PB85-224632

Testing of Wall-Fired Furnaces to Reduce Emissions of NO(sub X) and SO(sub X)
Volume 1. Final Report

Energy and Environmental Research Corp.
Irvine, CA

Prepared for

Environmental Protection Agency
Research Triangle Park, NC

Jun 85

U.S. Department of Commerce
National Technical Information Service
NTIS

PB85-224632

EPA/600/7-85/026a
June 1985

TESTING OF WALL-FIRED FURNACES TO REDUCE EMISSIONS OF NO_x AND SO_x

Volume 1

Final Report

by

P. L. Case
L. Ho
W. D. Clark
E. Kau
D. W. Pershing
R. Payne
M. P. Heap

Energy and Environmental Research Corporation
18 Mason
Irvine, California 92718

EPA Contract 68-02-3921

EPA Project Officer
D. C. Drehmel
LIMB Development Branch
Air and Energy Engineering Research Laboratory
U.S. Environmental Protection Agency
Research Triangle Park, NC 27711

AIR AND ENERGY ENGINEERING RESEARCH LABORATORY
OFFICE OF RESEARCH AND DEVELOPMENT
U.S. ENVIRONMENTAL PROTECTION AGENCY
RESEARCH TRIANGLE PARK, NC 27711

REPRODUCED BY
NATIONAL TECHNICAL
INFORMATION SERVICE
U.S. DEPARTMENT OF COMMERCE
SPRINGFIELD, VA. 22161

TECHNICAL REPORT DATA

(Please read Instructions on the reverse before completing)

1. REPORT NO EPA/600/7-85/026a	2.	3. RECIPIENT'S ACCESSION NO. PB85 224632/AS
4. TITLE AND SUBTITLE Testing of Wall-fired Furnaces to Reduce Emissions of NO_x and SO_x: Volume 1. Final Report		5. REPORT DATE June 1985
		6. PERFORMING ORGANIZATION CODE
7. AUTHOR(S) P. L. Case, L. Ho, W. D. Clark, E. Kau, D. W. Pershing, R. Payne, and M. P. Heap		8. PERFORMING ORGANIZATION REPORT NO.
9. PERFORMING ORGANIZATION NAME AND ADDRESS Energy and Environmental Research Corporation 18 Mason Irvine, California 92718		10. PROGRAM ELEMENT NO.
		11. CONTRACT/GRANT NO. 68-02-3921
12. SPONSORING AGENCY NAME AND ADDRESS EPA, Office of Research and Development Air and Energy Engineering Research Laboratory Research Triangle Park, NC 27711		13. TYPE OF REPORT AND PERIOD COVERED Final; 8/82 - 11/83
		14. SPONSORING AGENCY CODE EPA/600/13

15. SUPPLEMENTARY NOTES AEERL project officer is Dennis C. Drehmel, Mail Drop 4, 919/541-7505. Volume 2 consists of appendices.

16. ABSTRACT The report gives results of a study to clarify the processes that control sulfur capture by dry sorbents injected directly into a pulverized-coal-fired system, and to develop methods for generalizing data from one test furnace to another and from test facilities to fired application. Most experiments were conducted in a 1 million Btu/hr down-fired furnace to determine the effects of: fuel type, sorbent type, injection location, peak flame temperature, SO2 concentration, and burner zone stoichiometry. Conclusions of the study include: (1) the concentration of SO2 in the natural-gas-fired tests had a slight effect on sulfur capture, increasing capture at Ca/S = 2 from 26% at 500 ppm to 40% at 3500 ppm SO2; (2) the concentration of mineral matter in the system had a very strong impact on capture at all SO2 concentrations and Ca/S ratios tested; (3) injecting the sorbent downstream from the main flame resulted in improved utilization in coal flames; and (4) the effect of sorbent type on capture with a given fuel was dependent on the firing conditions--including sorbent injection location and thermal conditions (the hydrated limes seemed to be most sensitive to thermal conditions and the Vicron limestone least sensitive). Dolomite gave the highest capture with all of the fuels tested.

17. KEY WORDS AND DOCUMENT ANALYSIS

a. DESCRIPTORS		b. IDENTIFIERS/OPEN ENDED TERMS	c. COSATI Field/Group
Pollution	Natural Gas	Pollution Control	13B
Nitrogen Oxides		Stationary Sources	07B
Sulfur Oxides		Wall-fired Furnaces	
Furnaces		Dry Sorbents	13A
Sorbents			11G
Pulverized Fuels			21D

18. DISTRIBUTION STATEMENT Release to Public	19. SECURITY CLASS *(This Report)* Unclassified	21. NO. OF PAGES 336
	20. SECURITY CLASS *(This page)* Unclassified	22. PRICE

EPA Form 2220-1 (9-73)

NOTICE

This document has been reviewed in accordance with U.S. Environmental Protection Agency policy and approved for publication. Mention of trade names or commercial products does not constitute endorsement or recommendation for use.

ABSTRACT

The report gives results of a study to clarify the processes that control sulfur capture by dry sorbents injected directly into a pulverized-coal-fired system, and to develop methods for generalizing data from one test furnace to another and from test facilities to fired application.

Most experiments were conducted in a 1 million Btu/hr down-fired furnace to determine the effects of: fuel type, sorbent type, injection location, peak flame temperature, SO_2 concentration, and burner zone stoichiometry.

Conclusions of the study included:

(1) The concentration of SO_2 in the natural-gas-fired tests had a slight effect on sulfur capture, increasing capture at Ca/S = 2 from 26 percent at 500 ppm to 40 percent at 3500 ppm SO_2;

(2) The concentration of mineral matter in the system had a very strong impact on capture at all of the SO_2 concentration levels and Ca/S ratios tested;

(3) Injecting the sorbent downstream from the main flame resulted in improved utilization in coal flames; and

(4) The effect of sorbent type on capture with a given fuel was dependent on the firing conditions--including sorbent injection location and thermal conditions (the hydrated limes seemed to be most sensitive to thermal conditions and the Vicron limestone least sensitive).

TABLE OF CONTENTS

Section | Page

1.0 SUMMARY 1-1

1.1 Purpose and Scope 1-1
1.2 Results of Detailed Measurements in Gas and Coal Flames 1-5
1.3 Results - Thermal Effects 1-8
1.4 Sulfur Capture Model 1-12
1.5 Sorbent/Mineral Matter Interactions 1-13
1.6 Fuel Sorbent Interactions 1-18
1.7 Downstream Sorbent Injection 1-26
1.8 Furnace Thermal and Capture Modeling 1-33
1.9 System Effects 1-40
1.10 Effect of LIMB Boiler Operation 1-42
1.11 Conclusion and Recommendations 1-42

2.0 BACKGROUND, PURPOSE AND SCOPE 2-1

2.1 Background 2-1
2.2 LIMB Technology Development 2-14
2.3 Purpose and Scope 2-15

3.0 DETAILED MEASUREMENTS IN GAS AND COAL FLAMES 3-1

3.1 Experimental Approach and Scope of Detailed Measurements 3-1
3.2 Characterization of Natural Gas Flames 3-5
3.3 Coal Flame Characterization 3-16
3.4 Conclusions - Detailed Measurements 3-28

4.0 THERMAL EFFECTS - BURNER AND OPERATIONAL EFFECTS, HIGH TEMPERATURE FLAMES 4-1

4.1 Burner Effects 4-1
4.2 Operational Effect - Effect of Load 4-11
4.3 High Temperature Flames 4-11
4.4 Conclusions 4-16

5.0 SULFUR CAPTURE MODEL 5-1

5.1 Sorbent Activation Model 5-1
5.2 Sorbent Sulfation Model 5-3
5.3 Sulfur Capture Model - Conclusions 5-13

6.0 SORBENT MINERAL MATTER INTERACTIONS 6-1

6.1 Effect of Mineral Matter on Sorbent 6-1

Preceding page blank

TABLE OF CONTENTS (CONCLUDED)

Section / Page

6.2 SO_2 and Mineral Matter Concetration Effects 6-19
6.3 Morphological Characteristics of Ash/Sorbent Mixtures 6-21
6.4 Conclusions - Mineral Matter Effects 6-28

7.0 FUEL AND SORBENT INTERACTIONS 7-1

7.1 Sorbent Effects 7-1
7.2 Fuel Effects 7-17
7.3 Conclusions, Fuel and Sorbent Interactions 7-27

8.0 DOWNSTREAM SORBENT INJECTION 8-1

8.1 Downstram Injection: Fuel/Sorbent Effects 8-1
8.2 Effect of Sorbent Location 8-14
8.3 Conclusions Downstram Sorbent Injection 8-27

9.0 FURNACE MODELING 9-1

9.1 Furnace Modeling Objectives 9-1
9.2 Boiler Performance Code 9-1
9.3 Two-Dimensional Furnace Modeling 9-5
9.4 Three-Dimensional Furnace Modeling 9-25
9.5 Combined Thermal/Sulfation Modeling 9-27

10.0 SYSTEM EFFECTS 10-1

11.0 EFFECT OF SORBENT INJECTION ON BOILER OPERATING CHARACTERISITCS 11-1

11.1 Review: Effects on Boiler Operating Characteristics 11-1
11.2 Boiler Simulator Furnace Tests of Sorbent Effect on Ash Characteristics 11-10
11.3 Conclusion - Effect of LIMB on Boiler Operation 11-19

12.0 CONCLUSIONS AND RECOMMENDATIONS 12-1

12.1 Conclusions - Experimental Results 12-2
12.2 Conclusions - Analytical Methods Development 12-5

13.0 REFERENCES 13-1

LIST OF FIGURES

Figure Page

1-1 LIMB Technology Development 1-2
1-2 Detailed Gas Temperatures, Natural Gas Flame 1-6
1-3 Detailed Gas Temperautres, Indiana Coal (Lot 3) Flame 1-7
1-4 Effect of Fuel Injector and SR_b on Sulfur Capture, Natural Gas + H_2S Flames 1-9
1-5 Comparison of Sulfur Capture in High and Low Temperature Gas Flames with Indiana Coal Flame 1-10
1-6 Conceptual Illustration of Pore Model for CaO/SO_2 Reaction 1-11
1-7 Effect of Ash Addition on Sulfur Capture - Vicron 45-3 Plus Fly Ash. Natural Gas/H2S Flame, DMB, Axial Injector and Sorbent with Fuel 1-14
1-8 Effect of Mineral Addition on Sulfur Capture by Vicron 45-3, Natural Gas/H_2S Flame, Port #3 (Exit Convective Section) 1-15
1-9 Effect of Al_2O_3 Content of Solid on Capture by Vicron 45-3 1-16
1-10 Effect of Al_2O_3 Content of Solid on Sulfur Capture by Dolomite 1-17
1-11 Effect of Sorbent Type, Natural Gas Flame 1-20
1-12 Effect of Sorbent Type on Sulfur Capture, Indiana Lot 3 Coal 1-21
1-13 Effect of Input Vircron Particle Size on SO_2 Capture, Comparison of BSF Data with Model 1-23
1-14 Effect of Fuel on Sulfur Capture and Thermal History of Vicron 45-3 with Fuel 1-25
1-15 Effect of Fuel on Sulfur Capture and Thermal History of Dolomite, Sorbent with Fuel 1-25
1-16 Boiler Simulator Furnace 1-27
1-17 Effect of Srobent Type on Sulfur Capture - Downstream Injection, Indiana L3 Coal 1-29
1-18 Comparison of Srobent Injection Location, with Utah and Indiana Coal, Vicron 45-3 1-30
1-19 Effect of Kaolin Addition, Sorbent and Kaolin with Fuel, Natural Gas + H_2S-Firing 1-31
1-20 Effect of Kaolin Addition to Fuel, Sorbent Injected in PFC. Natural Gas + H_2S-Fired 1-32
1-21 Scanning Electron Micrographs of Vicron and Kaolin in Natural Gas Flame 1-34
1-22 Scanning Electron Micrographs of Indiana Coal with Vicron 1-35
1-23 LWS Temperature Profiles 1-37
1-24 Furnace Comparison 1-39
1-25 Effect of Firing System on Sulfur Capture, Vicron 45-3 with Two Fuels in LWS and BSF 1-41

LIST OF FIGURES (CONTINUED)

Figure		Page
2-1	LIMB Process	2-3
2-2	Comparison of Steinmuller and DMB Data - Limestone Injected in Tertiary Ports	2-7
2-3	Influence of Heat Extraction Rate - Base Case Conditions	2-9
2-4	Effect of Fuel on Sulfur Capture (Vicron 45-3)	2-11
2-5	LIMB Technology Development	2-13
2-6	Program Technical Approach	2-17
3-1	Comparison of Coal and Propane Capture and Thermal History	3-2
3-2	Sulfur Capture, Natural Gas Flame	3-3
3-3	Sulfur Capture, Indiana Coal Flame	3-4
3-4	Comparison of Capture for Indiana Coal Flames	3-4
3-5	Temperature Profile and Sulfur Capture for Gas and Coal Flames	3-7
3-6	Temperature Profile and Sulfur Capture for Natural Gas and Propane Flames	3-8
3-7	Detailed Gas Temperatures Natural Gas Flame	3-9
3-8	Radial Gas Temperatures, Natural Gas Flame	3-10
3-9	Gas Species Profiles, Natural Gas Flame	3-12
3-10	Solids Loading (Centerline), Vicron 45-3 in Natural Gas Flame, Axial	3-13
3-11	Solids Loading, Vicron 45-3 in Natural Gas Flame, Radial	3-14
3-12	Summary of Sorbent Thermal History, Surface Area and Utilization, Natural Gas/H_2S Flame	3-15
3-13	Detailed Gas Temperatures - Indiana Coal Flame	3-17
3-14	Gas Species Profiles, Indiana Coal Flame	3-18
3-15	Solids Loading, Indiana 3 Coal Flame, Axial	3-19
3-16	Solids Loading, Indiana 3 Flame, Radial	3-20
3-17	Evolution of Species from Indiana 3 Coal (Radiant Furnace)	3-21
3-18	Retention of Sulfur in Solid, Indiana 3 Coal	3-22
3-19	Solids Loading, Vicron 45-3, with Indiana 3 Coal, Axial	3-23
3-20	Solids Loading, Vicron 45-3 with Indiana 3 Coal, Radial	3-24
3-21	Evolution of Species from Indiana 3 Coal with Vicron 45-3 (Radiant Furnace)	3-25
3-22	Retention of Sulfur in Solid, Indiana 3 Coal with Vicron 45-3	3-26
3-23	Calcium Retention in Ash, Boiler Simulator Furnace	3-29
4-1	Effect of Fuel Injection on Capture Natural Gas + H_2S Flame, Sorbent with Fuel	4-2

LIST OF FIGURES (CONTINUED)

Figure		Page
4-2	Effect of Burner Zone Stoichiometry on Sulfur Capture and NO_x, Axial Injector	4-4
4-3	Effect of Burner Zone Stoichiometry on Sulfur Capture and NO_x, Radial Injector, with Air Heat	4-5
4-4	Thermal History Comparison: Two Fuel Injectors, Staged . . .	4-6
4-5	Thermal History Comparison: Two Fuel Injectors Unstaged . . .	4-7
4-6	Detailed Temperature Measurements, Natural Gas Flame, Radial Injector with 400°F Heat	4-8
4-7	Detailed Temperature Measurements, Natural Gas Flame, Axial Injector, Unstaged, No Air Heat	4-9
4-8	Thermal History and Sulfur Capture for Staged and Unstaged Indiana 3 Coal Flames	4-10
4-9	Sulfur Caputre at Baseload (1.0 MBtu/hr) BSF, Natural Gas + H_2S with Vicron 45-3	4-12
4-10	Sulfur Capture at High Load (1.6MBtu/hr) BSF, Natural Gas + H_2S with Vicron 45-3	4-13
4-11	Effect of Load on Thermal History and Sulfur Capture, BSF, Natural Gas, Vicron 45-3	4-14
4-12	Effect of Oxygen Addition on Thermal History and Sulfur Capture, Natural Gas/H_2S Flames	4-15
4-13	Comparison of Sulfur Capture in High and Low Temperature Gas Flames with Indiana Coal Flame	4-17
5-1	Zone Approach to Sulfur Capture Model	5-2
5-2	Effect of Peak Temperature on Sorbent Surface Area	5-4
5-3	Conceptual Illustration of Pore Model for CaO/SO_2 Reaction	5-6
5-4	Application of Random Pore Model to Data of Borgwardt (1970)	5-8
5-5	Model Comparison	5-10
5-6	Effect of Pore Structure Parameters	5-11
5-7	Effect of Temperature	5-12
5-8	Effect of Ca/S Ratio	5-14
5-9	Effect of SO_2 Concentration	5-15
5-10	Effect of Intrinsic Rate Constant	5-16
5-11	Effect of Product Layer Diffusivity	5-17
5-12	Effect of Particle Density	5-18
5-13	Effect of Particle CaO Content	5-19
5-14	Effect of Particle Size	5-20
6-1	Effect of Ash Addition on Sulfur Capture - Vicron 45-3 Plus Fly Ash. Natural Gas/H_2S Flame, DMB, Axial Injector and Sorbent with Fuel	6-2
6-2	Effect of Mineral Addition on Sulfur Capture by Vicron 45-3, Natural Gas/H_2S Flame, Port #3 (Exit Convective Section)	6-6

LIST OF FIGURES (CONTINUED)

Figure		Page
6-3	Effect of Mineral Addition on Sulfur Capture by Dolomite, Natural Gas/H_2S Flame, Port 3 (Exit Convective Section)	6-7
6-4	Effect of Al_2O_3 Content of Solid on Capture by Vicron 45-3	6-9
6-5	Effect of Al_2O_3 Content of Solid on Sulfur Capture by Dolomite	6-10
6-6A	Vicron 45-3 and Kaolin Particle Size Distribution - as Injected	6-12
6-6B	Marblewhite 125 and Kaolin Particle Size Distribution - as Injected	6-12
6-7	Dolomite and Kaolin Particle Size Distribution - as Injected	6-13
6-8	Effect of Mineral Matter Concentration on Decrease in SO_2 Capture with Vicron 45-3	6-15
6-9	Effect of Mineral Matter Concentration on Decrease SO_2 Capture for Marblewhite 125	6-16
6-10	Effect of Mineral Matter Concentration on SO_2 Capture for Dolomite	6-17
6-11	Effect of Al_2O_3 and SO_2 Concentration on SO_2 Capture, Natural Gas + H_2S, Vicron 45-3/Kaolin, Ca/S = 1.0	6-22
6-12	Effect of Al_2O_3 and SO_2 Concentration on SO_2 Capture, Natural Gas + H_2S, Vicron 45-3/Kaolin, Ca/S = 2.0	6-23
6-13	Effect of Al_2O_3 and SO_2 Concentration on SO_2 Capture, Natural Gas + H_2S, Vicron 45-3/Kaolin Ca/S = 3.0	6-24
6-14A	Vicron/Kaolin Mixture Injected at Fuel	6-26
6-14B	High Magnification Mixed-Composition Particle	6-27
6-15	Phase Diagram for CaO - Al_2O_3 - SiO_2 System	6-29
7-1	Fuel/Sorbent Interactions Test Matrix	7-2
7-2	Test Matrix for Sorbent Particle Size Effect	7-3
7-3	Effect of Sorbent Type, Natural Gas Flame	7-8
7-4	Effect of Sorbent Type on Sulfur Capture, Indiana Lot 3 and Lot 4 Coals	7-9
7-5	Effect of Sorbent Type on Sulfur Capture, Indiana Lot 3 and Lot 4 Coals	7-9
7-6	Effect of Sorbent on Sulfur Capture, Utah and Illinois Coals	7-11
7-7	Effect of Sorbent on Sulfur Capture, Utah and Illinois Coals	7-11
7-8	Effect of Hydrated Lime Type, Colton and German, on Sulfur Capture. Sorbent with Fuel, DMB, Uncooled	7-12
7-9	Effect of Hydrated LIme Type, Colton and German, on Sulfur Capture. Sorbent with Fuel, DMB, Uncooled	7-12
7-10	Relative Particle Size Distributions, Colton and "Steinmuller" Calcium Hydroxides	7-13
7-11	Particle Size Distributions foir Vicron and Fredonia Sorbents	7-14

LIST OF FIGURES (CONTINUED)

Figure		Page
7-12	Particle Size Distributions for Dolomite Sorbents	7-15
7-13	Effect of Input Vicron Particle Size on Sulfur Capture, Natural Gas and Indiana L3 Coal	7-16
7-14	Effect of Input Vicron Particle Size on SO_2 Capture, Comparison of BSF Data with Model	7-18
7-15	Effect of Fredonia Sorbent Particle Size on SO_2 Capture, Natural Gas and Indiana L3 Coal	7-19
7-16	Effect of Dolomite Particle Size on Sulfur Capture, Gas Flame	7-20
7-17	Effect of Dolomite Particle Size on Sulfur Capture, Indiana (Lot 3) Coal	7-21
7-18	Effect of Fuel on Sulfur Capture and Thermal History of Vicron 45-3 with Fuel	7-24
7-19	Effect of Fuel on Sulfur Capture and Thermal History of Dolomite, Sorbent with Fuel	7-25
7-20	Effect of Fuel on Sulfur Capture for Fredonia (Coarse) and Lime (Colton)	7-26
7-21	Effect of Fuel on Sulfur Capture for Fredonia (Coarse) and Lime (Colton)	7-26
7-22	Effect of Fuel Sulfur Content on Sulfur Capture, Vicron 45-3	7-28
7-23	Effect of Fuel Sulfur Content on Sulfur Capture - Dolomite	7-29
7-24	Correlation of Ash/Sorbent Alumina Content with Sulfur Capture	7-31
8-1	Boiler Simulator Furnace	8-2
8-2	Effect of Sorbent Location on Sulfur Capture - Fuel and Downstream Injection	8-3
8-3	Effect of Sorbent Type on Sulfur Capture - Downstream Injection, Indiana L3 Coal	8-4
8-4	Temperature Profile for Downstream Injection, Indiana (Lot 5) Coal	8-7
8-5	Effect of Sorbent Type on Sulfur Capture, Downstream Injection, Indiana L5 Coal	8-9
8-6	Temperature Profile for Downstream Sorbent Injection, Illinois Coal	8-10
8-7	Effect of Sorbent Type on Sulufr Capture, Downstream Injection, Illinois Coal	8-11
8-8	Temperature Profile for Downstream Sorbent Injection, Utah Coal	8-12
8-9	Effect of Sorbent Type of Sulfur Capture, Downstream Injection, Utah Coal	8-13
8-10	Temperature Profile for Downstream Sorbent Injection, Saar Coal	8-15
8-11	Effect of Sorbent Type on Sulfur Capture, Downstream Injection, Saar Coal	8-16

LIST OF FIGURES (CONTINUED)

Figure | Page

8-12 Temperature Profile for Downstream Sorbent Injection, Natural Gas + H_2S 8-17
8-13 Effect of Sorbent Type on Sulfur Capture, Downstream Injection, Natural Gas = H_2S 8-18
8-14 Comparison of Sorbent Injection Location, with Utah and Indiana Coal, Vicron 45-3 8-19
8-15 Comparison of Sorbent Injection Location, with Utah and Indiana Coals, Dolomite 8-20
8-16 Effect of Kaolin Addition, Sorbent and Kaolin with Fuel, Natural Gas + H_2S-Firing 8-21
8-17 Effect of Kaolin Addition to Fuel, Sorbent Injected in PFC. Natural Gas + H_2S-Fired 8-23
8-18 Sorbent Injection and Sample Locations for Surface Area Measurements 8-24
8-19 Furnace Temperature Profile, Sorbent with Fuel 8-25
8-20 Furnace Temperature, Sorbent in Post-Flame Cavity 8-26
8-21 Natural Gas Flame. Vicron and Kaolin Injected at Fuel 8-28
8-22 Natural Gas Flame. Kaolin Injected at Fuel and Vicron Injected Downstream 8-29
8-23 Indiana Coal with Vicron Injected at Fuel 8-30
8-24 Indiana Coal with Vicron Injected Downstream 8-31

9-1 SWS Flow and Heat Release Patterns 9-10
9-2 Effect of Load on SWS Exit Temperature 9-13
9-3 0.5 m Off-Centerline Gas Temperatures 9-14
9-4 Centerline Gas Temperatures 9-15
9-5 SWS Wall Temperatures 9-17
9-6 SWS Heat Flux to Walls 9-18
9-7 MT Flow and Heat Release Patterns 9-21
9-8 MT Gas Temperatures 9-22
9-9 MT Wall Temperatures 9-23
9-10 MT Heat Flux to Wall 9-24
9-11 LWS Zoning 9-26
9-12 Effect of Load on LWS Exit Temperature 9-28
9-13 LWS Temperature Profiles 9-29
9-14 LWS Temperature Profiles 9-30
9-15 Particle Tracking Example 9-32
9-16 SWS Mean Particle Temperature History 9-34
9-17 SWS Distribution of Particle Residence Times at Exit 9-35
9-18 SWS Peak Particle Temperature Distribution 9-36
9-19 SWS Particle Temperature Distribution 9-38
9-20 Sulfur Capture in SWS 9-40
9-21 Sulfur Capture in MT 9-44
9-22 Sulfur Capture in LWS 9-48
9-23 Furnace Comparison 9-50

10-1 Characteristics of the LWS Test Furnace 10-2

LIST OF FIGURES (CONCLUDED)

Figure		Page
10-2	Effect of Firing System on Sulfur Capture, Vicron 45-3 with Two Fuels in LWS and BSF	10-3
11-1	Size Distribution With and Without Added Sorbents; Detroit Edison Tests	11-4
11-2	TVA Shawnee Effect of Limestone Injection on Particle Size - Inlet of Collector	11-5
11-3	Effect of Sorbent on Fly Ash Resistivity TVA Shawnee, B & W - Pilot and Detroit Edison - St. Clair	11-6
11-4	In-situ Resistivity vs. Temperature Relationship for Various Coal Sulfurs (No Limestone Injection)	11-7
11-5	In-situ Resistivity vs. Temperature Relationship for Various Coal Sulfurs (with Limestone Injection)	11-8
11-6	Furnace Temperatures and Sulfur Capture -Illinois Coal Fired with Vicron 45-3	11-11
11-7	Furnace Temperatures and Sulfur Capture - Utah Coal Fired with Vicron 45-3	11-13
11-8	Fouling Characteristics - Heat Extraction (q) and Cooling Probe Temperature (T). Illinois Coal Fired	11-14
11-9	Fouling Characteristics - Heat Extraction (q) and Cooling Probe Temperature (T). Illinois Coal with Vicron 45-3 (Ca/S = 2.0)	11-15
11-10	Fouling Characteristics - Heat Extraction (q) and Cooling Probe Temperature (T). Utah Coal Fired	11-16
11-11	Fouling Characteristics - Heat Extraction (q) and Cooling Probe Temperature (T). Utah Coal + Vicron 45-3 (Ca/S = 2.25)	11-17
11-12	Particle Size Distribution, Flue, Illinois Coal With and Without Sorbent	11-21
11-13	Particle Size Distribution, Flue, Utah Coal and Utah Coal with Sorbent	11-22

LIST OF TABLES

Table Page

1-1 Sorbent Characteristics 1-19
1-2 Fuel Characteristics 1-24

5-1 Basline Conditions 5-22

6-1 Ash-Sorbent Mixture Compsition 6-3
6-2 Typical Compositions of Mineral Additives 6-5
6-3 Sorbent Mineral Mixtures Characteristics 6-8
6-4 Sorbent/Kaolin Mixture Compositions 6-14
6-5 Sulfur Capture for Various Al_2O_3, SO_2 Concentration 6-20
6-6 Effect of Mineral Addition on Surface Area 6-25

7-1 Sorbent Characteristics 7-5
7-2 Fuel Characteristics 7-23
7-3 Coal (Ash) Sorbent Mixture Characteristics
(Equivalent Ca/S = 2.0) 7-30

8-1 Downstream Sorbent Injection Tests 8-5
8-2 Sorbent Surface Area Results 8-8

9-1 Utah Coal Analysis 9-6
9-2 Versatile Burner Dimensions 9-9
9-3 V50 Burner Dimensions 9-19
9-4 SWS Baseline Conditions 9-39
9-5 Sulfur Capture in SWS 9-42
9-6 MT Baseline Conditions 9-43
9-7 Sulfur Capture in MT 9-45
9-8 LWS Baseline Conditions 9-46
9-9 BSF Baseline Conditions 9-49

11-1 LIMB Effluent Stream Characteristics 11-18
11-2 Effect of Sorbent Addition on Total Solids
Load and Carryover 11-20

1.0 SUMMARY

This report summarizes the research program and results obtained under EPA Contract 68-02-3921. This research project is one of several programs sponsored by the EPA to investigate and develop simultaneous NO_x/SO_x emission control using limestone injection in multi-stage burners. The overall technology development programs range from small-scale fundamental investigations to pilot-scale development studies. This overall EPA program includes analysis of boiler design aspects of LIMB technology and a probable full-scale utility boiler demonstration. One concept of the EPA LIMB program is shown in Figure 1-1. There are three basic facets shown: scientific aspects, pilot-scale studies, and application. LIMB application is likely to be very system-specific, involving analysis of a particular fuel/boiler/burner system, selection of a sorbent and injection method and consideration of the impact of LIMB on operation of the boiler. As indicated in Figure 1-1, the results of investigations of the fundamental aspects of sulfur capture, pilot-scale studies and the development of models for the process will aid in the application of LIMB technology.

The research program summarized here feeds into the development effort at several levels. The shaded areas in Figure 1-1 show the areas in which results of this research program are of use. The work reported here involved direct investigations of the role of fuel and sorbent properties and fuel mineral matter interactions. Results of these experimental efforts can be used to clarify the sulfate formation process and to derive guidelines for determining sorbent injection locations. In addition to the experimental work, analytical development work including the development of a sulfur capture model, and the application of heat transfer models was performed.

1.1 Purpose and Scope

The overall goal of the research program was the clarification of means to reduce emissions of nitrogen oxide (NO_x) and sulfur oxides (SO_x) from the pulverized-coal, wall-fired, combustion systems found in utility boilers. The work was divided into four separate tasks. The purpose of Task 1 was to

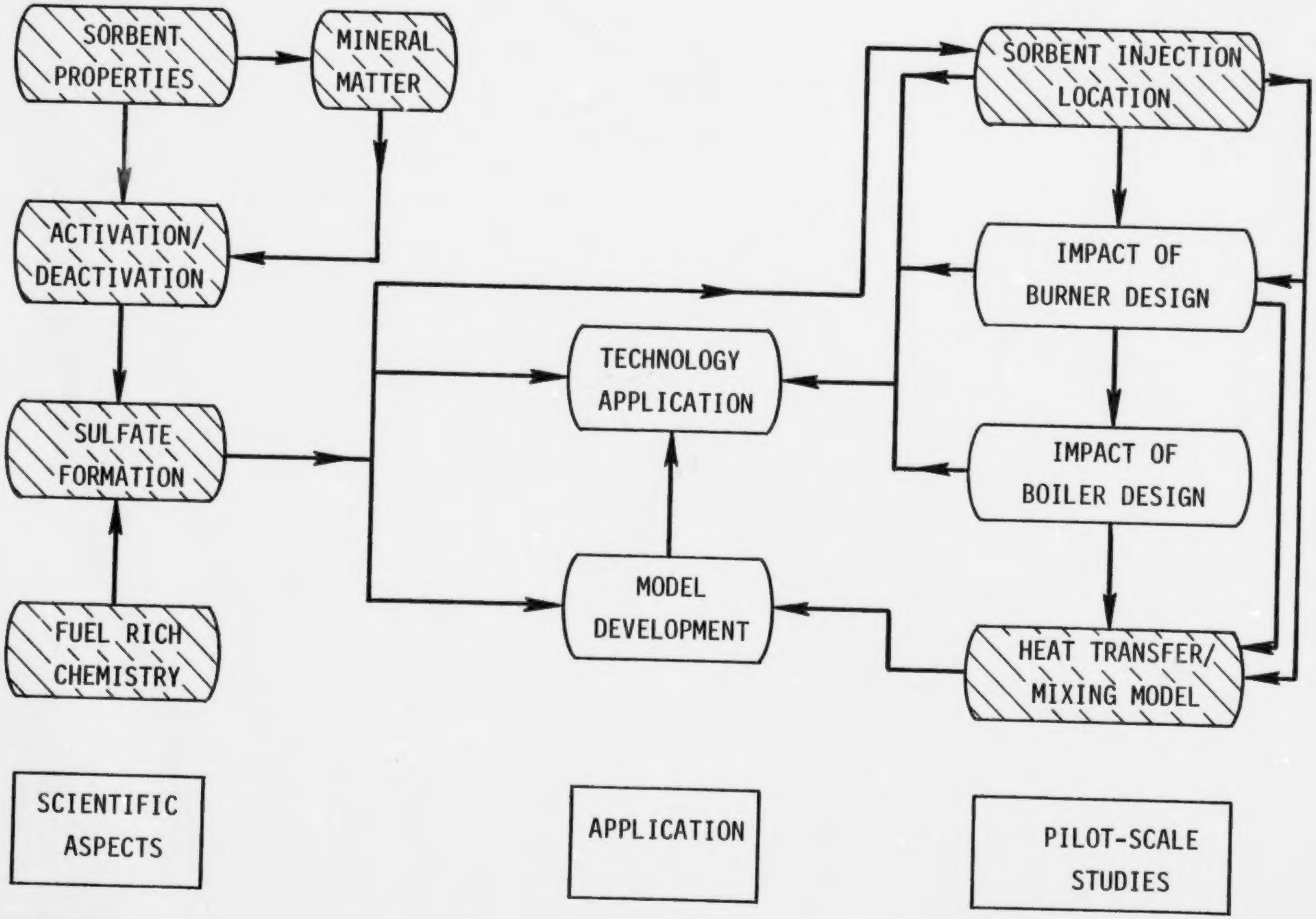
SORBENT PROPERTIES
MINERAL MATTER
ACTIVATION/ DEACTIVATION
SULFATE FORMATION
FUEL RICH CHEMISTRY
TECHNOLOGY APPLICATION
MODEL DEVELOPMENT
SORBENT INJECTION LOCATION
IMPACT OF BURNER DESIGN
IMPACT OF BOILER DESIGN
HEAT TRANSFER/ MIXING MODEL
SCIENTIFIC ASPECTS
APPLICATION
PILOT-SCALE STUDIES

Figure 1-1. LIMB technology development.

provide detailed information about sorbent and sulfur reactions under conditions of particular interest. Task 2 was designed to evaluate the potential of a number of design and sorbent options. Task 3 provided some information on the effect of scale on the performance of systems designed to reduce NO_x and SO_x, and Task 4 provided for summarizing the data produced, providing recommendations concerning optimum systems and potential operational problems.

1.1.1 Task 1 - Detailed Measurements

The major goal of this task was to clarify the effect of the immediate flame zone on sorbent reactivity and overall sorbent utilization. In particular, there were several conditions encountered in earlier (EPA Contract 68-02-2667) parameter screening studies which indicated that processes occurring in the immediate flame region (less than 1 sec. residence time) may have a controlling effect on sorbent reactivity and overall sorbent utilization. The task was made up of two phases: The first phase was the measurement of detailed temperature and species profiles in the near-burner region in an attempt to identify conditions which would explain observed differences in sulfur capture. The second phase provided for the detailed measurement of temperatures, species, and sorbent properties from conditions of particular interest resulting from the sorbent and design option investigation.

A model of the sulfur capture process was developed for use as a tool in evaluating the application of the dry limestone injection process to practical systems. Results from earlier studies, most notably the EPA in-house studies, the EPA sponsored project at the Tennessee Valley Authority and work performed at Battelle, have been used to generate models of the reactions between limestone and sulfur dioxide. One modeling approach (the pore model) was selected for development as part of Task 1.

1.1.2 Task 2 - Sorbent and Design Options

The purpose of this task was to evaluate the potential of various sorbent and design options to improve the performance of LIMB. This task included: investigation of: burner parameters such as fuel injector type and burner zone stoichiometry; sorbent parameters such as sorbent type, particle size and composition; operational characteristics such as load, high temperature flames (O_2 enriched) and sorbent injection location; fuel effects using coals and gaseous fuels; and the effect of ash/mineral matter components on sorbent reactivity.

1.1.3 Task 3 - Effect of Scale

As originally conceived, the objective of Task 3 was to investigate scale effects on the performance of systems designed for the simultaneous reduction of NO_x and SO_x emissions. This was to be achieved both though the use of mathematical models for the prediction of furnace performance and through tests carried out on a range of furnace sizes. The experimental studies were to produce data directly related to scale effects. The mathematical model development was to provide a tool for the interpretation and eventual extrapolation of the data. It was planned that the work carried out under this task should make extensive use of data generated at bench-scale in this and earlier programs, and should be closely linked to the pilot-scale studies planned under the EPA Contract 68-02-2667 pilot-scale test program. Scheduling problems (the 2667 pilot-scale tests have yet to be completed) and the need to investigate ash/mineral matter and fuel/sorbent effects in a less expensive, more easily controlled system resulted in a redefinition of the Task 3 scope. The pilot-scale experiments were eliminated and the analysis of data from the BSF studies and other pilot-scale LIMB investigations was emphasized.

1.1.4 Task 4 - Summary and Recommendations

The purpose of Task 4 was to review the data generated in the other three tasks in order to rank possible options and provide recommendations for optimum systems. In a sense, this report is Task 4, however, the experimental results (as is often the case) have raised nearly as many questions as have been answered. Thus, the purpose of this task is to summarize the experimental results and analytical procedures, to describe a method of analyzing and rationalizing data from various systems, and to discuss remaining problems which should be addressed.

1.2 Results of Detailed Measurements in Gas and Coal Flames

One of the primary goals of this research program was to provide data which would clarify some of the puzzling results from earlier work. In particular, the effect of changing from gas to coal firing was of interest. In earlier parameters screening studies, Indiana coal and propane doped with H_2S were fired under the same conditions. The overall thermal history of the sulfur/sorbent utilization in the propane-fired case was dramatically better than in the coal-fired case. It appeared that some process in the near-burner region had a dominant effect on sorbent reactivity. The first task of this program was to identify temperature and species profiles in the immediate flame region which might explain the observed differences in sorbent utilization.

Detailed temperature and species measurements in the region near the burner were made for both Indiana coal and gas flames. Gas temperature maps of the radiant portion of the Boiler Simulator Furnace (BSF) fired with natural gas and with Indiana (lot 3) coal are shown in Figures 1-2 and 1-3. Measurements of gas species, solids loading and solids composition for the two flames were also made. These detailed measurements showed slight differences in flame shape and peak flame temperatures (the coal flame was somewhat shorter and hotter near the burner than the gas flame) and confirmed the difference in sorbent utilization in the two flames. There was some loss of calcium (sorbent) in the furnace when coal was fired and considerable dropout of solids through the furnace with either fuel. The measured differences in temperature and flame shape hardly seem sufficient to account for the observed difference in sulfur capture. It appeared that some fuel effect not directly

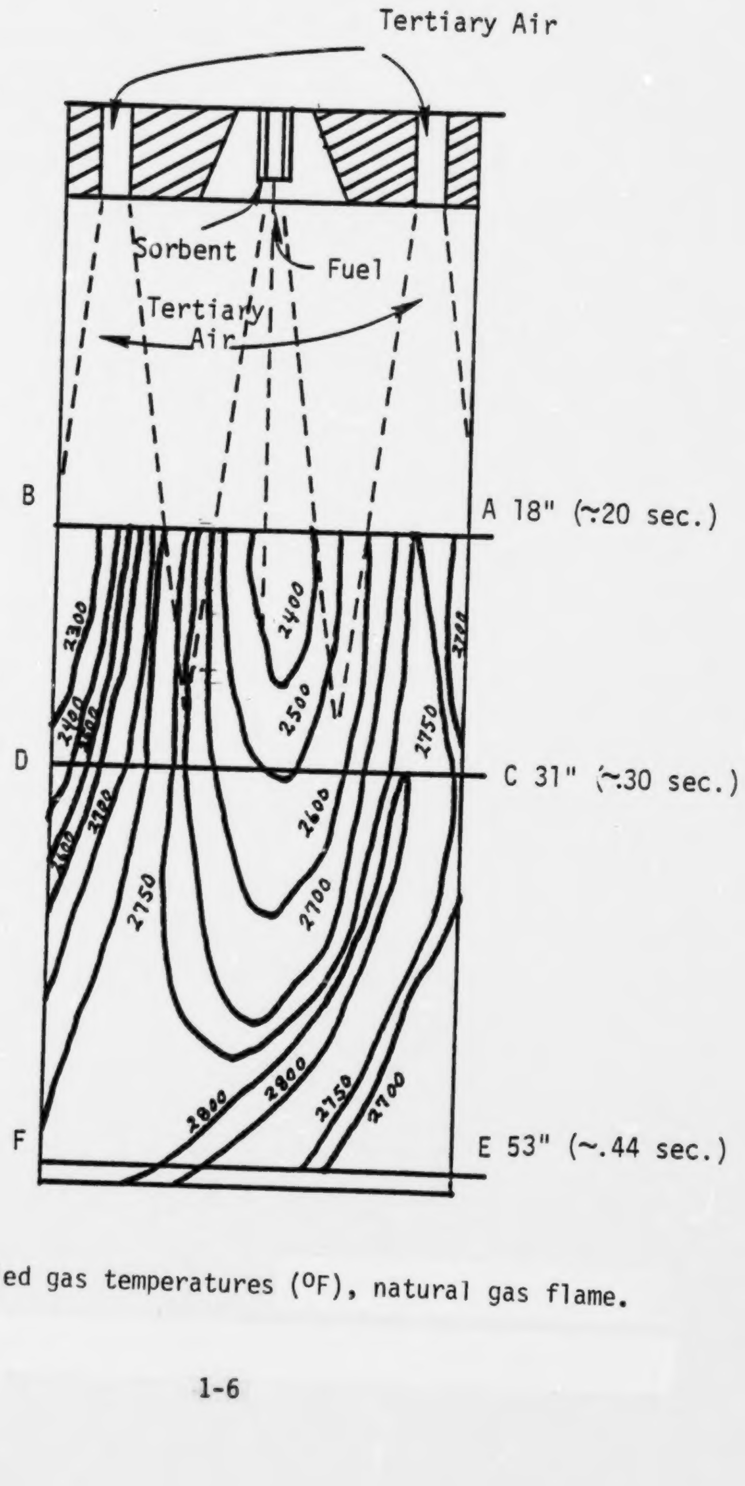
Tertiary Air
Sorbent
Fuel
Tertiary Air
B
A 18" (~.20 sec.)
D
C 31" (~.30 sec.)
F
E 53" (~.44 sec.)
2300
2400
2400
2500
2700
2750
2400
2600
2700
2750
2800
2800
2750
2700

Figure 1-2. Detailed gas temperatures (°F), natural gas flame.

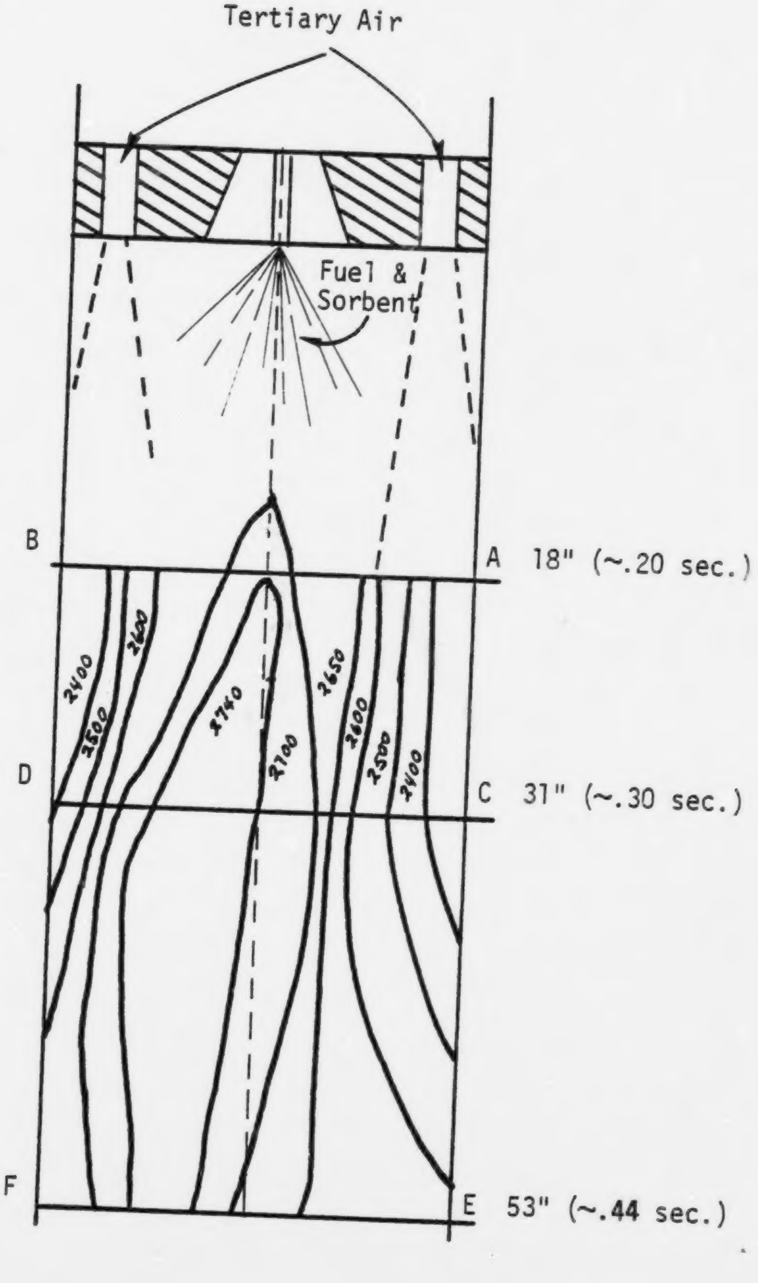
Tertiary Air
Fuel &
Sorbent
B
A
18" (~.20 sec.)
2400
2500
2600
2740
2700
2650
2600
2500
2400
D
C
31" (~.30 sec.)
F
E
53" (~.44 sec.)

Figure 1-3. Detailed gas temperatures (^{o}F), Indiana coal (lot 3) flame.

reflected in temperature or gaseous species concentrations was responsible for the lower sulfur capture in the coal flame.

1.3 Results - Thermal Effects

Even though thermal differences in the gas and coal flames tested did not seem great enough to account for the observed difference in sorbent utilization, thermal differences, especially peak temperature, have been shown in the other studies to have a dramatic effect on sorbent reactivity. In order to ascertain the effect of temperature differences on capture in a simple system (gas fuel only) several experiments emphasizing high temperatures were performed. Experiments investigating burner effects, including fuel injector type and burner zone stoichiometry, the effect of load (especially concerned with changes in residence times), and high temperature (O_2 enriched) flames were also done.

Under the same conditions - the burner fired at 1.0 MBtu/hr and SR_b = 0.6, SR_t = 1.2 sorbent injected with the fuel gave the same capture regardless of the fuel injector (axial or radial) used. The effect of burner zone stoichiometry depended to some extent on the fuel injector used as can be seen from the data plotted in Figure 1-4. Oxygen enrichment and increasing load had some effect on sulfur capture, changing load changed the region in the furnace where sulfation occurred and very high temperature oxygen enriched (30 percent in the oxidant O_2) flames decreased sorbent utilization somewhat.

In these tests the change in sulfur capture produced by altering the thermal characteristics of the natural gas flame were much less dramatic than the difference in capture between gas and coal flames as can be seen by the data plotted in Figure 1-5. Temperature profiles for natural gas/H_2S at two thermal conditions are shown with the Indiana coal temperature profile. Capture throughout the BSF at a constant calcium-to-sulfur ratio is also shown for the three conditions. The temperature profiles from the two gas fired cases essentially bracket the coal profile, but the capture for both gas fired tests was higher than for the coal. These results combined with the detailed measurements indicate that the effect of fuel type on sulfur capture is not a simple, direct result of thermal differences in the flames.

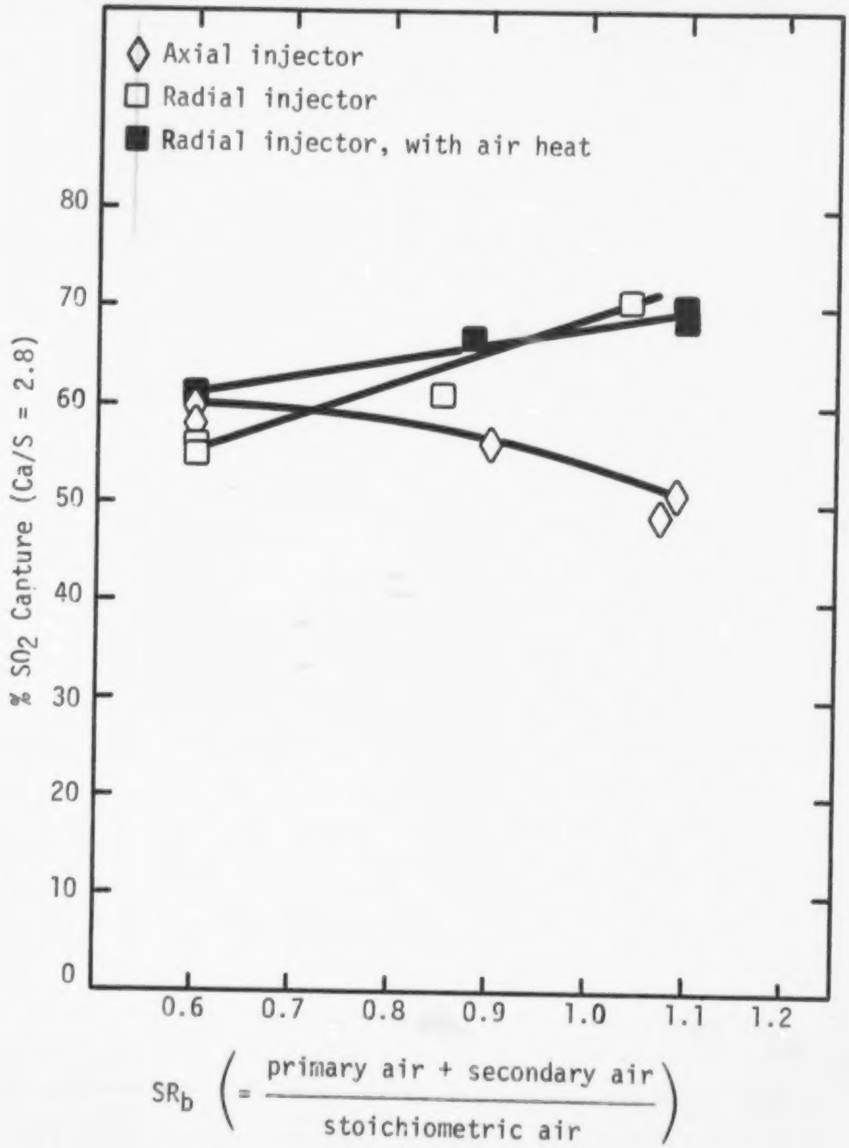

Figure 1-4. Effect of fuel injector and SR_b on sulfur capture, natural gas + H_2S flames.

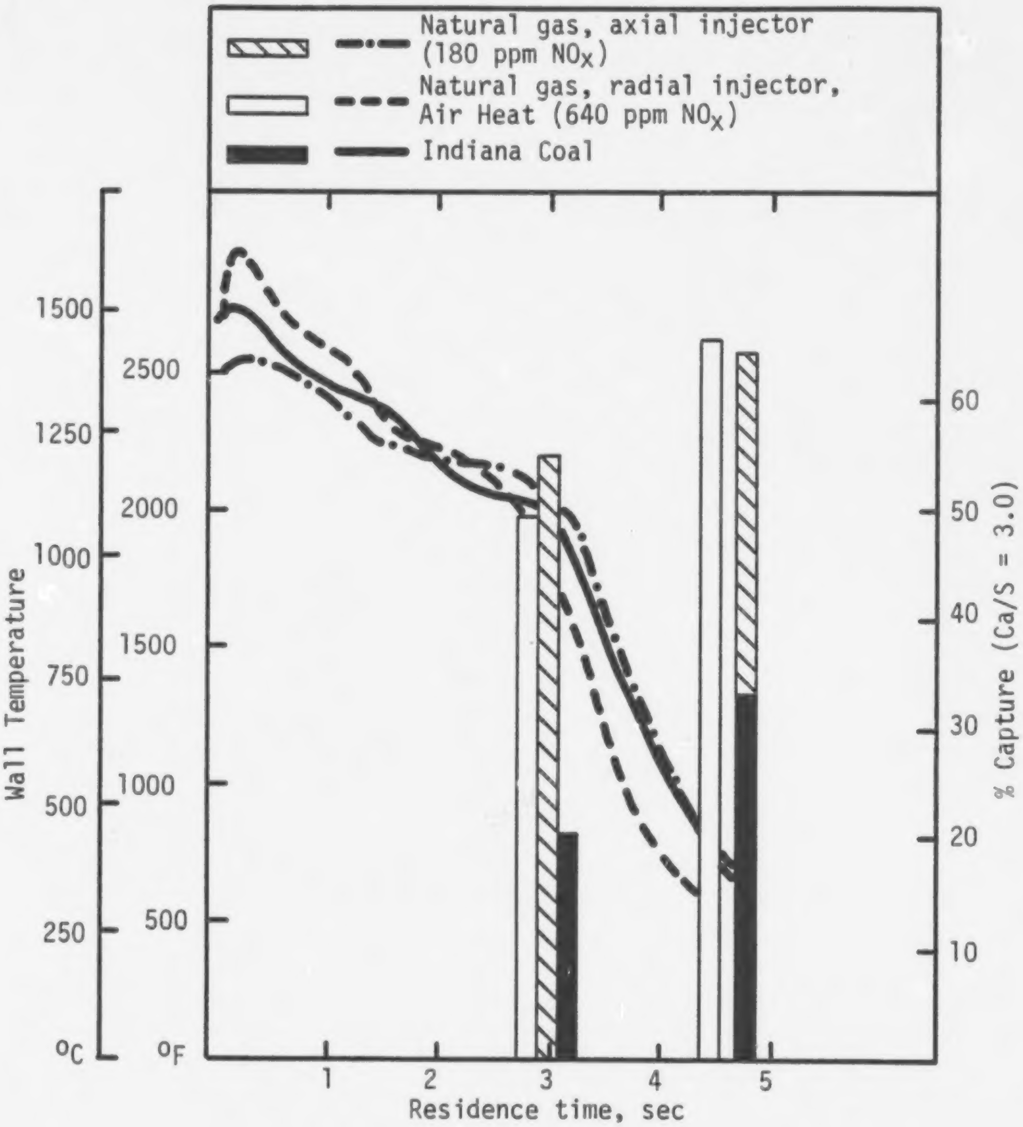

Figure 1-5. Comparison of sulfur capture in high and low temperature gas flames with Indiana coal flame.

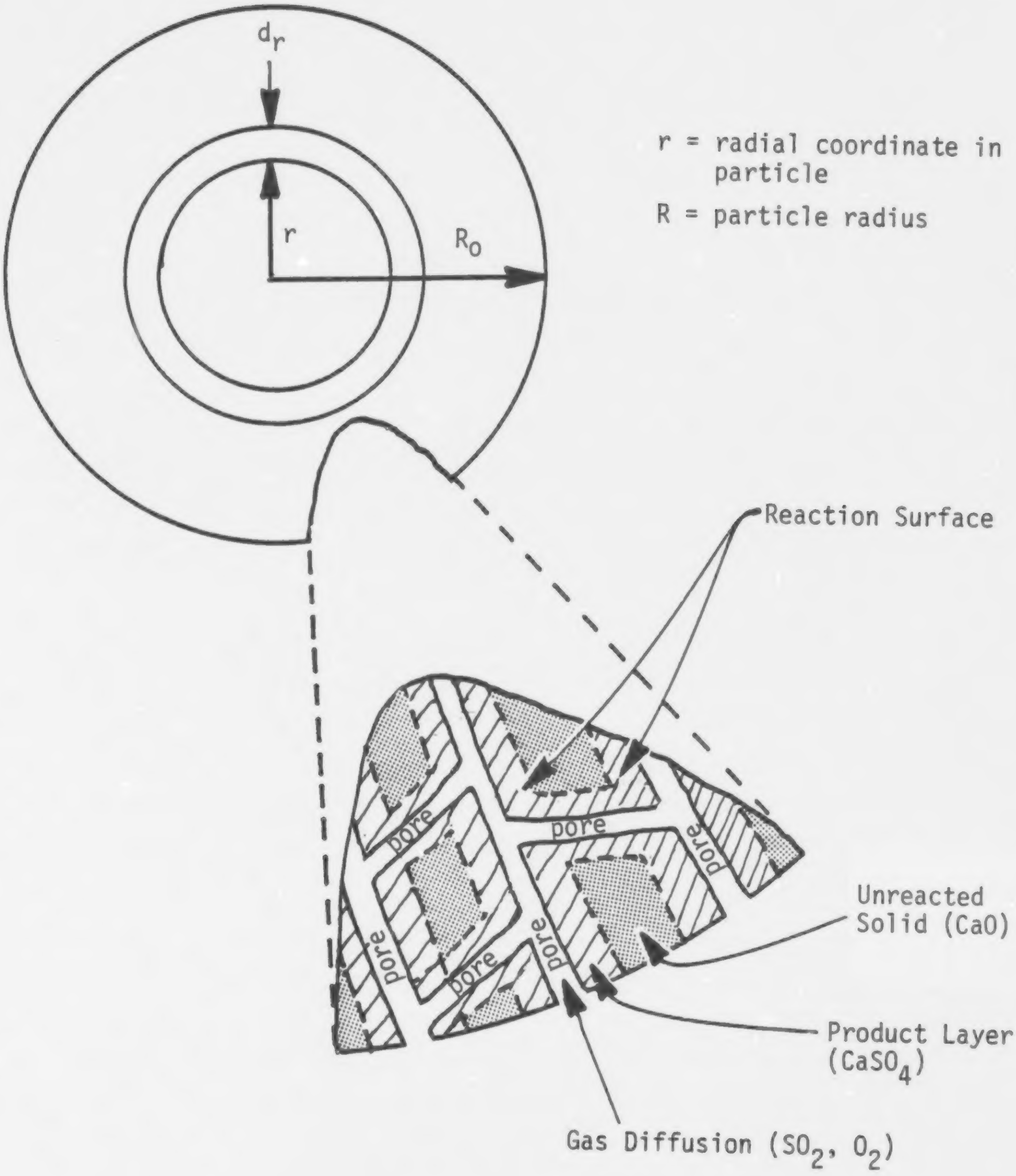
d$_r$
r
R$_o$
r = radial coordinate in particle
R = particle radius
Reaction Surface
pore
pore
pore
pore
pore
pore
Unreacted Solid (CaO)
Product Layer ($CaSO_4$)
Gas Diffusion (SO_2, O_2)

Figure 1-6. Conceptual illustration of pore model for CaO/SO_2 reaction.

1.4 Sulfur Capture Model

The capture of sulfur by solid sorbents injected directly into the furnace is a complex process. Modeling helps to understand and clarify the parameters involved in the sulfur capture process. The general approach has been to divide the process into two zones: sorbent activation and sorbent sulfation. The first zone, sorbent activation, includes the processes which ultimately govern sorbent reactivity and sulfation capacity; these processes include: particle heat-up, calcination, and deactivation as a result of overheating and/or interfering chemical reactions. The second zone, sulfation includes the processes which control sulfate formation including: diffusion within the particle pores, chemisorption, reaction with the solid, diffusion through the reactant layer, blockage of the pores due to sulfate formation, and the thermal stability limits of the sulfate.

The activation portion of the model is basically empirical and was derived from data produced by another EPA Contract (68-02-3633) described in detail by Cole, et al., (1983).

The sulfation portion of the model is based on an approach developed by Bhatia and Perlmutter (1981) which treats the calcined (CaO) particles as spheres enveloping a random distribution of cylindrical pores which provide the overall particle surface areas. The reaction is initiated at the pore surface and a layer of reaction product (calcium-sulfate) forms around the pore. This reaction product layer separates the pore surface and the solid reactant surface. The gas (SO_2) must diffuse through the product layer to the surface of the solid reactant (CaO) where the sulfation reaction takes place. The model scheme for a single particle is shown conceptually in Figure 1-6.

A computer program of this random pore model applied to the SO_2-lime reaction has been coded for use at EER. This computer program was then tested against the original, reference, development of the pore model (Bhatia and Perlmutter); was compared with a grain-type model applied by a group at the University of Utah (Silcox, et al.); and was tested against sulfation data obtained by Borgwardt (1971) with good agreement.

The sensitivity of the model to various parameters including pore-size characteristics, surface area, temperature, calcium-to-sulfur ratio, the selected intrinsic rate constant (derived from kinetic data and subject to some variation in interpretation), sulfate product layer diffusivity and Sherwood number (which influences the SO_2 concentration gradient at the particle surface) was tested. The parameters which had a significant effect on capture were the porosity/pore size/surface area of the sorbent (these are interrelated, see Section 5.2.3) and to a lesser extent, time, temperature, SO_2 concentration and Ca/S ratio.

1.5 Sorbent/Mineral Matter Interactions

There were greater differences in sulfur capture between coal and gas flames than were easily explained with thermal arguments. The possibility of interference by the coal ash or some component of the ash was investigated. Fly ash collected from one of the pilot-scale facilities was mixed with the sorbent (Vicron 45-3) and tested for sulfur capture in a H_2S-doped natural gas flame. The added ash decreased capture by the sorbent significantly. Figure 1-7 summarizes sulfur capture data for plain Vicron and two ash-sorbent mixtures in the gas-fired system.

An interference in sulfur capture by fly ash from a coal-fired system implies a coal sorbent interaction. Fly ash from a coal is, however, considerably different than the mineral matter in the parent coal. The mineral material in the fuel oxidizes, some components vaporize and recondense, others melt. Coal mineral components were, therefore, tested for interferences with injected sorbents. Two common clay minerals were used - Kaolin and bentonite. Figure 1-8 summarizes captures for plain sorbent and for the sorbent mineral mixtures. Both minerals reduced sulfur capture; the Kaolin had the largest effect, decreasing capture from about 50 percent to 10 percent at a Ca/S ratio of two. The bentonite did not decrease capture as much as the Kaolin. Tests mixing dolomite (which gave higher sulfur captures than Vicron when fired with coal) showed a similar effect of mineral material addition. The two additive minerals have different compositions which may account for their different effect on the sorbents. Figures 1-9 and 1-10 show

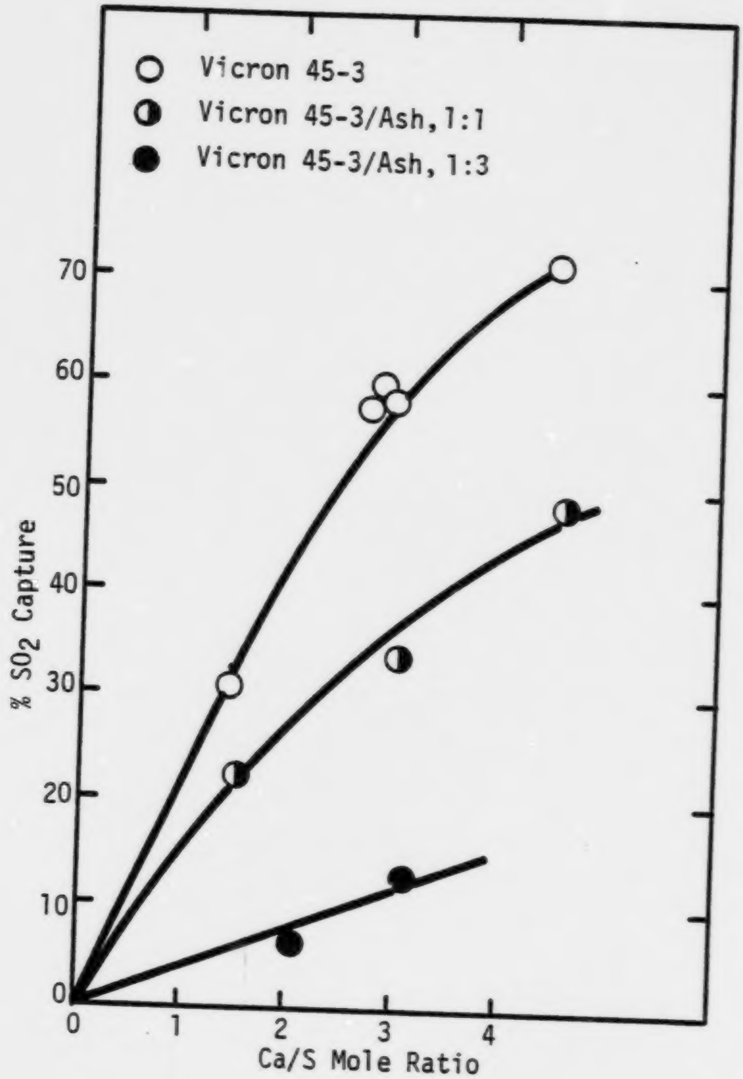

Figure 1-7. Effect of Ash Addition on Sulfur Capture - Vicron 45-3 Plus Fly Ash. Natural Gas/H_2S Flame, DMB, Axial Injector and Sorbent with Fuel.

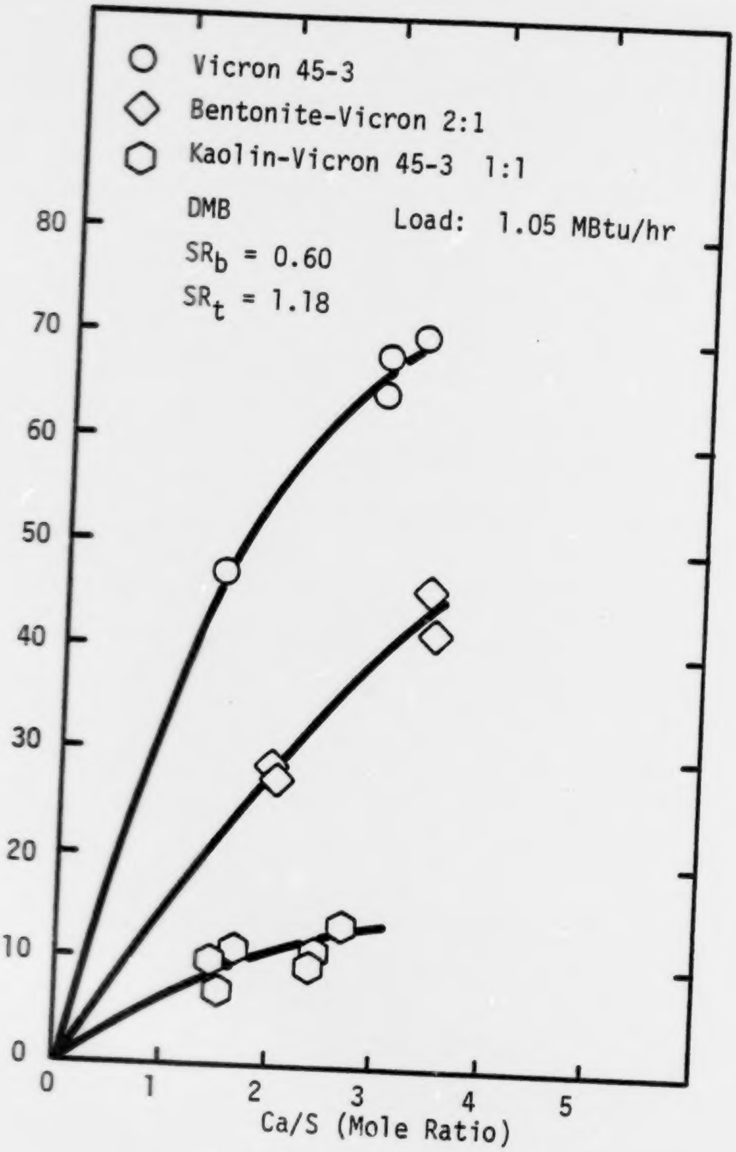

Figure 1-8. Effect of mineral addition on sulfur capture by Vicron 45-3, natural gas/H_2S flame, port #3 (exit convective section).

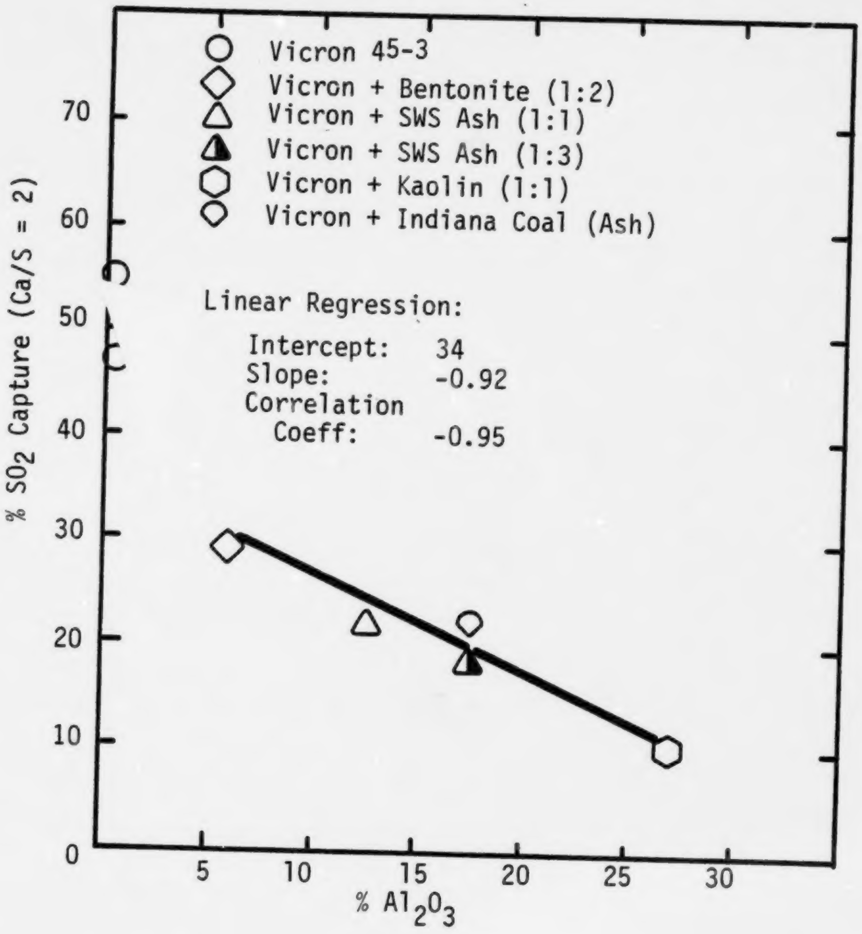

Figure 1-9. Effect of Al_2O_3 content of solid on capture by Vicron 45-3.

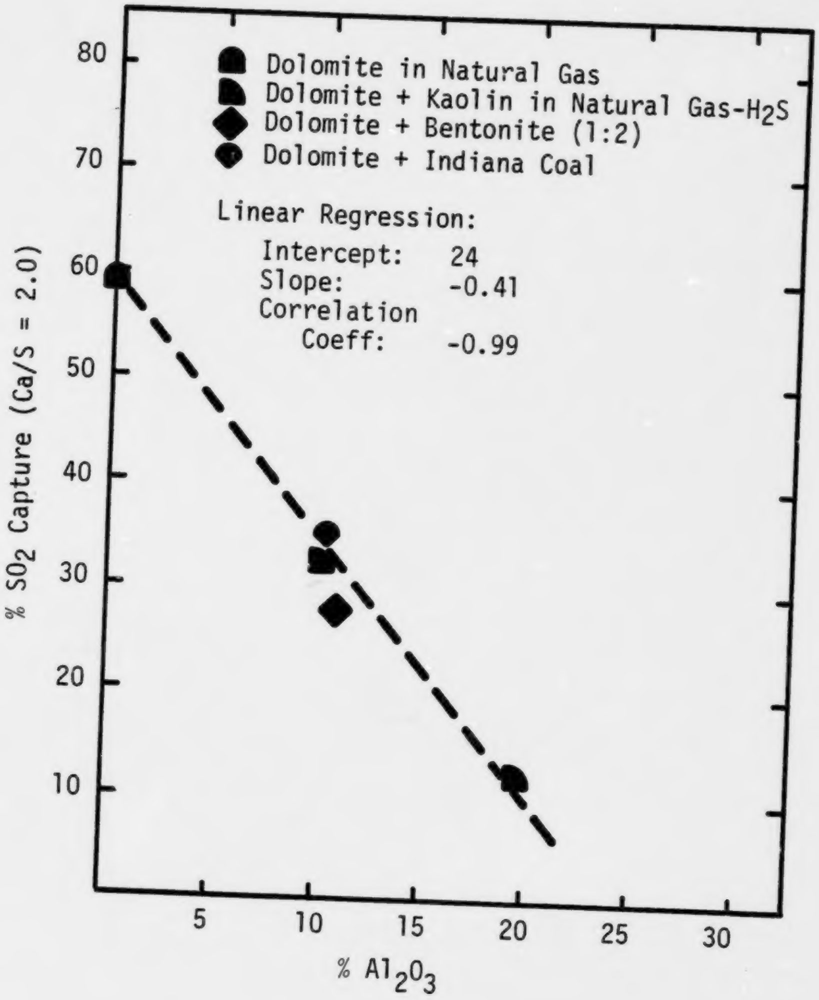

Figure 1-10. Effect of Al_2O_3 content of solid on sulfur capture by Dolomite.

sulfur capture for the various Vicron and dolomite mixtures plotted against the alumina content of the mixture. There is a reasonably good negative correlation between alumina content and SO_2 capture.

The realtive size of the sorbent and Kaolin particles was investigated using two sizes of Vicron limestone and dolomite. Changing the added mineral size had little effect on the decrease in sulfur capture due to mineral material addition for either limestone. The concentration of SO_2 in the natural gas-fired tests had a slight effect on sulfur capture, increasing capture at Ca/S = from 26 percent at 500 ppm to 40 percent at 3500 ppm SO_2. The concentration of mineral matter (correlated as gm Al_2O_3 per dry normal cubic meter of flue gas) in the system had a very strong impact on capture at all of the SO_2 concentration levels and Ca/S ratios tested. At a calcium-to-sulfur mole ratio of 2 and 3500 ppm SO_2 the capture went from 40 percent with no mineral material to 8 percent with 7 gm/DNCM Al_2O_3 in the flue gas.

1.6 Fuel Sorbent Interactions

In order to begin assembling a systematic data base on the effect of fuel and sorbent type on sulfur capture several fuel/sorbent pairs were tested at the same firing conditions in the BSF. All of the fuels and sorbents scheduled for pilot-scale testing at EER under various other contracts were included in the range of BSF tests. Using the same fuels and sorbents in different, well characterized, systems allows some assessment of particular systems effects on sulfur capture.

The sorbents tested included three limestones, two hydrated limes, and a dolomite. Table 1-1 summarizes characteristics of the sorbents used. (There was more than one particle size of some of the sorbents tested.)

Sulfur capture by these six sorbents injected into natural gas/H_2S flame in the BSF is summarized by the data in Figure 1-11. Dolomite gave the highest capture, the Colton hydrated lime gave the lowest capture. Similar data for the baseline Indiana coal (lot 3) is shown in Figure 1-12, again dolomite gave the highest capture and the Colton lime the lowest. Capture for

TABLE 1-1. SORBENT CHARACTERISTICS

Sorbent	Dolomite ◗	SM Carbonate ○	Fredonia C ◺	SM Ca(OH)$_2$ ⌂	Vicron 45-3 ⬡	Colton Lime ◇
Petrographic Charact. Type	Dolomite	---	Calcite	Hydrated Lime	Calcite	Hydrated Lime
Composition	$CaCO_3$ $MgCO_3$	$CaCO_3$	$CaCO_3$	$Ca(OH)_2$	$CaCO_3$	$Ca(OH)_2$
Grain Size μm	---	---	Fine	500-700	---	N.A.
Top Size μm	<100	>100	>100	30	45,40	80
Mean Size μm	34.0,40	16	10	3.5	11,12	12.5
Bottom Size μm	1.0	1.5	0.4	0.3	0.3,0.8	0.7,4
Density gm/cc	2.855	2.76	2.76	2.35	2.757	2.353
Oil Absorption	---	---	---	---	14	---
Surface Area	0.64,0.60	3.42	5.06	13.5,12.1	0.9,0.6	10.4,13.8
Ignition Wt. Loss 1000^{o}C	47.1,44.2	---	43.3	25.3	44.0,41.0	26.4,26.0
SA (1000^{o}C) m^2/gm	9.17	---	1.34	1.64	6.7,3.7	1.86
Hydration Wt. Gain (1000^{o}C)	67.5	---	31.6	---	33.08	33.25
Chemical Comp. (%)						
Ca	21.0	38.9	40.0	51.0	39.2	48.9
Al	0.09	0.09	---	0.26	0.07	0.28
Si	0.37	0.76	---	0.80	0.07	1.08
Fe	0.102	0.09	---	0.22	0.037	0.164
Na	0.033	---	---	---	0.022	0.034
Mg	12.1	0.35	0.74	---	0.485	0.255
K	0.039	---	---	0.51	0.011	0.129
Cr	0.27	---	---	---	0.006	0.005

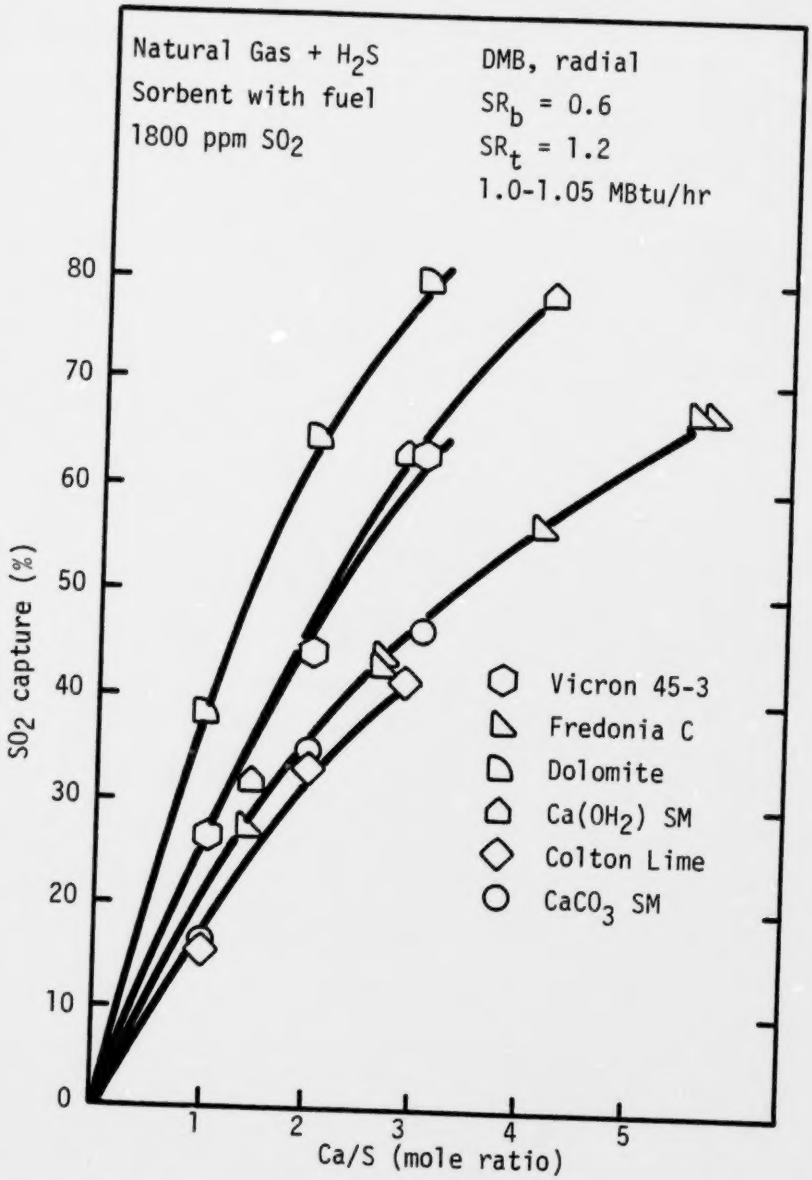

Figure 1-11. Effect of sorbent type, natural gas flame.

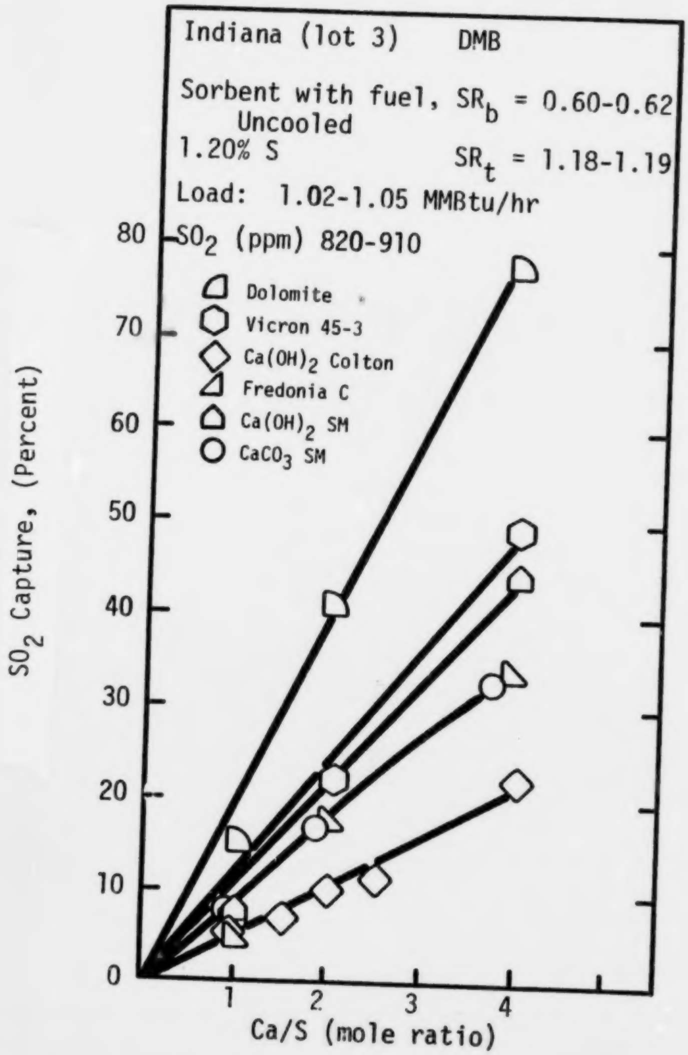

Figure 1-12. Effect of sorbent type on sulfur capture, Indiana Lot 3 coal.

all of the sorbent was lower than with the natural gas H_2S flame. Two other fuels, Utah (a western low-sulfur, sub-bituminous coal) and Illinois (an eastern high-sulfur, bituminous coal) were tested. Dolomite gave the highest capture with these fuels also, and again with the Utah coal the Colton lime gave the least capture.

The effect of the Vicron particle size on sulfur capture with Indiana coal and natural gas is summarized in Figure 1-13a. Increased sorbent particle size slightly reduced capture with natural gas. The effect of sorbent size on sulfur capture was slightly greater with the Indiana coal. The expected effect of particle size on sulfur capture was determined using the sulfation model. Figure 7-13b shows the calculated effect of sorbent particle size and the measured effect with the gas and coal flames. (Data from earlier tests (2667) with Vicroin 15-15 were added to extend the data base.) The calculated values are based on in-situ sorbent size, which is not necessarily the injected sorbent size. Vicron has been demonstrated to fragment when flame calcined. It is very difficult to estimate in-flame particle sizes for the vicrons except to say they are probably smaller than the injected size. The model predicts that particle size has little effect with fine (<10 μm) particles. The natural gas and coal data show the same trend though not as clearly (perhaps in the coal case because of an interaction with the coal mineral matter).

The effect of fuel type and sulfur content on sulfur capture was investigated. Samples of five coals and natural gas were tested with Vicron 45-3, dolomite and a calcium hydroxide under the same general firing and sampling conditions. The fuels used were all fuels scheduled for pilot-scale (10-100 MBtu/hr) testing at EER under various other contracts. Table 1-2 summarizes the characteristics and of the fuels used during these tests.

Vicron 45-3 was tested with four coals, the results of these tests are summarized in Figure 1-14. The figure shows sulfur capture as a function of Ca/S ratio, based on fuel sulfur content and sorbent feed rate. The Utah coal has considerable calcium in the ash so the Ca/S mole ratio including the fuel calcium is also shown. The high sulfur Illinois coal gave the highest capture

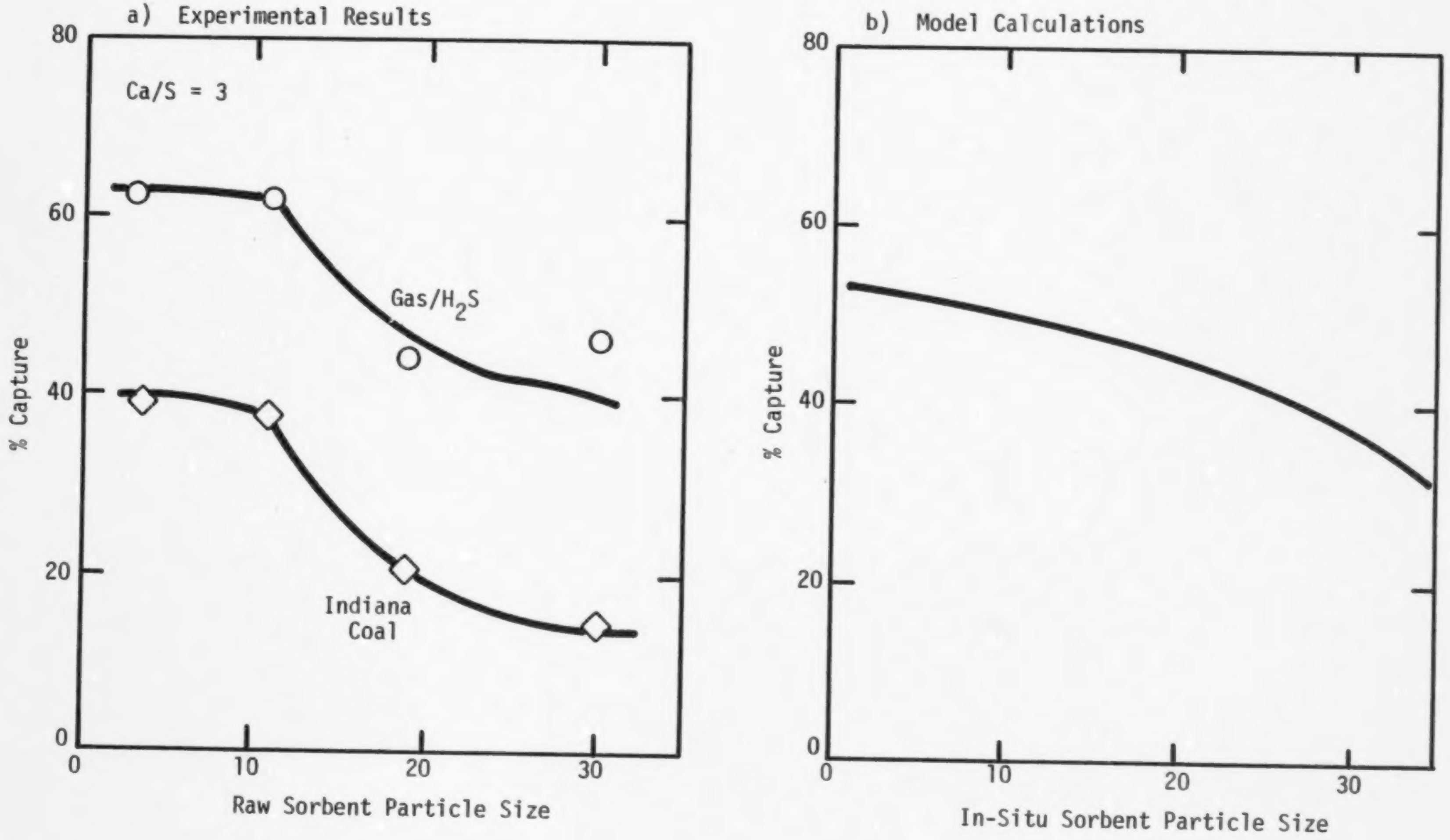

Figure 1-13. Effect of input Vicron particle size on SO_2 capture, comparison of BSF data with model.

TABLE 1-2. FUEL CHARACTERISTICS

Fuel	Indiana L3 ○	Illinois ◇	Utah △	Indiana L4 ◊	Saar ⌂
Proximate (a.r., %)					
Volatiles	29.98	38.22	40.0	32.93	31.37
Fixed C	54.99	46.07	48.48	53.0	59.38
Ash	9.96	9.52	7.62	8.81	7.25
H_2O	5.07	6.19	3.90	5.26	2.0
Ultimate (dry %)					
C	69.65	64.85	69.92	71.65	74.8
H	4.43	4.53	5.07	4.63	4.77
N	1.41	1.23	1.41	1.4	1.21
S	1.15	3.70	0.88	1.37	0.79
O (diff)	12.88	15.54	14.79	12.03	10.55
Btu/lb (dry)	12,721	11,947	12,740	12,188	13,374
Ash Composition (%)					
SiO_2	58.63	52.58	64.06	57.6	44.99
Al_2O_3	23.56	17.62	18.89	23.82	25.0
TiO_2	0.99	0.59	0.78	0.91	0.77
Fe_2O_3	10.26	15.83	4.78	10.28	10.49
CaO	0.95	4.40	5.21	1.37	4.7
MgO	0.36	1.22	0.71	0.73	3.06
K_2O	1.49	2.21	1.16	2.4	3.27
Na_2O	0.22	1.18	0.77	0.45	0.485
SO_3	0.43	4.51	4.95	0.80	5.615
P_2O_5	0.47	0.28	0.43	0.29	0.175
Ash Melting pts					
(°F, red.) IDT	2360	2035	2240	2400	2235
AFT	2590	2070	2380	2540	2360
HT	2615	2240	2480	2630	2450
FT	>2700	2380	2700	>2700	2555
(°F, oxi.) IDT	2600	2250	2320	2520	2317
AFT	>2700	2340	2440	2680	2405
HT		2460	2520	>2700	2490
FT		2540	2700	>2700	2600
Forms of Sulfur (a.r.)					
Pyrite	0.3	0.5	0.1	0.3	0.37
Sulfate	0.41	2.3	0.6	0.4	0.46
Organic	0.33	0.6	0.1	0.5	0.02
Total	1.09	3.4	0.8	1.2	0.78

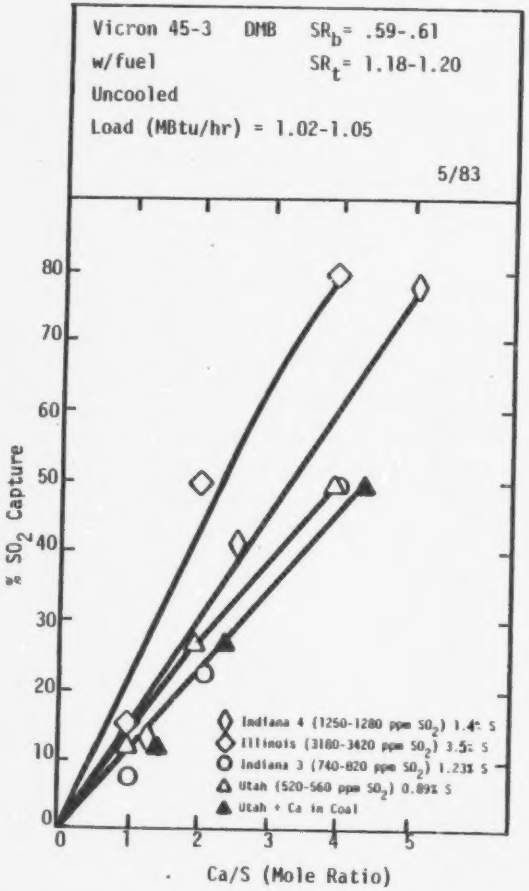

Figure 1-14. Effect of fuel on sulfur capture and thermal history of Vicron 45-3 w/fuel.

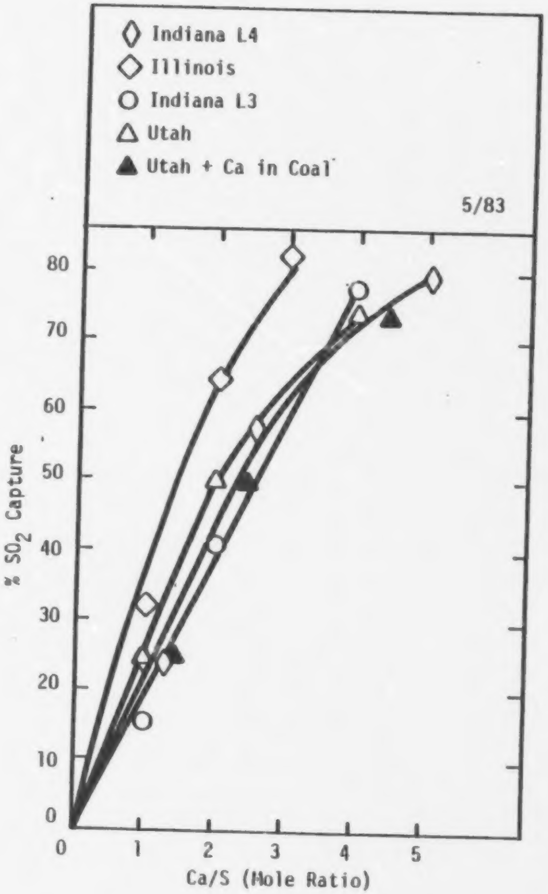

Figure 1-15. Effect of fuel on sulfur capture and thermal history of Dolomite, sorbent w/fuel.

while Utah and Indiana (lot 3) gave the lowest. Sulfur capture data for dolomite with the sample four fuels is shown in Figure 1-15. Again, the high-sulfur Illinois coal gave the highest capture, though the difference was not as striking as with the Vicron 45-3.

The effect of sorbent type on capture with a given fuel was dependent on the firing conditions - including sorbent injection location and thermal conditions. The hydrated limes seemed to be most sensitive to thermal conditions and the Vicron least sensitive. The German hydroxide gave better capture than the Colton hydroxide - it was not clear why the two stones had different captures. Dolomite give the highest capture with all of the fuels tested.

The effect of fuel type on capture with a given sorbent was also system (injection method, firing characteristics and thermal conditions) dependent. Capture with natural gas was higher for all of the sorbents than with coal - due, in part, to deactivation of the sorbent by coal mineral matter.

1.7 Downstream Sorbent Injection

One of the most interesting results of earlier experiments (2667) in the BSF was the effect of physical staging on sulfur capture. The BSF can be fired in two general modes: internally staged, or DMB (Distributed Mixing Burner), where all of the combustion air is added at the burner face, through the main burner and the tertiary air ports; and physically, or externally staged, where part of the combustion air is added downstream at the base of the post-flame section. A schematic of the BSF is shown in Figure 1-16. Staging air addition at location A is internal staging, air addition at location B is physical staging.

When the furnace was fired in the internally staged mode, capture by Vicron injected at the burner was rather low. When the furnace was externally staged and sorbent was added with the staging air captures were considerably higher. The increase in sulfur capture with downstream sorbent injection could be due to the different thermal environment experienced by the sorbent

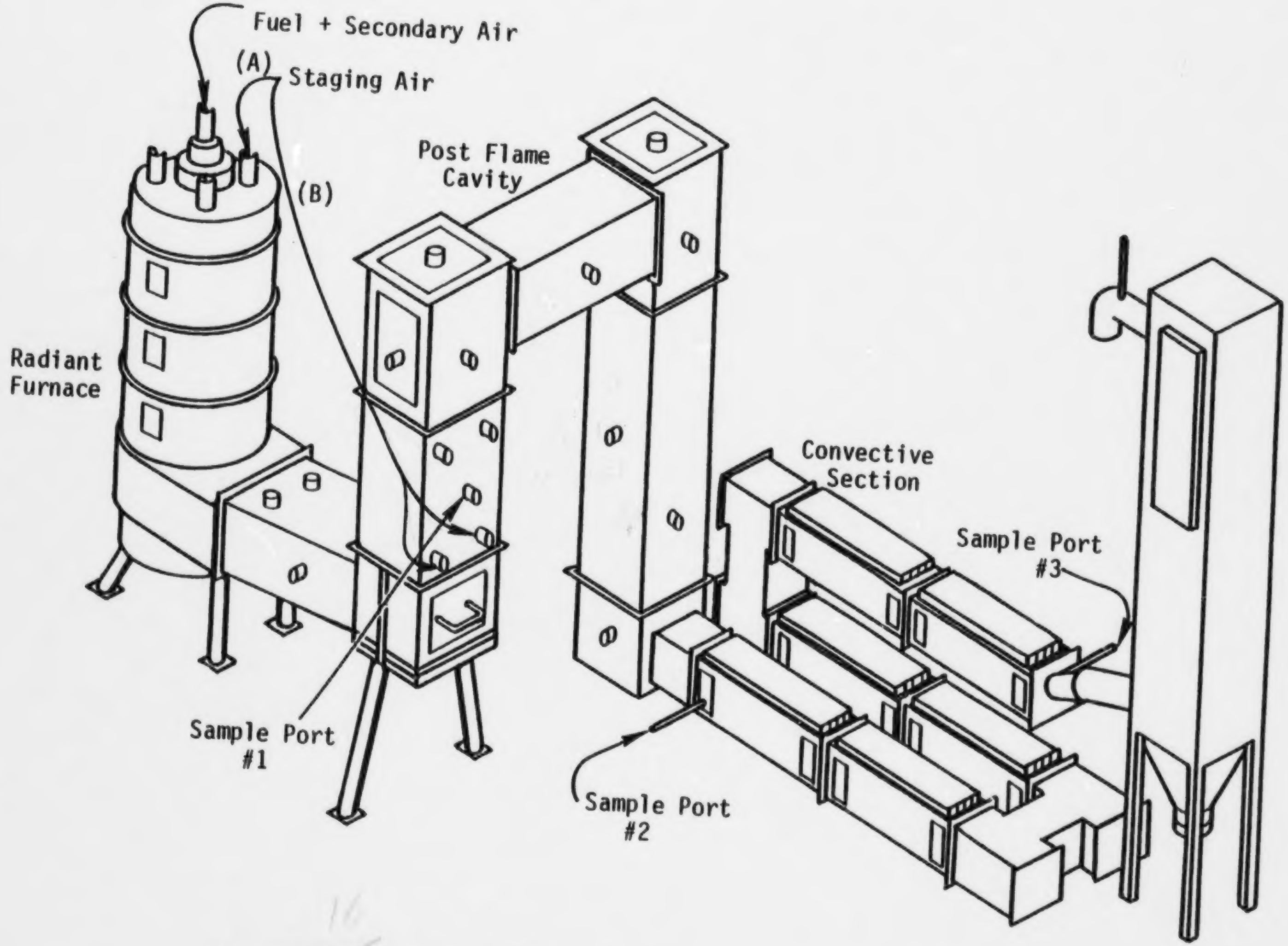
Fuel + Secondary Air
(A)
Staging Air
(B)
Post Flame Cavity
Radiant Furnace
Convective Section
Sample Port #3
Sample Port #1
Sample Port #2

16

Figure 1-16. Boiler simulator furnace.

or to a decrease in the effect of coal ash on the sorbent. In order to further explore downsteam injection and to assess the effect of fuel sorbent interactions in this firing configuration, downstream injection tests of four sorbents with Indiana (lot 3) coal were performed. Three of the sorbents had been used earlier in physically staged experiments. The results of the sorbent injection tests are summarized in Figure 1-17. The figure also shows the earlier data for comparison. In general, the data were repeatable and captures were higher than fuel injection for all of the sorbents.

The difference in capture for the two sorbent locations when firing Indiana (lot 3) and Utah coals is shown by the data in Figure 1-18. Downstream injection gave slightly greater improvement for the Indiana coal.

Downstream sorbent injection results in a different sorbent thermal history as well as different sorbent mineral material contacting. The improved capture may be due to either difference, both were explored.

The coal-fired system was simulated using natural gas doped with H_2S. Kaolin was added to simulate the mineral material of the coal. Sorbent was added to either the fuel or downstream at the post-flame cavity. Figure 1-19 shows captures for dolomite and Vicron in the fuel with and without Kaolin; Figure 1-20 shows similar data for the two sorbent injected downstream. The Kaolin had a much greater impact on capture when the sorbent was injected with the fuel. This result implies that part of the injection location effect when coal firing is due to a change in the mineral matter interference.

Sorbent samples were taken at the top of the post-flame cavity when firing natural gas and injecting sorbent either with the fuel or at the base of the post-flame cavity. For all of the sorbents tested, the sorbent surface area at the sample point was higher when it was injected at the base of the post-flame cavity.

The physical characteristics of the solid samples were investigated using high-resolution scanning electron microscopy (SEM). The SEMs show particle morphology, information on the composition of particular particle may also be

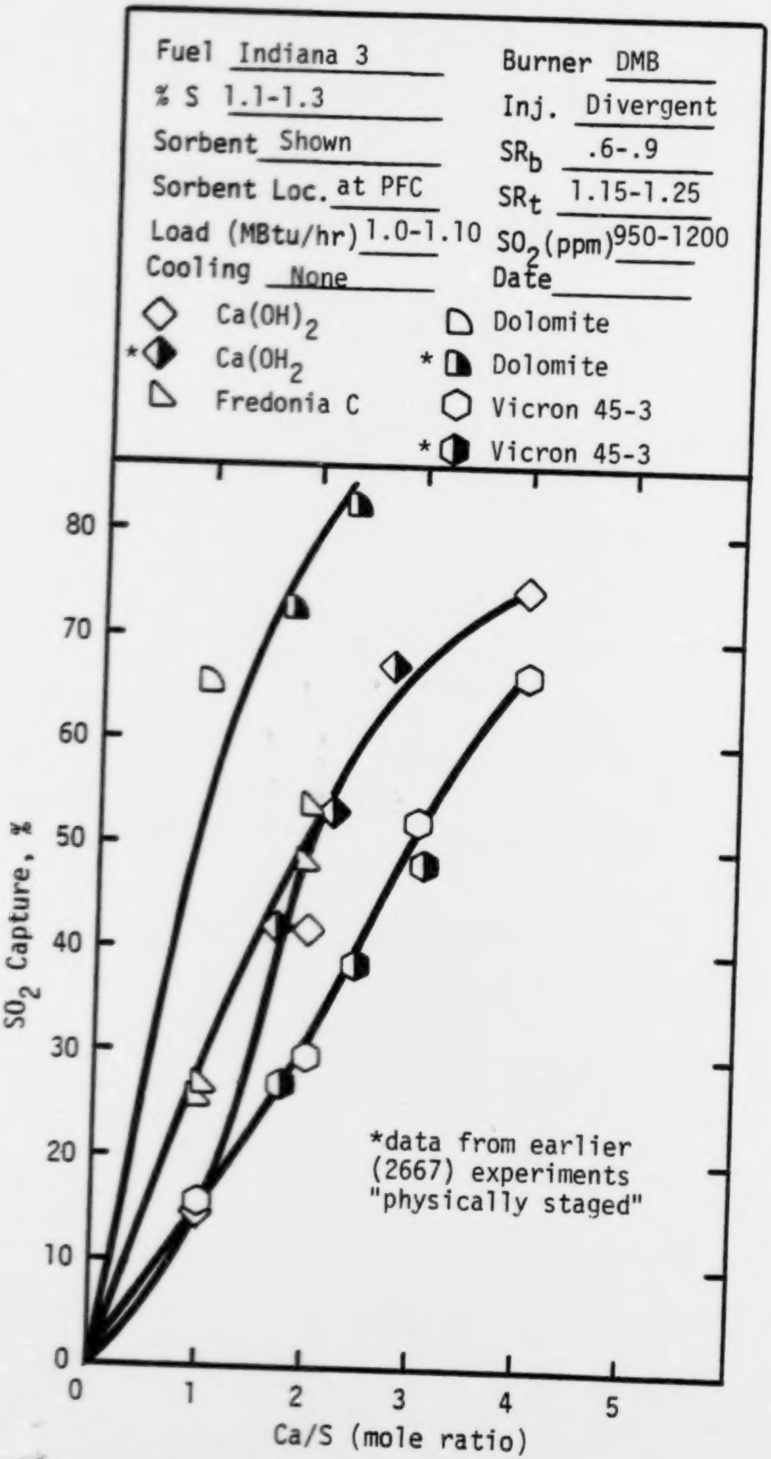

Figure 1-17. Effect of sorbent type on sulfur capture - downstream injection, Indiana L3 coal.

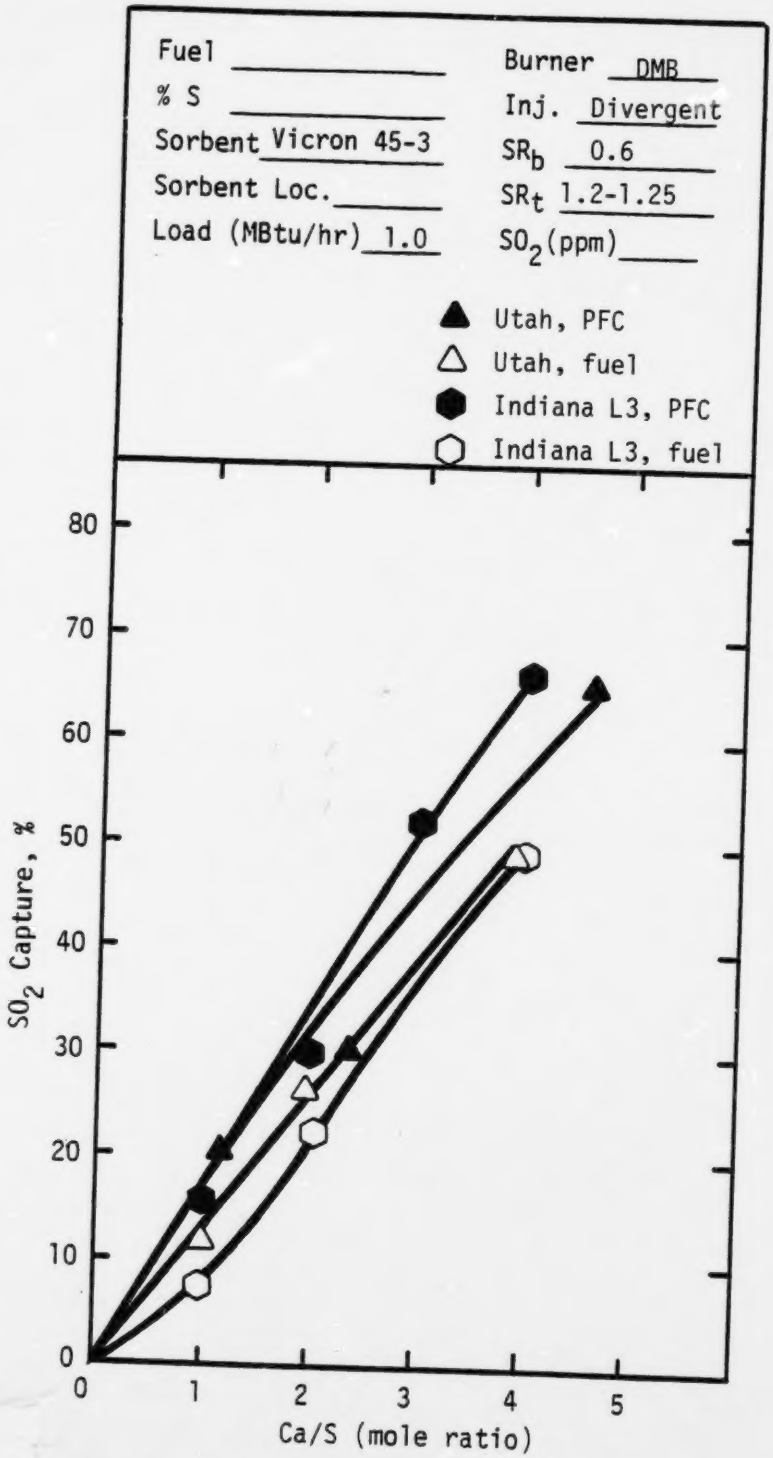

Figure 1-18. Comparison of Sorbent Injection Location, with Utah and Indiana Coal, Vicron 45-3.

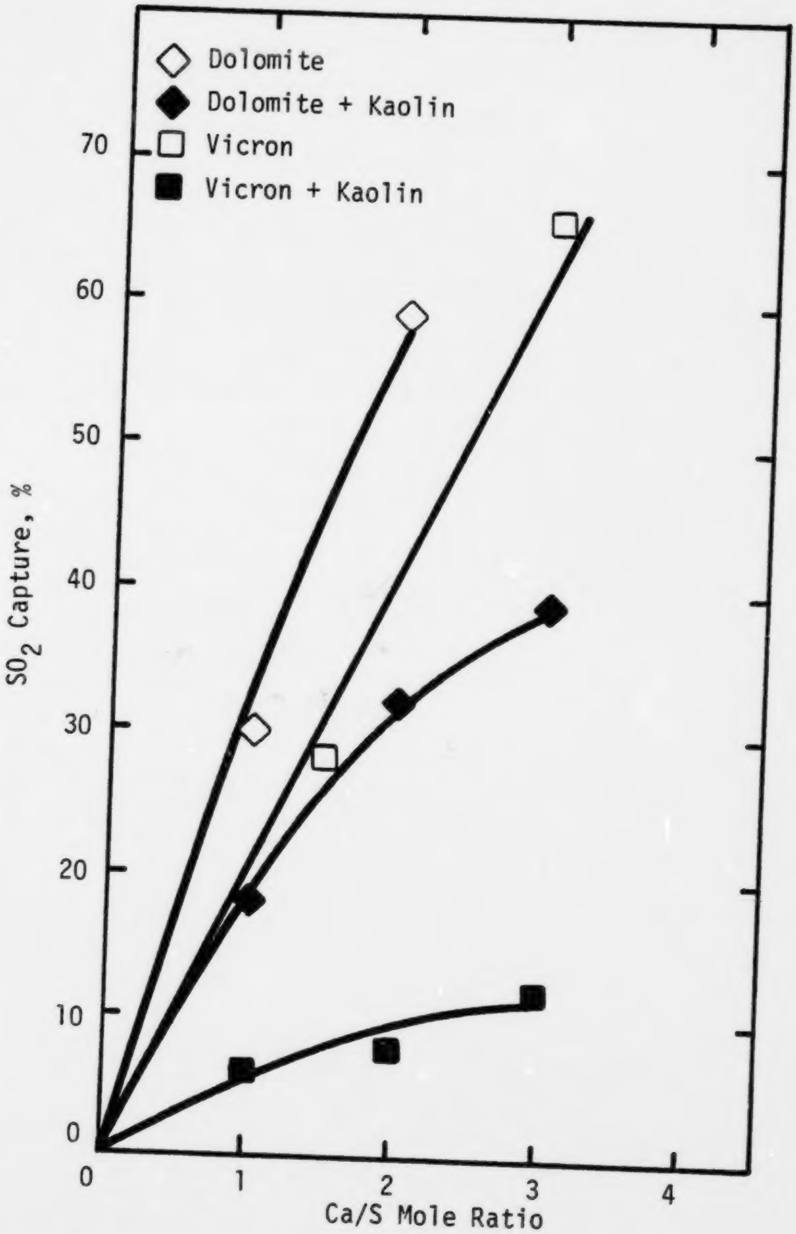

Figure 1-19. Effect of Kaolin addition, sorbent and Kaolin with fuel, natural gas + H_2S-firing.

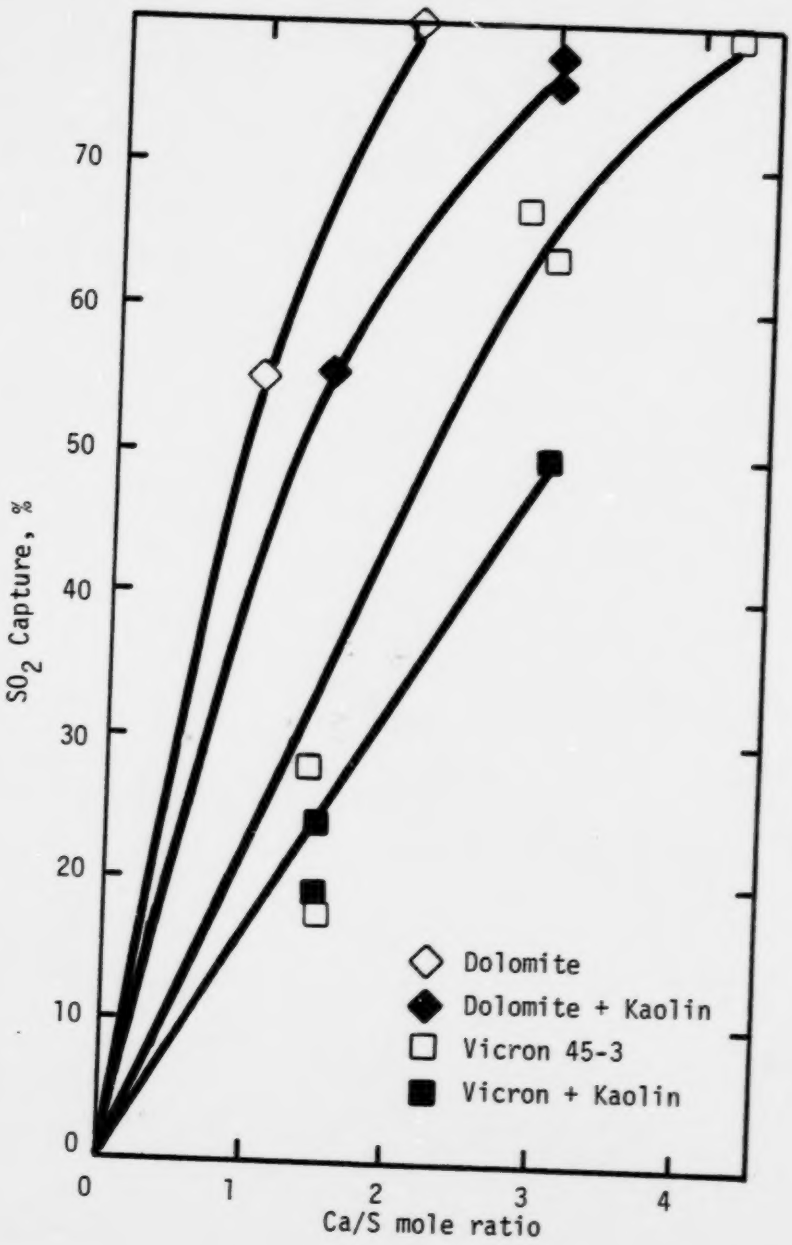

Figure 1-20. Effect of Kaolin Addition to Fuel, Sorbent Injected in PFC. Natural Gas + H_2S-Fired.

obtained. Figure 1-21 shows SEMs of solid samples taken from natural gas/ Kaolin flames with Vicron added. In photo 1-21a the sorbent and Kaolin were mixed and injected with the fuel, in Figure 1-21b the Kaolin was injected with the fuel and the sorbent was injected downstream. The particles in from the mixed Kaolin/Vicron injection are typically spherical and analysis indicated they are made up of various proportions of Al/Si/Ca. (Kaolin is $Al_2O_3 \cdot 2SiO_2$ and Vicron is essentially pure CaO.) When the sorbent was injected downstream, discrete irregular sorbent particles mixed with smooth, spherical, melted Kaolin particles can be easily identified (see 1-21b).

Samples of Indiana coal ash with Vicron 45-3 injected with the fuel or downsteam show characteristics similar to the Kaolin/Vicron in natural gas samples. Scanning electron micrographs of the two samples are shown in Figure 1-22. Figure 1-22a shows many fused spherical particles which, when analyzed, are composed of Ca, Al, Si, Fe and other typical ash metals. There are essentially no irregular high surface area sorbent (nearly pure Ca) particles in the field. In contrast, two types of particles can be seen in the micrograph of the "downstream-injection" samples: irregular sorbent particles and smooth mineral ash particles.

1.8 Furnace Thermal and Capture Modeling

The primary objective of Task 3 was to investigate scale effects on the performance of systems designed for the simultaneous reduction of NO_x and SO_x emissions. The temperature history of gases and particles is a key factor in the capture of sulfur compounds. However, reliable information on time/ temperature profiles in large-scale systems is, at best, fragmentary. Even in experimental systems data is seldom taken in such a manner that comprehensive scale relationships can be observed. A model is necessary to fill in the gaps between data points to obtain the detailed temperature/flow field map necessary to track particles through a furnace. Such a model allows the experimenter to rationalize sulfur capture data, to explain observed trends in terms of the effects of parameters and scale, and to extrapolate data to different and larger-scale systems.

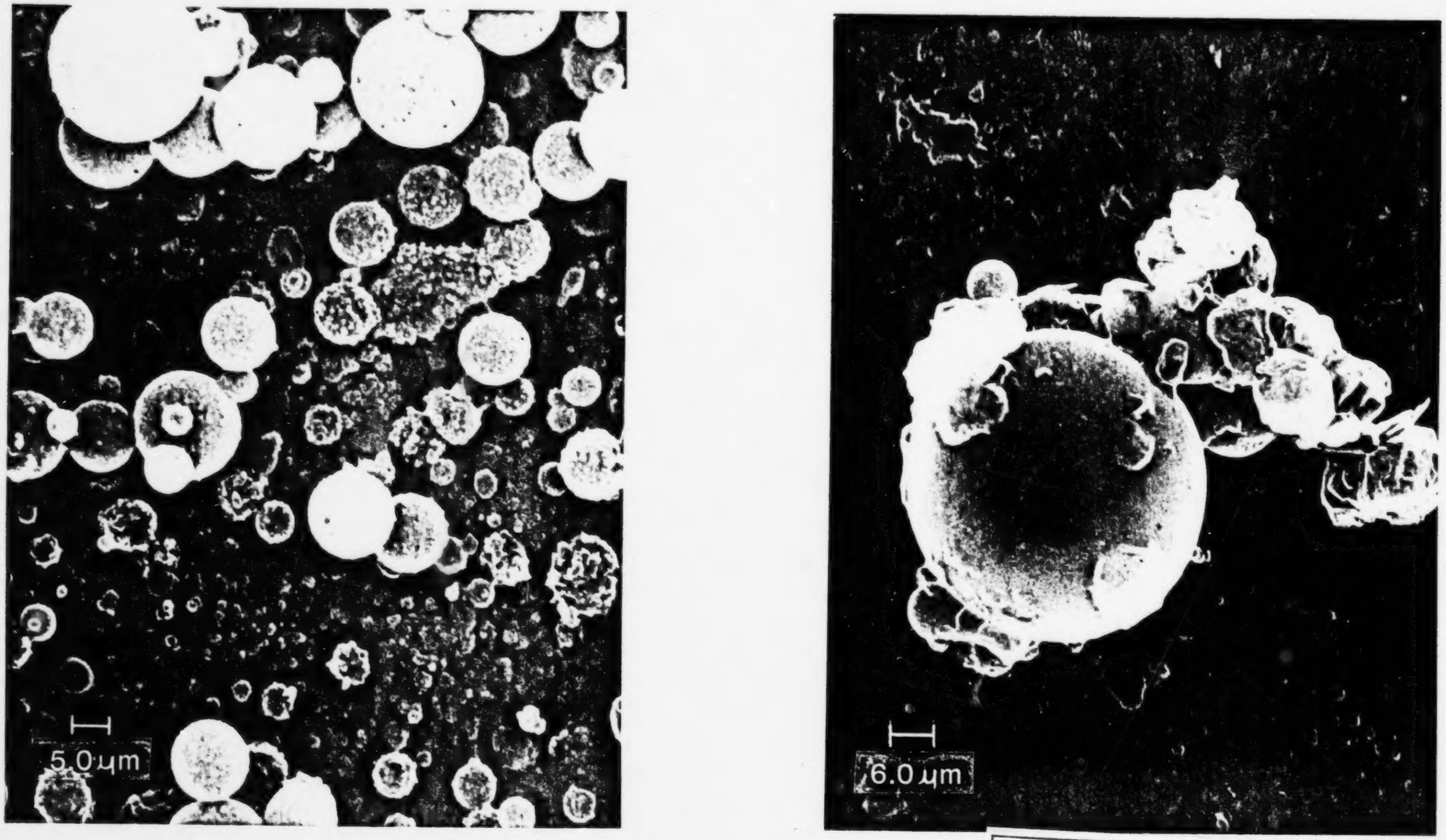

Reproduced from
best available copy.

a) Vicron and Kaolin with Fuel

b) Kaolin with Fuel, Vicron Downstream

Figure 1-21. Scanning electron micrographs of Vicron and Kaolin in natural gas flame.

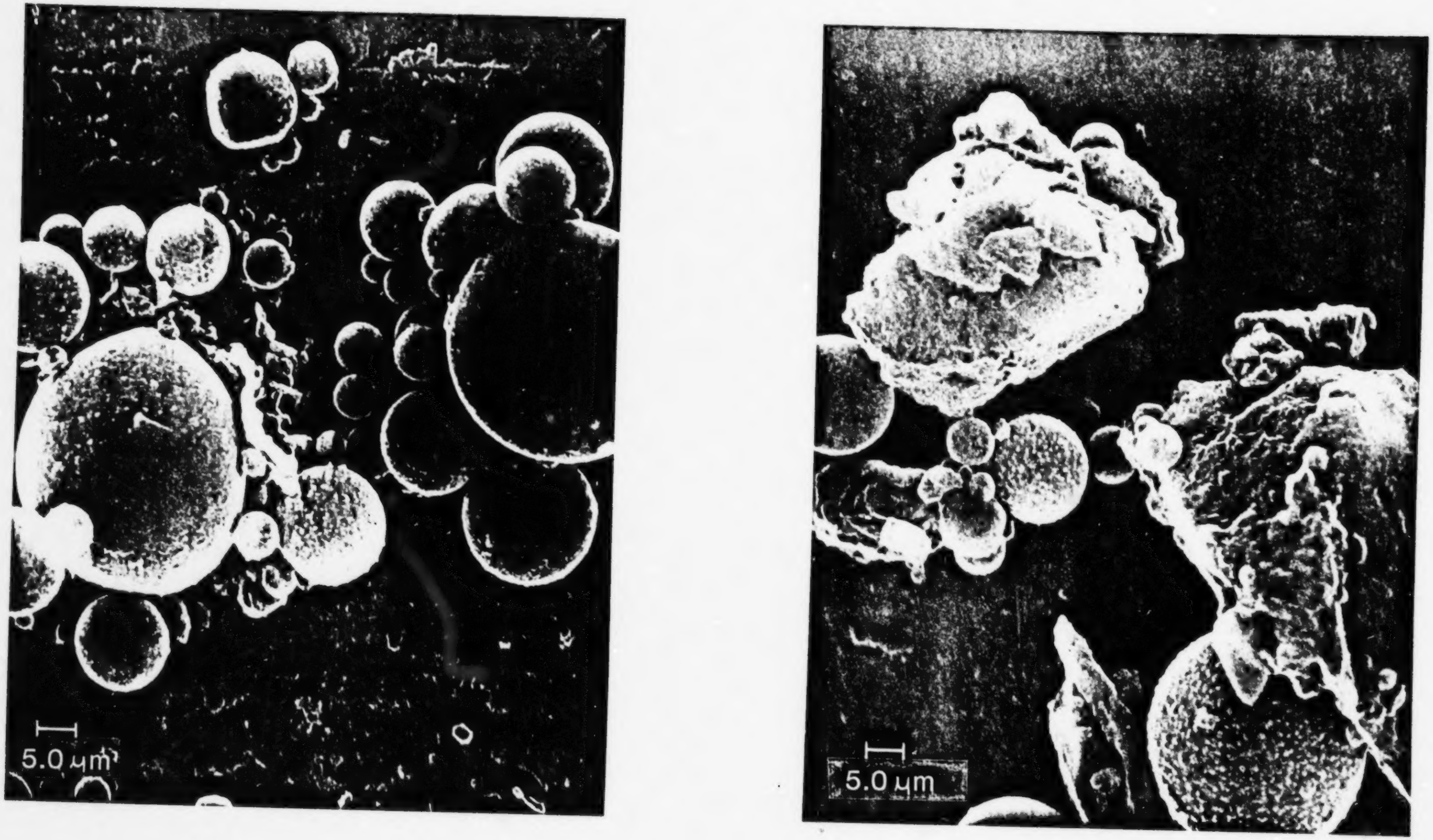

a) Vicron Injected with Fuel

b) Vicron Injected Downstream

Figure 1-22. Scanning electron micrographs of Indiana coal with Vicron.

The modeling work included the use of a sulfation model (discussed earlier), the thermal modeling of three experimental facilities at EER, and the coupling of the two models to predict SO_2 capture. An existing boiler performance code, developed by Wolfgang Richter at EER was used for the thermal modeling. The code allows predictions of local and overall heat transfer and fuel burnout in boiler combustion chambers and industrial furnaces. The results are dependent on furnace geometry and operating conditions, characteristics of fuel and characteristics of wall deposits. The flow pattern within the furnace and the distribution of heat release due to combustion of volatile or gaseous fuel species is prescribed. Predictions of local furnace variables include:

- Gas temepratures;
- Incident and net radiative and total heat fluxes to heat sink surfaces;
- Temperatures of refractory walls and wall deposits;
- Burnout of solid fuel particles of up to ten size classes;
- Equilibrium concentrations of major gaseous species corresponding to the progress of fuel burnout;
- Complete time/temprature histories of real or imaginary tracer particles or material within the furnace;
- Time dependent representation of all considered dependent variable, if requested.

There are two and three-dimensional codes available at EER; the three-dimensional code was used to model the LWS and the two-dimensional code was used to model the axi-symmetric SWS and MT furnaces. Figure 1-23 shows a typical predicted temperature map of one section of the LWS.

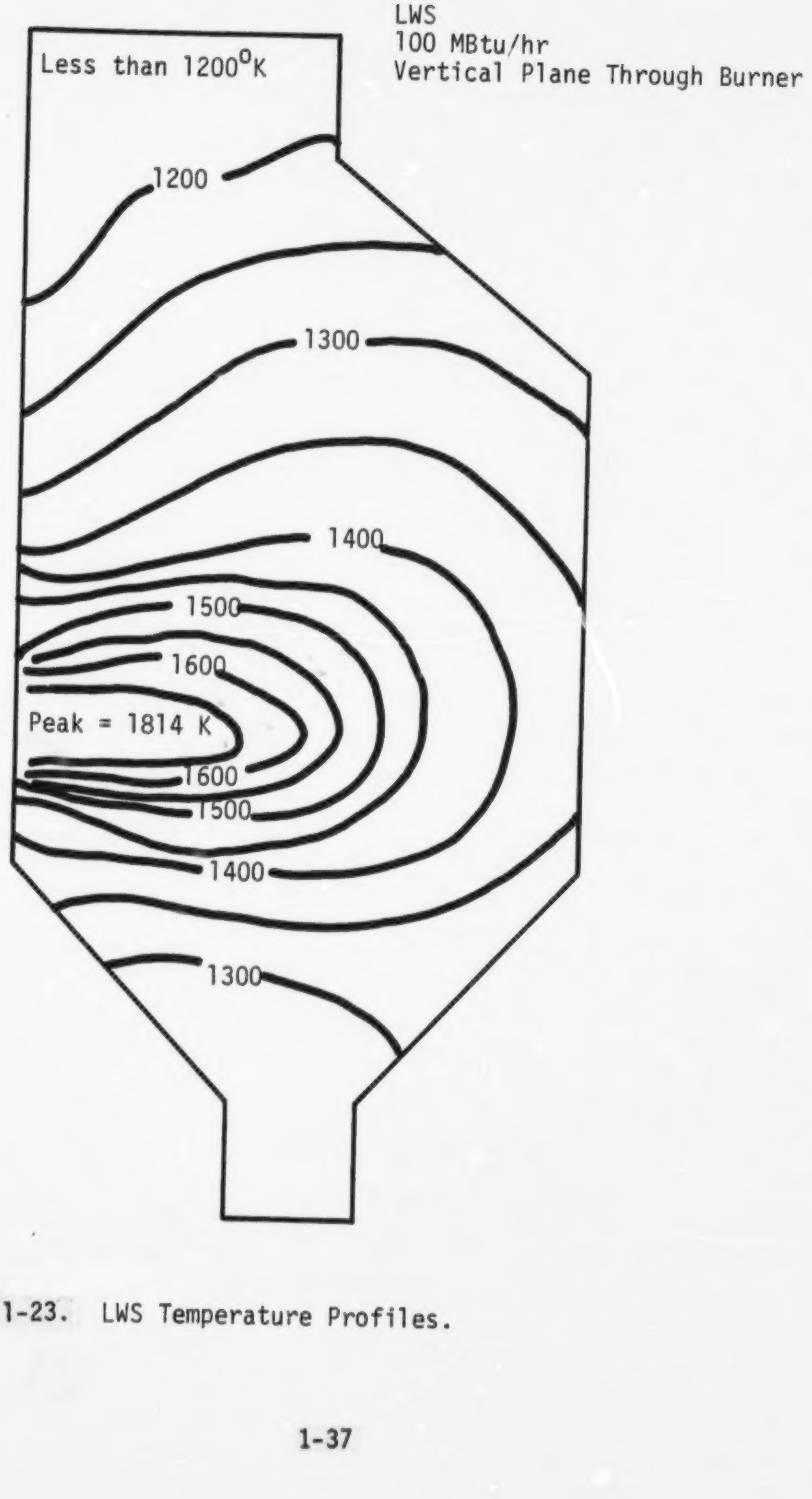
LWS
100 MBtu/hr
Vertical Plane Through Burner
Less than 1200°K
1200
1300
1400
1500
1600
Peak = 1814 K
1600
1500
1400
1300

Figure 1-23. LWS Temperature Profiles.

Combined thermal sulfation modeling consisted of the following steps:

- The furnace heat transfer model was used to produce a temperature/flow map of the furnace.
- A large number of particles were tracked through the furnace, passing from zone to zone at random, weighted by the gas flow.
- The distribution of peak particle tempertures was used to calculate a mean particle surface area according to the sorbent activation correlation.
- The mean temperature and the mean residence time were used to calculate sulfation according to the sorbent sulfation model.

The combined thermal/sulfation modeling approach was used on the SWS, MT, and LWS furnaces. The importance of assumptions inherent to the approach was investigated, and the results from the three furnaces were compared with each other and with results obtained applying the sulfation model to measured temperature profiles on the BSF.

Effects of scale were investigated by comparing sulfur capture predictions for the four furnaces under baseline conditions for sorbent injection with the fuel . Results are shown in Figure 1-24. The three parameters which primarily affect sulfur capture are temperature, surface area and residence time. Averaging techniques were used to estimate these three parameters for each furnace. The predicted sulfur capture of 44 percent for the LWS was highest due to its long residence time and high surface area which more than offset its low mean temperature. A fairly high sulfur capture of 39 percent was predicted for the MT. This is due to its high mean temperature, and relatively flat temperature profile resulting in a fairly high surface area. The SWS had a predicted sulfur capture of only 23 percent. Its average temperature was cool, but its peak temperatures were not, so its mean surface

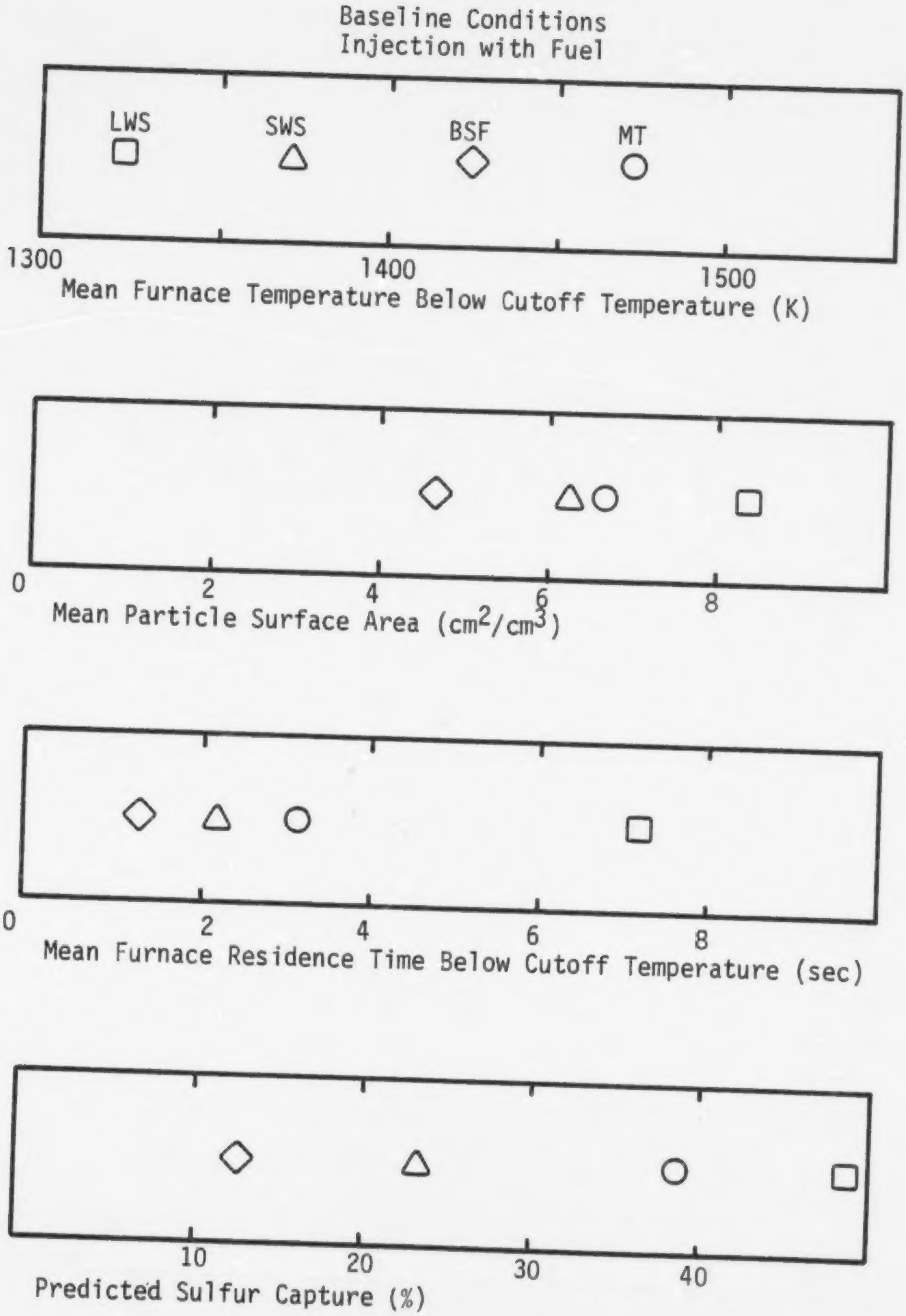

Figure 1-24. Furnace Comparison.

area was not high. The 13 percent capture predicted for the BSF was the lowest. The BSF had highest peak temperature resulting in the lowest surface area and it had the shortest residence time.

1.9 System Effects

Although the LIMB process is conceptually simple, sulfur capture can be affected by so many variables that actual analysis of the process and prediction of results is very complex. In addition to the effects due to fuel and sorbent characteristics, sorbent location and injection method and furnace operating conditions, the firing/boiler system itself has an effect on sulfur capture. System effects are due to different thermal, mixing and residence time characteristics of different facilities. The effects of these variables are difficult to separate, although judicious application of modeling procedures is of some help.

A comparison of the LWS and BSF systems can be made by comparing data obtained from similar firing schemes using the same fuel and sorbent. Figure 1-25 a and b shows such a comparison. The LWS was fired at 100 MBtu/hr using the subscale distributed mixing burner, staged with Vicron 45-3 injected with the fuel. Figure 1-25a shows sulfur capture by Vicron 45-3 as a function of Ca/S ratio for two coals in the two furnaces. The Indiana (lot 4) coal had 1.9 percent S and the Utah coal had .9 percent S.

In earlier pilot-scale studies, multiplying the calcium-to-sulfur ratio by the square root of the coal sulfur content was effective in eliminating some of the apparent effect of fuel sulfur content on sulfur capture (Payne, et al. 1983). Figure 1-25b shows this correlation applied to the BSF and LWS data. Data from the BSF with the two fuels becomes very comparable while the fuel effect in the LWS is exaggerated. Clearly some property or set of properties of the two systems, aside from fuel or fuel sulfur content has an effect on sorbent injection performance.

The analysis performed on the two systems using thermal and sulfation models (Chapter 9) indicated that all other things being equal (fuel sorbent

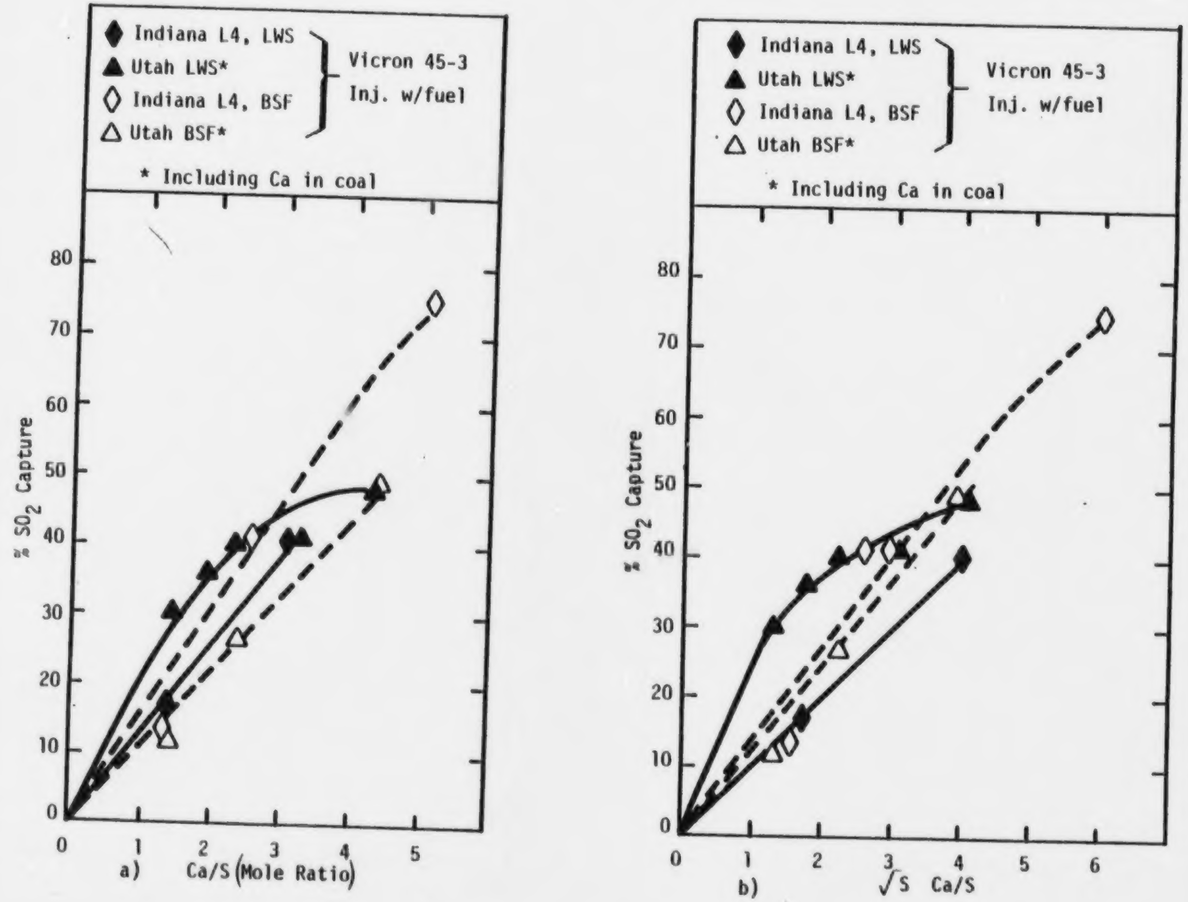

Figure 1-25. Effect of firing system on sulfur capture, Vicron 45-3 with two fuels in LWS and BSF.

interactions, ash interference, mixing, etc.) injection of Vicron 45-3 with the fuel should give higher capture in the LWS than in the BSF. This appears to be the case for the Utah coal, but not for the Indiana. The modeling/analysis method cannot take account of ash and/or sorbent distribution effects. This may account for the difference between observed and expected system effects.

1.10 Effect of LIMB Boiler Operation

All of the results to date, in both pilot-demonstrations and in smaller-scale work such as the BSF experiments indicate that injecting sorbent into the boiler will affect the boiler operating characteristics. Increases in fouling rates and convective section plugging have been documented. Limestone injection may affect both slagging characteristics (decreasing or increasing ash fusion temperatures depending on the original fuel characteristics) and the hardness of fouling deposits. Limestone injection may affect flame characteristics - changing emissivities, flame and/or wall temperatures - but such effects have not been studied.

Particulate removal systems will be affected by changes in solids loading and size distribution and in fly ash resistivity and flue-gas SO_3 content. All of these effects have been observed and general trends can be predicted-such as increased resistivity and fouling - but the data base needed to predict the particular effects of LIMB on the operation characteristics of a given boiler is simply not yet available. More experience with limestone injection in various systems is required in order to begin assessing acutal effects on operating systems.

1.11 Conclusion and Recommendations

The overall goals of this research were the clarification of the processes which control sulfur capture by dry sorbents injected directly into a pulverized coal fired system, and the development of methods for generalizing data from one test furnace to another and from test facilities to fired application.

The experimental portion, carried out in the BSF, included investigation of:

- The effect of fuel type and fuel mineral material on sulfur;
- The effect of sorbent type on sulfur capture;
- Detailed temperature and species characteristics of flares which gave significantly different sulfur captures;
- The effort of operational characteristics such as fuel injector, burner zone stochiometry, peak flare temperature, and load on sulfur capture;
- The effect of sorbent injection location;
- and the effect of LIMB on various furnace operational characteristics such as slagging, fouling, solids loads and size distribution and fly ash resistivity.

The analytical portion included the development of a computer code to model sulfur capture by sorbents and the application of an existing boiler performance/heat transfer code to model facilities at EER, providing a prediction of thermal characteristic.

Conclusions from the experimental portion of this work include:

- The observed fuel effect, whch gave much lower captures for coal fired sorbent injection experiments than for gas fired experiments, has been shown to be a result of deactivation of the sorbent by fuel mineral material.
- A reasonably good correlatlion between solid (sorbent/ash) sample alumina (Al_23) content and sulfur capture has been observed; the

more alumina in the solid the lower the capture, using either Vicron or dolomite.

- Sulfur capture for the fuels tested with Vicron 45-3 and dolomite also showed a fairly consistant inverse correlation with the calculated $A/_2O_3$ content of the ash sorbent mixture (at a Ca/S=2.0).

- Electron micrographs of sorbent mineral samples taken from the BSF show particles composed of a mixture of Al/Si and Ca. The particles are spherical and have been molten at some point in the furnace. The mechanism of mineral deactivation and formation of these spherical particles is not clear and should be the subject of further investigation.

- Electron micrographs of coal/sorbent samples also showed spherical particles composed of calcium and ash minerals such as Al, Si and Fe.

- The concentration of SO_2 in the natural gas-fired tests had a slight effect on sulfur capture, increasing capture at Ca/S = 2 from 26 percent at 500 ppm to 40 percent at 3500 ppm SO_2. The concentration of mineral matter (correlated as gm Al_2O_3 per dry normal cubic meter of flue gas) iln the system had a very strong impact on capture at all of the SO_2 concentration levels and Ca/S ratios tested. At a calclium-to-sulfur mole ratio of 2 and 3500 ppm SO_2 the capture went from 40 percent with no mineral material to 8 percent with 7 gm/DNCM Al_2O_3 in the flue gas.

- A fairly extensive data base of sulfur capture in the BSF for various fuel-sorbent pairs was established. Six fuels and five sorbents were tested (not all possible combinations of fuel-sorbent pairs were included).

  - The effect of sorbent type on capture with a given fuel was dependent on the firing conditions - including sorbent injection location and thermal conditions. The hydrated limes seemed to be most sensitive to thermal conditions and and the Vicron least sensitive. The German hydroxide gave better capture than the Colton hydroxide - it was not clear why the two had different captures. Dolomite gave the highest capture wilth all of the fuels tested.

  - The effect of fuel type on capture with a given sorbent was also system, (injection method, firing characteristics and thermal condiltions) dependent. Capture with natural gas was higher for all of the sorbents than with coal.

- In general, sorbent size affected capture only for large particles, at mean sizes less than 10 μm particle size had little effect on sulfur capture. A comparison of the predicted effect of particle size and the observed effect using various sizes of Vicron was in fairly good agreement.

- Injecting the sorbent downstream from the main flame resulted in improved utilization in coal flames. Experiments with natural gas flames showed that the sorbents had somewhat higher surface areas in the reaction zone when injected downstream. Gas-fired experiments using mineral matter additives showed that mineral material deactivation of the sorbent could be reduced by injecting the sorbent downstream of the main flame.

- Electron micrographs of solid samples from experiments where Kaolin was injected with the fuel (natural gas) and the sorbent was injected downstream showed discrete irregular sorbent particles and spherical milneral material particles.

- Electron micrographs of samples taken from coal-fired, downstream sorbent injection tests showed spherical ash particles and discrete irregular sorbent particles.

- Injecting sorbent to control SO_2 emissions from pulverized coal fired boilers will result in changes in the boiler operating characteristics. Changes measured in the BSF due to sorbent injection included:
    - Increased solids loading from 35 percent to as much as three times depending on the fuel sulfur content,
    - Changes in particle size distribution resulting in an increase in fines,
    - Increased fouling on the simulated convective passes,
    - And increases in fly ash resistivity of as much as 30 times for the higher sulfur coal tested.

The analytical/engineering tools developed included a computer program for modeling the sulfur capture process, the application of an existing boiler performance/heat transfer code to specific thermal characteristics of a given system, and a scheme for using the two codes to predict sulfur capture and analyze results from sorbent injection tests.

The sulfation portion of the model is probably adequate for the model application needs except that the predicted effect of SO_2 concentration does not match the available data very well. The sorbent activation portion of the model is the best currently available, but is over-simplified and should be refined as data on the effects of calcination conditions and input sorbent characteristics becomes available.

The two and three dimensional furnace models are well developed. The application of these is only limited by available data on specific burner/furnace characteristics (i.e., flame shape, size, thermal conductivity and thickness of slag deposits, emissivity of injected sorbent, etc.).

An approach to combining the two models has been attempted. The furnace heat transfer model was used to predict a temperature/flow map of the furnace. A large number of particles were tracked through the furnace giving a distribution of peak temperature and residence times. The peak temperature distribution was then used to give an average sorbent surface area and the mean temperature and residence time were used with this surface area to predict sulfur capture.

This scheme was applied to the three pilot scale furnaces in order to predict the effect of scale for a standard condition using the same sorbent, injected with the same fuel (which only affects SO_2 concentration in the current scheme).

The model predictions of capture in the three pilot facilities are fairly good at predicting overall ranking of capture in the furnaces - LWS better than MT better than SWS. Capture measured in the LWS ranged from 40 to 53% depending on the burner and sorbent injection location. (The model predicts slightly higher capture for sorbent injection with the tertiary air in the LWS which was also apparent in some of the LWS tests.) Captures measured in the MT ranged from 10 to 29% again depending on burner and sorbent injection location. The highest capture measured in the SWS was 30%, higher than the predicted 23%. The model also does not predict a difference in capture due to sorbent injection location in the SWS while experimental results showed a difference as great as from 10% to 30% capture.

The analytical tools developed are promising and prediction of some general capture trends is possible but several gaps in the data and in the data and in modeling techniques remain. The avaliable analytical methods do not give sufficient refinement of the processes occurring in the near burner region which, from the experimental results, can have a profound impact on sorbent reativity and sulfur capture. The prediction of sorbent reactivity from measureable properties and projected thermal history is still very inadequate. Insufficient data on the effects of parent stone characteristics, such as grain size, composition and particle size, as well as the effect of various flame-calcination regions (heating rate, peak temperature, quench rate, etc.) on sorbent reactivity currently exist. These areas should receive further experimental and analytical attention.

The experiments performed have provided some clarification of the effect of various system parameters on sulfur capture by direct injection of sorbents. Fuel mineral matter has been shown to deactivate the sorbent if the two are injected together in a high temperature ($>$ 2300 $_{o}$F). Downstream sorbent injection (at temperatures around 2200 ^{O}F) gave higher captures than injection with the fuel for coal fired tests, because of decreased mineral matter interference and some increase in sorbent surface area. Further experimental work investigating the mechanism of mineral deactivation, the possibility of generating high surface area (highly reative) sorbents and the effect of sorbent injection on boiler operating characteristics (especially heat transfer concerns such as flame emissivity) should be performed.

2.0 BACKGROUND, PURPOSE AND SCOPE

This report summarizes the experimental and analytical effort performed for EPA Contract No. 68-02-3921 "Testing and Evaluation of Experimental Wall-Fired Furnaces to Determine Optimum Means to Reduce Emissions of Nitrogen and Sulfur Oxides", a one-year research effort executed at Energy and Environmental Research Corporation. The work summarized in this report was in part a continuation of effort initiated under EPA Contract 68-02-2667. The 2667 program, initiated in 1977, was aimed at providing a wider data and design base for application of the delayed mixing burner (DMB) concept. The objectives of the DMB program were extended to include the generalization of low NO_x burner technology for combined NO_x/SO_x control. The SO_x control program goal was to ascertain whether calcium containing sorbents (or other materials) can be used to provide an economically satisfactory combined NO_x/SO_x control strategy for pulverized coal-fired boilers without reducing boiler availability. This chapter gives a brief description of the low NO_x burner/sorbent-injection process and discusses results of several current investigations (including 2667) which helped direct the program effort. A brief overview of the EPA Limestone Injected Multi-staged Burner Program is given and the role of this program outlined. The purpose, scope and organization of the contract effort is presented.

2.1 Background

Coal sulfur does not necessarily convert quantitatively to sulfur oxides when coal is burned. Coals with high alkali metal oxide contents retain significant quantities of sulfur in the ash as sulfates. Thus, one method of preventing the emission of sulfur oxides is to effectively increase the alkali metal concentration in the system. This may be accomplished by adding alkali to the coal or by injecting an alkali sorbent which will capture sulfur into the combustion chamber. The sorbent (generally calcium carbonate) flash calcines when it is injected into the furnace and reacts with gaseous sulfur species. Depending on local stoichiometries, solid calcium sulfite and/or calcium sulfate may be formed. The solid sulfur compounds continue through the boiler and are collected with the fly ash at the boiler exit.

Considerable effort was expended in the late 1960's and early 1970's on development and demonstration projects based on this process. Although pilot plant studies showed promise, the results could not be duplicated in full-scale systems. The poor sorbent utilization efficiencies observed in the full-scale systems were attributed to dead-burning and maldistribution of the sorbent. Recent pilot-scale studies with low NO_x coal burners suggest that sorbent injection could be more effective under conditions which minimize NO_x formation in pulverized coal flames.

The technology which has the potential to provide simultaneous control of nitrogen and sulfur oxides has been dubbed LIMB - Limestone Injection into Multi-stage Burners. A simplified description of the LIMB process is illustrated in Figure 2-1. Coal, combustion air and the sorbent are injected into the furnace. The sorbent may be mixed with the coal or injected with one of the combustion air streams such as the staging air. Subsequent events can be considered to take place in three regions, namely:

1. Particle Heating - a short residence time region where the coal and sorbent are heated, typically at rates of 10^4 K/sec.

2. Fuel-Rich - an oxidizing region where the coal is burned out and the combustion products are cooled before entering the convective section.

The oxidation of fuel-bound nitrogen (producing fuel NO) accounts for 80 percent of the total oxides of nitrogen formed during the combustion of pulverized coal. The minimization of fuel NO formation requires that volatile fuel nitrogen species are prevented from reacting with oxygen and forming NO. During combustion the volatile fuel nitrogen species (XN) can follow two general paths:

- Fuel-lean

$$XN + O_2 \longrightarrow NO \qquad (1)$$

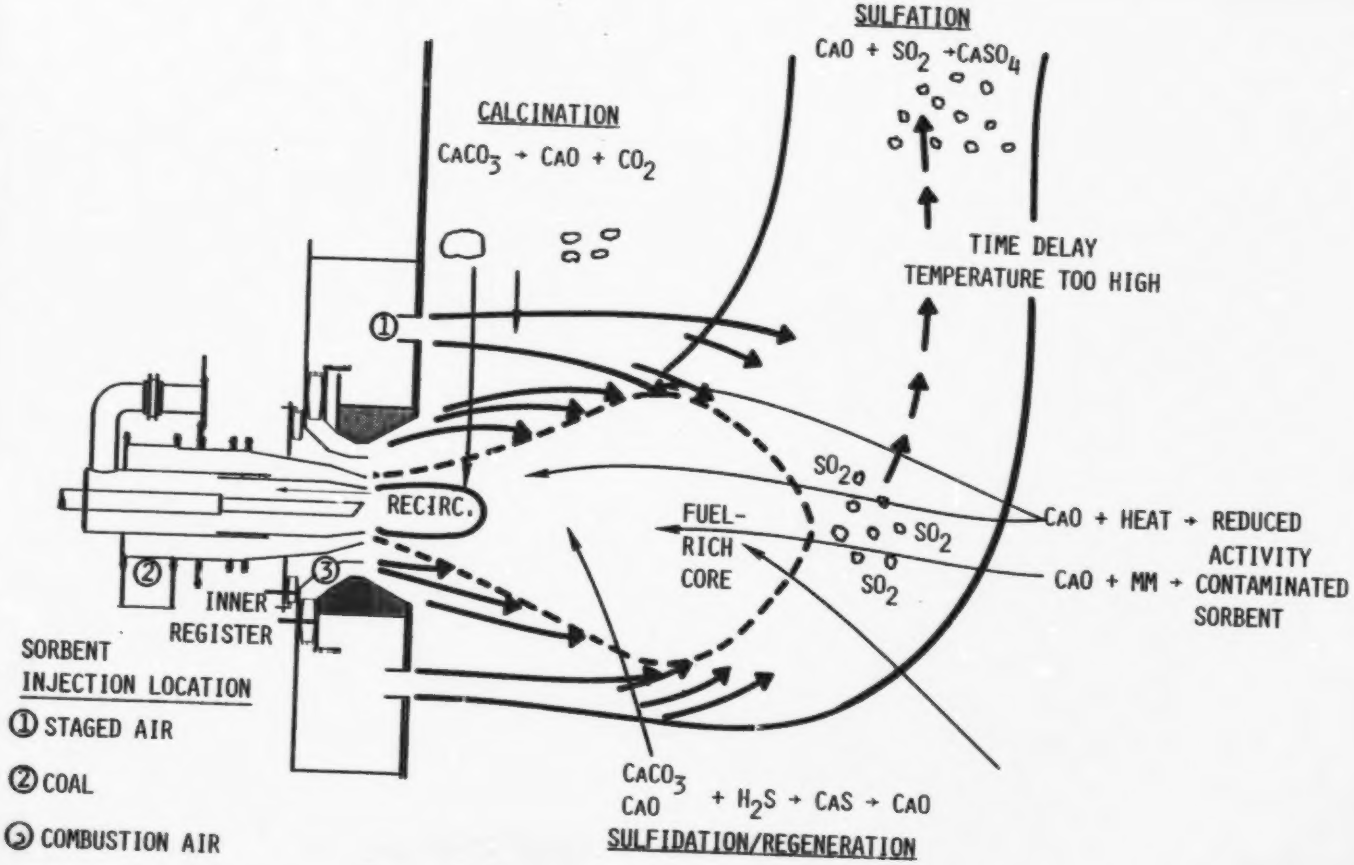
SULFATION
CAO + SO2 →CASO4
CALCINATION
CACO3 → CAO + CO2
TIME DELAY
TEMPERATURE TOO HIGH
①
RECIRC.
SO2
FUEL-
RICH
CORE
SO2
SO2
CAO + HEAT → REDUCED ACTIVITY
CAO + MM → CONTAMINATED SORBENT
②
③
INNER
REGISTER
SORBENT
INJECTION LOCATION
① STAGED AIR
② COAL
③ COMBUSTION AIR
CACO3
CAO + H2S → CAS → CAO
SULFIDATION/REGENERATION

Figure 2-1. LIMB Process.

- Fuel-rich

$$XN \longrightarrow HCN \longrightarrow N \longrightarrow NH \longrightarrow NH_2 \longrightarrow NH_3 \qquad (2)$$

$$N + NO \longrightarrow N_2 + O \qquad (3)$$

The reaction sequence 2 summarizes the nitrogen shift reactions which produce HCN or NH_3 under fuel-rich condtions. Reaction 3 is the most probable path forming N_2 in pulverized coal flames. All fuel-bound nitrogen is not volatile and the coal char contains nitrogen which can be oxidized. Since char burnout must be accomplished under oxidizing conditions, NO production from char nitrogen is unavoidable. Consequently, it is important that the conditions in the heating and fuel-rich zones promote the evolution of fuel nitrogen species.

The oxidation of both organic and inorganic coal sulfur produces SO_2 emissions from pulverized coal combustion. The ultimate gas-phase sulfur speciation depends upon the temperature and gas-phase stoichiometry. In the fuel-rich region sulfur will exist as H_2S, COS, or CS_2 and in the fuel-lean region almost all the sulfur will exist as SO_2. An injected sorbent can capture sulfur in both the fuel-rich and fuel-lean regions (see Figure 2-1). In the fuel-rich region the reduced sulfur species can react with sorbent directly producing calcium sulfide:

$$CaCO_3 + H_2S \longrightarrow CaS + H_2O + CO_2 \qquad (4)$$

Under fuel-lean conditions sulfur dioxide reacts with the calcined sorbent producing calcium sulfate:

$$CaO + SO_2 + 1/2\ O_2 \longrightarrow CaSO_4 \qquad (1)$$

The rates of both reactions are expected to be dependent upon the gas-phase sulfur concentration which benefits the fuel-rich capture because the reactants are more concentrated (provided the sulfur content of the char is minimized). Fuel-rich capture could have the further advantage that calcium sulfide, which has a small molar-volume, may not block the pore structure of the calcined sorbent allowing a greater utilization of the limestone.

Before the fuel-lean capture process can take place, the sorbent must be calcined. The reactivity of the calcine appears to be most strongly dependent upon peak temperatures. If temperatures are too high the material is dead-burned, resulting in a dramatic reduction in the BET surface area and a loss of reactivity. Consequently, the thermal history experienced by the sorbent particles is critical and it may be advantageous if they are excluded from the heat release zone where peak temperatures are highest. Regeneration of SO_2 can occur, the sulfide is more stable at higher temperatures than the sulfate, but if capture occurs under fuel-rich conditions the sulfide must be converted to sulfate in the fuel-lean region without decomposition to CaO and SO_2.

The sulfur capture process results in particulate emissions which consist of:

- fly ash;
- partially calcined sorbent;
- calcined sorbent with varying degrees of reactivity;
- partially sulfated sorbent

The composition and properties of the solid emissions will depend upon coal and sorbent properties as well as the LIMB process.

The LIMB process has been under investigation for several years in studies sponsored by the U.S. EPA and other governmental divisions as well as by commercial organizations and research organizations in Europe such as the IFRF (International Flame Research Foundations) and Rheinisch-Westfalischeswerk (RWE), a West German utility. The results of these investigations have been reviewed and were used as a basis for planning the program effort reported in this work. Detailed descriptions of the experiments and results are reported elsewhere (see references).

The results of the 2667 investigations were particularly significant in influencing the direction of this work. The 2667 effort involved two parallel investigations, which will be briefly reviewed, at two scales. These were:

- Bench-scale investigations using a purpose-built Boiler Simulator Furnace (BSF) firing at a nominal rate of 10^6 Btu/hr. The main purpose of these studies was to define the phenomenon controlling sulfur capture in pulverized coal flames.

- Pilot-scale investigations involving full-scale low NO_x coal burners tested in an environment (the LWS furnace) designed to simulate the burner heat release zones of a small utility boiler.

The pilot-scale SO_2 emission control studies were "piggy-backed" onto low NO_x burner studies. Two low NO_x distributed mixing burner, the EPA prototype DMB and the Steinmuller burner, were tested in the LWS, (the furnace is described in detail by Payne, et al., 1982). The studies were carried out without burner modification and only at conditions which had been optimized for NO_x emissions. No attempt was made to optimize the system for sulfur capture.

Results of the sorbent injection tests for the two burners in the LWS indicate that sorbent type [$Ca(OH)_2$ or $CaCO_3$] and injection location (with fuel or staging air) had small effects on the sulfur capture in either burner. The effect of sorbent location was more pronounced with the prototype burner and appears to be a result of changes in sorbent thermal history. The data also indicate that sulfur capture increases with coal sulfur content. The data in Figure 2-2 summarize results from studies with the EPA prototype and Steinmuller burners in several furnaces. Results from Steinmuller tests in the LWS and in the IFRF furnace (see Flamet, 1981) are included along with data from the prototype burner. Comparing the LWS results using the prototype and Steinmuller burners with Indiana coal, it is seen that use of the prototype burner resulted in higher sulfur capture even though the burners were operated at comparable conditions. This is perhaps indicative of the influence of burner design conditions. The LWS results using prototype burner

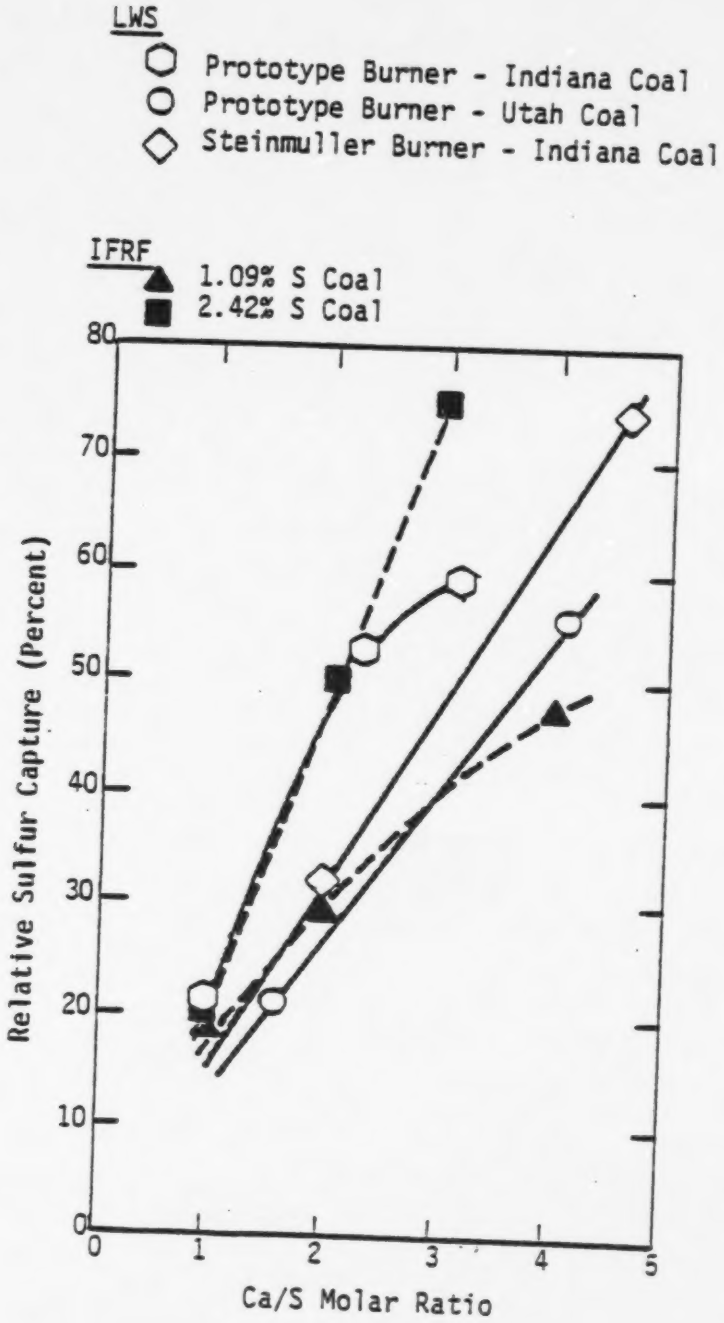

Figure 2-2. Comparison of Steinmuller and DMB Data - Limestone Injected in Tertiary Ports.

with Utah coal and the low sulfur coal IFRF test results show good general agreement, indicating that burner effects may be unimportant for low sulfur coals. All of these results are from burners which were not optimized for SO_2 capture, and therefore, should be treated with caution. The good agreement between the LWS data for Indiana coal and the IFRF data with the high sulfur coal is somewhat surprising in light of the higher furnace temperature (1000°C versus 600°C in the LWS) employed at IFRF.

The bench-scale limestone injection studies were performed concurrently with the pilot-scale studies. The 2667 bench-scale studies consisted of three experimental phases, namely:

Series A - Combustion Parameter Screening
Series B - Thermal History/Sulfur Chemistry
Series C - Fuel and Sorbent Studies

The bench-scale experiments were performed in the Boiler Simulator Furnace (BSF) which is described in detail in Appendix A (Volume II) and by Case, et al., 1983. The results of the bench-scale studies (discussed in detail by Case, et al., 1983) and questions raised by the data were used to plan the 3921 effort. Two basic firing conditions were used: burner-staging where a sub-scale Distributed Mixing Burner was used to deliver fuel, sorbent and all of the combustion air, and physically-staged where part of the combustion air was added downstream producing a long residence time fuel-rich region in the radiant furnace.

The results of the experimental studies conducted in the boiler simulator furnace indicated that the parameters of major importance were thermal environment, calcium-to-sulfur ratio, and sorbent composition. Thermal environment (local temperature) was shown to have a strong effect on the utilization of dry sorbents injected directly into the furnace. The burner staged experiments showed the influence of temperature most clearly; a reduction in peak flame temperature, due to cooling in the radiant zone (as shown by the data in Figure 2-3) or to a reduction in load, increased the sulfur capture significantly. Changes in other combustion parameters, such as

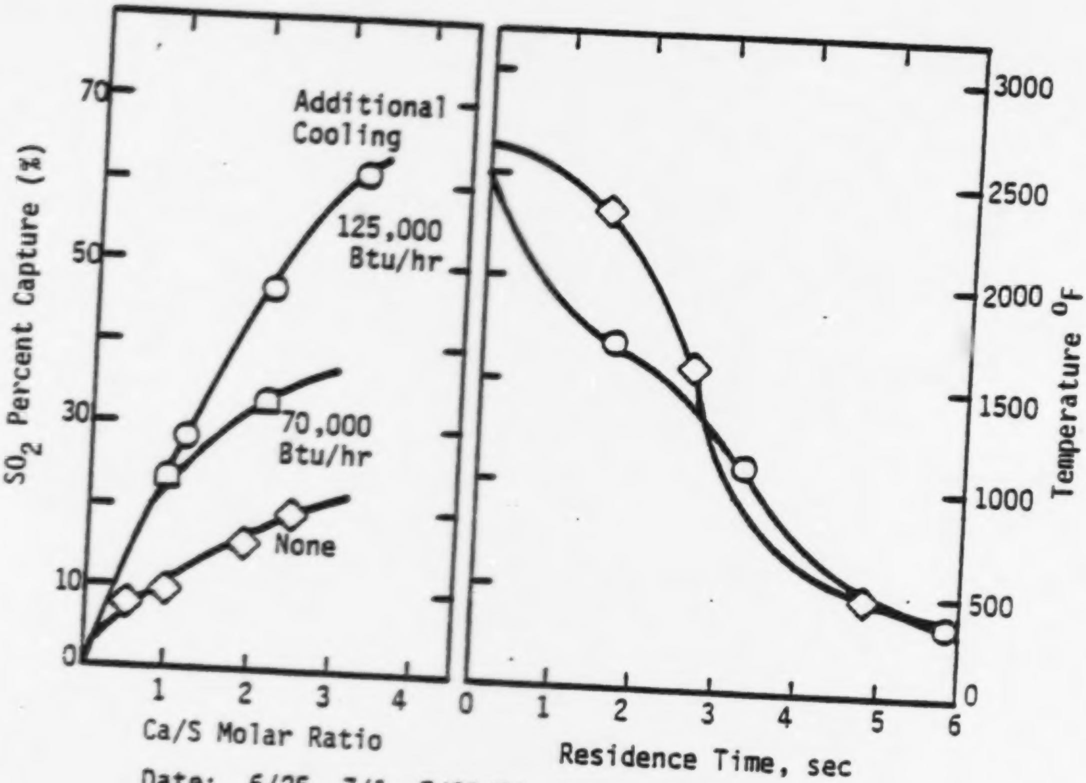

Date: 6/25, 7/1, 7/29/81
Rate: 800,000 Btu/hr
Cooling: As Shown
SR_P: 0.2
SR_B: 0.6
SR_T: 1.20

Coal: Indiana
Ca/S Mole Ratio:
Sample Port: #3
Sorbent: $CaCO_3$, 45-3
Injection Loc.: Tertiary Air

Figure 2-3. Influence of Heat Extraction Rate - Base Case Conditions.

sorbent locations and injection velocity, had secondary effects on sulfur capture.

The effect of thermal history under physically-staged conditions was less clear. Changes in both load and thermal cooling in the radiant furnace were complicated by the changes in furnace temperature due to the physical staging itself, since physically staging the coal flame significantly altered the furnace temperature profile. First-stage stoichiometry and sorbent location both influenced sulfur capture under externally-staged conditions; however, the results suggest that these influences may be more strongly related to thermal changes than to chemical changes. There was no clear evidence that sorbent utilization under fuel-rich conditions was much higher than under fuel-lean conditions.

The influence of sorbent type on sulfur capture was studied at different combustion conditions. The sorbents examined included:

- Vicron 45-3
- Vicron 15-15
- Michigan Marl
- Hydrated Lime [$Ca(OH)_2$]
- Dolomite

These sorbents were tested with Indiana (lot 3) coal and propane. In general, the Dolomite gave good capture under all conditions examined. The hydrated lime appeared to be most sensitive to thermal enivornment. High captures were observed for all of the sorbents when the primary fuel was propane/H_2S. The effect of fuel sulfur on sorbent utilization was investigated by studying: Indiana (lot 3) coal, Beulah lignite (from North Dakota), propane doped with H_2S, and a coal/water slurry. All of the fuel screening tests were conducted with Vicron 45-3 as the sorbent. Figure 2-4 summarizes capture for the fuels

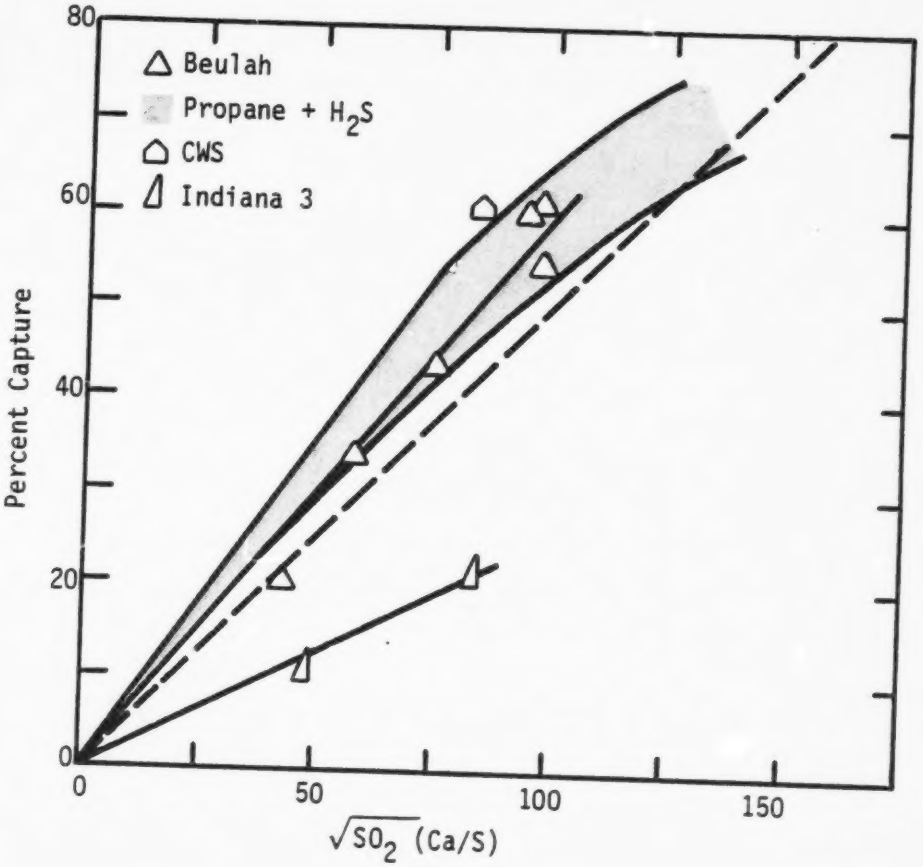

Figure 2-4. Effect of fuel on sulfur capture (Vicron 45-3).

as a function of Ca/S $\sqrt{SO_2}$, the SO_2 correlation was used in an attempt to eliminate the effect of fuel sulfur content. The sorbent utilization was significantly less when the primary fuel was the Indiana coal than in all of the other cases tested. Adiabatic flame temperatures were calculated for all of the fuels at stoichiometric ratios from 0.6 to 1.2 and the calculated temperatures for the solid fuels rank in the same order as the sulfur capture obtained; the highest sorbent utilization was achieved with the fuel producing the lowest theoretical tmeperature. However, the differences in calculated temperature do not appear to be significant enough to explain the large differences in capture.

The 2667 bench-scale and pilot-scale studies provided a considerable amount of data on the sulfur capture process, however, a clear picture describing the precise sequence of events and controlling parameters which dictate overall sulfur capture could not be assembled. There have, in fact, been a number of anomalous results in the 2667 and other sorbent injection studies. These results include: the difference in sorbent utilizatin in gas and coal-fired flames, the effect of fuel sulfur content on SO_2 capture - which correlates well with $\sqrt{S}$ for some burners and firing conditions (notably the EPA prototype burner in the MT and LWS) and does not correlate data reported from other facilities such as the Steinmuller burner fired in the IFRF furnace and does not correlate data obtained in the same facility with different burners. Simple thermal differences are not sufficent to explain differences in data obtained in various tests. Figure 2-5 summarizes data obtained in four facilities using a $CaCO_3$ sorbent injected through the tertiary air ports of a Distributed Mixing Burner. The $\sqrt{S}$ correlation was used in an attempt to eliminate some of the effect due to different fuel sulfur contents. The BSF and LWS data were obtained under similar thermal conditions, which are somewhat colder than typical boiler operating conditions. These results show good agreement and appear to show some promise for the translation of data to different furnace scales.

When the same burner which was used in the LWS tests was fired in the MT furnace, where the thermal environment, firing arrangement and confinement are similar to those of the IFRF furnace, a significant reduction in SO_2 capture

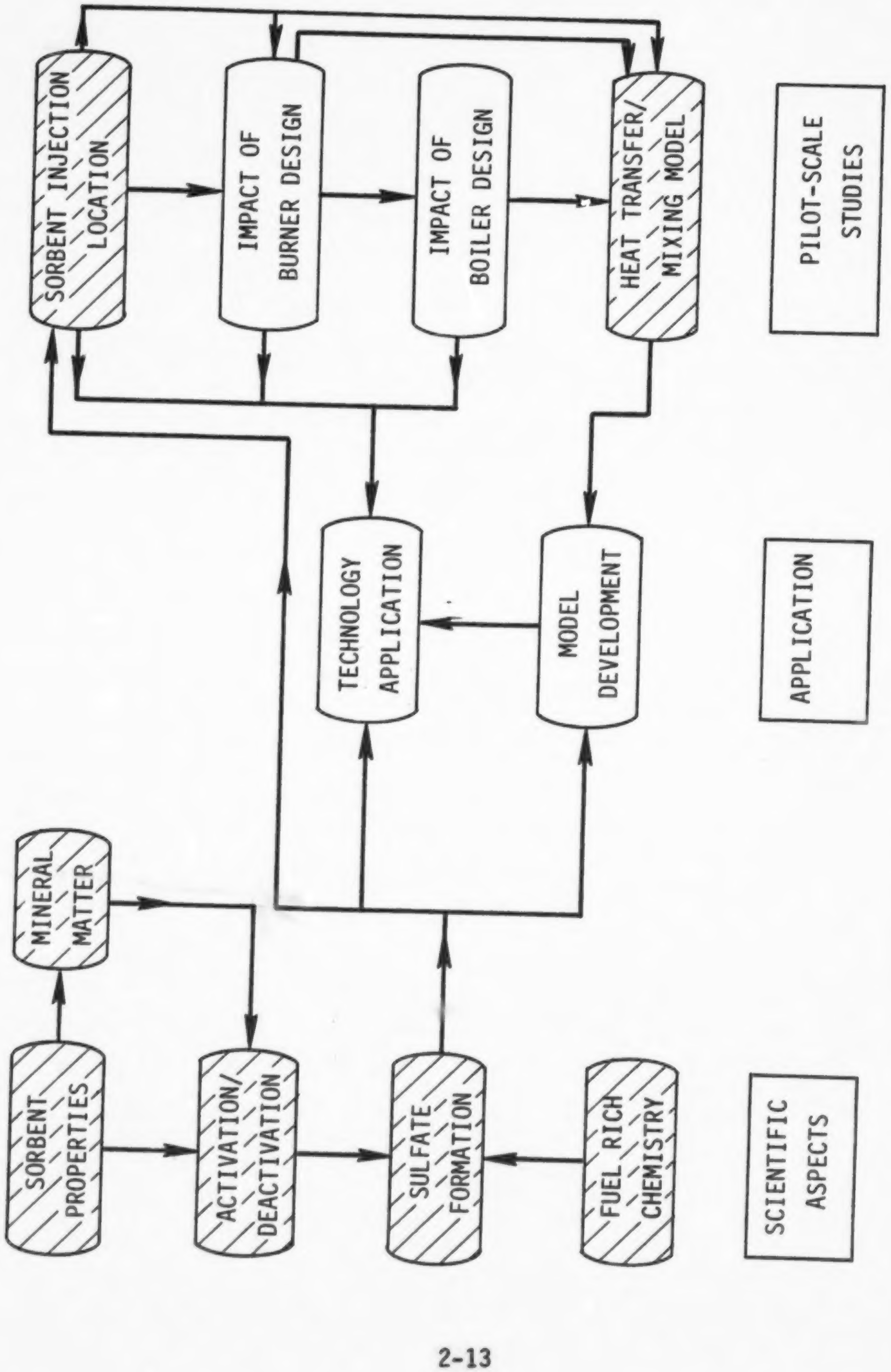
SORBENT PROPERTIES
MINERAL MATTER
ACTIVATION/ DEACTIVATION
SULFATE FORMATION
FUEL RICH CHEMISTRY
SCIENTIFIC ASPECTS
TECHNOLOGY APPLICATION
MODEL DEVELOPMENT
APPLICATION
SORBENT INJECTION LOCATION
IMPACT OF BURNER DESIGN
IMPACT OF BOILER DESIGN
HEAT TRANSFER/ MIXING MODEL
PILOT-SCALE STUDIES

Figure 2-5. LIMB technology development.

was observed. This latter trend appears to be consistent with thermal environment effect arguments, from which the higher temperature environment would be expected to be less conducive to sulfur capture, but conflicts with the IFRF furnace data. The data from the IFRF studies were obtained in a furnace very similar to the MT which was also considerably hotter than the LWS (flue gas temperature 1600°C compared to 800°C). The captures in the IFRF furnace were as high as the LWS captures when thermal arguments would suggest they should be lower.

The questions raised by these and other data formed the basis for planning the 3921 program effort as well as other investigations of the sorbent injection/sulfur capture process.

2.2 LIMB Technology Development

This research project is one of several programs sponsored by the EPA to investigate and develop simultaneous NO_x/SO_x emission control using limestone injection in multi-stage buners. The overall technology development programs ranging from small-scale fundamental investigations to pilot-scale development studies and includes analysis of boiler design aspects of LIMB technology and a probable full-scale utility boiler demonstration.

One overall concept of the LIMB program is shown in Figure 2-5. There are three basic facets shown: scientific aspects, pilot-scale studies and application. Scientific questions still incompletely understood include: the role of sorbent properties, especially predicting sorbent properties in the furnace from characteristics of the raw stone; the effect of thermal history or fuel mineral material on sorbent reactivity; the time and temperature requirements for sulfation; and the role of fuel-rich reactions (CaS formation oxidation and/or decomposition) in sulfur capture in a staged mixing system. Pilot-scale studies using various burners in various pilot furnaces (at scales from 1 to 150 MBtu/hr) include investigation and analysis of the effects of sorbent injection location, burner design and boiler design. Analytical tools which are being developed include methods for modeling furnace thermal and mixing characteristics using an existing boiler performance heat-transfer code and developing models for analyzing furnace flow fields.

LIMB application is likely to be very system-specific, involving analysis of a particular fuel/boiler/burner system, selection of a sorbent and injection method and consideration of the impact of LIMB on operation of the boiler. Both the scientific aspects and the pilot-scale studies will influence the application of LIMB. As indicated in Figure 2-5, the results of investigations of the fundamental aspects of sulfur capture, pilot-scale studies and the devleopment of models for the process will aid in the application of LIMB technolgy.

The research program summarized here feeds into the development effort at several levels. The shaded areas in Figure 2-5 show the areas in which results of this research program are of use. The work reported here involved direct investigations of the role of fuel and sorbent properties, fuel mineral matter interactions, and fuel-rich capture. Results of these experimental efforts can be used to clarify the sulfate formation process and to derive guidelines for determining sorbent injection locations. In addition to the experimental results, analytical development work played a significant role in this research program. The development of a sulfur capture model, and the application of heat transfer models were a significant portion of the program results.

Methods for modeling, or engineering analysis of LIMB application in a given system are invaluable for the successful development of this NO_x/SO_x control strategy. The model development and application performed for this program are part of the creation of an overall modeling and analysis strategy which will be used to aid the application of the LIMB technology.

2.3 Purpose and Scope

The overall goal of the research program was the clarification of means to reduce emissions of nitrogen oxide (NO_x) and sulfur oxides (SO_x) from the pulverized-coal, wall-fired, combustion systems found in utility boilers. The work was divided into four separate tasks, each of which is discussed below. The purpose of Task 1 was to provide detailed information about sorbent and sulfur reactions under conditions of particular interest. Task 2 was designed to evaluate the potential of a number of design and sorbent options. Task 3 provided some information on the effect of scale on the performance of systems designed to reduce NO_x and SO_x , and Task 4 provided for summarizing the data produced, providing recommendations concerning optimum systems and potential operational problems. The interrelationship of these tasks and the relationship of the proposed effort to current and recently completed work is shown in Figure 2-6.

2.3.1 Task 1 - Detailed Measurements

The major goal of this task was to clarify the effect of the immediate flame zone on sorbent reactivity and overall sorbent utilization. In particular, there were several conditions encountered in earlier (2667) parameter screening studies which indicated that processes occuring in the immediate flame region (less than 1 sec. residence time) may have a controlling effect on sorbent reactivity and overall sorbent utilization. The task was made up of two phases: The first phase was the measurement of detailed temperature and species profiles in the near-burner region in an attempt to identify conditions which would explain observed differences in sulfur capture. The second phase provided for the detailed measurement of temperatures, species and sorbent properties from conditions of particular interest resulting from investigations of sorbent and design options.

In addition to clarifying observed phenomonen, it was expected that the detailed measurements in Task 1 could be used to answer key questions about sorbent activation and reactivity. These questions included:

- What temperature is necessary for complete calcination in the times available?

- What temperature, for how long, causes sorbent deactivation, dead-burning?

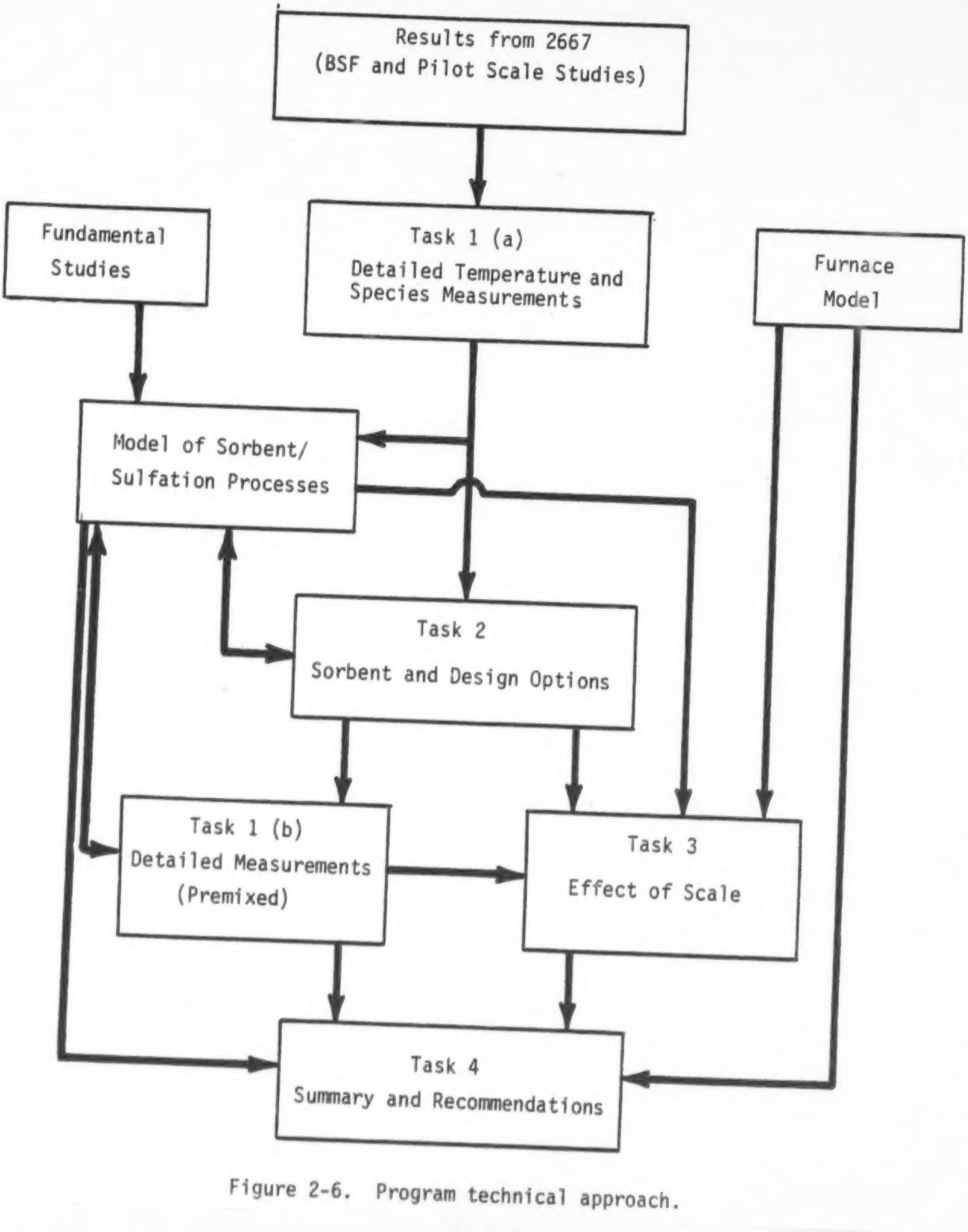
Results from 2667
(BSF and Pilot Scale Studies)
Fundamental Studies
Task 1 (a)
Detailed Temperature and Species Measurements
Furnace Model
Model of Sorbent/ Sulfation Processes
Task 2
Sorbent and Design Options
Task 1 (b)
Detailed Measurements (Premixed)
Task 3
Effect of Scale
Task 4
Summary and Recommendations

Figure 2-6. Program technical approach.

- Is there a minimum time at temperature for sorbent activation?

- Is there a time-temperature scheme which creates a "super active" sorbent?

- Does local stoichiometry have an effect on sorbent calcination?

- Are there physical/chemical processes occuring in the immediate zone which affect sorbent utilization? In particular, what effect does the mineral component of the coal have on sorbent reactivity?

The generalization of the sulfur capture process and the application of information generated by these and other LIMB was a major objective of the research. A model of the sulfur capture process was developed for use as a tool in evaluating the application of the dry limestone injection process to practical systems. Results from earlier studies, most notably the EPA in-house studies, the EPA sponsored project at the Tennessee Valley Authority and work performed at Battelle, have been used to generate models of the reactions between limestone and sulfur dioxide. One modeling approach (the pore model) was selected for development as part of Task 1. The development of this model is described in Section 5.0.

2.3.2 Task 2 - Sorbent and Design Options

The purpose of this task was to evaluate the potential of various sorbent and design options to improve the performance of LIMB. The task also included considerable investigation into the mechanisms by which various options affected sulfur capture. This task included: investigation of burner parameters such as fuel injector type and burner zone stoichiometry. Sorbent parameters such as sorbent type, particle size and composition; operational characteristics such as load, high temperature flames (O_2 enriched) and sorbent injection location; fuel effects using coals and gaseous fuels and investigating the effect of ash/mineral matter components on sorbent reactivity.

Detailed measurements of temperature and species profiles in Task 1 failed to sufficiently explain differences between SO_2 capture by sorbents injected with coal or natural gas in the BSF. The results of other studies had implied that thermal differences especially differences in peak temperature could have a dramatic effect on sorbent utilization. A simple system, using gas fuel was used to investigate the effects of high temperatures on sorbent reactivity. The results of these tests are discussed in Section 4.0.

Thermal differences in certain gas and coal flames in the BSF were slight, while SO_2 captures were very different. The possibility that inorganic mineral material in the coal ash was in some fashion deactivating the sorbent was investigated. Sorbent/coal-fly ash mixtures and sorbent mixed with common coal mineral materials were tested in the BSF. These tests indicated a strong interference by particular coal minerals which bears further investigation. The experiments and results are discussed in Section 6.0.

In order to explore the effect of sorbent type on capture, and to provide a comparative data base for planned and in-progress pilot-scale studies, a series of fuel/sorbent interaction tests were preformed. Four coals (and three different batches of the baseline Indiana coal) were used. Sorbents tested included three limestones, two hydrated limes and a dolomite. Sorbent particle size effects, with both gas and coal using limestones and dolomite were also investigated. The fuel sorbent interactions studies are described in Section 7.0.

The effect of downstream sorbent injection for a number of fuel sorbent pairs was also investigated. Injection downstream, after the main flame zone had been shown to improve sulfur capture in earlier studies. The extent and possible mechanism of this effect were explored as is described in Section 8.0.

2.3.3 Task 3 - Effect of Scale

As originally conceived, the objective of Task 3 was to investigate scale effects on the performance of systems designed for the simultaneous reduction of NO_x and SO_x emissions. This was to be achieved both through the use of mathematical models for the prediction of furnace performance and through tests carried out on a range of furnace sizes. Bench-scale data indicated that the time/temperature history of gases and particles is a key factor in the capture of sulfur compounds. However, reliable information on time/temperature profiles in large-scale systems is at best fragmentary. Even in experimental systems data is seldom taken in such a manner that comprehensive scale realtionships can be observed. There is, therefore, a need to devleop an understanding of the effects of scale both to aid in the interpretation of large-scale data (based upon the results of small bench-scale studies), and to provide the tools whereby the technology may be more confidently assessed in terms of its application to full-scale installations.

The technical approach envisaged for this task followed two lines of attack: one involving the use and development of mathematical modeling techniques, and the second requiring experimental studies at a range of furnace scales. The experimental studies were to provide data directly related to scale effects. The mathematical model development was to provide a tool for the interpretation and eventual extrapolation of the data. It was anticipated that both together will yield a predictive capability for the extrapolation of results to full-scale installations.

It was planned that the work carried out under this task should make extensive use of data generated at bench-scale in this and earlier programs, and should be closely linked to the pilot-scale studies planned under the EPA Contract No. 68-02-2667 pilot-scale test program. Scheduling problems (the 2667 pilot-scale tests have yet to be completed) and the need to investigate ash/mineral matter and fuel/sorbent effects in a less expensive, more easily controlled system resulted in a redefinition of the Task 3 scope. The pilot-scale experiments were eliminated and emphasis on the analysis of data from the BSF studies and ther pilot-scale LIMB investigations was emphasized.

A fully developed furnace heat transfer model was set-up and used to predict the complete temperature field for the three experimental furnace configurations used in the 68-02-2667 contract pilot-scale studies. The gross time-temperature histories generated in this way were then used in conjunction with small-scale (BSF and fundamental work) experimental data, and with the sulfur capture model developed in Task 1 to predict sulfur captures in the various facilities. This analytical effort is described in Section 9.0. A summary of some observed system effects which are not easily explained in terms of the thermal analysis is presented in Section 10.0.

2.3.4 Task 4 - Summary and Recommendations

The purpose of Task 4 is to review the data generated in the other three tasks in order to rank possible options and provide recommendations for optimum systems. In a sense this report is Task 4, however, the experimental results (as is often the case) have raised nearly as many questions as have been answered. Thus, the purpose of this task (and report) is then to summarize the results of these experiments and analytical procedures, to describe a method of analyzing and rationalizing data from various systems and to discuss remaining problems which should be addressed. The conclusions chapter (Section 13.0) and the project summary (Section 1.0) comprise Task 4.

3.0 DETAILED MEASUREMENTS IN GAS AND COAL FLAMES

One of the primary goals of this research program was to provide data which would clarify some of the puzzling results from earlier work. In particular, results from the bench-scale Boiler Simulator Furnace studies performed under EPA Contract 68-02-2667 were of interest. One inexplicable result of the 2667 bench-scale studies was the effect of fuel type. Indiana coal and propane doped with H_2S were fired under the same conditions: DMB (internally staged), $SR_b = 1.2$, full load (1.0 MBtu/hr), uncooled, sorbent with the fuel. The overall thermal history of the sulfur/sorbent system was virtually identical, but sorbent utilization in the propane-fired case was dramatically better than in the coal-fired case (Figure 3-1). It appeared that some process in the near-burner region had a dominant effect on sorbent reactivity. The first task of this program was to identify temperature and species profiles in the immediate flame region which might explain the observed differences in sorbent utilization.

3.1 Experimental Approach and Scope of Detailed Measurements

The major goal of this task was to clarify the effect of the immediate flame zone on sorbent reactivity and overall sorbent utilization. A phased approach was used. The first step was to reestablish the observed difference in capture with the coal and gas flames. The gas fuel was changed from propane to natural gas for economic reasons, therefore, a comparison of capture in propane and natural gas flames was made. After the difference in capture in the two flames was established, measurements of gas temperatures in the radiant furnace were made. Permanent gas species (O_2, CO, CO_2) concentrations were measured and isokinetic solid samples were taken. The sampling and analytical systems used are described in detail in Appendix B Volume II).

Sulfur capture for Vicron 45-3 with the natural gas/H_2S flame was measured. Captures on the order of 50 percent at a Ca/S mole ratio of 2 were measured (see Figure 3-2). The Vicron 45-3 injection test was repeated with Indiana (lot 3) coal giving SO_2 capture of less than 25 percent at a calcium-to-sulfur ratio of 2 (see Figure 3-3). This capture was slightly higher than

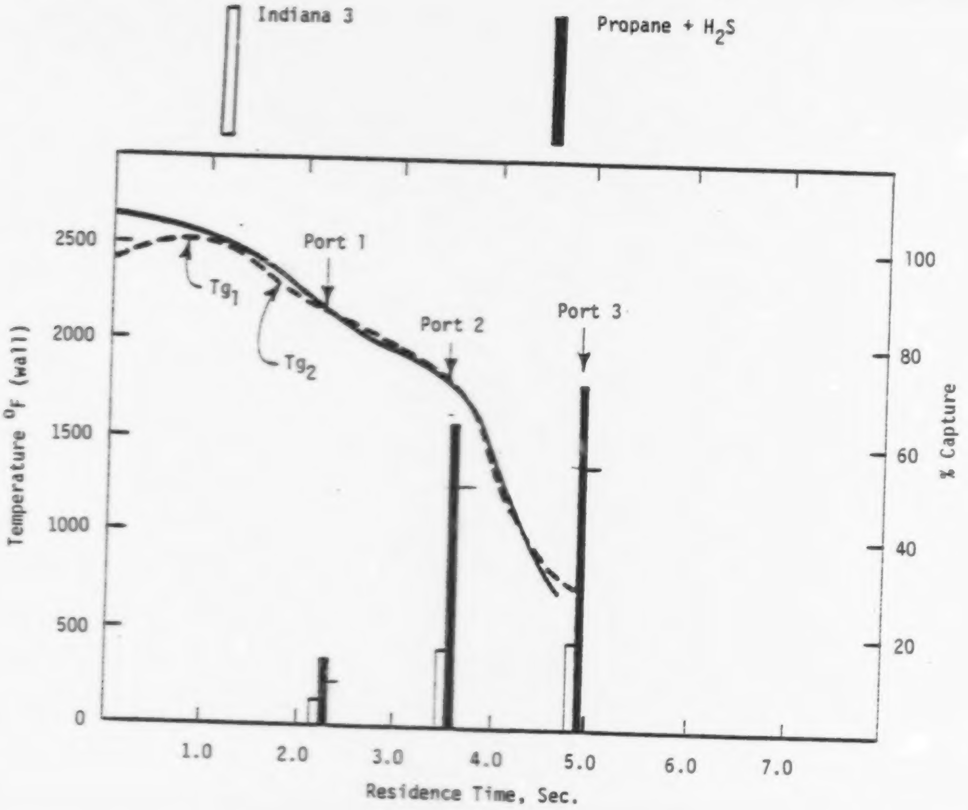

Figure 3-1. Comparison of coal and propane capture and thermal history.

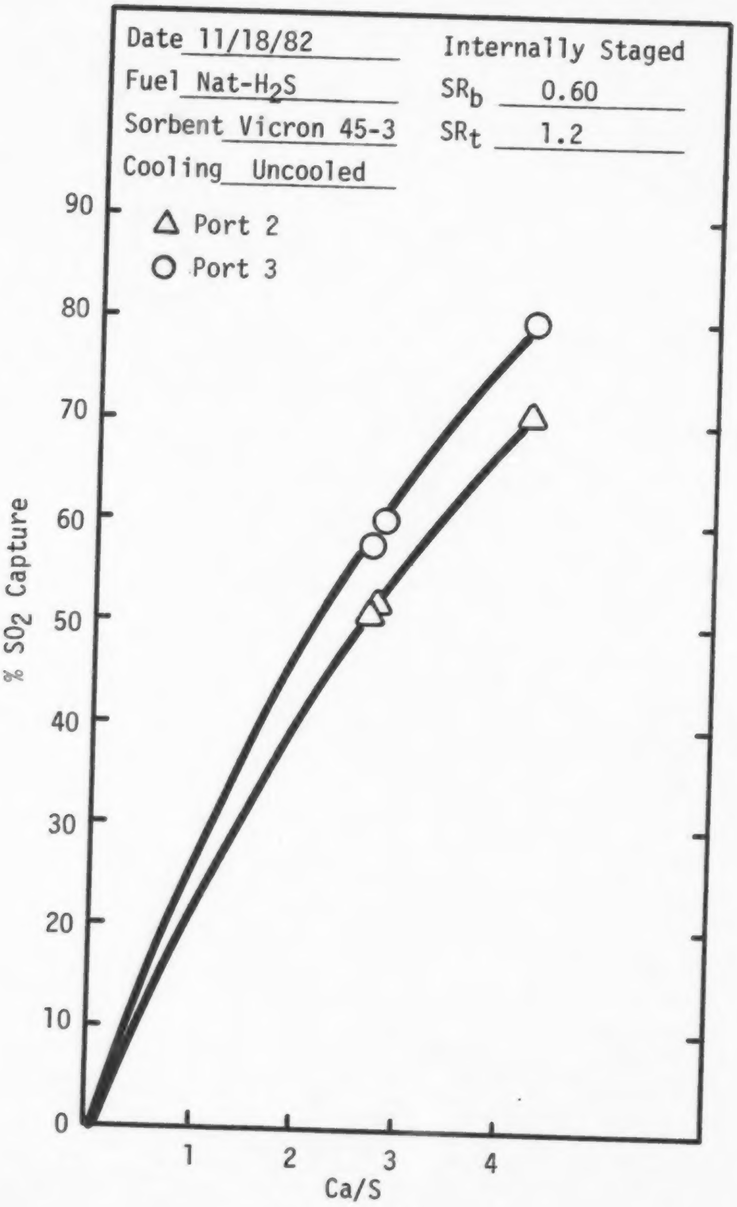

Figure 3-2. Sulfur Capture, Natural Gas Flame.

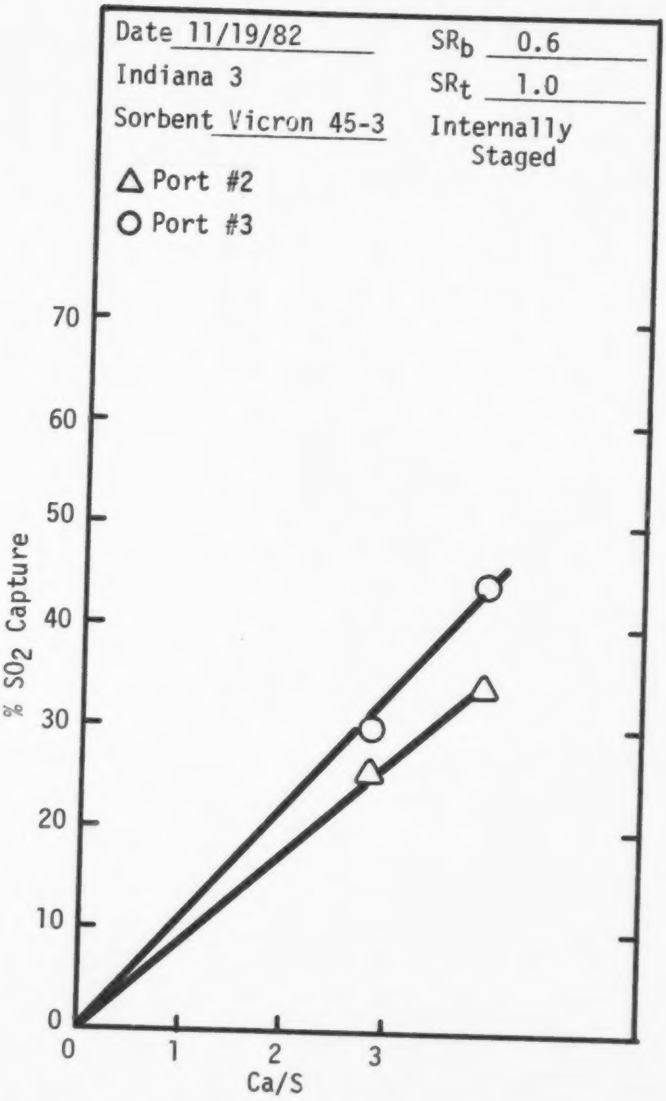

Figure 3-3. Sulfur Capture, Indiana Coal Flame.

measured for the Indiana coal earlier. A comparison of the temperature profiles for the two cases (shown in Figure 3-4) indicates that the longer residence time in the sulfation reaction zone (200°F) for the second test is a reasonable explanation for the improved capture.

The difference between captures in the coal and gas flames was still dramatic, and the wall temperature profiles were not sufficiently different to explain the change in sorbent utilization (see Figure 3-5). A comparison of the propane and natural gas wall temperature profiles and sulfur capture measurements (Figure 3-6) showed little effect of the gas-fuel type on sulfur capture.

Having reestablished the difference in sorbent utilization for the coal and gas fuels, detailed measurements in the radiant furnace were made for both flames.

3.2 Characterization of Natural Gas Flames

In order to clarify the differences between the coal and gas flames, detailed maps of gas temperatures, permanent gas species, solids loading (with sorbent added to the gas fuel) and sorbent utilization were made. The flow and temperature fields in the BSF are most complex in the radiant furnace, near the burner. Radial traverses at three axial locations were used to establish the temperature and gas concentration fields.

Gas temperatures were measured with a suction pyrometer (see Appendix A). Radial and axial traverses were used to construct the temperature field maps shown in Figures 3-7 and 3-8. The vertical cross-section shown in Figure 3-7 indicates the complexity of the temperature field in the region near the burner. Low temperature regions downstream of the tertiary air injectors indicate the penetration of the tertiary jets. The radial temperature profile flattens considerably as the axial distance increases; becoming rather flat at the third traverse point 53 inches below the burner. Temperature fields at the first two horizontal planes (A-B, 18 in. below the burner and C-D, 31 in.

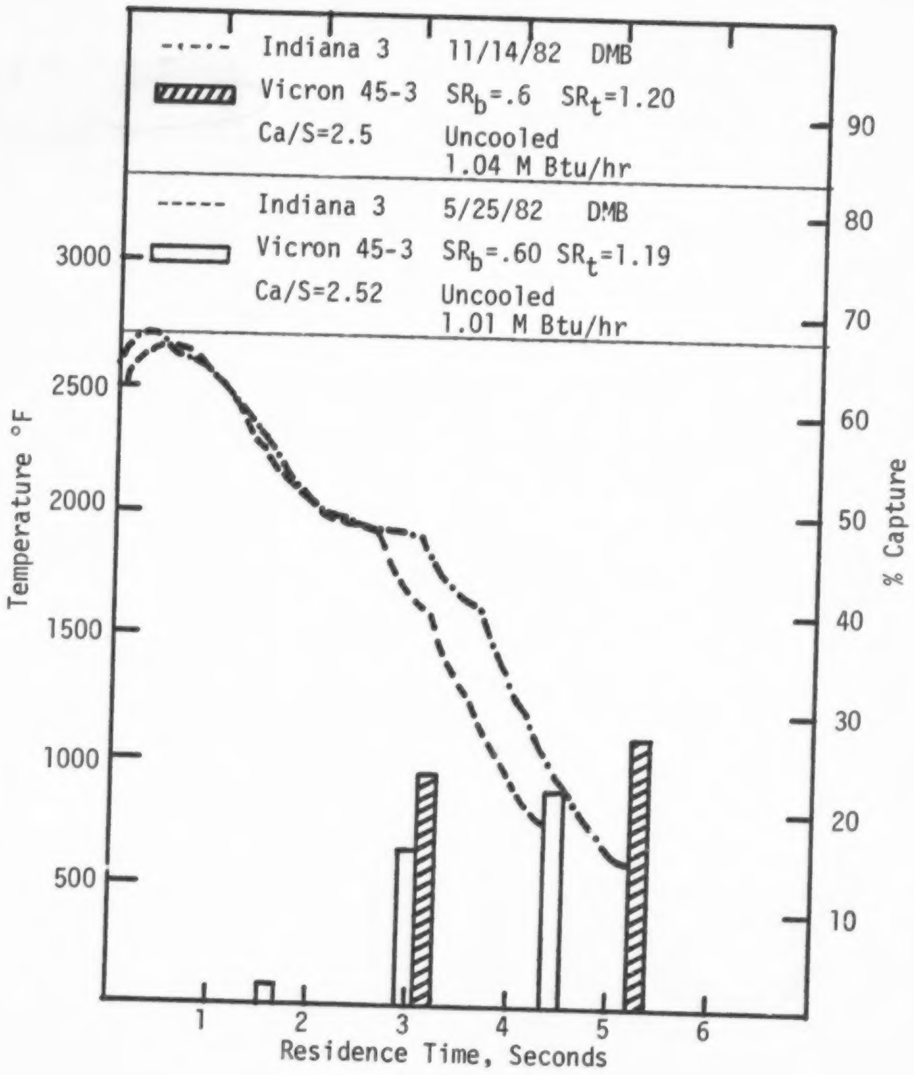

Figure 3-4. Comparison of capture for Indiana coal flames.

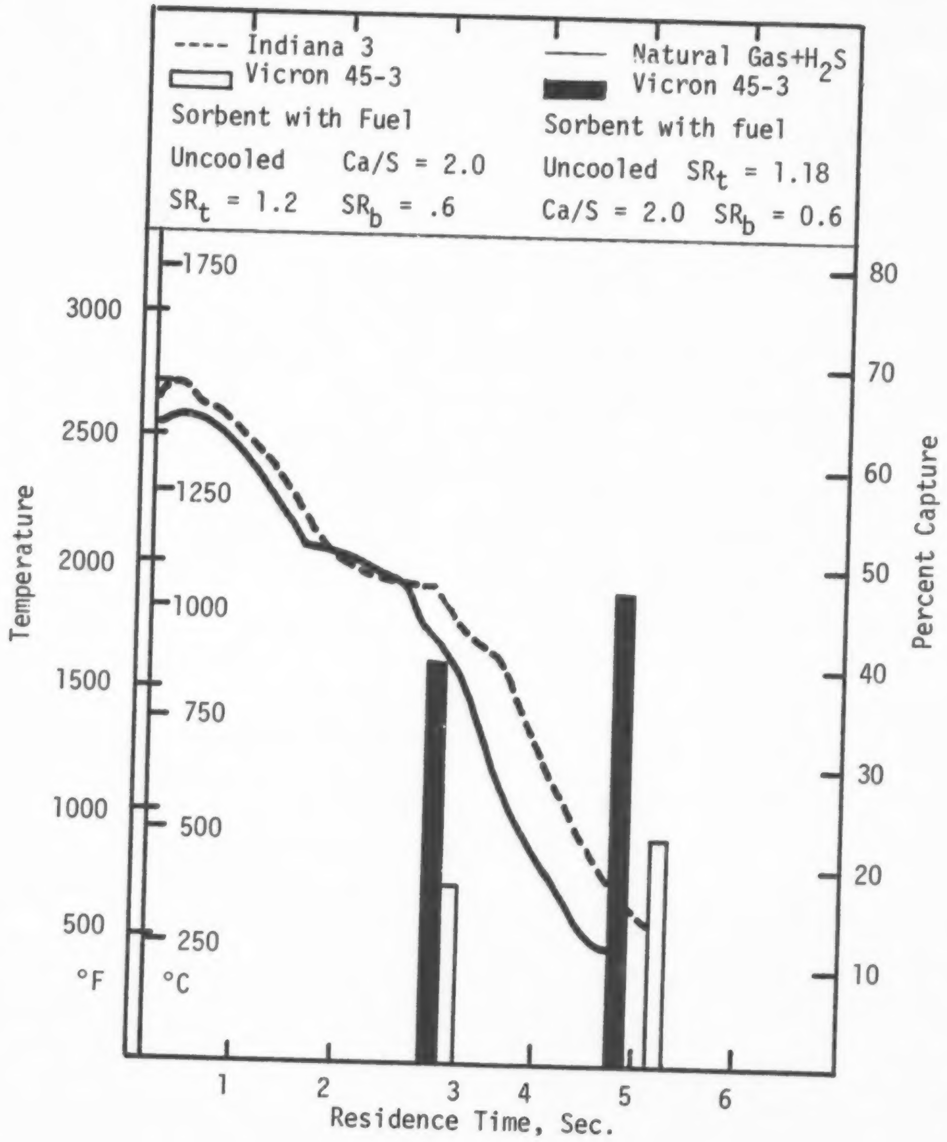

Figure 3-5. Temperature profile and sulfur capture for gas and coal flames.

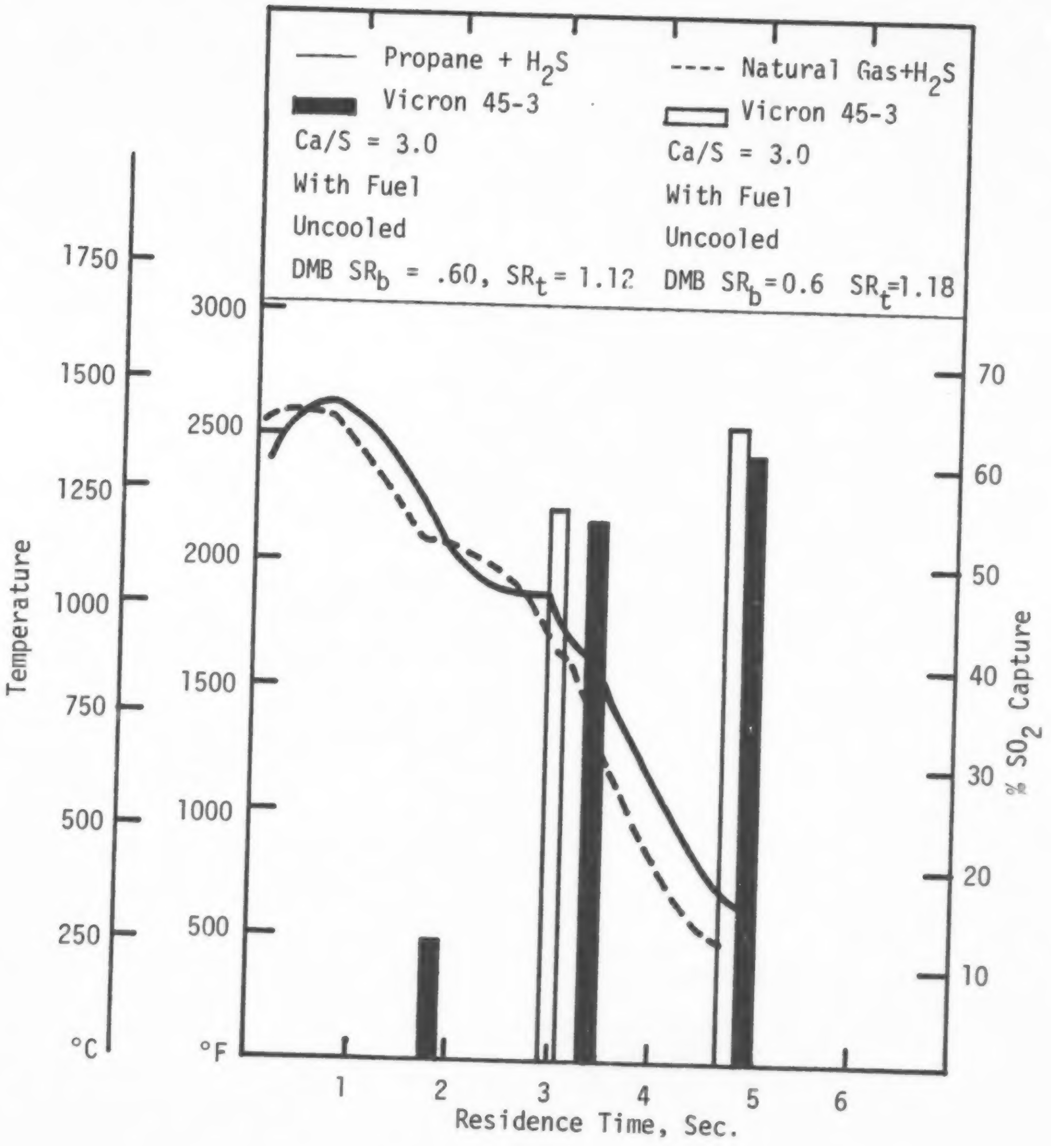

Figure 3-6. Temperature profile and sulfur capture for natural gas and propane flames.

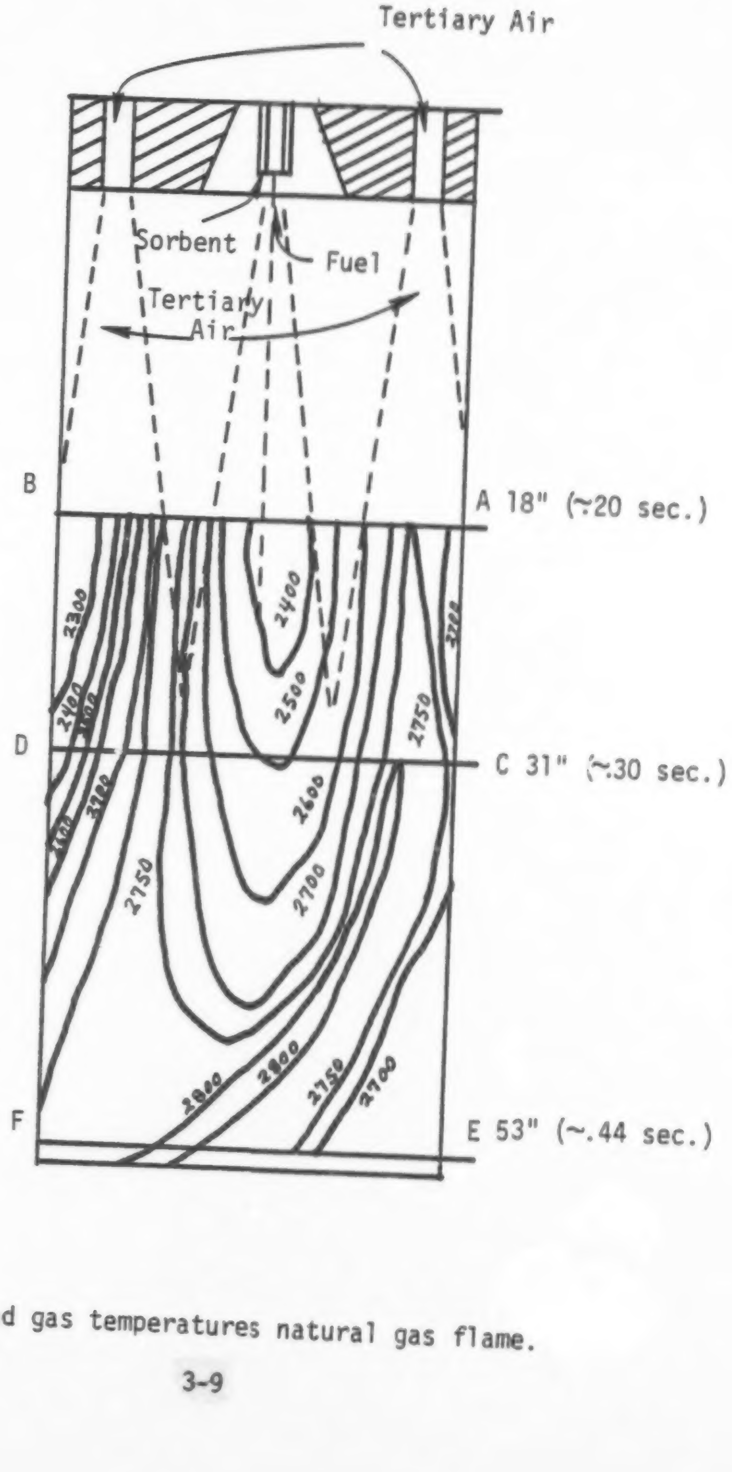
Tertiary Air
Sorbent
Fuel
Tertiary Air
B
A 18" (~.20 sec.)
2300
2400
2400
2500
2750
D
C 31" (~.30 sec.)
2600
2750
2700
F
2800
2800
2750
2700
E 53" (~.44 sec.)

Figure 3-7. Detailed gas temperatures natural gas flame.

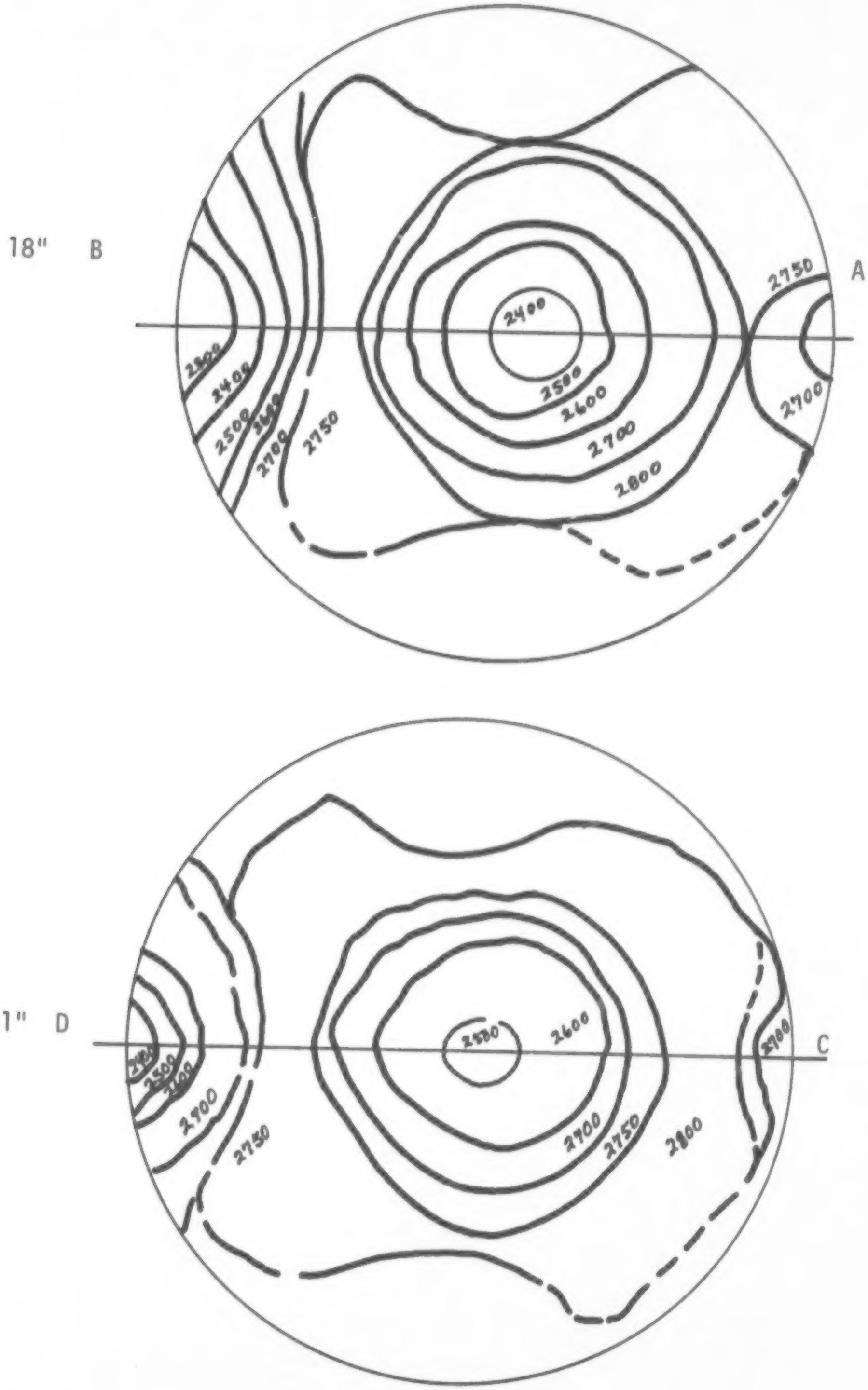

Figure 3-8. Radial gas temperatures, natural gas flame (as in Fig. 5-9).

below the burner) are indicated in Figure 3-7. Details of the temperatures in the tertiary jets are shown only for the jets in the traverse plane. Measurements could not be made at 90° from this plane, but the detailed structure of the other two tertiary jets is unlikely to be different than those measured.

Gas species concentration measurements, radial traverses at the the same axial location, are summarized in Figure 3-9. The measurements correlate well with the temperature maps. Oxygen concentrations were highest in the tertiary jet regions and the radial profile became more uniform farther from the burner. Both sets of measurements indicate that the flame was not perfectly centered in the radiant tunnel but tended to cling to one wall of the furnace.

Vicron 45-3 was injected with the natural gas and isokinetic solids samples were taken at various locations in the furnace. Figure 3-10 shows the measured solids loading as a function of axial distance from the burner. Figure 3-11 shows radial variations at three locations in the radiant furnace. It appears that the solid sorbent jet spread out in the first 50 or less inches from the burner and from that point the solids loading across the furnace was rather flat. The solids dropout (settling to the walls and sticking to the convective tubes was on the order of 85 percent from the burner to the flue; there was a 22 percent dropout in the radiant furnace and another 9 percent (from theoretical) in the post-flame cavity giving 31 percent loss before the convective sections. The theoretical solids loading was based on the the flue gas volume and the sorbent feed rate assuming 100 percent calcination of the Vicron 45-3 to calcium oxide.

The Vicron 45-3 was added to an H_2S-doped flame. The samples collected for the solids loading measurements were analyzed for calcium and sulfur. Sorbent utilization was calculated from the composition measurements. Figure 3-12 shows the sorbent utilization as a function of axial distance. Wall temperatures and gas temperatures (at the centerline) are also shown. Utilization calculated from measured SO_2 capture, and the input calcium-to-sulfur ratio are also shown. Sulfur captures based on gas measurements and solid sample analysis are in reasonable agreement except at port 2 (near the

5-1

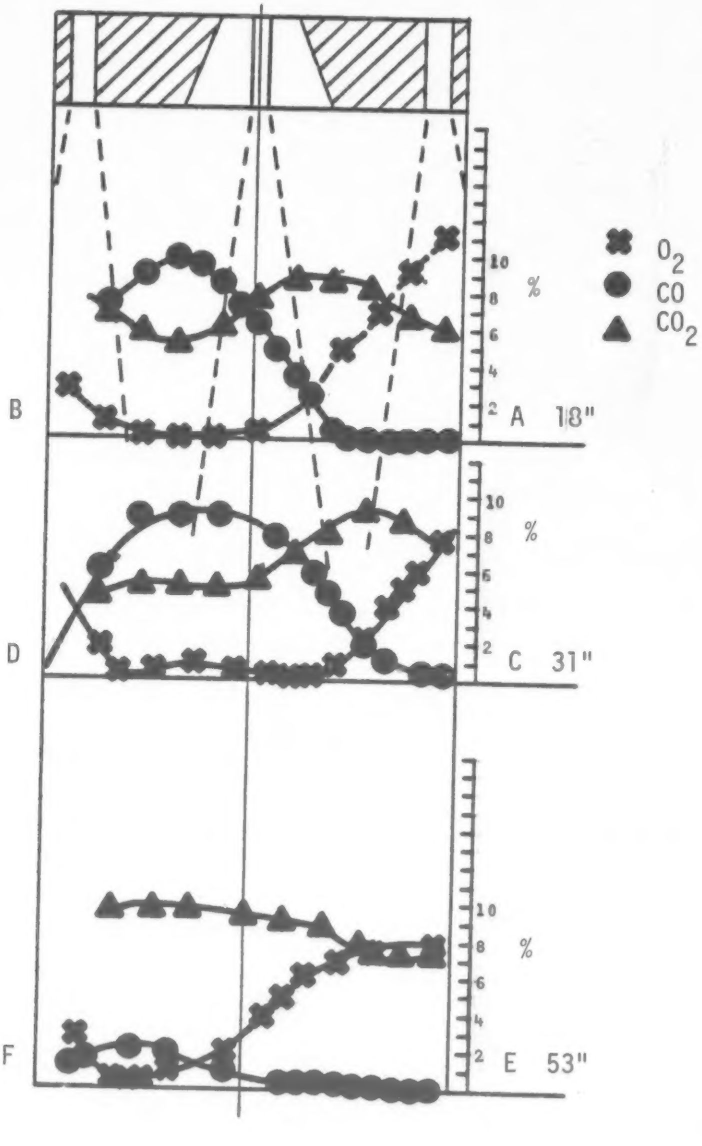

Figure 3-9 . Gas species profiles, natural gas flame.

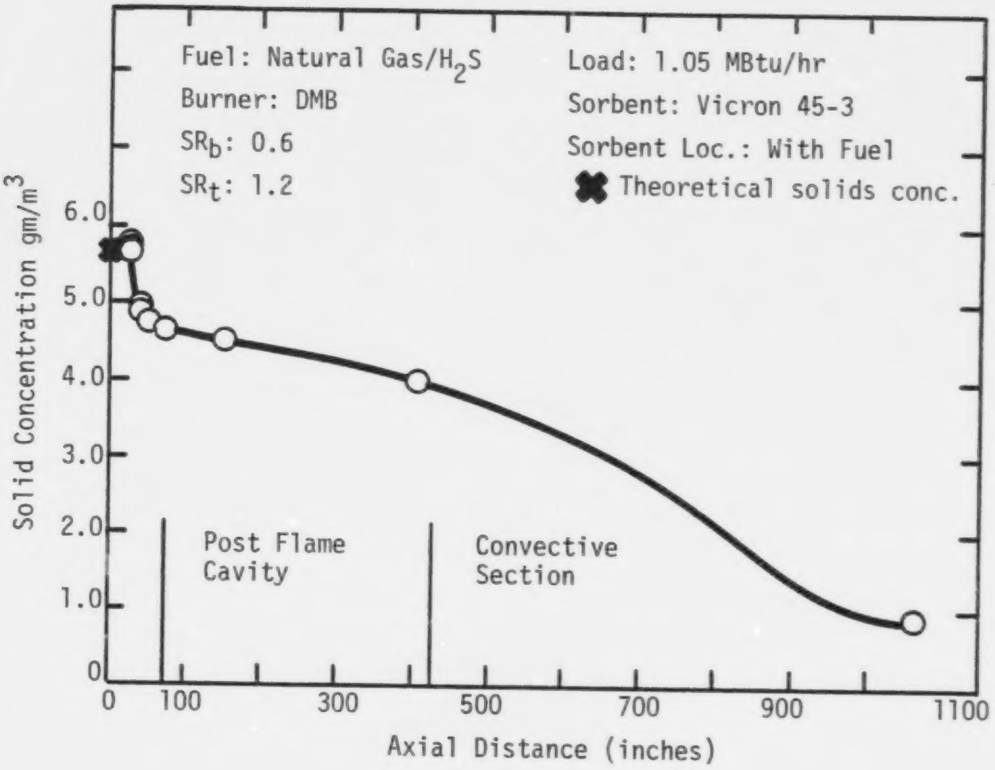

Figure 3-10. Solids loading (Centerline), Vicron 45-3 in natural gas flame, axial.

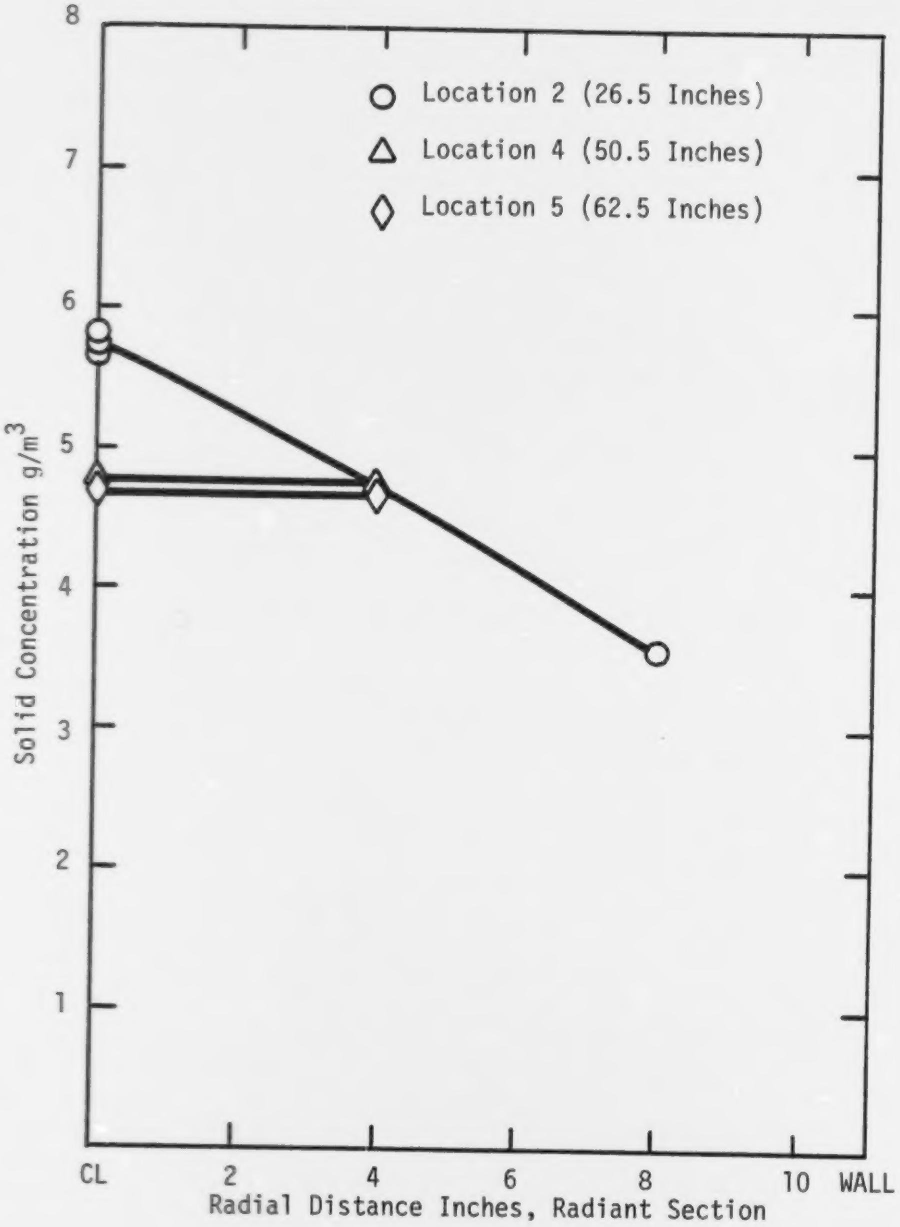

Figure 3-11. Solids loading, Vicron 45-3 in natural gas flame, radial.

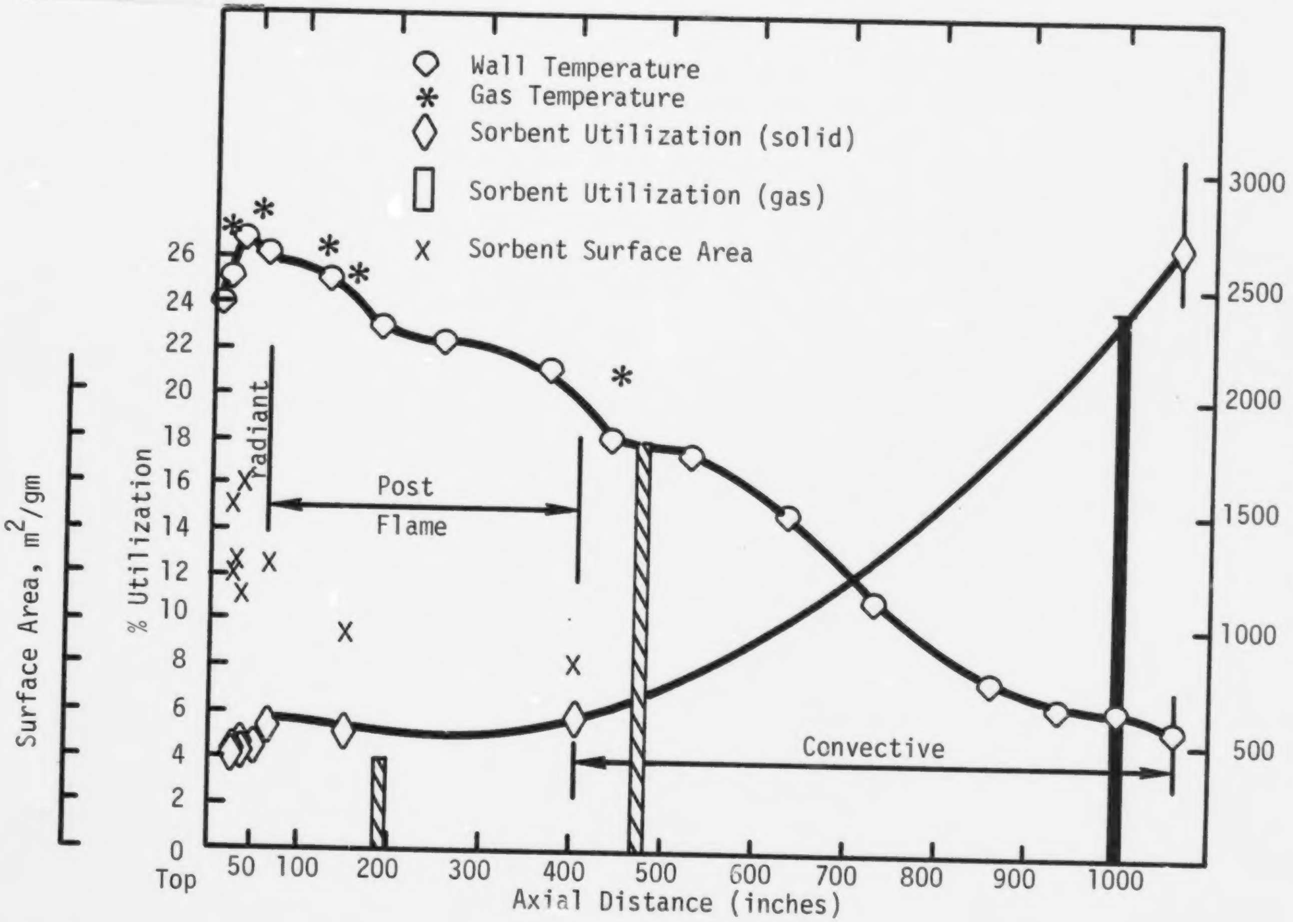

Figure 3-12. Summary of Sorbent Thermal History, Surface Area and Utilization, Natural Gas/H_2S Flame.

exit of the post-flame cavity) where capture in the gas was much higher than in the solid. The samples were not taken at exactly the same location and were in a temperature region where the sulfation reaction is fast. This may account for the higher capture at the downstream (gas sample) location.

3.3 Coal Flame Characterization

The Indiana (lot 3) coal flame was characterized in a manner similar to the gas flame. A gas temperature map was constructed from the downfired portion of the furnace. Figure 3-13 shows this temperature map. Again, the tertiary air jets are apparent and the temperature field is more complex near the burner and the profile is nearly flat at the plane E-F 53 inches from the burner. The flame temperatures are slightly higher near the burner than the gas flame was.

Radial traverses of the furnace were made at three axial planes to measure O_2, CO_2, and CO in the coal flame. The gas concentration profiles are shown in Figure 3-14. The temperature and species maps are in good agreement. The O_2 concentration was highest in the air jets and the radial profiles were fairly flat at the 53 inch, E-F plane. The essentially zero CO concentration at this point implies that the coal flame was somewhat shorter than the gas flame (where the CO concentration was .5-15 percent at 53 inches from the burner.

Isokinetic solids samples were taken on the centerline of the down-fired tunnel at several axial locations. Samples were also taken at the post-flame cavity and at the exit of the convective section. The results of these measurements are summarized in Figure 3-15. The theoretical ash loading is based on the ash content of the fuel and the flue gas volume assuming 100 percent carbon burnout. The higher than theoretical solid concentrations measured in the radiant furnace were due to incomplete fuel burnout (see Figure 3-17). Solids dropout through the furnace was about the same as the sorbent/natural gas flame (85 percent loss before the flue). A radial traverse of the furnace 38.5 inches below the burner (see Figure 3-16) indicated little difference in solids distribution across the furance.

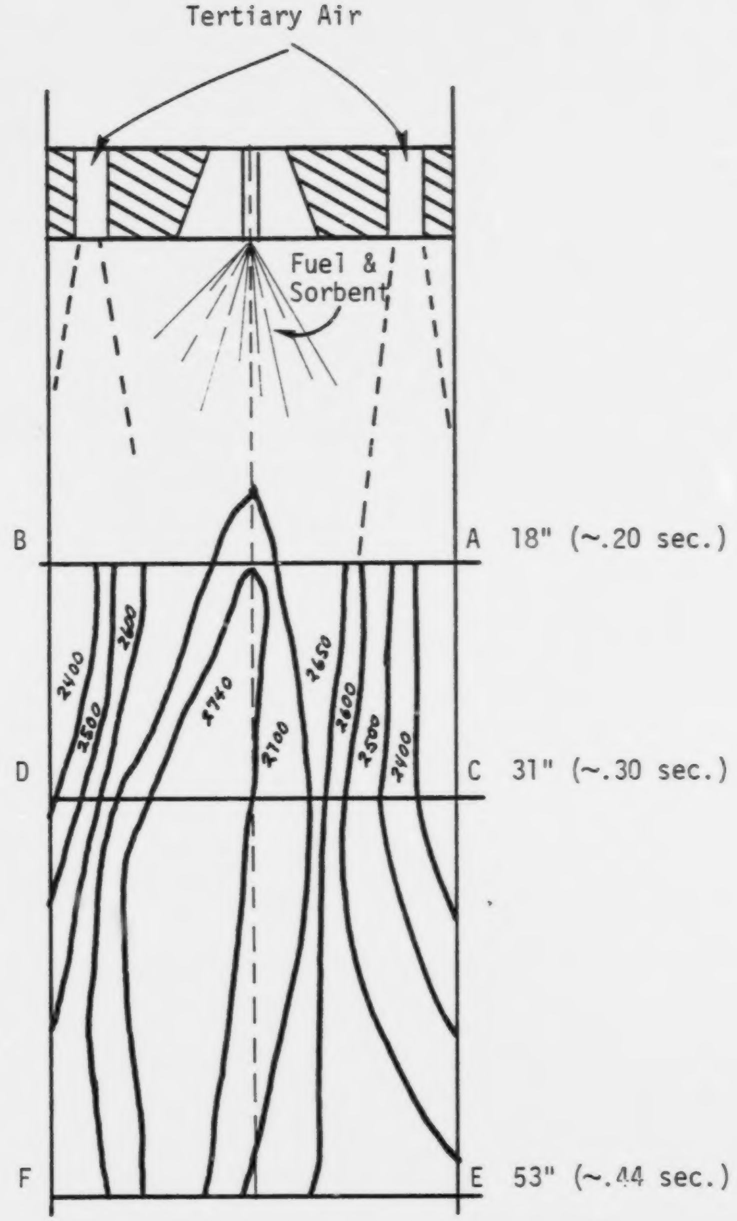
Tertiary Air
Fuel &
Sorbent
B
A
18" (~.20 sec.)
D
C
31" (~.30 sec.)
F
E
53" (~.44 sec.)
2400
2500
2600
2740
2700
2650
2600
2500
2400

Figure 3-13. Detailed gas temperatures - Indiana coal flame.

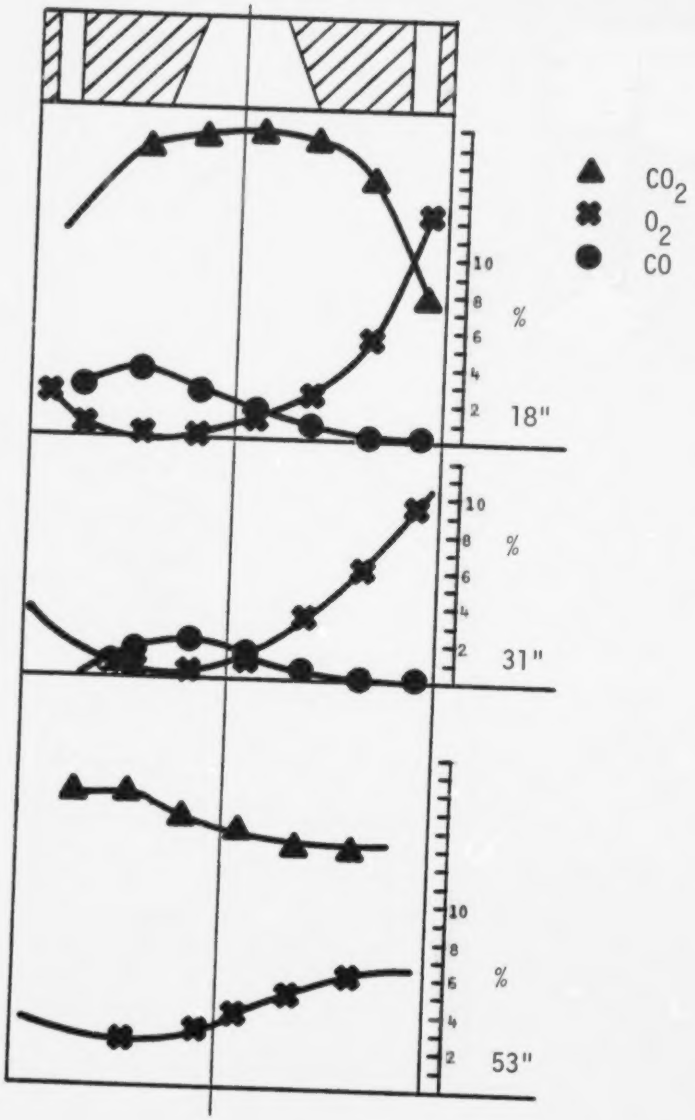

Figure 3-14. Gas species profiles, Indiana coal flame.

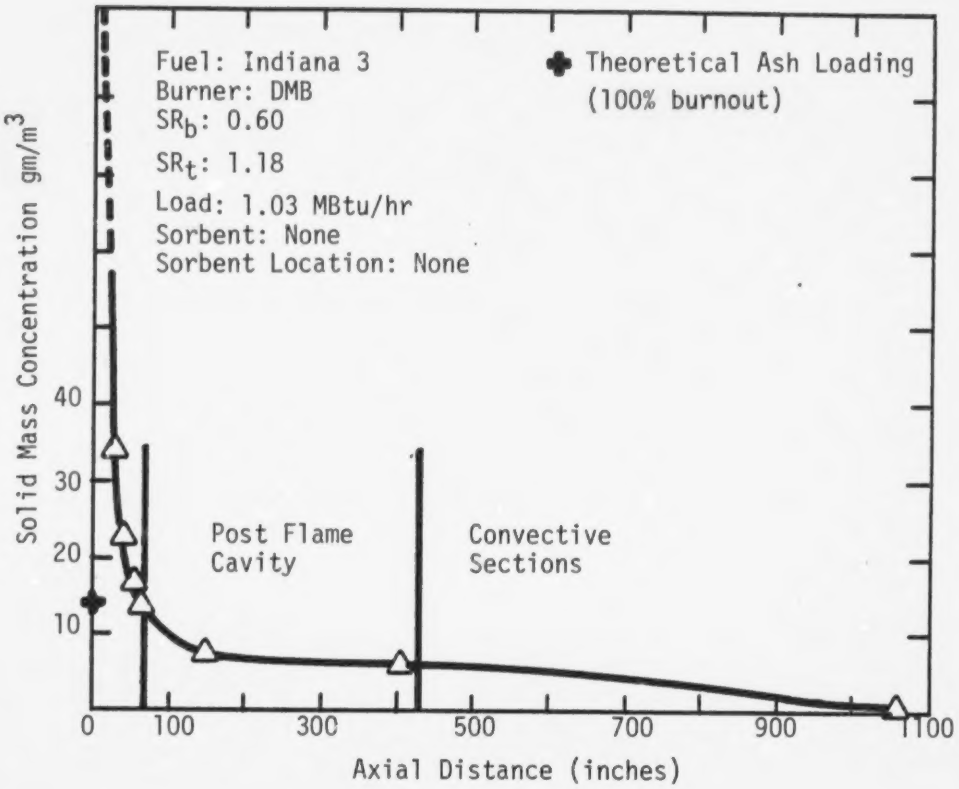

Figure 3-15. Solids loading, Indiana 3 coal flame, axial.

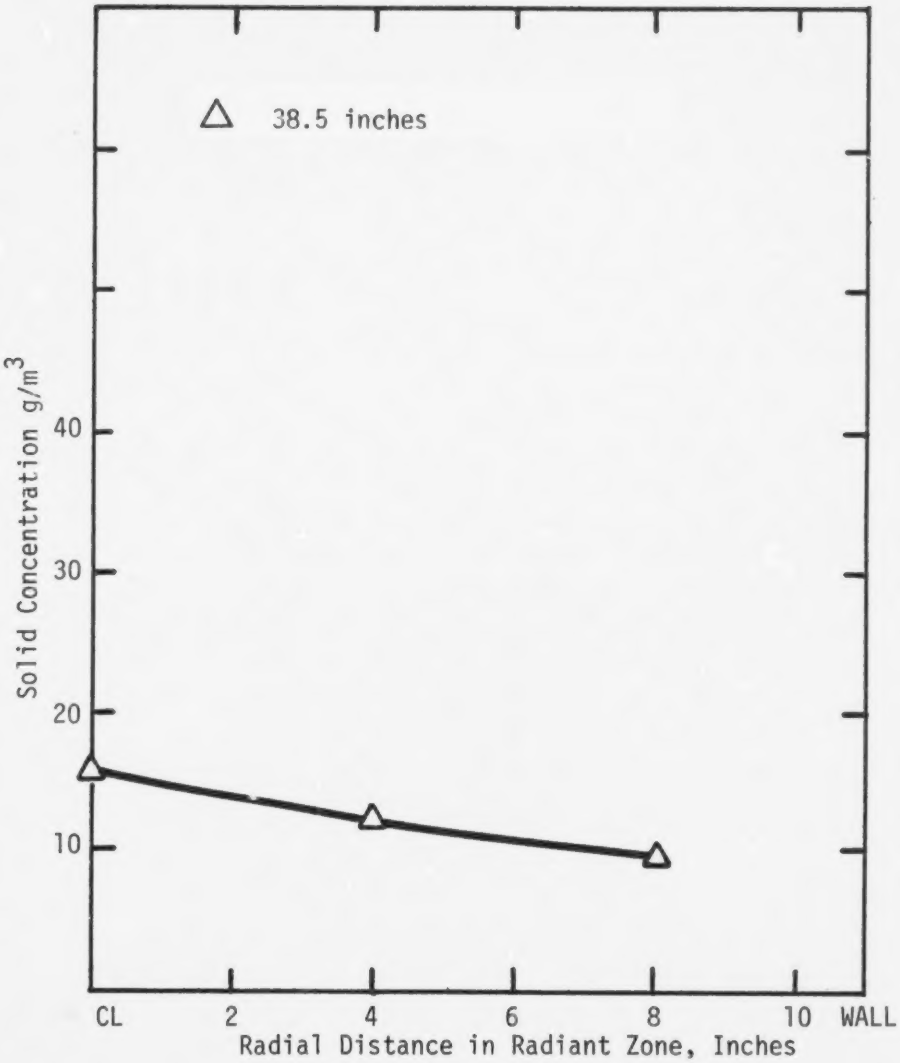

Figure 3-16. Solids loading, Indiana 3 flame, radial.

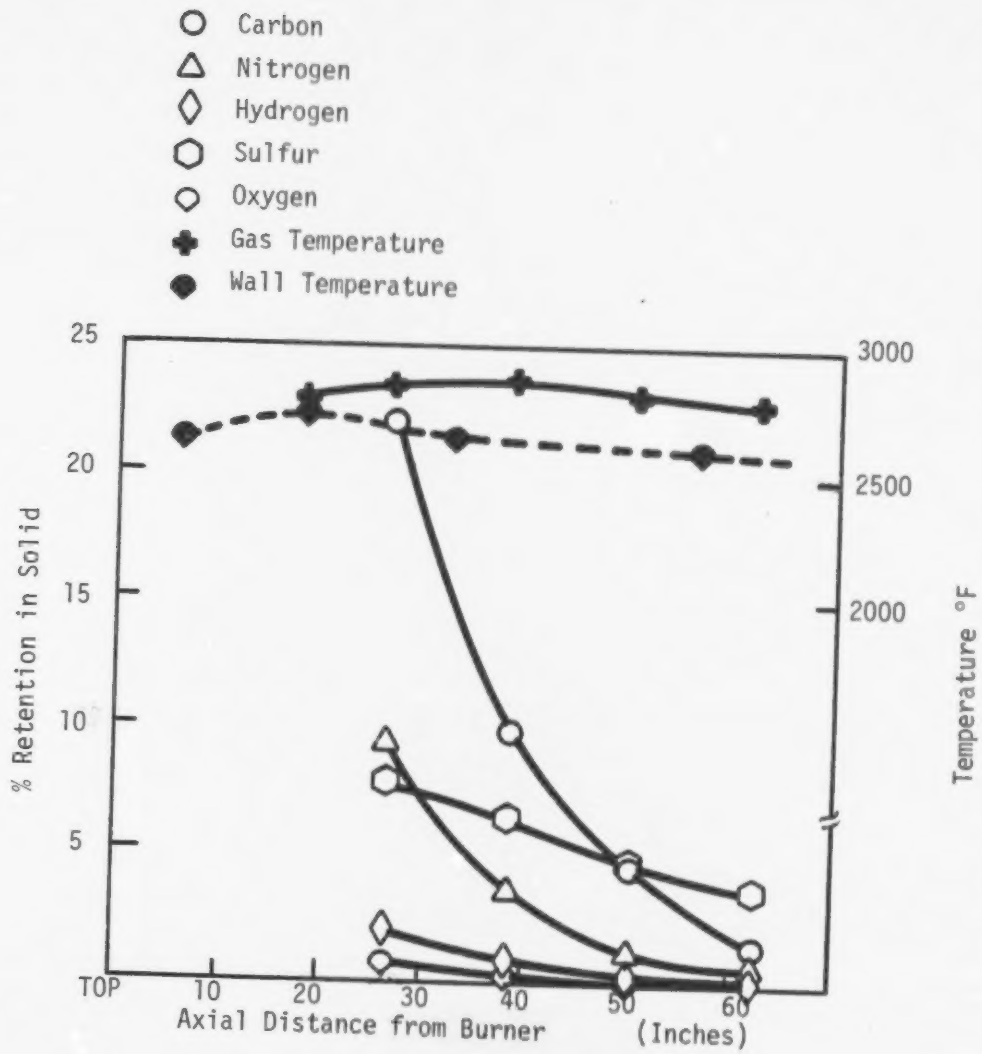

Figure 3-17. Evolution of species from Indiana 3 coal (radiant furnace).

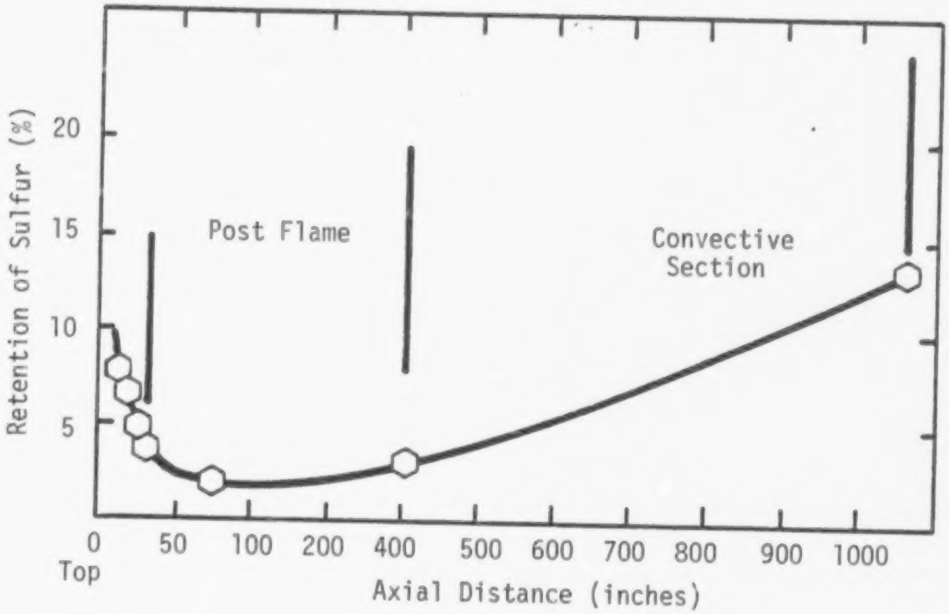

Figure 3-18. Retention of sulfur in solid, Indiana 3 coal.

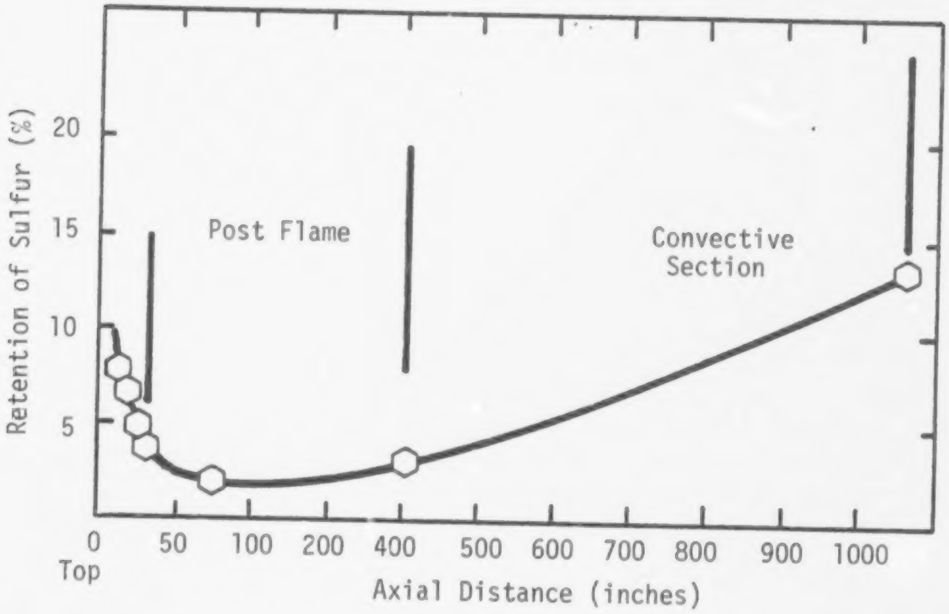

Figure 3-18. Retention of sulfur in solid, Indiana 3 coal.

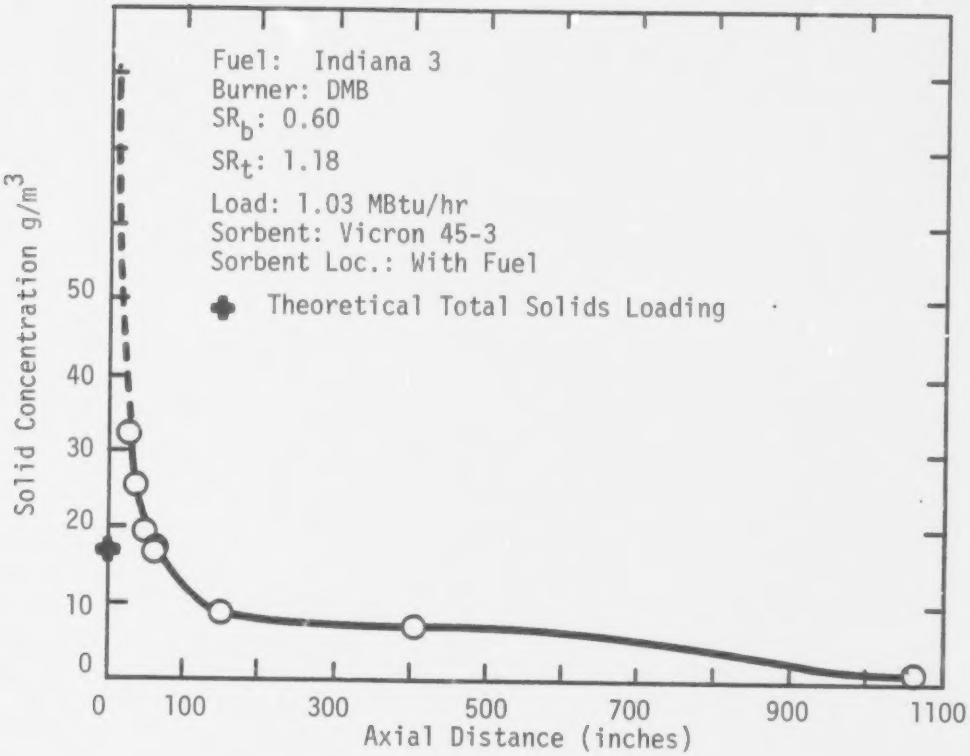

Figure 3-19. Solids loading, Vicron 45-3, with Indiana 3 coal, axial.

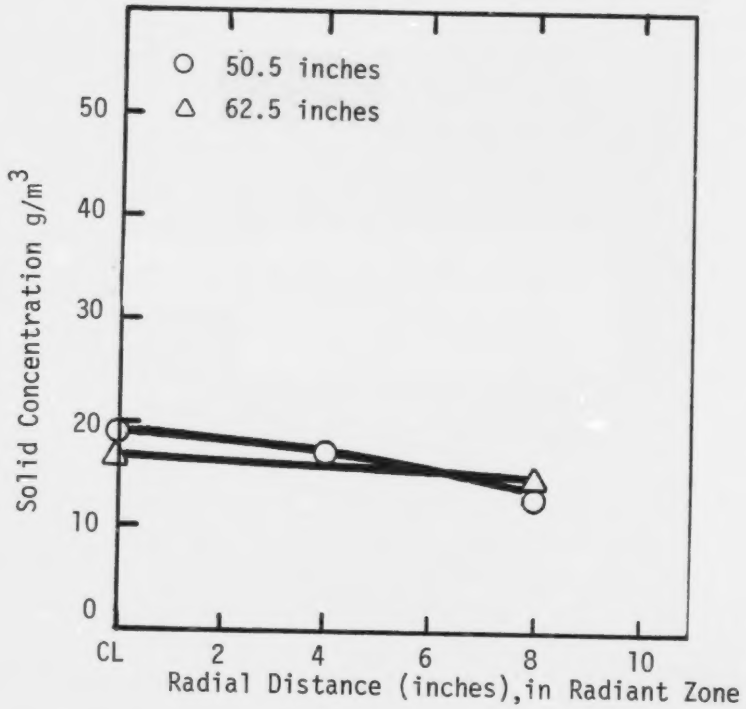

Figure 3-20. Solids loading, Vicron 45-3 with Indiana 3 coal, radial.

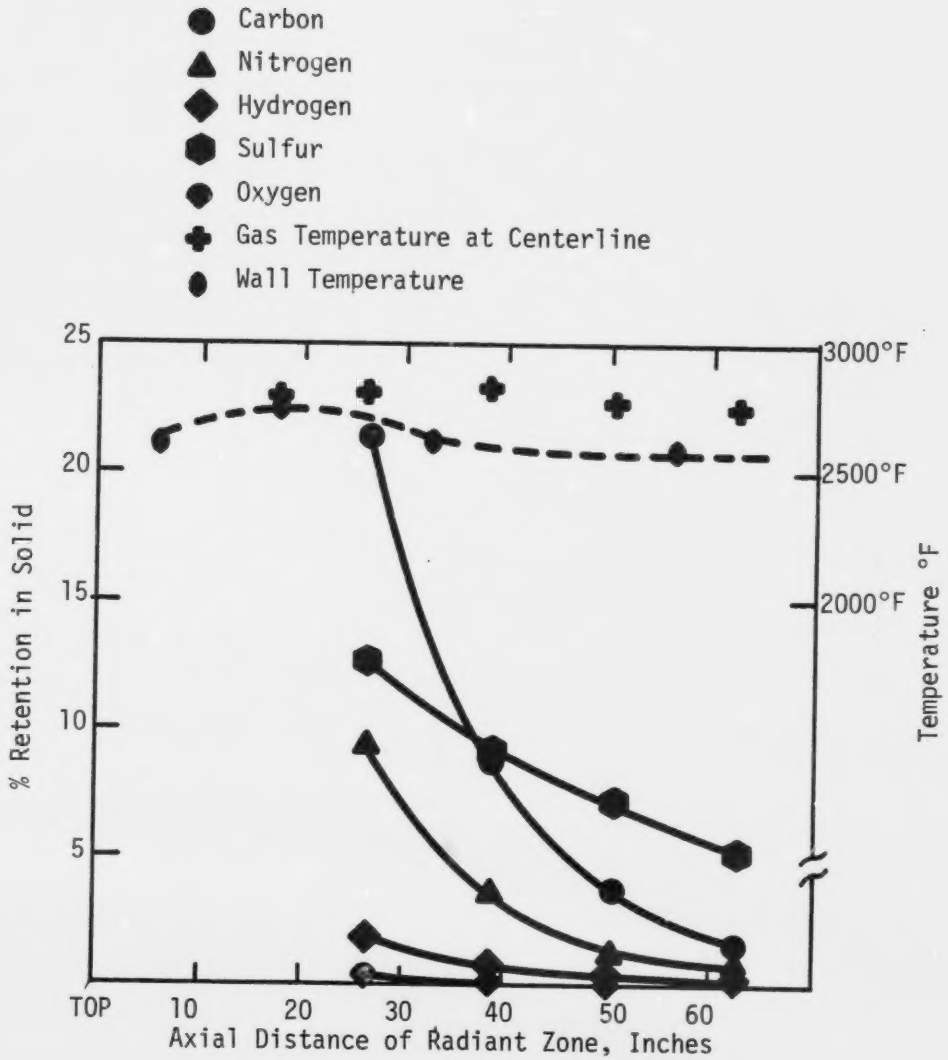

Figure 3-21. Evolution of species from Indiana 3 coal with Vicron 45-3 (radiant furnace).

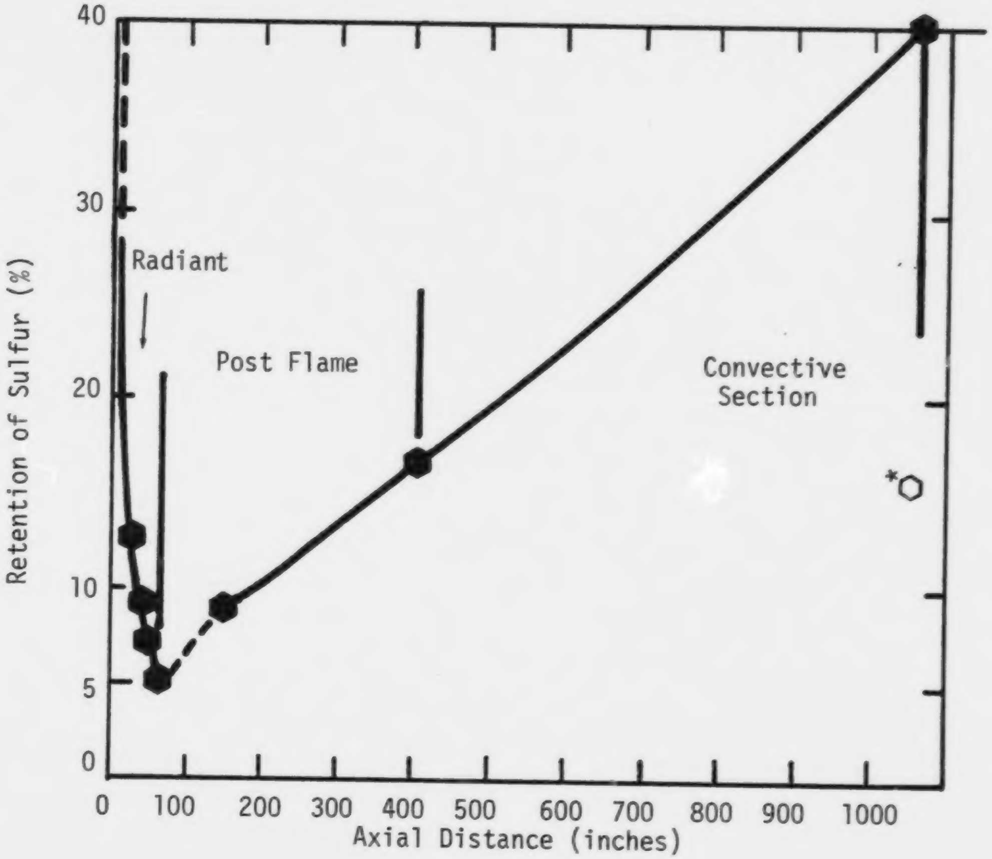

*Total retention without sorbent

Figure 3-22. Retention of sulfur in solid, Indiana 3 coal with Vicron 45-3.

The solid samples were analyzed for carbon, hydrogen, nitrogen and sulfur. These analyses were used to calculate retention of the various species in the solid using as ash a tracer. Figure 3-17 shows the results of these calculations. Retention of the various species in the solid is plotted as a function of axial location in Figure 3-17. Gas (centerline) and wall temperatures are also indicated. Carbon burnout is essentially complete at the exit of the radiant furnace. Nitrogen and hydrogen are also burned out, but some sulfur is retained in the the solid. Sulfur retention through the furnace is plotted in Figure 3-18. Solid sulfur decreases in the radiant furnace as the fuel burns out, remains low in the high temperature post-flame section and increases through the convective section. Inherent sulfur capture - retention of sulfur in the ash - is common for coal-fired systems and is a function of the fuel, the ash composition (especially alkali metal content) and the thermal characteristics of the combustor.

Similar samples (an axial profile at the centerline through the furnace) were taken for the Indiana coal flame with Vicron 45-3 injected with the coal. Solids concentration as a function of axial distance is plotted in Figure 3-19. The theoretical total solids loading was based on the coal/ash content, the flue gas volume and the sorbent feed rate assuming 100 percent burnout and 100 percent calcination of the sorbent. The solid retention characteristics of the furnace were essentially the same for the sorbent/ash and ash cases. Radial profiles at two locations in the coal/sorbent case (see Figure 3-20).

Analyses of the solid samples were used to calculate species retention in the radiant furnace. Carbon, hydrogen and nitrogen burnout characteristics were the same as for the plain coal conditions. Sulfur retention was higher for the sorbent added case (see Figure 3-21). Sulfur retention in the ash as a function of axial location is shown in Figure 3-22. As with the coal only case, sulfur in the solid dropped in the radiant furnace and was low in the high temperature portion of the post-flame section. The sulfur content of the solid rose considerably through the post-flame cavity to the exit of the convective section reflecting the sorbent/sulfur capture.

The calcium content of the ash/sorbent samples was also measured. The calcium carryover of the solid is indicated in Figure 3-23. Theoretical calcium was based on 100 percent carbon burnout and complete calcination of the sorbent. The calcium content of the ash at the furnace exit was seventy percent of theoretical reflecting some preferential loss of calcium in the furnace. From the data, most of this loss occurred in the first part of the post-flame section. It is not apparent why calcium would be retained at this point.

3.4 Conclusions - Detailed Measurements

Detailed measurements of temperatures, gas species and solids in the near-burner region were performed to better define two flames (coal and gas) which gave disparate sorbent utilizations. These detailed measurements showed slight differences in flame shape and peak flame temperatures (the coal flame was somewhat shorter and hotter near the burner than the gas flame) and confirmed the difference in sorbent utilization in the two flames. There was some loss of calcium (sorbent) in the furnace when coal was fired and considerable dropout of solids through the furnace with either fuel. The measured differences in temperature and flame shape hardly seem sufficient to account for the observed difference in sulfur capture. It appeared that some fuel effect not directly reflected in temperature or gaseous species concentrations was responsible for the lower sulfur capture in the coal flame.

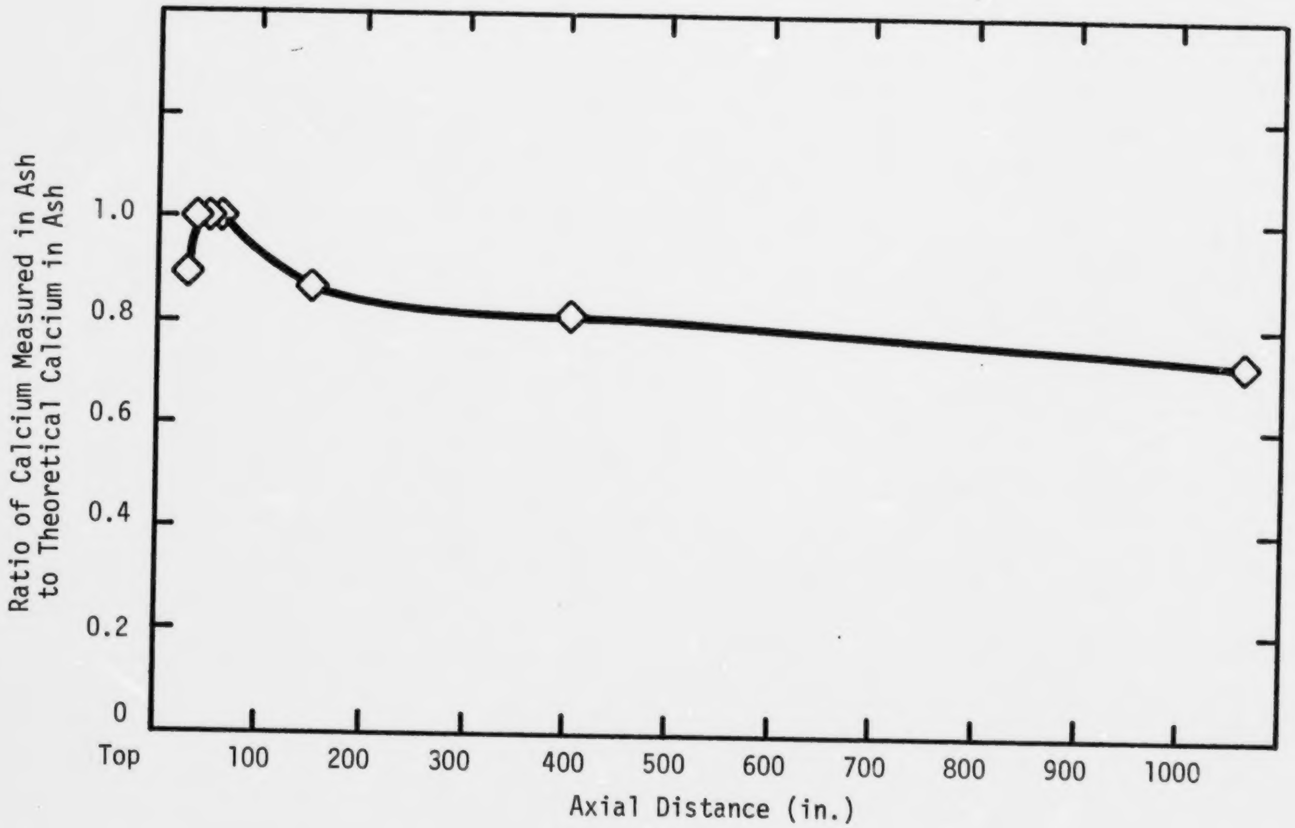

Figure 3-23. Calcium retention in ash, Boiler Simulator Furnace.

4.0 THERMAL EFFECTS - BURNER AND OPERATIONAL EFFECTS, HIGH TEMPERATURE FLAMES

Detailed measurements of gas temperatures and species concentrations in a natural gas flame and a coal flame which gave very different sorbent utilizations showed small differences in peak flame temperature and flame shape. These differences did not appear to be great enough to account for the observed difference in sorbent utilization, however, thermal differences, especially peak temperature, have been shown in other studies to have a dramatic effect on sorbent reactivity. In order to ascertain the effect of temperature differences on capture in a simple system (gas fuel only), several experiments were performed. These experiments emphasized high temperature conditions and were mostly concerned with changes in the region near the burner. Experiments investigating burner effect, including fuel injector type and burner zone stoichiometry, the effect of load (especially concerned with changes in residence times), and high temperature (O_2 enriched) flames were performed.

4.1 Burner Effects

Natural gas doped with H_2S was fired using two fuel injectors, radial and axial. The axial fuel injector was simply an open-ended straight pipe which delivered the fuel at the center of the burner throat. The radial injector consisted of a pipe (the same size as the axial injector) with one small hole (3/16") at the end and eight similar holes spaced evenly around the outside of the pipe 1/2" back from the end. The flames produced by these fuel injectors were different, the axial flame was much longer and narrower than the radial flame and produced lower levels of NO than the radial flame. Sulfur capture by Vicron 45-3 injected with the fuel was measured for both the radial and axial flames. The radial configuration was also fired using 400°F air preheat to give a higher temperature, higher NO_x condition. The burner was staged at SR_b 0.6 and SR_t 1.2 for all of these conditions. Figure 4-1 summarizes the sulfur capture measured. The fuel injection method and air heat with the radial injector made essentially no difference in the sulfur capture measured.

Fuel Nat-H_2S
% S
Sorbent Vicron 45-3
Sorbent Loc. w/fuel
Load (MBtu/hr) 1.04
Burner DMB
Inj. Shown
SR_b 0.6
SR_t 1.2
SO_2(ppm) 1800

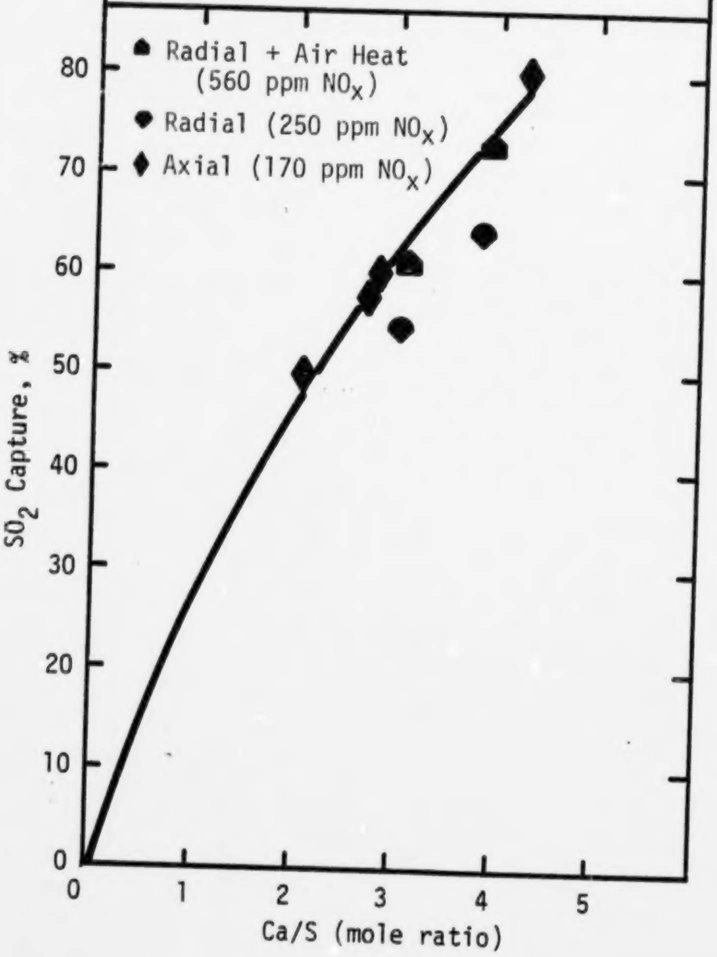

Figure 4-1. Effect of Fuel Injection on Capture Natural Gas + H_2S Flame, Sorbent with Fuel.

The effect of staging on both SO_2 capture and NO_x emissions was investigated with both injections (the radial injector with air heat). Sulfur capture and NO_x emissions are shown as a function of burner zone stoichiometry in Figures 4-2 and 4-3. Sorbent was added with the fuel in all of the tests. Several results are of interest. Sorbent addition resulted in a decrease in NO_x emissions, no matter which injector was used or at what burner zone stoichiometry. This decrease in NO_x is probably a thermal effect. Calcination of $CaCO_3$ is an endothermic reaction. The heat required to calcine the sorbent comes from the gas flame in the region very near the burner. The calcination reaction probably requires enough heat to drop the gas flame temperature and, therefore, decrease the formation of thermal NO.

Burner zone stoichiometry had a slight effect on sulfur capture for both flames. Capture was higher for the unstaged flame with the high temperature, radial flame and lower for the axial flame than when the burner was staged. It was also apparent that in the high temperature system more of the total sulfur capture occurred in the convective passes (which were hotter) than with the cooler axial-flame system. The shift in sulfur capture location is consistant with the change in temperature profile for the two firing modes (see Figure 4-4), but the different effect of burner zone stoichiometry is not easily explained.

Gas temperature measurements of the two flames were made at three locations in the radiant furance. Temperatures in the unstaged flames are summarized in Figures 4-7 and 4-8. The air heat/radial injector was indeed considerably hotter than the axial flame and the high temperatures were maintained longer (2900°F vs 2700°F at the bottom of the radiant furnace). One would have expected that the extremely high temperatures in the radial flame would have deactivated the sorbent, resulting in lower capture. In fact, the overall capture was higher, with a significant portion taking place in the convective section. This implies that the sorbent retained sufficent reactivity even though it passed through very high temperature regions.

The effect of unstaged firing on sulfur capture with the Indiana coal was tested. There was essentailly no differnce in capture with the two firing

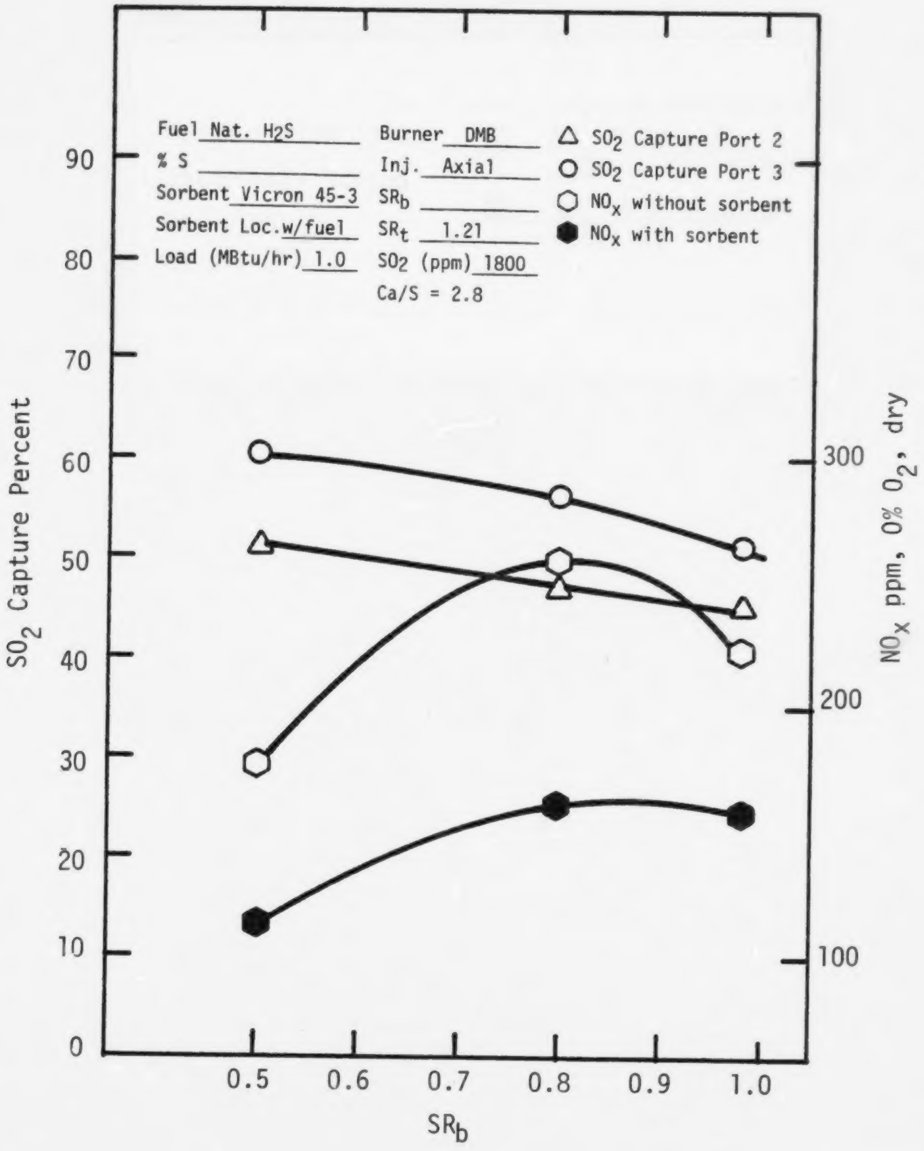

Figure 4-2. Effect of burner zone stoichiometry on sulfur capture and NO_x, axial injector.

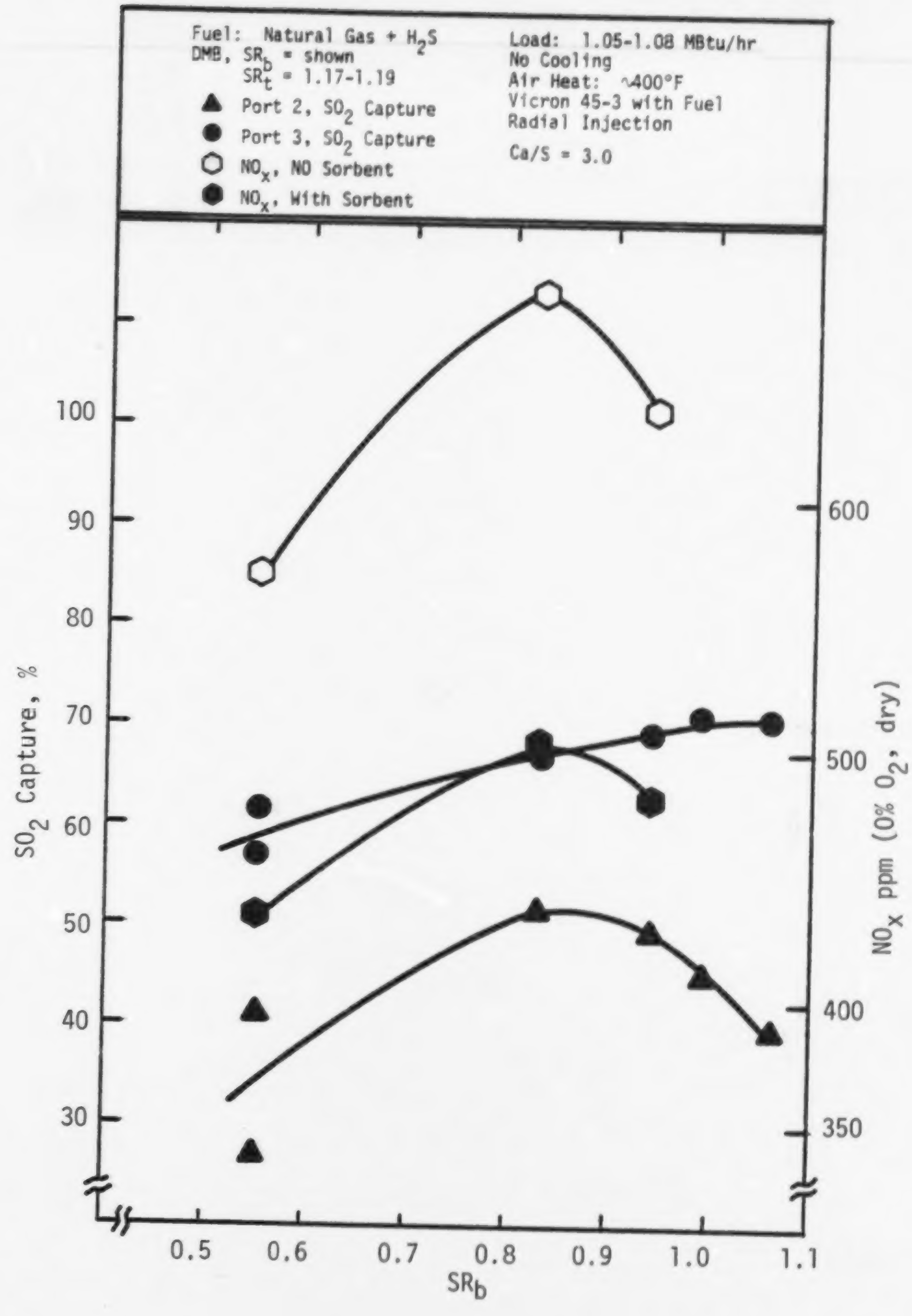

Figure 4-3. Effect of burner zone stoichiometry on sulfur capture and NO_x, radial injector, with air heat.

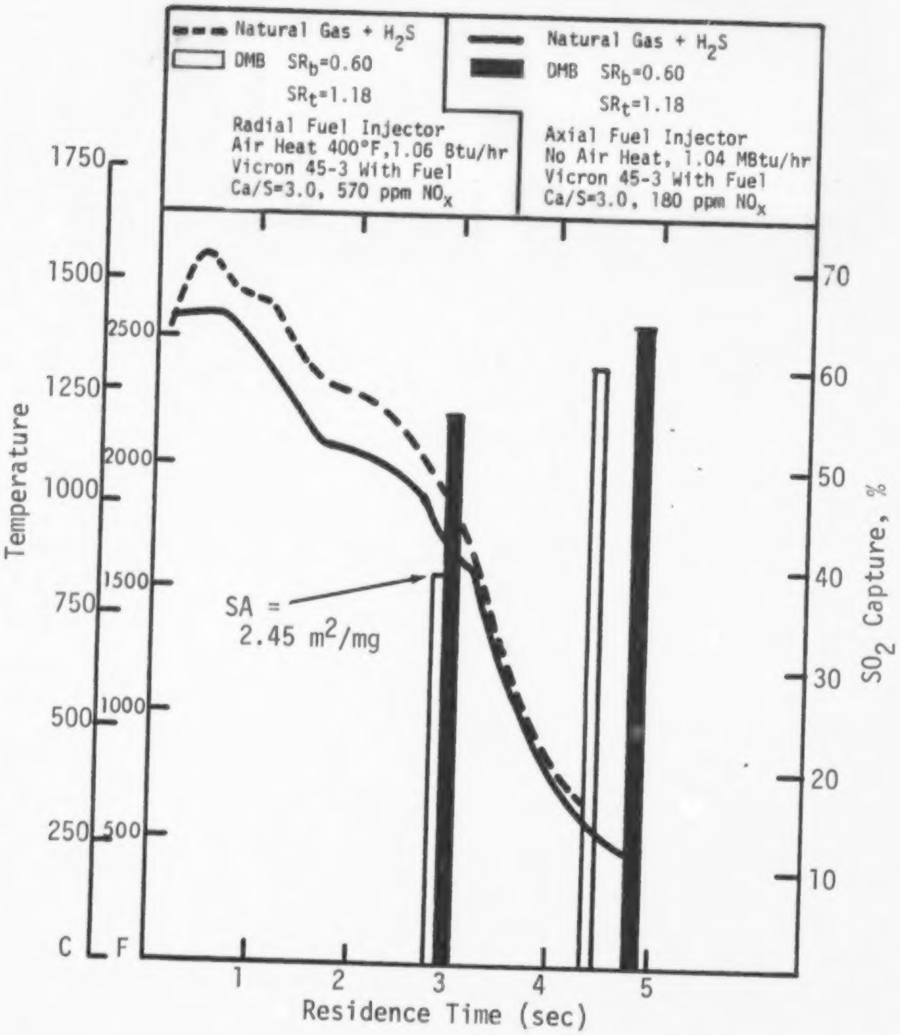

Figure 4-4. Thermal history comparison: two fuel injectors, staged.

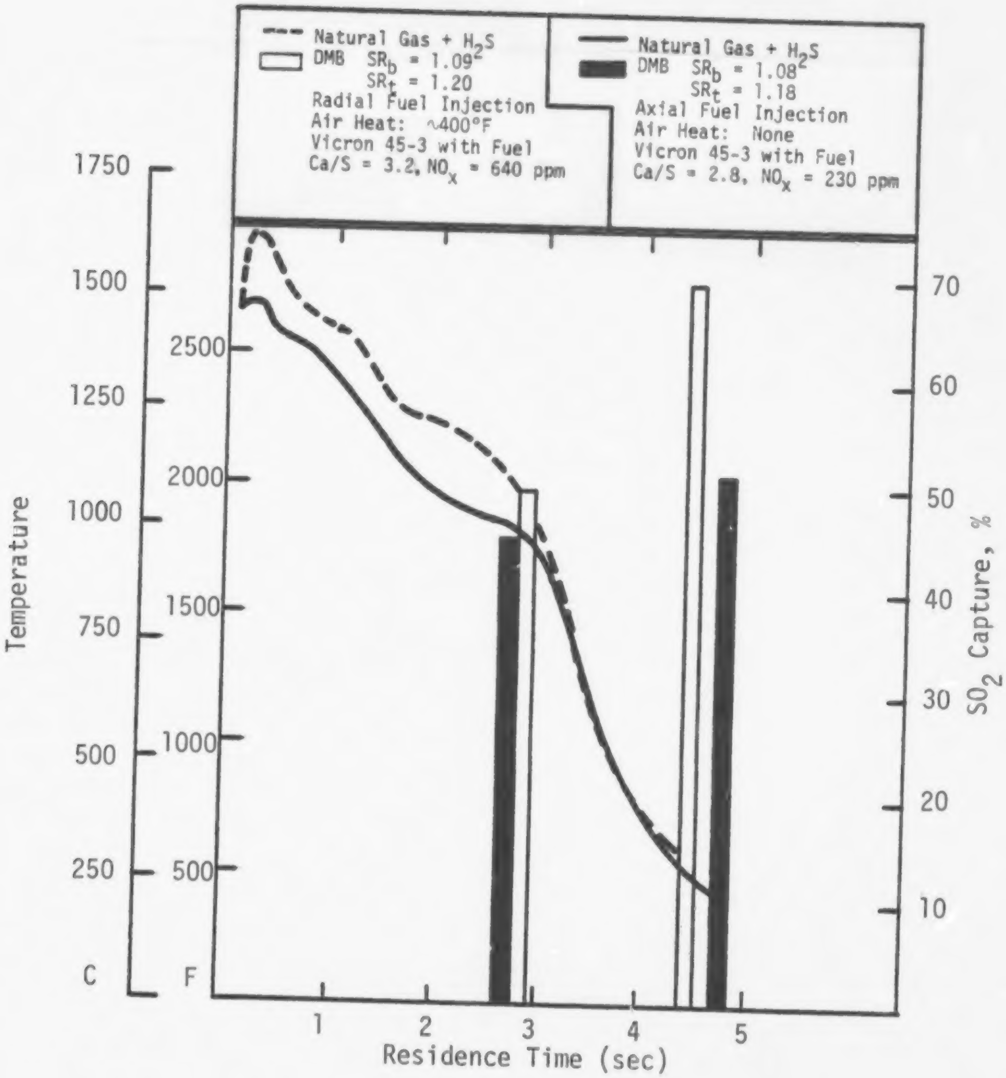

Figure 4-5. Thermal history comparison: two fuel injectors unstaged.

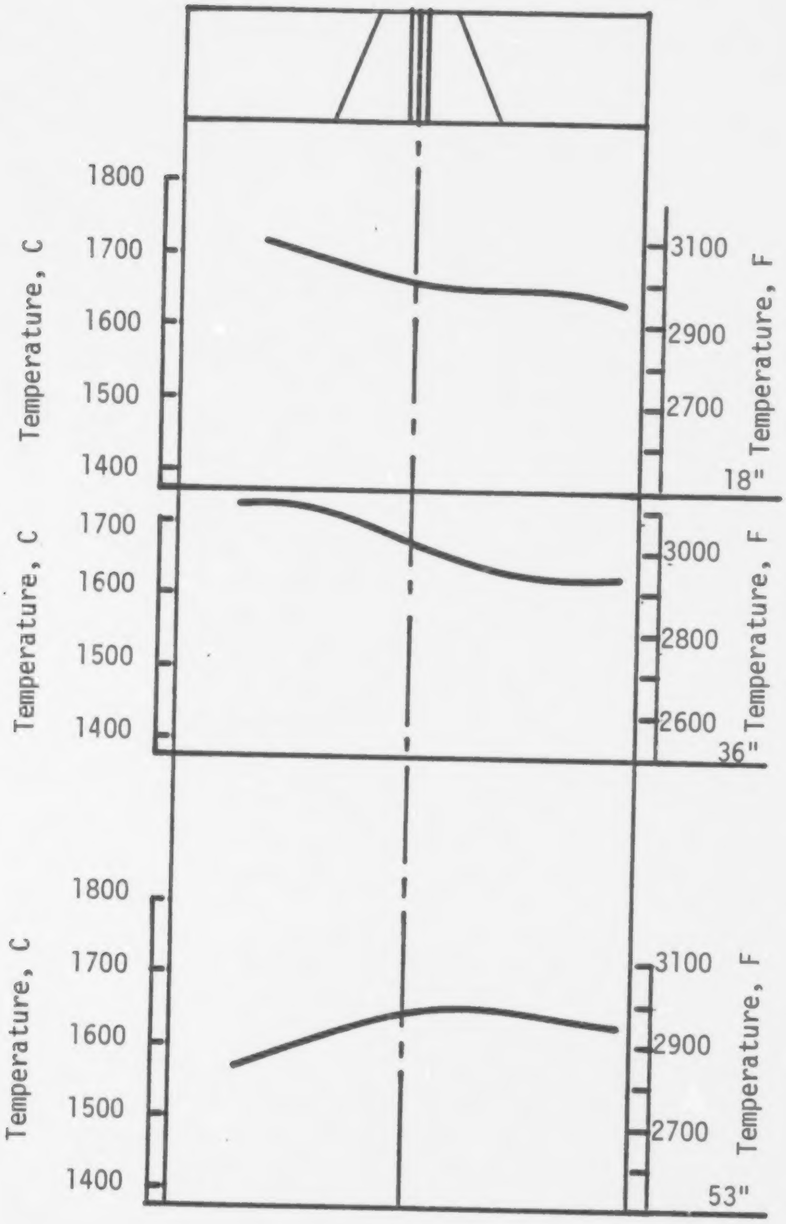

Figure 4-6. Detailed temperature measurements, natural gas flame, radial injector with 400°F heat.

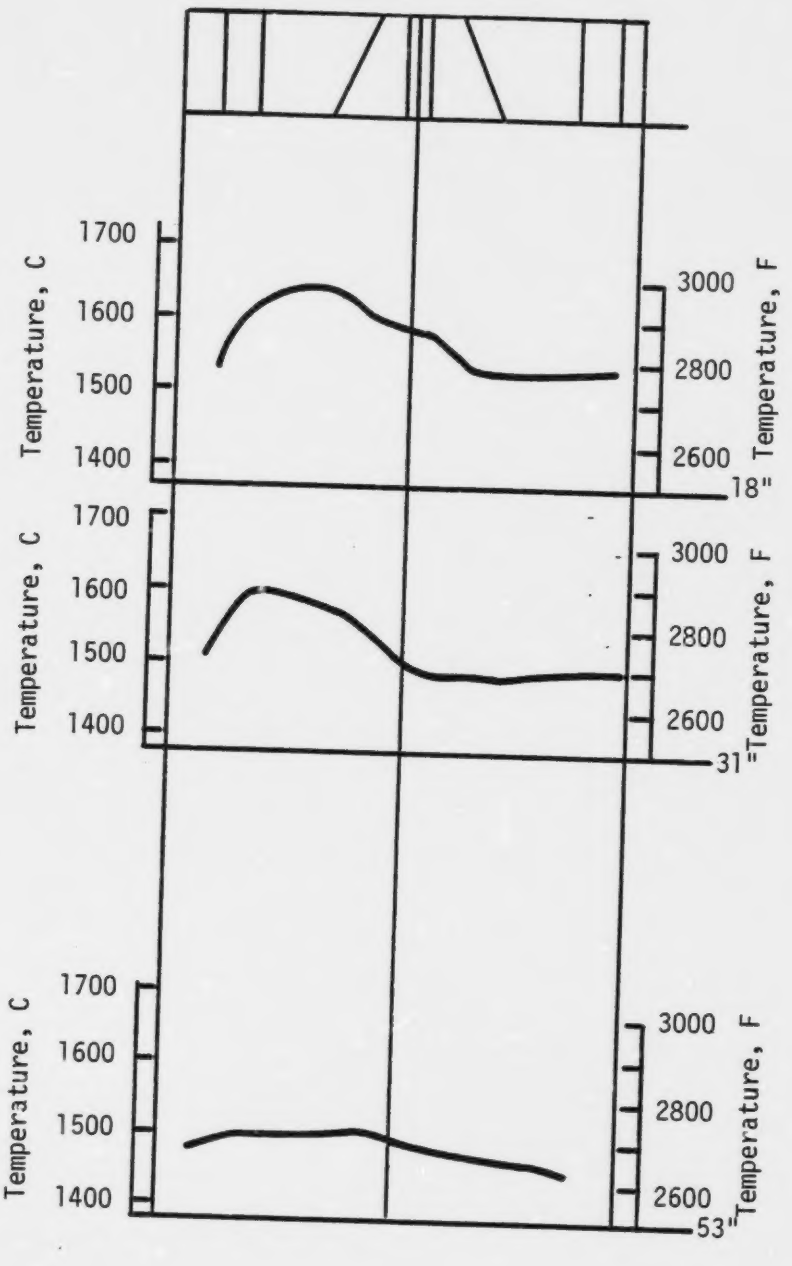

Figure 4-7. Detailed temperature measurements, natural gas flame, axial injector, unstaged, no air heat.

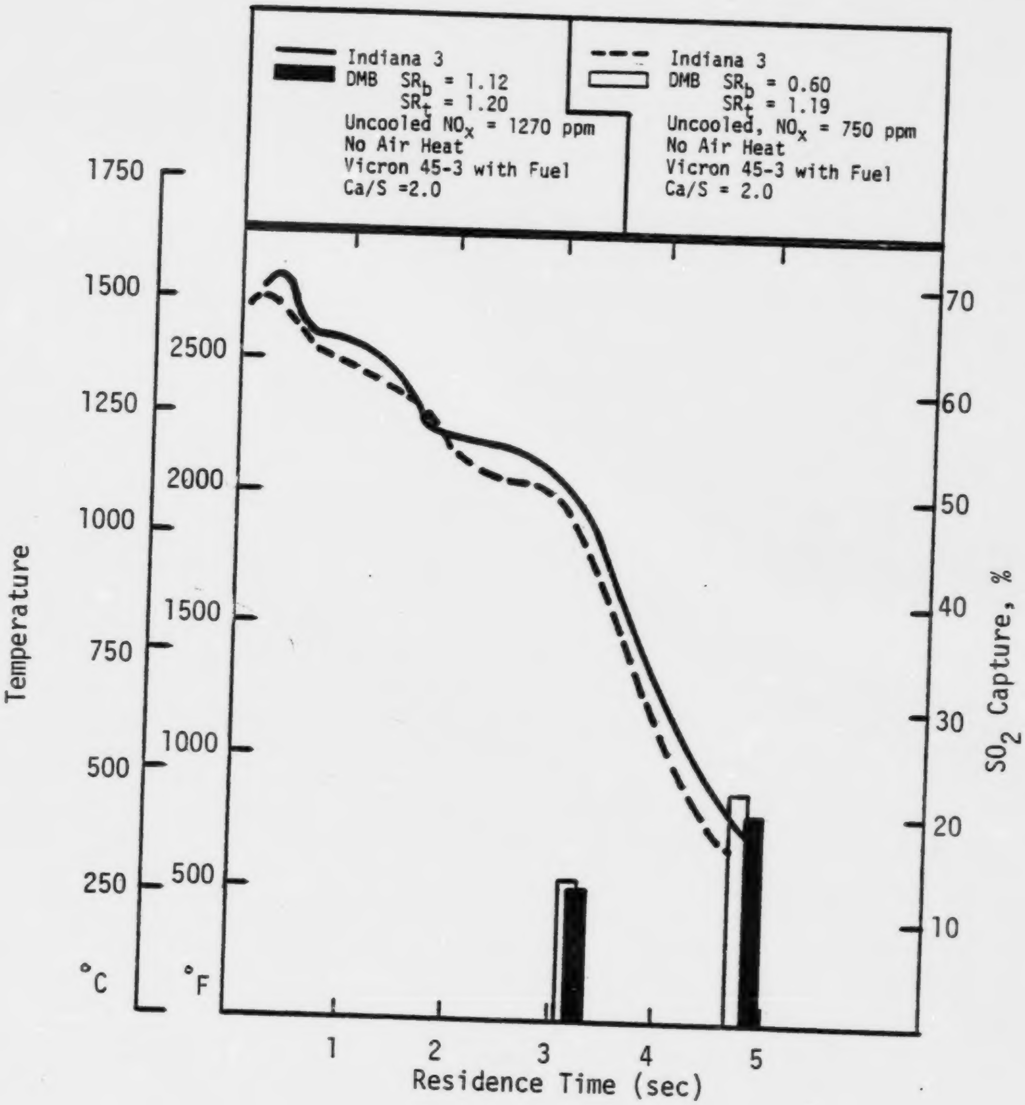

Figure 4-8. Thermal history and sulfur capture for staged and unstaged Indiana 3 coal flames.

conditions even though the peak temperature was somewhat higher for the unstaged case (see Figure 4-8).

4.2 Operational Effect - Effect of Load

The boiler simulator furnace was fired with natural gas/H_2S at two loads, 1.0 and 1.8 MBtu/hr. Vicron 45-3 was injected with the fuel and sulfur capture was measured at three locations. Figure 4-9 shows sulfur capture as a function of Ca/S mole ratio of the baseline, 1.0 MBtu/hr load. Capture at a load of 1.6 MBtu/hr is summarized in Figure 4-10. Overall capture at the two loads was similar, however the location in the furnace where capture took place, and the residence times involved were quite different. Figure 4-11 shows temperature profiles and sulfur captures for the two cases. The peak temperature was higher and the total residence time was shorter at the high load. More sulfur capture took place in the convective section (between port 2 [1.9 sec.] and port 3 [2.8 sec.] than for the low load case. The convective section was hotter (entrance temperature 2000°F rather than 1800°F) at high load, which probably explains the higher capture in that section. It is not apparent why the higher temperatures and shorter residence times at the high load did not yield lower capture.

4.3 High Temperature Flames

None of the high temperature gas-fired conditions investigated resulted in decreased sulfur capture due to the high temperature. In order to produce an extreme condtion the BSF was fired on natural gas doped with H_2S using oxygen-enriched air. The burner was unstaged and the radial fuel injector used to produce the highest temperature flames. Sorbent was injected with the fuel.

The temperature profiles and sulfur captures obtained with these flames are summarized in Figure 4-12. Oxygen enrichment increased overall furnace residence time and peak flame temperature by reducing the overall mass throughput rate. NO_x levels increased from 500 ppm for the air-fired case to 3200 ppm for the 30 percent O_2-fired case. Peak gas temperatures increased

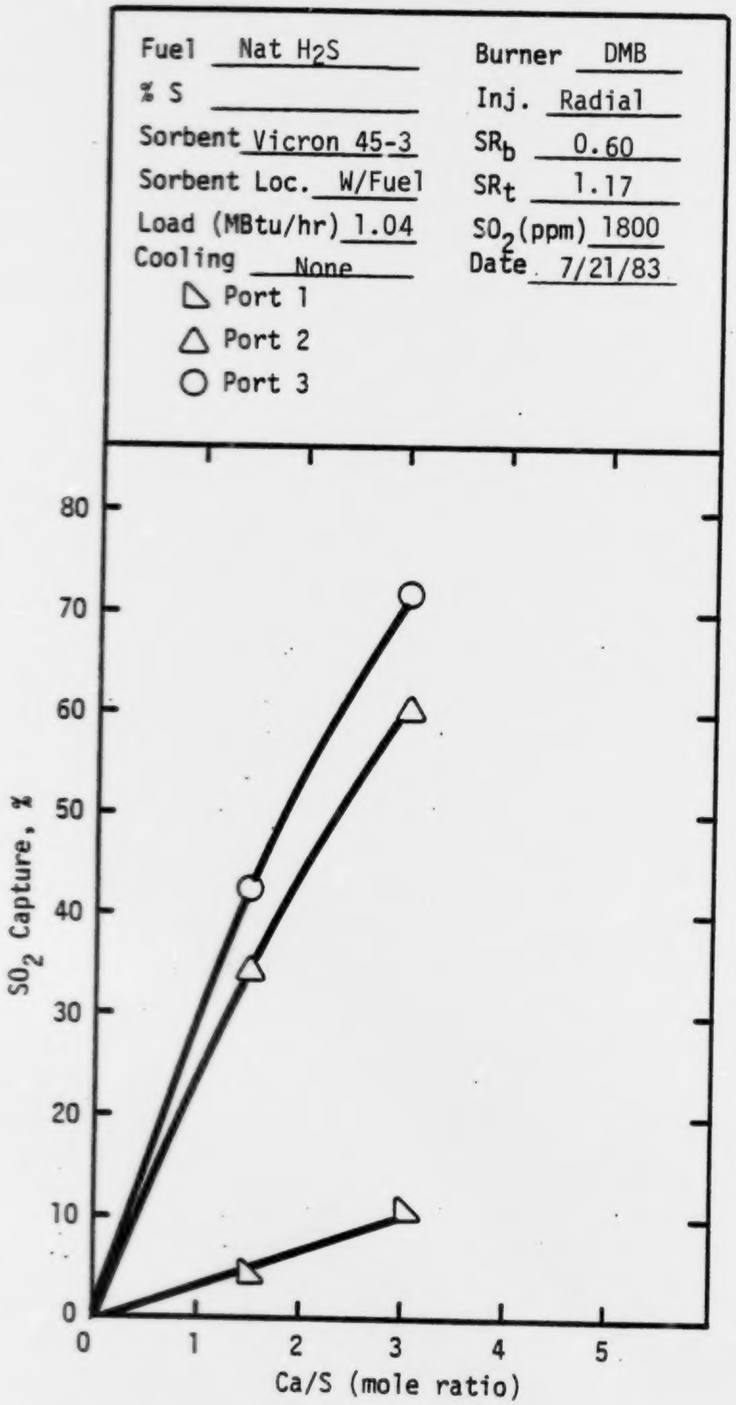

Figure 4-9. Sulfur Capture at Baseload (1.0 MBtu/hr) BSF, Natural Gas + H_2S with Vicron 45-3.

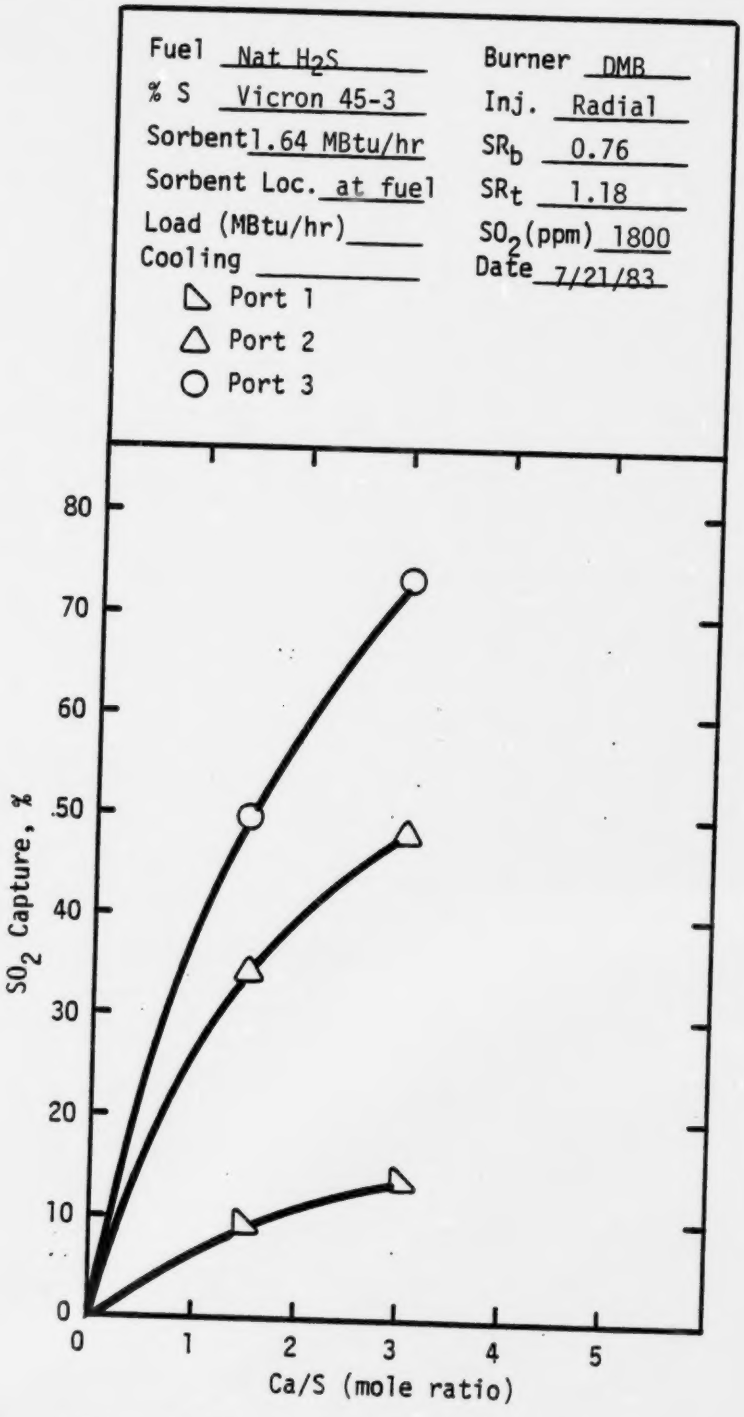

Figure 4-10. Sulfur Capture at High Load (1.6 MBtu/hr) BSF, Natural Gas + H_2S with Vicron 45-3.

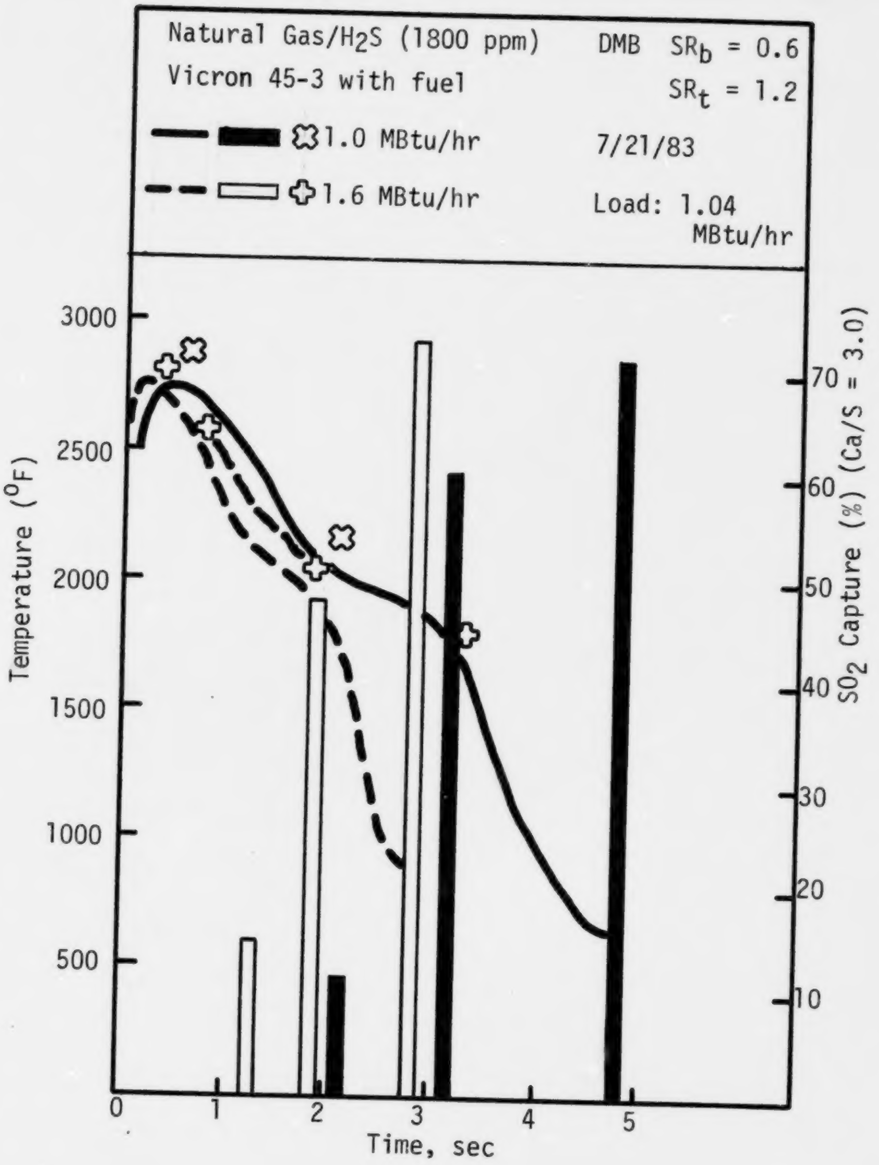

Figure 4-11. Effect of load on thermal history and sulfur capture, BSF, natural gas, Vicron 45-3.

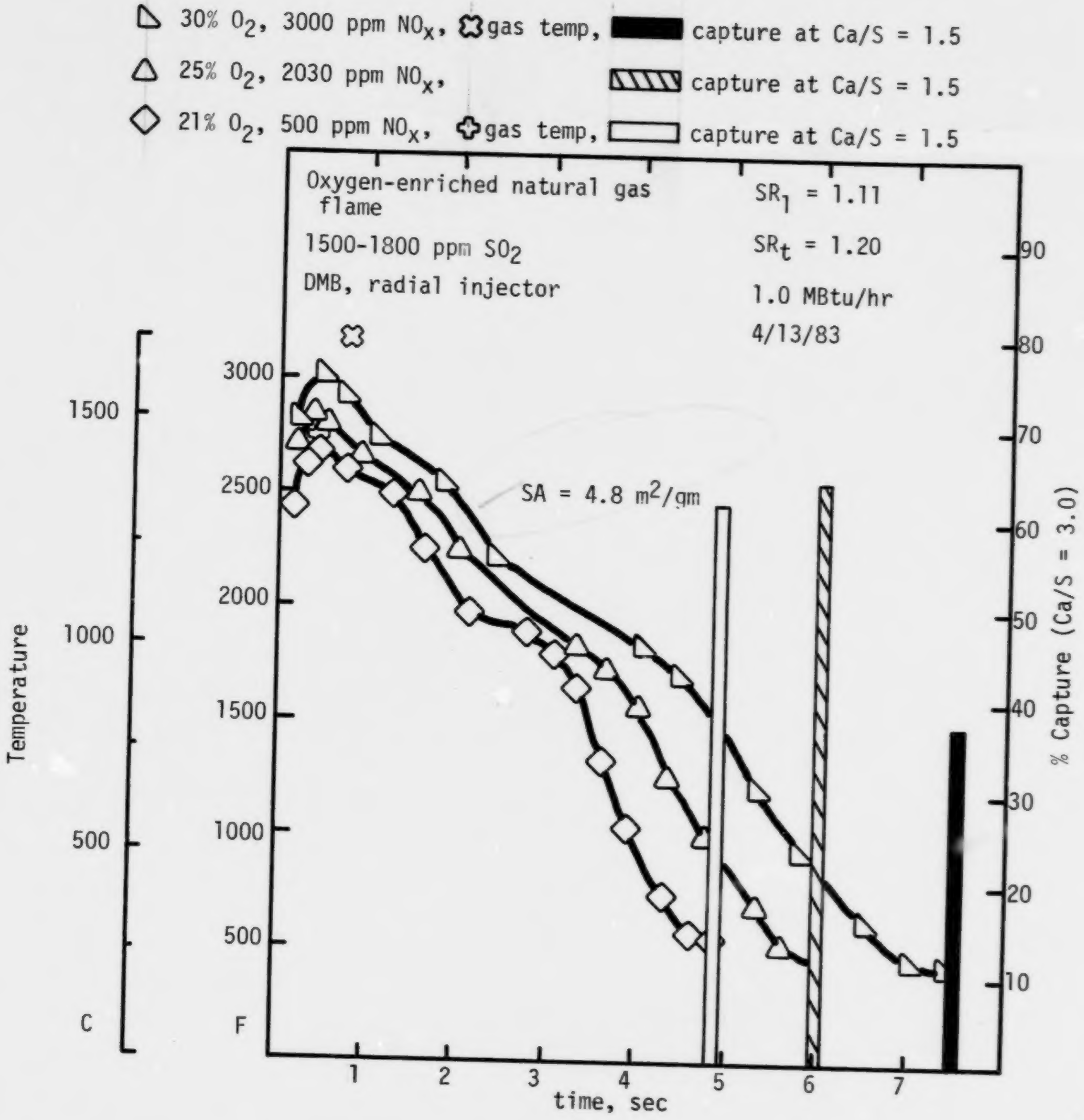

Figure 4-12. Effect of oxygen addition on thermal history and sulfur capture, natural gas/H_2S flames (conditions as in Figure 5-11).

from 2800 to 3100°F. Sorbent utilization was lower in the high temperature flame, but not dramatically so, possibly because the increased residence time compensated somewhat for the change in sorbent reactivity.

4.4 Conclusions

Investigation of the effect of various thermal conditions on sulfur capture from gas flames indicated that overall sulfur capture in the BSF was only slightly affected by very significant increases in flame temperature. Changes in burner characteristics, including fuel injector and staging level also had minor effects on sulfur capture. The change in sulfur capture produced by altering the thermal characteristics of the natural gas flame were much less dramatic than the difference in capture between gas and coal flames.

The data in Figure 4-13 show how much more significant the fuel change was than the change in temperatures. Temperature profiles for natural gas/H_2S at two thermal conditions are shown with the Indiana coal temperature profile. Capture throughout the BSF at a constant calcium-to-sulfur ratio is also shown for the three conditions. The gas temperature profiles essentially bracket the coal profile, but the capture for both gas conditions was higher than for the coal. These results combined with the detailed measurements discussed in Chaper 3 indicate that the effect of fuel type on sulfur capture is not a simple, direct result of thermal differences in the flames. These results strongly reinforced the concept that some other component of the coal, most likely the ash, was having a deactivating effect on the sorbent. The role of ash and the mineral components contained in coal were explored - the results of these studies are discussed in the next chapters.

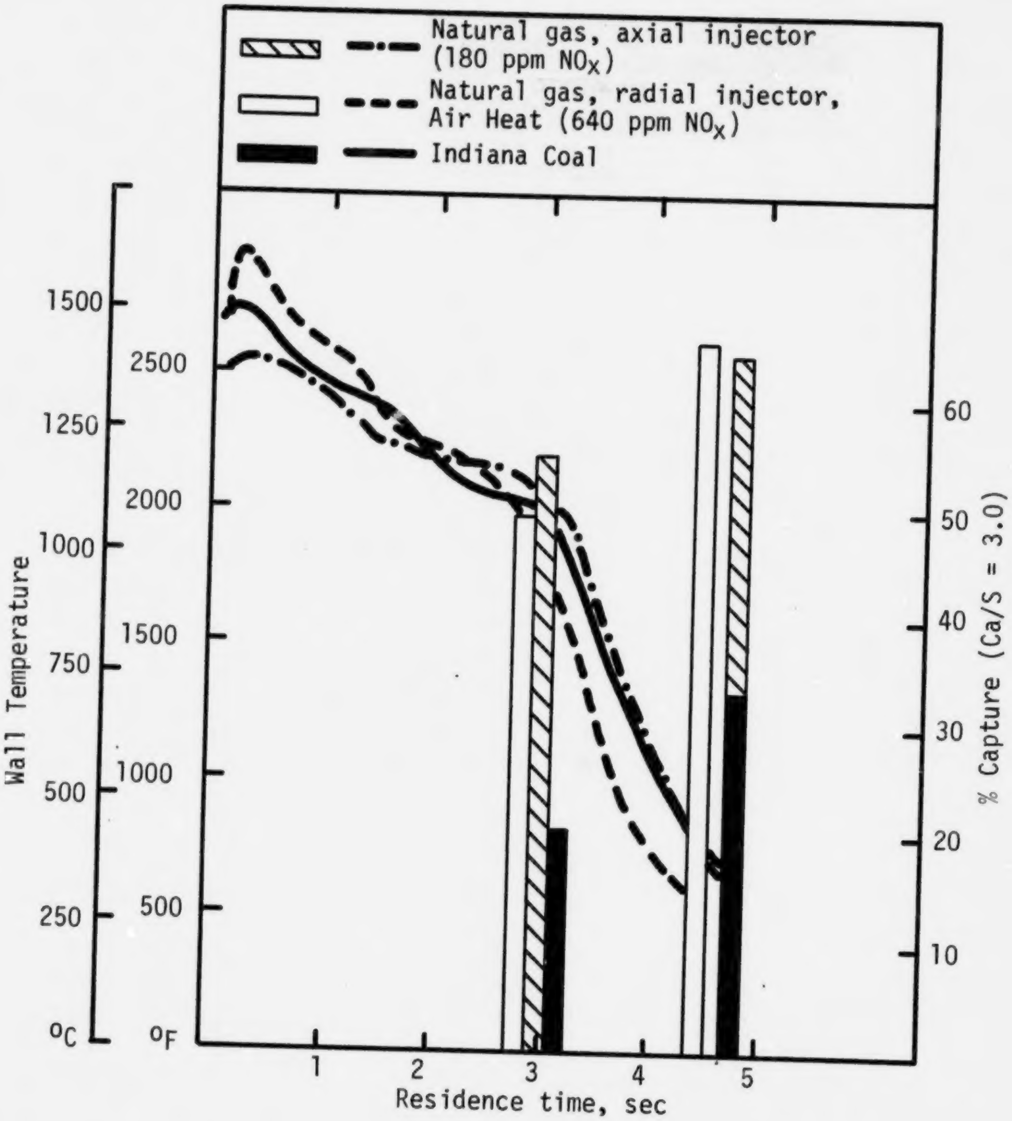

Figure 4-13. Comparison of Sulfur Capture in High and Low Temperature Gas Flames with Indiana Coal Flame.

5.0 SULFUR CAPTURE MODEL

The capture of sulfur by solid sorbents injected directly into the furnace is a complex process. Modeling helps to understand and clarify the parameters involved in the sulfur capture process. The general approach has been to divide the process into the two zones of sorbent activation and sorbent sulfation as shown in Figure 5-1, and to model each zone separately. The first zone, sorbent activation, includes the processes which ultimately govern sorbent reactivity and sulfation capacity; these processes include: particle heat-up, calcination, and deactivation as a result of over-heating and/or interfering chemical reactions. The second zone, sulfate formation, includes the processes which control sulfate formation, including: diffusion within the particle pores, chemisorption, reaction with the solid, diffusion through the reactant layer, blockage of the pores due to sulfate formation, and the thermal stability limits of the sulfate.

5.1 Sorbent Activation Model

Sorbent activation has been studied in detail under EPA contract 68-02-3633 as described by Cole, et al. (1983). This section is a brief summary of the major conclusions concerning sorbent activation.

The rate at which a sorbent particle calcines depends upon the heat capacity of the particle, convective heat transfer between the particle and the surrounding gas, radiative heat transfer between the particle and the walls of the combustion system, and heat consumption in the endothermic calcination process. Within the ranges of interest, particle heat-up is generally dominated by convection; and both heat-up and calcination are essentially complete within 1 to 10 milliseconds. Thus, unless low temperatures (below $1500^{o}K$) or large particles (above 100 μm) are encountered, calcination is fast compared to sulfation.

As a sorbent particle calcines, its internal surface area increases due to the conversion of $CaCO_3$ to less bulky CaO. At high temperatures, internal surface area decreases as sintering or dead-burning results in pore closure.

5.0 SULFUR CAPTURE MODEL

The capture of sulfur by solid sorbents injected directly into the furnace is a complex process. Modeling helps to understand and clarify the parameters involved in the sulfur capture process. The general approach has been to divide the process into the two zones of sorbent activation and sorbent sulfation as shown in Figure 5-1, and to model each zone separately. The first zone, sorbent activation, includes the processes which ultimately govern sorbent reactivity and sulfation capacity; these processes include: particle heat-up, calcination, and deactivation as a result of over-heating and/or interfering chemical reactions. The second zone, sulfate formation, includes the processes which control sulfate formation, including: diffusion within the particle pores, chemisorption, reaction with the solid, diffusion through the reactant layer, blockage of the pores due to sulfate formation, and the thermal stability limits of the sulfate.

5.1 Sorbent Activation Model

Sorbent activation has been studied in detail under EPA contract 68-02-3633 as described by Cole, et al. (1983). This section is a brief summary of the major conclusions concerning sorbent activation.

The rate at which a sorbent particle calcines depends upon the heat capacity of the particle, convective heat transfer between the particle and the surrounding gas, radiative heat transfer between the particle and the walls of the combustion system, and heat consumption in the endothermic calcination process. Within the ranges of interest, particle heat-up is generally dominated by convection; and both heat-up and calcination are essentially complete within 1 to 10 milliseconds. Thus, unless low temperatures (below 1500^{o}K) or large particles (above 100 μm) are encountered, calcination is fast compared to sulfation.

As a sorbent particle calcines, its internal surface area increases due to the conversion of $CaCO_3$ to less bulky CaO. At high temperatures, internal surface area decreases as sintering or dead-burning results in pore closure.

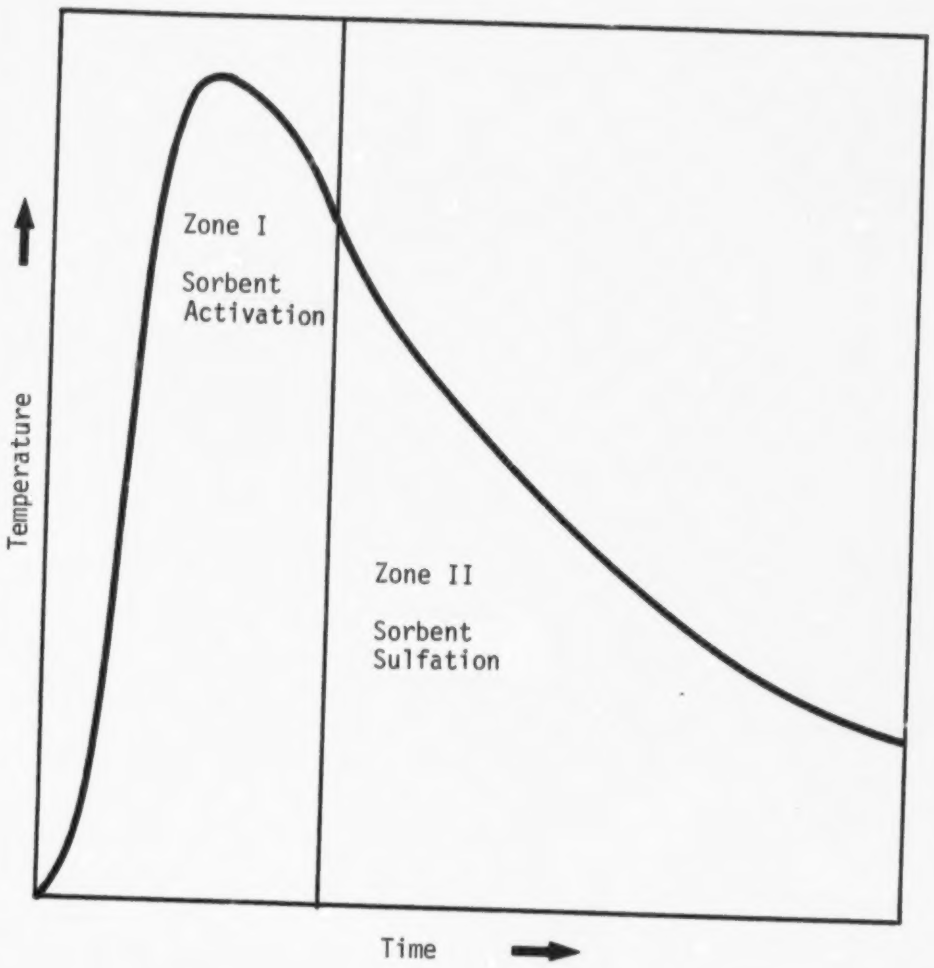

Figure 5-1. Zone approach to sulfur capture model.

A fundamental model describing the growth and decay of surface area has not yet been developed, however, a simple empirical curve fit relating ultimate surface area to peak particle temperature appears to be an adequate substitute. Figure 5-2 shows such a correlation for limestone.

Thus the sorbent activation model is very simple. Particle heat-up and complete calcination is assumed to occur instantaneously resulting in a particle surface area which depends on the peak temperature which the particle encounters.

5.2 Sorbent Sulfation Model

Two basic methods of modeling the SO_2-lime (CaO) reaction are currently available, having been developed by various workers to model reactions occuring in fluidized-bed combustors. The two main approaches to modeling the sulfation processes are: 1) The grain model which treats the sorbent as single calcium/oxide particles made up of tiny, non-porous micro-pellets; the void spaces between these micro-pellets being the pores of the larger particles. SO_2 in the gas-phase diffuses through these pores to the surface of the micro-pellets where reaction with CaO occurs. As reaction proceeds, a shell of reaction product uniformly accumulates around the surface of the CaO micro-pellets. Further reaction occurs only after gas diffuses through the pore structure of the particle and then through the reaction product layer around the micro-pellets to the inner core of the fresh, unreacted calcium/oxide which gradually shrinks in size until only a pellet of reaction product remains (Hartman, 1976). 2) The pore model (developed by Bhatia and Perlmutter, 1981) which treats the particles as spheres enveloping a random distribution of cylindrical pores which provide the overall particle surface area. A computer program of this random pore model applied to the SO_2-lime reaction has been coded for use at EER. This section describes the pore model, and outlines the procedures used to verify the model and to identify the most sensitive parameters.

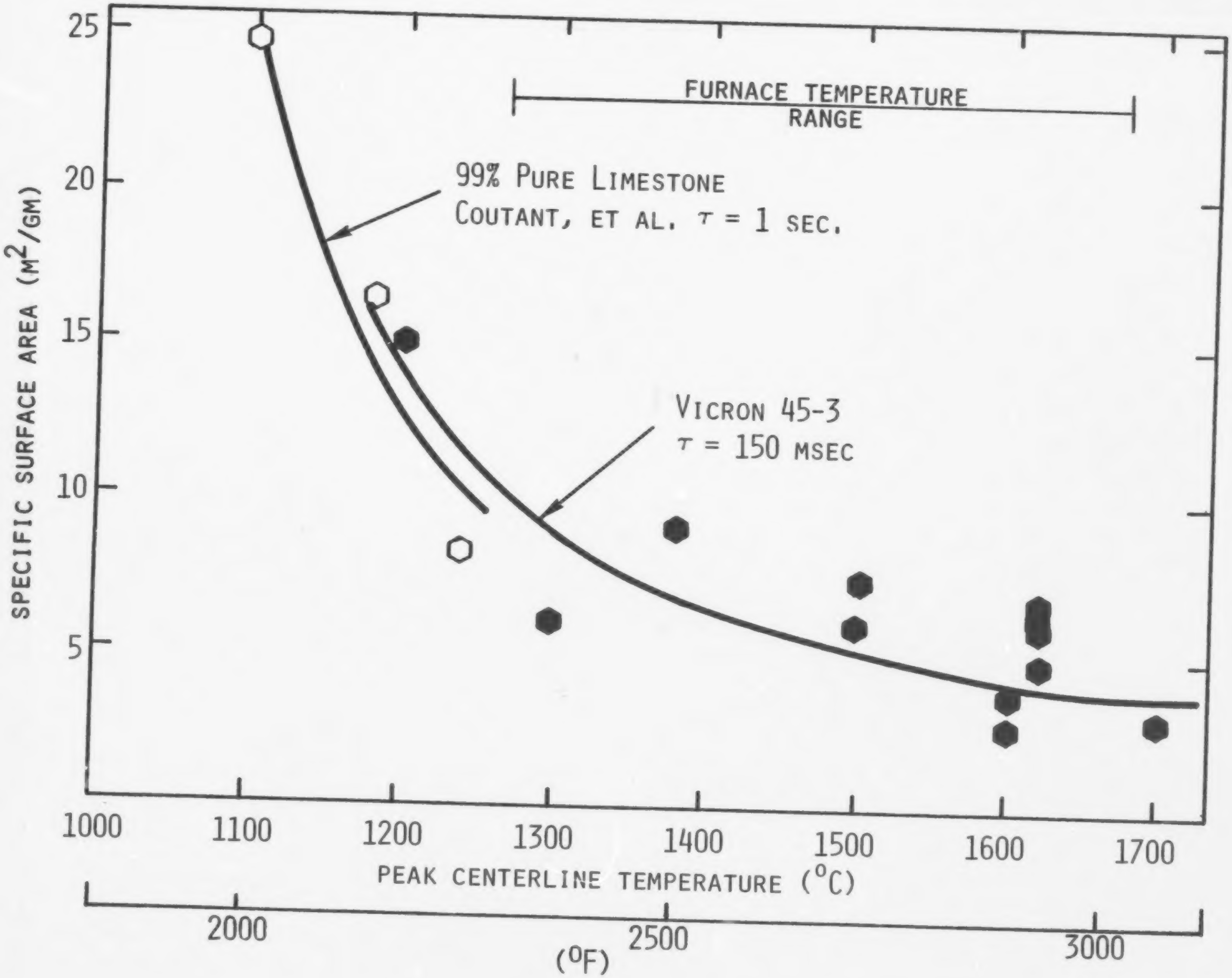

Figure 5-2. Effect of peak temperature on sorbent surface area.

5.2.1 Pore Model Description

The model considers the internal structure of the particle to be given by a set of overlapping, random-size, cylindrical pores. The reaction is initiated at the pore surface and a layer of reaction product (calcium-sulfate) forms around the pore. This reaction product layer separates the pore surface and the solid reactant surface. The gas (SO_2) must diffuse through the product layer to the surface of the solid reactant (CaO) where the sulfation reaction takes place. The model scheme for a single particle is shown conceptually in Figure 5-3.

The model also considers boundary layer diffusion and pore diffusion of the gas reactant. The resulting governing equations are:

$$\frac{1}{r^2}\frac{\partial}{\partial r}\left(D_e r^2 \frac{\partial C}{\partial r}\right) = \frac{a\rho\,(1 - \varepsilon_o)}{Mb}\,\frac{dX}{dt} \qquad (1)$$

and

$$\frac{dX}{dt} = \frac{K_s\, S_o\, C\,(1-X)\sqrt{1 - \psi \ln(1-X)}}{(1-\varepsilon_o)\left[1 + \frac{\beta Z}{\psi}\left(\sqrt{1 - \psi \ln(1-x)} - 1\right)\right]} \qquad (2)$$

Equation 1 describes the diffusion of gaseous reactant into the pore while Equation 2 gives the local rate of conversion (accounting for the effect of the product layer diffusional resistance).

The boundary conditions are:

$$\frac{\partial C}{\partial r} = 0 \qquad \text{at } r = o \qquad (3)$$

and

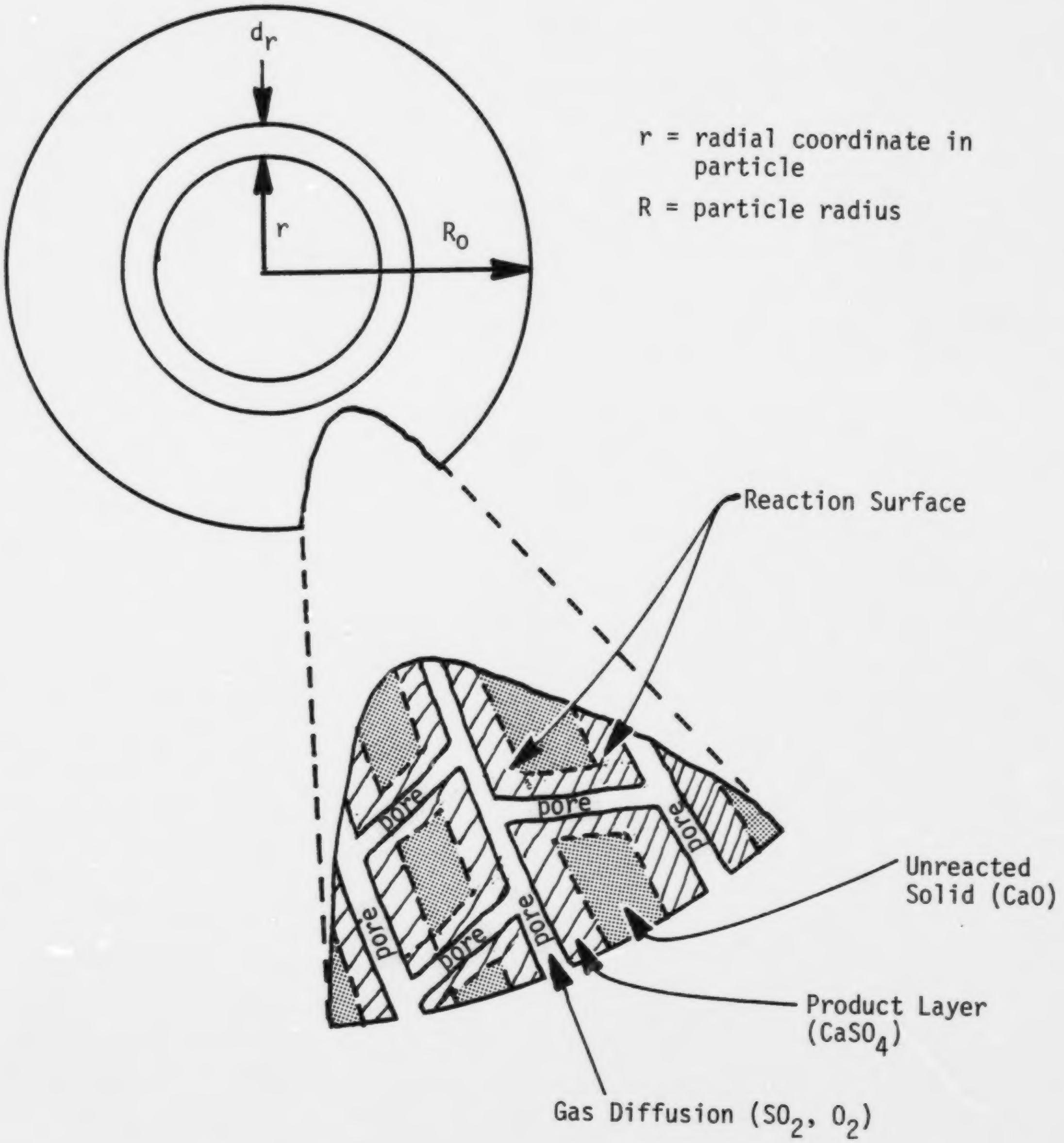
d_r
r
R_o
r = radial coordinate in particle
R = particle radius
Reaction Surface
pore
pore
pore
pore
pore
pore
Unreacted Solid (CaO)
Product Layer ($CaSO_4$)
Gas Diffusion (SO_2, O_2)

Figure 5-3. Conceptual illustration of pore model for CaO/SO_2 reaction.

$$D_e \frac{\partial C}{\partial r} = k_b (C_\infty - C) \quad \text{at} \quad r = R \qquad (4)$$

where k_b is the boundary layer mass transfer coefficinet and C is the concentration of gas reactant at the free stream. The governing equations, (1) and (2) and the boundary condition equations (3) and (4) constitute the complete system for the pore model. These equations are non-dimensionalized and solved numerically in the following manner:

- Equation (1) and boundary condition (3) and (4) are integrated numercially by finite-difference method to give the intra-particle concentration distribution.

- Equation (2) is simultaneously integrated (using a fourth-order Runge-Kutta scheme) to give local conversion.

A complete listing of the Fortran program developed for the pore model is given in Appendix G (Volume II).

5.2.2 Pore Model Verification

In order to test the program, the SO_2-lime reaction calculations, identical to those performed by Bhatia & Perlmutter (1981) were repeated. The results of these calculations (presented in terms of overall lime conversion as a function of time for various temperatures) are plotted in Figure 5-4. For comparison, Bhatia & Perlmutter's results and Borgwardt's data (1970) are also shown in Figure 5-4. The calculations and the data are in reasonable agreement. Slight discrepancies between the EER calculations and Bhatia's calculations may be attributed to the differences in numerical method of solution. The calculations assumed constant free-stream SO_2 concentrations (3000 ppm) at constant temperature (indicated).

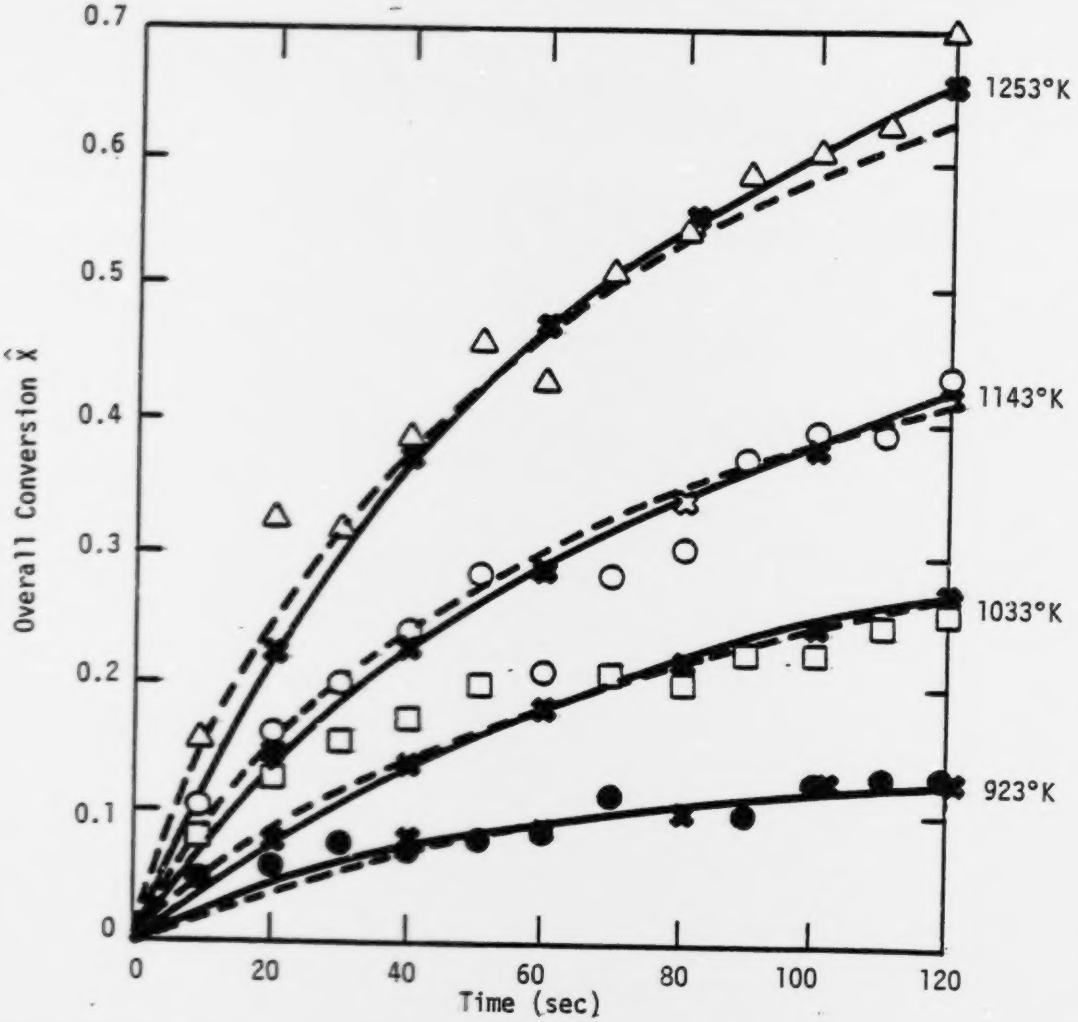

Figure 5-4. Application of random pore model to data of Borgwardt (1970). Solid lines represent the current model calculations, dotted lines represent Bhatia & Perlmutter's calculations (1981).

A second verification of the pore model was achieved by comparing pore model predictions with those of the grain model developed concurrently at the University of Utah by Silcox and Pershing. Figure 5-5 shows that, under similar conditions, the pore model and the grain model are in excellent agreement.

5.2.3 Sensitivity Study

In order to identify the most sensitive model parameters, calculations were performed varying input parameters about the baseline values listed in Table 5-1. These baseline values were chosen as representative of typical conditions for LIMB applications.

Three independent parameters are necessary to define the pore structure. Pore length, surface area, and porosity have been chosen as inputs to the model, but mean pore radius and/or the spread in the pore size distribution may be substituted for any of the three. Thus, in the sensitivity study, when any one of these five parameters is varied with two others held constant, the remaining two variables are dependent and cannot be held constant. Figure 5-6 shows the effect of particle surface area at two porosities. The spread in the log-normal pore size distribution is held constant. Total pore length increases and particle radius decreases with increasing surface area. Under these conditions, sulfur capture is quite sensitive to pore structure parameters, increasing with increasing surface area (decreasing pore radius) and increasing with increasing porosity.

Sulfur capture is only moderately dependent on temperature as shown in Figure 5-7. Capture increases with increasing temperature due to increasing rates of reaction and diffusion until the equilibrium cut-off temperature is reached. At temperatures above the equilibrium limit, it is assumed that no reaction occurs. This assumption does not allow for the regeneration of CaO at above-equilibrium temperatures. Such a modification to the model would require detailed data for the backward reaction rates which are currently unavailable.

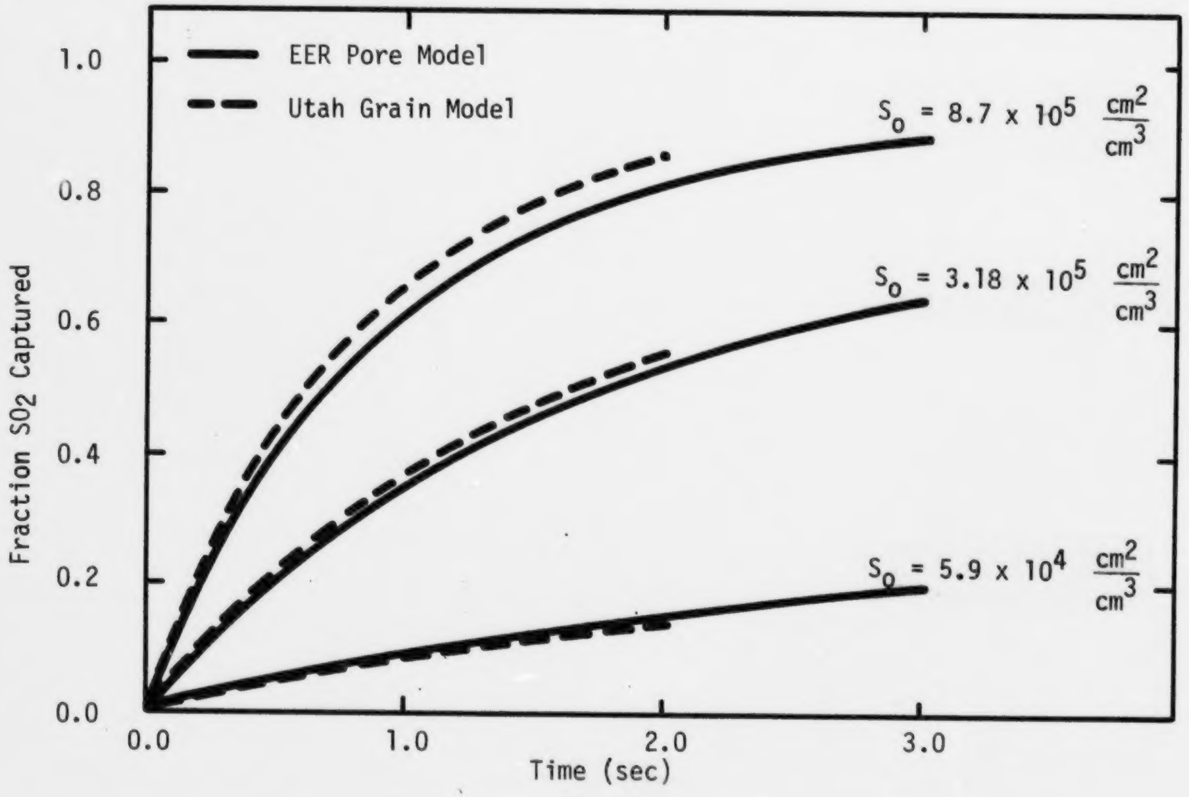

Figure 5-5. Model Comparison.

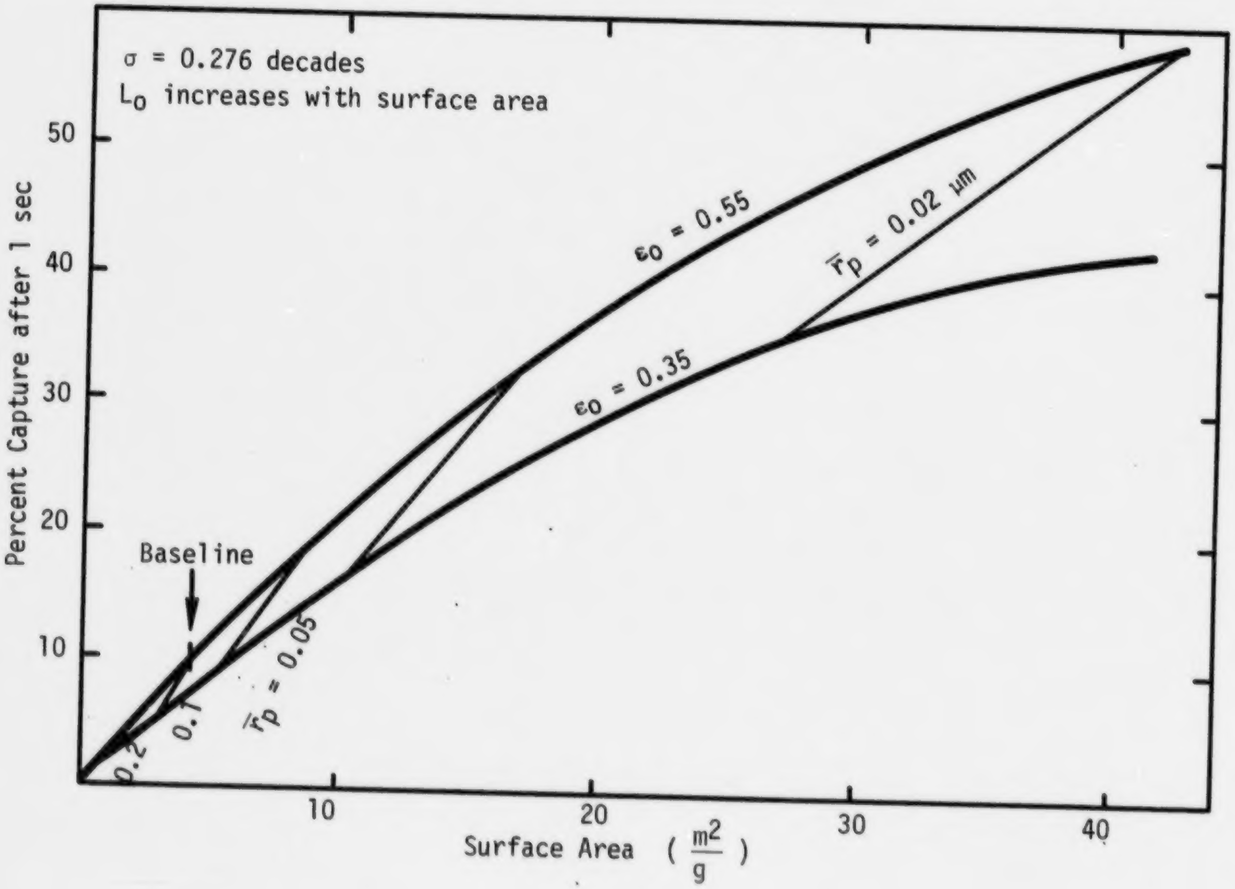

Figure 5-6. Effect of Pore Structure Parameters.

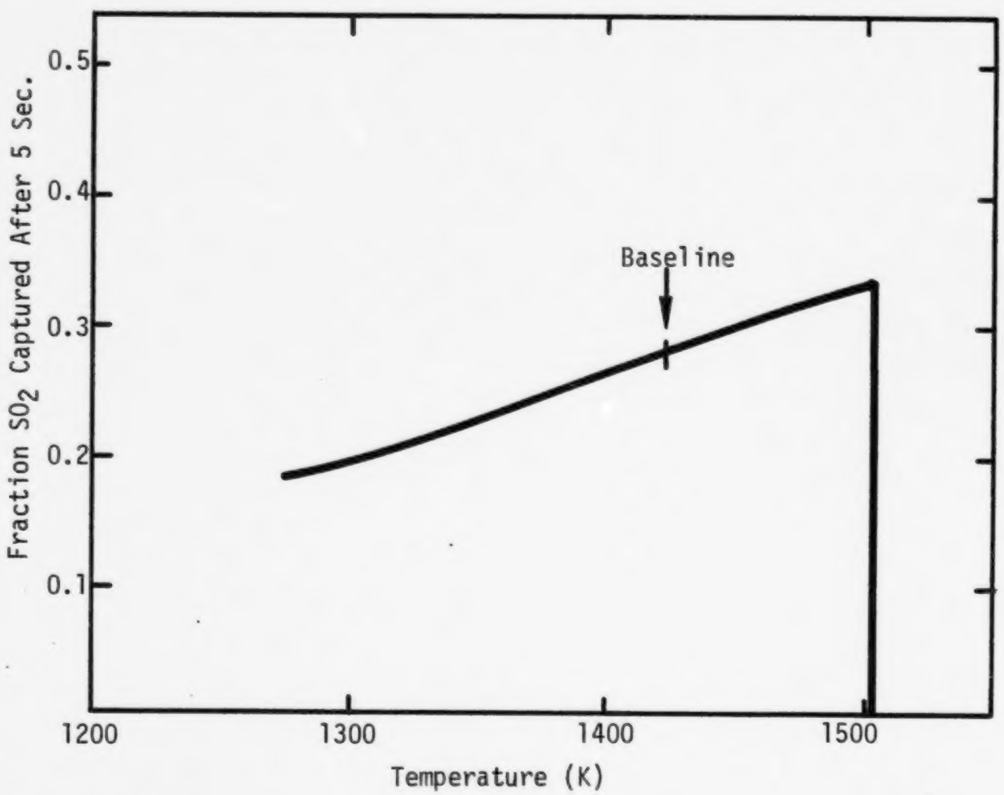

Figure 5-7. Effect of Temperature.

Effects of calcium-to-sulfur ratio and SO_2 concentration are shown in Figures 5-8 and 5-9. SO_2 capture increases with increasing Ca/S and with increasing SO_2 concentration. The predicted concentration effect is much stronger than most of the data indicates[*] suggesting that the assumed first-order dependence of intrinsic reaction rate on SO_2 concentration may be incorrect. Incorporation of variable-order kinetics into the pore model could rectify this discrepancy.

Parameters which have lesser effects on sulfur capture include intrinsic rate constant, product layer diffusivity, particle density, particle CaO content, particle size, and Sherwood Number as shown in Figures 5-10 through 5-14. Other parameters which had no effect on sulfur capture under investigated conditions were SO_2 diffusivity and Knudson diffusivity.

5.3 Sulfur Capture Model - Conclusions

A fairly simple model of sulfur capture has been produced. The model divides the process into two steps - sorbent activation and sorbent sulfation. The sorbent activation step is empirical. Results from recent studies of flash limestone calcination were used to derive a prediction of sorbent surface area from the peak temperature seen by the sorbent. Particle calcination is assumed to be instantanious and the model does not account for any effects of time-at-temperature on sorbent suface area. A pore model of the sulfation process is used. The pore model considers diffusion of SO_2 into the sorbent pores, chemisorbtion and reaction with the solid, diffusion of SO_2 through the sulfate layer, pore blockage and the limits of sulfate stability.

The sulfation portion of the model was tested against the original, reference, development of the pore model; was compared with a grain type model applied by a group at the University of Utah (Silcox, et al.) and against sulfation data obtained by Borgwardt with good agreement.

---

[*] See Section 6.3

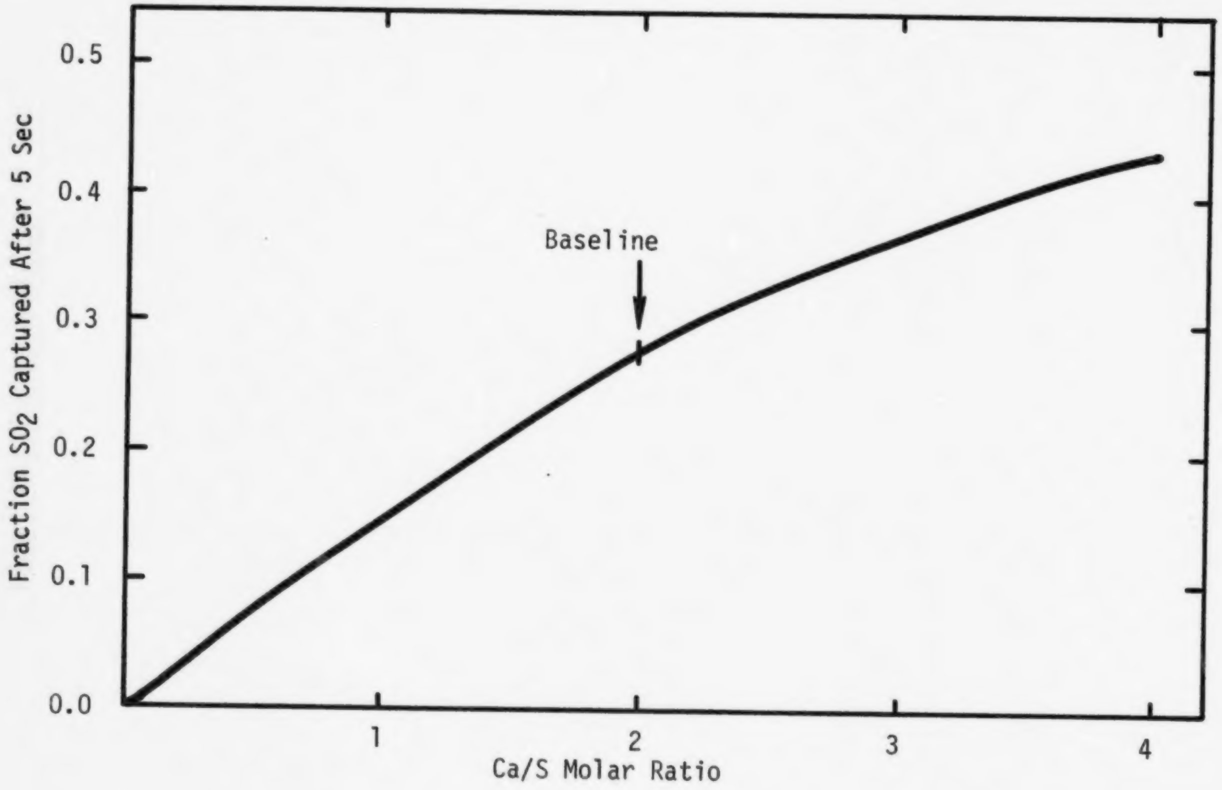

Figure 5-8. Effect of Ca/S Ratio.

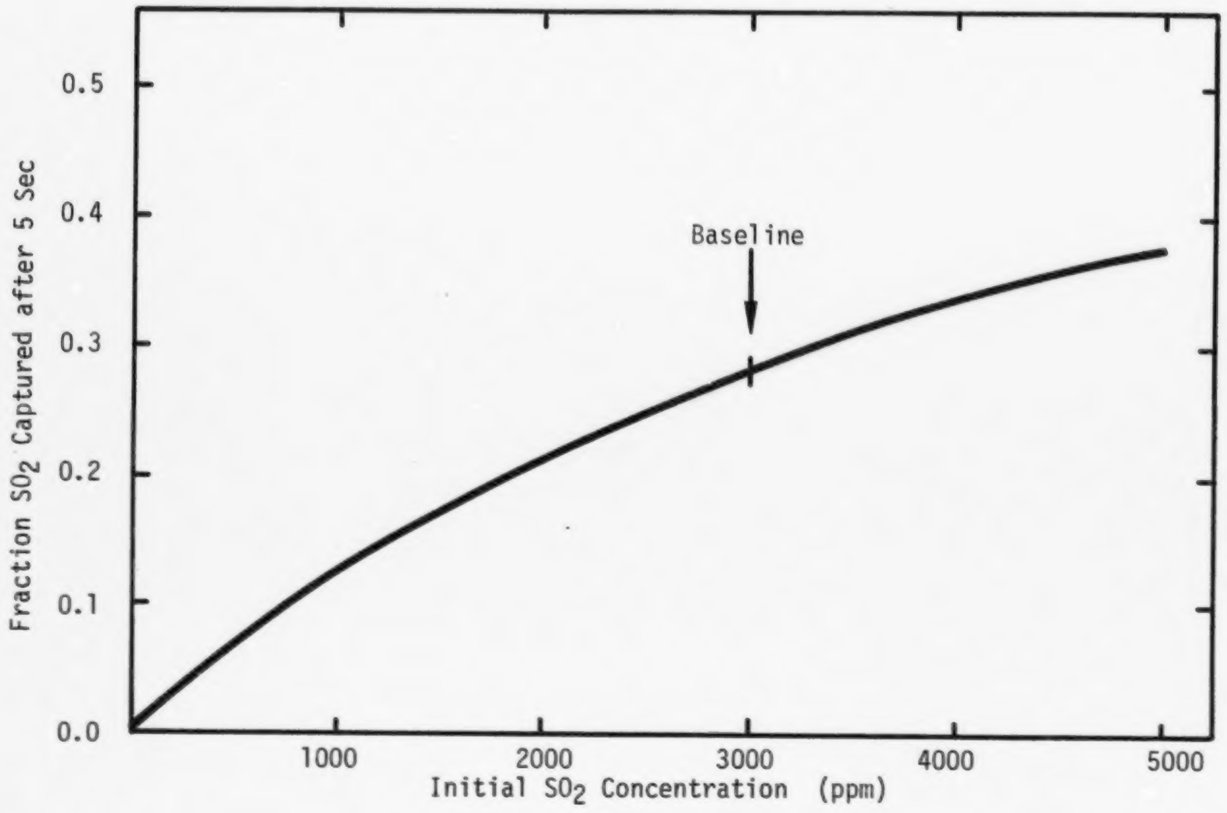

Figure 5-9. Effect of SO_2 Concentration.

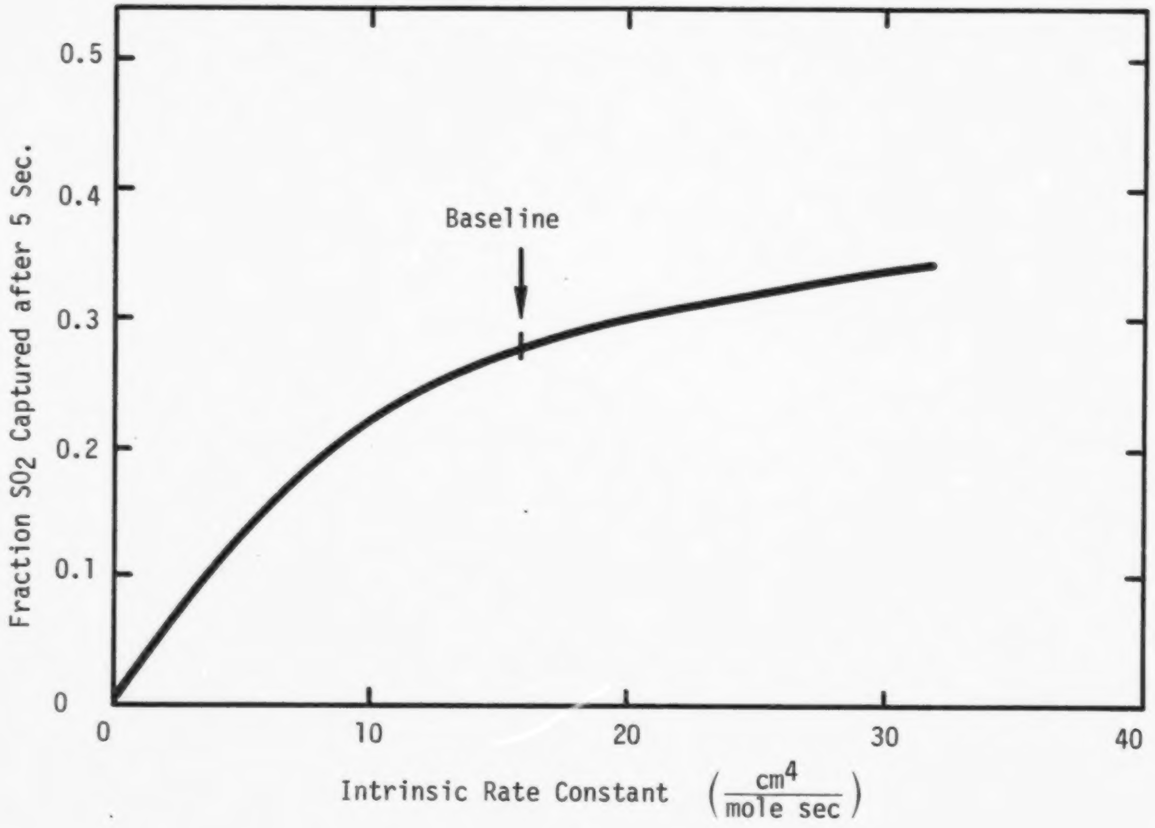

Figure 5-10. Effect of Intrinsic Rate Constant.

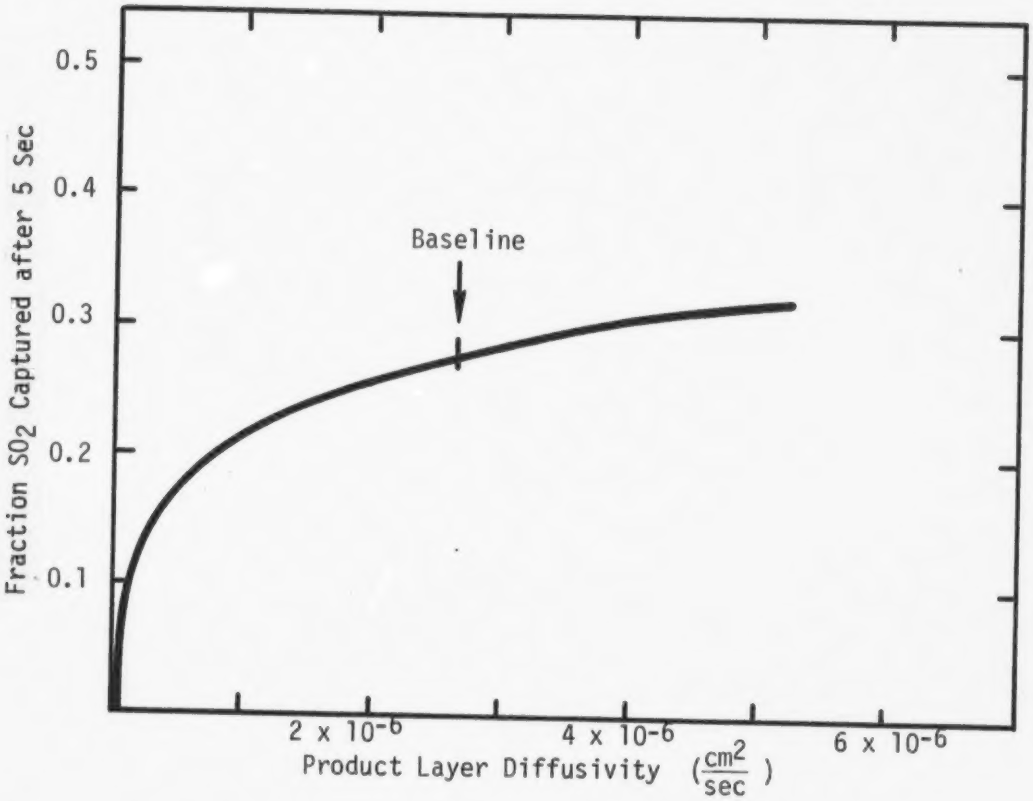

Figure 5-11. Effect of Product Layer Diffusivity.

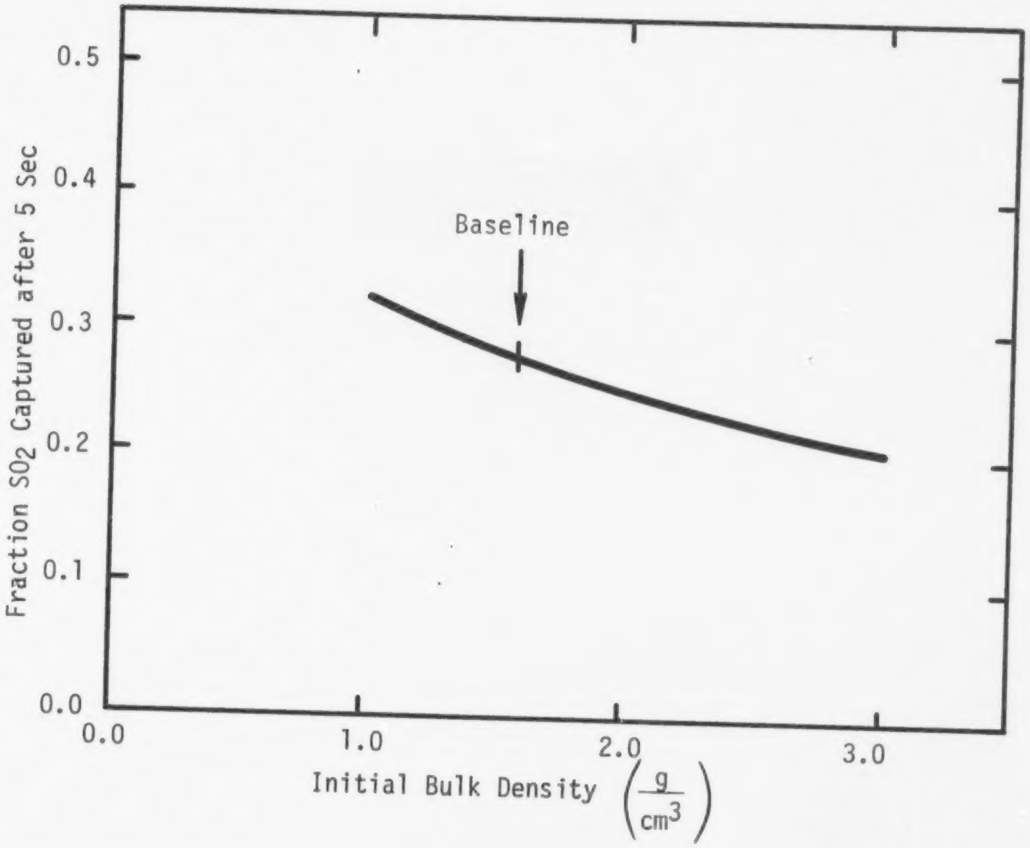

Figure 5-12. Effect of Particle Density.

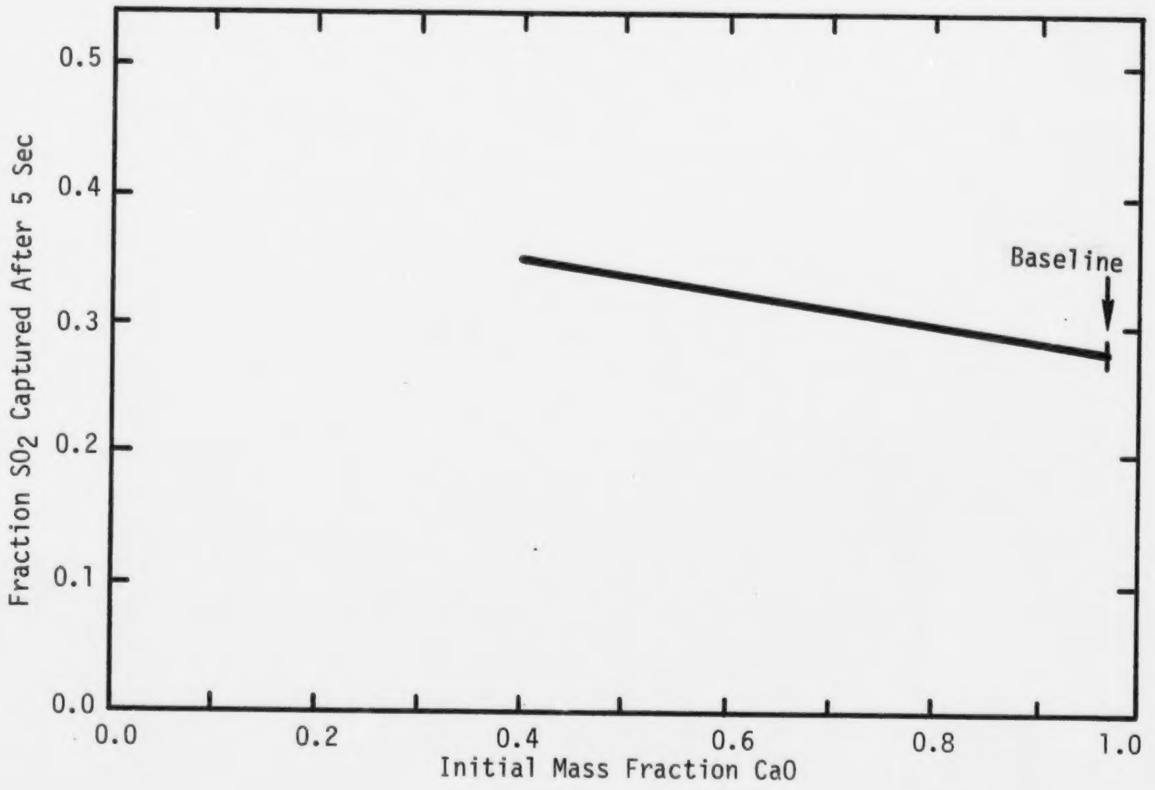

Figure 5-13. Effect of Particle CaO Content.

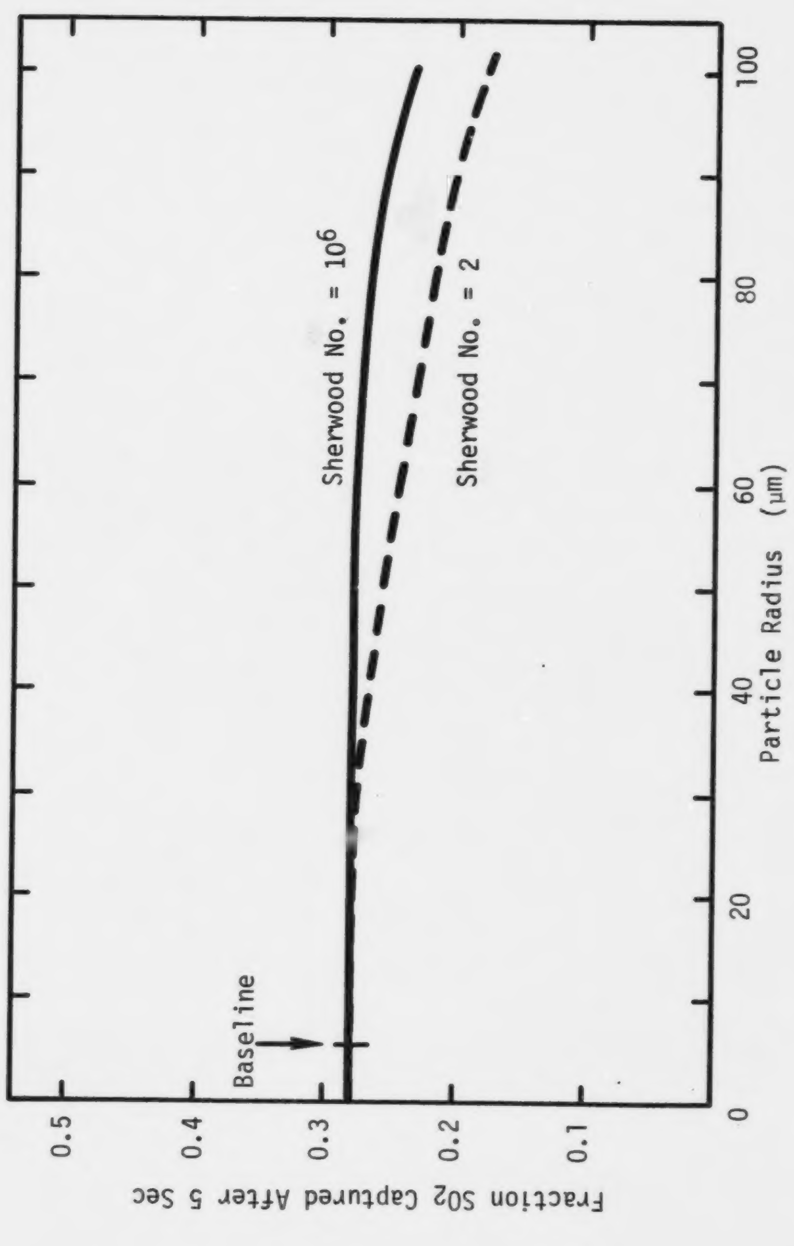

Figure 5-14. Effect of Particle Size.

The sensitivity of the model to various parameters including pore-size characteristics, surface area, temperature, calcium-to-sulfur ratio, the selected intrinsic rate constant (derived from kinetic data and subject to some variation in interpretation), sulfate product layer diffusivity and Sherwood number (which influences the SO_2 concentration gradient at the particle surface) was tested. The parameters which had a significant effect on capture were the porosity/pore size/surface area of the sorbent (these are interrelated, see Section 5.2.3) and to a lesser extent, time, temperature, SO_2 concentration and Ca/S ratio.

The sulfation portion of the model is probably adequate for the model application needs except that the predicted effect of SO_2 concentration does not match the available data very well. The sorbent activation portion of the model is the best currently available, but is over-simplified and should be refined as data on the effects of calcination conditions and input sorbent characteristics becomes available.

TABLE 5-1. BASELINE CONDITIONS

R_o Particle Radius = 5.5 μm

L_o Initial Pore Length = 7.55×10^8 cm/cm^3

S_o Initial Surface Area = 5.9×10^4 cm^2/cm^3

$_o$ Initial Porosity = 0.55 cm^3/cm^3

W_o Initial Mass Fraction CaO = 0.97

$_b$ Initial Bulk Density = 1.59 g/cm^3

Sh Sherwood Number = $1 \times 10^6 \simeq$ Infinite

C_o Initial Gas Phase SO_2 Concentration = 3000 ppm

Ca/S Ratio = 2.0

T Isothermal Temperature = 1422 ^{0}K

K_s Kinetic Rate Constant

$$K_s = \frac{1890 \text{ cm}^4}{\text{mole sec}} \exp \frac{-13500 \text{ cal}}{\text{RT mole}}$$

Dp Diffusivity through Product Layer

$$Dp = 0.0528 \frac{\text{cm}^2}{\text{sec}} \exp \frac{-28000 \text{ cal}}{\text{RT mole}}$$

Do Diffusivity through Pores

$$Do = \frac{1}{(^1/D_a) + (^1/DK_o)}$$

where

$$D_a = \exp\left[1.66 \ln(T) - 11.3\right] \text{ cm}^2/\text{sec}$$

$$DK_o = 9700 \frac{\text{cm}^2}{\text{sec}} \left(2\, \varepsilon_o/S_o\right) \quad T/M$$

NOMENCLATURE

a = stoichiometric coefficient for SO_2
b = stoichiometric coefficient for C_a
C = local concentration of SO_2 (mole/cm^3)
D_e = effective diffusivity of SO_2 in pores (cm^2/sec)
D_p = effective diffusivity of SO_2 in product layer (cm^2/sec)
L_o = total length of pore system per unit volume (cm/cm^3)
K_s = rate constant for surface reaction cm^4/mole-sec
M = Molecular weight of CaO (g/mole)
r = distance from the particle center (cm)
R = particle radius
S_o = initial pore surface area per unit volume (cm^2/cm^3)
t = time (sec)
X = local conversion
Z = ratio of volume of solid phase after rection to that before reaction

$$\beta = \frac{2K_s\ a\ \rho\ (1-\ {}_o)}{M\ b\ D_p\ S_o}$$

E_o = initial porosity (cm^3/cm^3)

W_o = Mass fraction of CaO in initial solid particle

$$\psi = \frac{4\ \pi\ L_o\ (1 - \varepsilon_o)}{\nu\ \ S_o2}$$

ρ = Mass of CaO per unit volume of solid phase

6.0 SORBENT MINERAL MATTER INTERACTIONS

There were significant differences in sorbent sulfur capture in gas and coal flames. These differences cannot be adequately explained with thermal arguments. Natural gas flames which had peak temperatures both lower and higher than the coal flame gave better overall sorbent utilization than the coal flames. The difference in sulfur capture seemed to be the result of some fuel characteristic other than flame temperature. The possibility of interference by the coal ash or some component of the ash was investigated.

Fly ash collected from one of the pilot-scale facilities (the SWS) was used to test the ash interference hypothesis. The ash was mixed with Vicron 45-3 at two ash-to-sorbent mass ratios. Samples of the mixtures were analyzed. Table 6-1 summarizes the composition of the mixtures. The two mixtures, and plain Vicron 45-3 were tested in the BSF. The furnace was fired with natural gas doped with H_2S and the sorbent, or sorbent/ash mixture, was injected with the fuel. The proportion of sorbent-to-fly ash for Indiana coal at a Ca/S mole ratio of 2.0 would be somewhere between the two Vicron/fly ash mixtures - at a sorbent-to-ash mass ratio of about 1:2 (1 lb. sorbent to 2 lb. ash).

Figure 6-1 summarizes the measured sulfur capture at various Ca/S ratios (based on the sorbent or sorbent/ash mixture composition and feed rate). Clearly the fly ash had a detrimental effect on sulfur capture. These results indicated that the ash in the Indiana coal may have been responsible for the low capture with the fuel. These results led to investigations of the effect of various coal mineral components on sulfur capture in clean, gas flames. Investigations of various mineral components, the relative size of the mineral and sorbent and the interaction of fuel sulfur and mineral matter were performed.

6.1 Effect of Mineral Matter on Sorbent

An interference in sulfur capture by fly ash from a coal-fired system implies a coal sorbent interaction. Fly ash from a coal is, however,

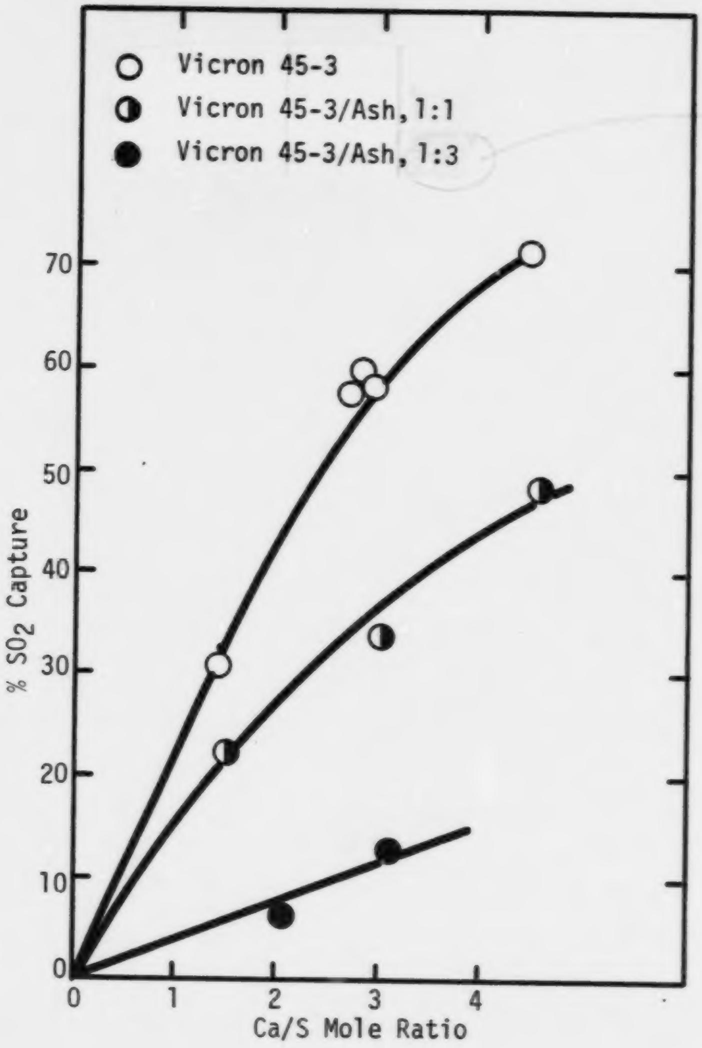

1:3

Figure 6-1. Effect of Ash Addition on Sulfur Capture - Vicron 45-3 Plus Fly Ash. Natural Gas/H_2S Flame, DMB, Axial Injector and Sorbent with Fuel.

TABLE 6-1. ASH-SORBENT MIXTURE COMPOSITION

	EER Analysis							Outside Analysis													
Sample	C	H	N	S	(diff) O_2	Ash*	CaO	Ash*	CaO	SiO_2	Al_2O_3	TiO_2	Fe_2O_3	MgO	Na_2O	K_2O	P_2O_5	SO_3	Size mm	SA M^2/gm
SWS Ash/Sorbent (Vicron 45-3) 50-50	8.2	0.1	0	0.3	16.5	74.9	31.4	76.3	31.7	26.6	9.5	.3	3.6	1.0	.2	.6	.1	1.3	12	
SWS Ash/Sorbent (Vicron 45-3) 75-25	5.8	0.1	0.4	0.4	7.9	85.4	17.4	85.6	17.9	42.2	15.0	.5	5.6	.9	.4	.9	.2	1.0		

* Based on ignition weight loss, will include CaO from sorbent as ash.

considerably different than the mineral matter in the parent coal. The mineral material in the fuel oxidizes, some components vaporize and recondense, others melt. It was important, therefore, to test coal mineral components for interferences with injected sorbents rather than simply testing fly ash for interactions. Two readily available minerals were tested. Kaolinite was common clay mineral found in many coals and bentonite - a mixed montmorillonite/chlorite clay, another common coal mineral, were mixed in varying proportions with the sorbent. These mixtures were injected with the fuel in a natural gas/H_2S flame. Table 6-2 summarizes the composition and some physical characteristics of the two minerals.

The data in Figure 6-2 show the effect of kaolin and bentonite on sulfur capture by Vicron 45-3. Figure 6-3 shows similar data for dolomite/kaolin and dolomite/bentonite mixtures. It is apparent that the kaolin had a profound impact on Vicron 45-3 reactivity and a somewhat smaller effect on dolomite reactivity. The bentonite reduced captures by both sorbents, but not nearly as profoundly as the kaolin, even though the proportion of mineral in the mixture was much higher for the bentonite/sorbent cases.

Some difference between the two mineral additives should account for the different effects on the sorbent. One possible difference is the alumina ($Al_2$03) content of the mineral. Table 6-3 summarizes the composition of the various sorbent mineral and sorbent ash mixtures. The calculated composition of Indiana coal ash mixed with sufficient Vicron 45-3 to give a Ca/S mole ratio of 2.0 is included in the table. Figure 6-4 and 6-5 show SO_2 capture measured at a Ca/S of 2 for the various sorbent/mineral (and the Indiana coal sorbent) cases. The Al_2O_3 content of the mixture correlates reasonably well with the SO_2 capture - the more Al_2O_3 in the solid, the lower the SO_2 capture.

The mechanism of ash interference is not clear. The mineral component of the coal may volatilize in the flame and then condense on the sorbent surface forming inactive calcium silicates or calcium aluminates. Volatilization data for coal ash components is sparse, however, the data available indicate rather low volatilities for Al_2O_3 and SiO_2 in coal at flame temperatures. The mineral matter addition tests showed a strong dependence of SO_2 capture on the

TABLE 6-2. TYPICAL COMPOSITIONS OF MINERAL ADDITIVES

	COMPOSITION	
Mineral Material	Kaolinite	Bentonite
Al_2O_3	38.38	16.0
SiO_2 (Combined)	45.30	40.3
Ignition loss at 950°C	13.97	14.4
Fe_2O_3	0.30	1.9
TiO_2	1.44	---
CaO	.05	10.4
MgO	.25	9.9
Na_2O	.27	---
K_2O	.04	---

TYPICAL PHYSICAL CHARACTERISTICS

	Median size (μm)	Oil Adsorption (%)	BET Surface Area m^2/gm
Kaolinite			
Hydrite Flat D	5.0	34	7
Hydrite 121 S	1.5	39	8
Hydrite PX	0.68	43	12
Ibex Bentonite	2.5	--	

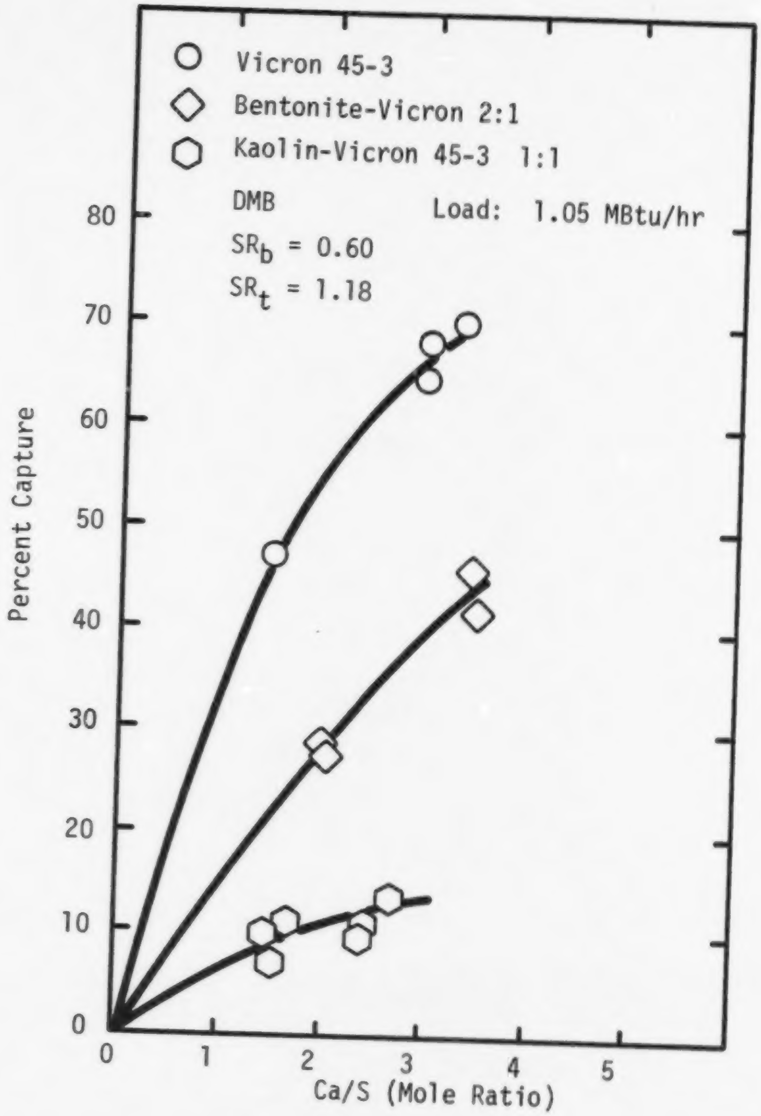

Figure 6-2. Effect of Mineral Addition on Sulfur Capture by Vicron 45-3, Natural Gas/H_2S Flame, Port #3 (Exit Convective Section).

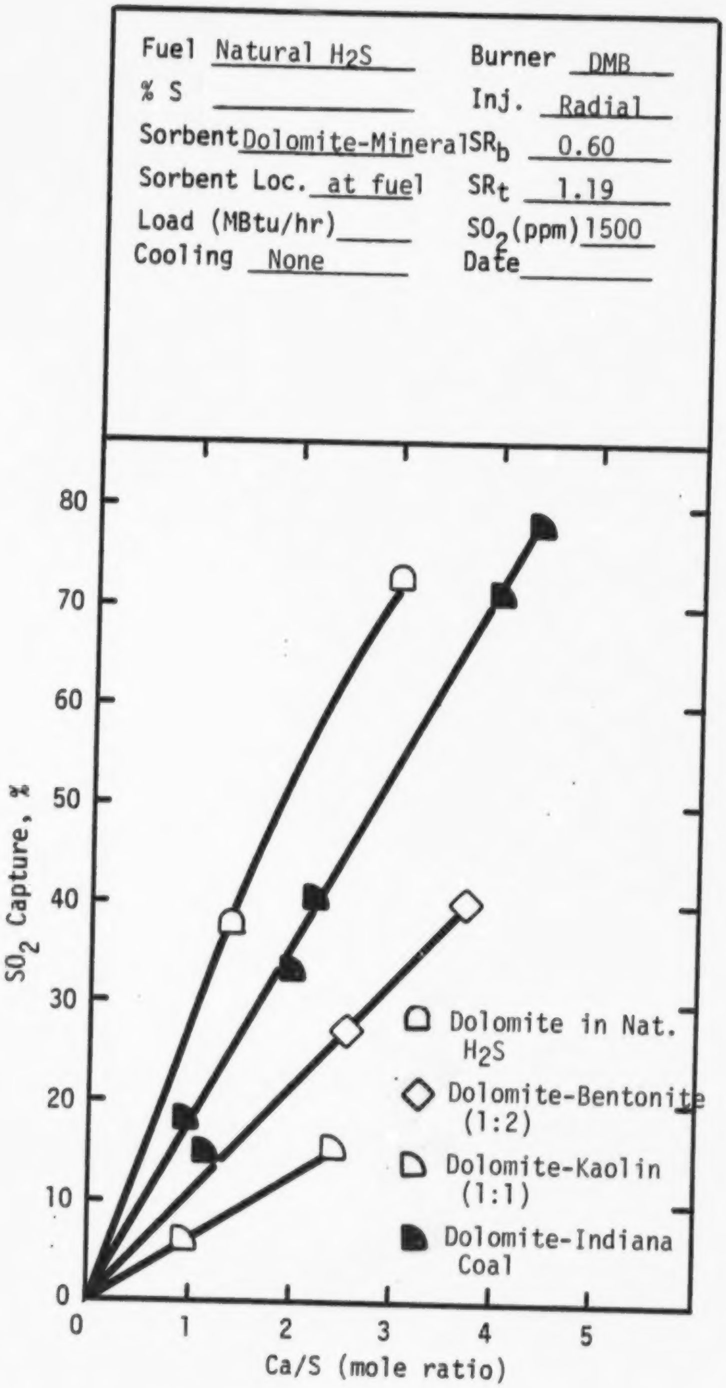

Fuel	Natural H_2S	Burner	DMB
% S		Inj.	Radial
Sorbent	Dolomite-Mineral	SR_b	0.60
Sorbent Loc.	at fuel	SR_t	1.19
Load (MBtu/hr)		SO_2(ppm)	1500
Cooling	None	Date	

Figure 6-3. Effect of Mineral Addition on Sulfur Capture by Dolomite, Natural Gas/H_2S Flame, Port 3 (Exit Convective Section).

TABLE 6-3. SORBENT MINERAL MIXTURES CHARACTERISTICS

Sorbent Mineral	1000°C Ig. Loss	S.A. 1000°C	Chemical Composition (Ignited Sample) Weight, %										
			CaO	SiO_2	Al_2O_3	Fe_2O_3	Na_2O	K_2O	MgO	TiO_2	P_2O_5	CRO_2	SO_3
Vicron 45-3	44.0	6.79	97.6	0.27	0.35	0.188	0.10	0.046	1.42			0.01	
Indiana 3 (Ash) + Vicron 45-3, Ca/S = 2.0	19.0		29.26	41.26	17.23	8.81	0.16	0.86	0.85	0.67	0.36	0.005	0.52
SWS Ash + Vicron 45-3 (1:1)	23.7		41.59	34.81	12.39	4.66	0.30	0.81	1.34	0.41	0.19		1.69
SWS Ash + Vicron 45-3 (3:1)	14.41		20.93	49.34	17.51	6.52	0.41	1.09	1.11	0.62	0.28		1.15
Bentonite + Vicron 45-3 (2:1)	27.88	.40	24.67	37.95	6.19	2.05	1.42	2.69	10.71	0.21	0.67	0.004	0.11
Kaolin + Vicron (1:1)	29.71	2.37	38.62	31.94	27.11	0.285	0.231	0.046	0.738	1.012		0.007	
Dolomite	47.1		57.18	1.54	0.49	0.57	0.17	0.18	39.02			0.848	
Indiana 3 (Ash) + Dolomite, Ca/S = 2	28.3		24.28	34.80	14.41	7.47	0.178	0.78	16.42	0.56	0.30	0.35	0.43
Dolomite + Bentonite (1:2)	25.3	0.89	24.08	39.06	15.47	1.96	0.043	0.045	19.12			0.209	
Dolomite + Kaolin (1:1)	31.2	6.49	21.42	33.53	28.11	0.43	0.261	0.097	14.78	1.04		0.317	

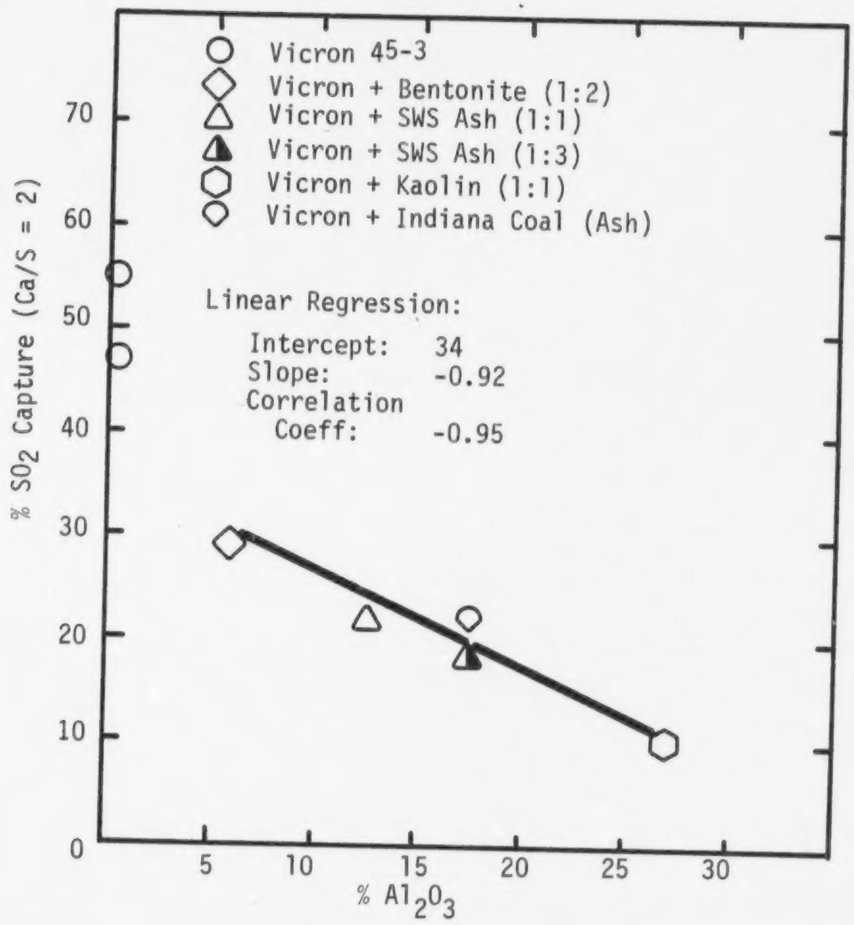

Figure 6-4. Effect of Al_2O_3 Content of Solid on Capture by Vicron 45-3.

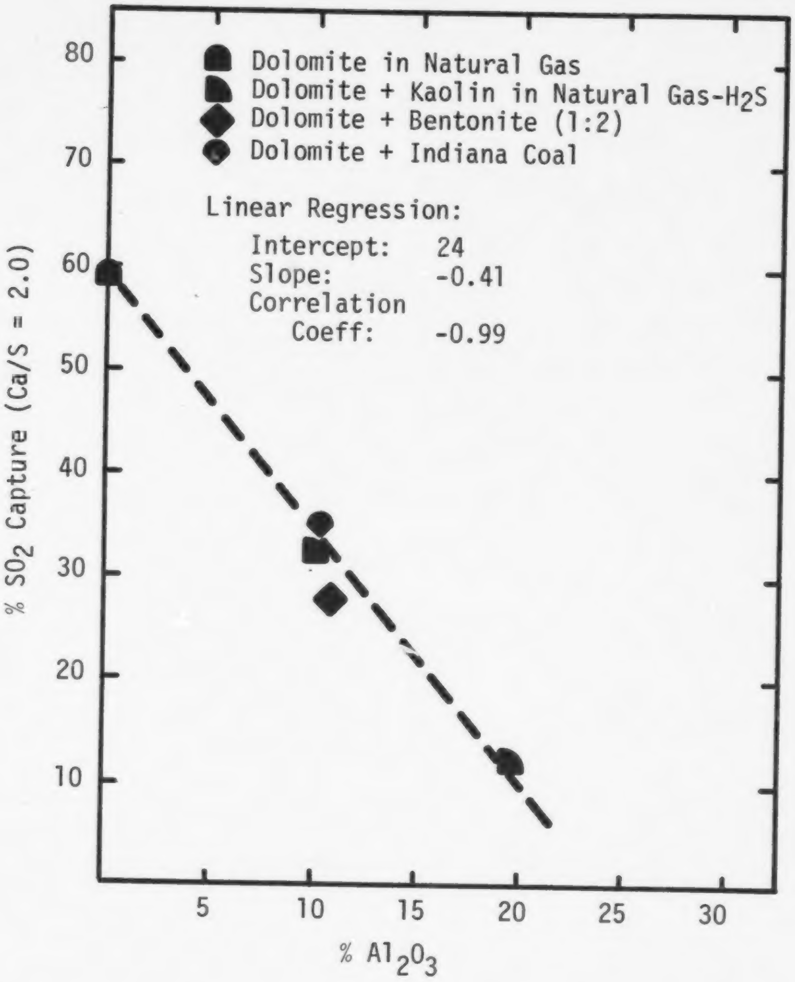

Figure 6-5. Effect of Al_2O_3 Content of Solid on Sulfur Capture by Dolomite.

Al_2O_3 content of the solid injected, with low volatility of the Al_2O_3 it seems unlikely that the Al_2O_3 is deactivating the sorbent by vaporizing and recondensing on the sorbent particles.

A second possibility is that the mineral matter melts at flame temperatures and is sticky. The sorbent may contact the sticky molten material and become deactivated. Another possibility is that the sorbent and mineral materials are in contact and the combined solid forms a low melting eutectic which deactivates the sorbent.

If particle collisions are an important step in the sorbent deactivation process the number of particles in the gas stream should have an effect on the deactivation process. An attempt to investigate the effect of particle size (and therefore number given the same mass) on sorbent reactivity was made. Two sizes of vicron and the dolomite were tested with different sizes of kaolin. The particle size distributions of the sorbents and kaolins are shown in Figure 6-6 and 6-7. (The effect of sorbent particle size on sulfur capture is discussed in Chapter 7. The effect of particle size on capture was different for coal and natural gas firing, this was another reason for the sorbent mineral matter size studies.)

The sorbents and kaolins were mixed and fed together with the fuel in a natural gas/H_2S flame in the BSF. Table 6-4 summarizes the composition of the sorbent mineral mixtures (after ignition which drives off the CO_2 in the sorbent and the H_2O in the kaolin). Sulfur capture at several calcium-to-sulfur ratios was measured with each mixture. Increasing the Ca/S ratio necessarily increased the solid feed rate and therefore, the concentration of Al_2O_3 in the furnace. The data from these tests is plotted as a function of the Al_2O_3 concentration in the furnace. The difference in SO_2 capture given by the plain sorbent and the sorbent-kaolin mixture [%SO_2 capture = %SO_2 capture (Vicron) - %SO_2 capture (Vicron/Kaolin)] was used to indicate the effect of the mineral addition and is plotted as the dependent variable in Figures 6-8 through 6-10.

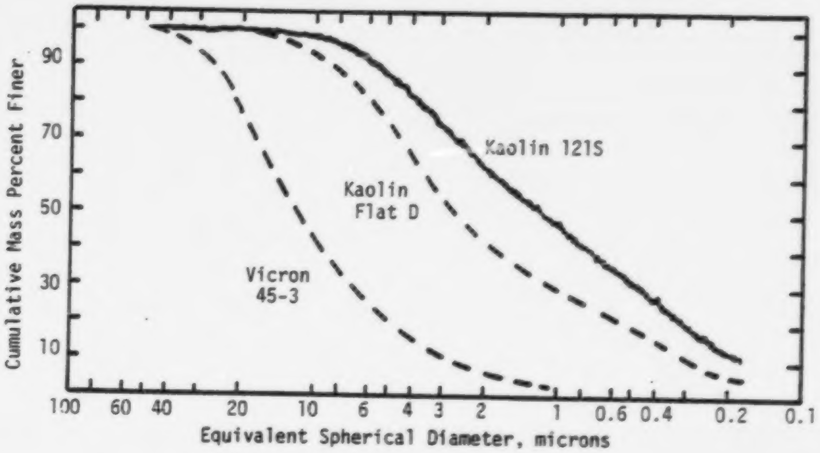

Figure 6-6a. Vicron 45-3 and Kaolin particle size distribution - as injected.

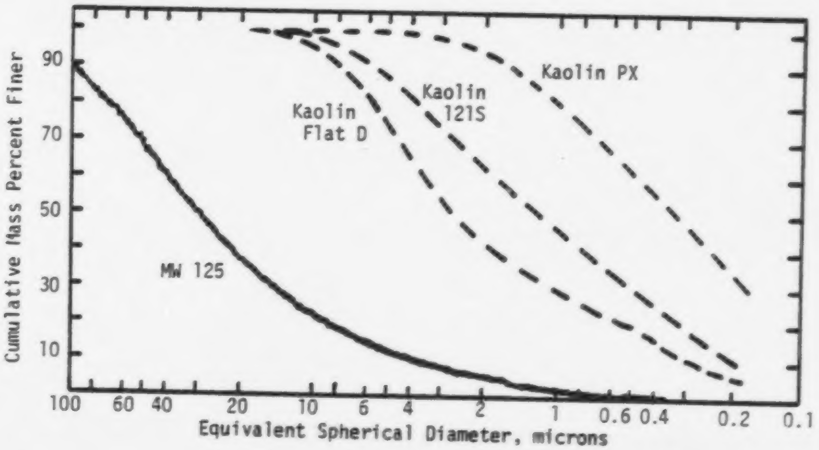

Figure 6-6b. Marblewhite 125 and Kaolin particle size distribution - as injected.

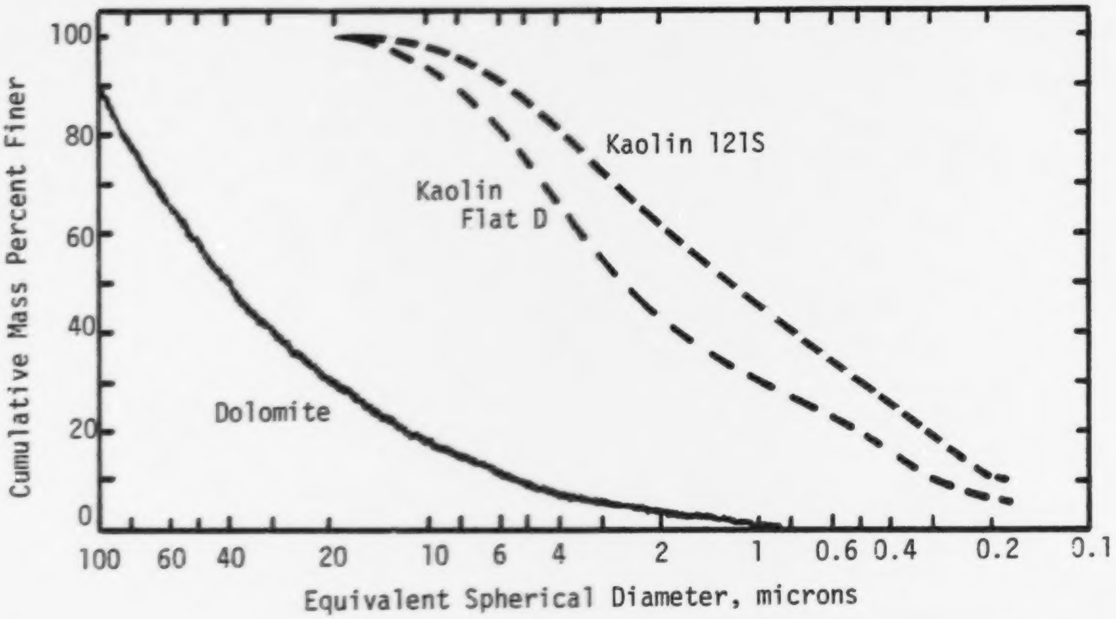

Figure 6-7. Dolomite and Kaolin particle size distribution - as injected.

TABLE 6-4. SORBENT/KAOLIN MIXTURE COMPOSITIONS

	CaO Meas	CaO Theo	Wt Loss 950	Al_2O_3	SiO_2	Fe_2O_3	T_iO_2	MgO	Na_2O	K_2O	Cr
Vicron 45-3/Kaolin FD	35.6	36.58	34.	12.923	15.2	.170	.48	.6194	.1295	.031	0.004
Vicron 45-3/Kaolin 121S	45.1	36.58	34.	12.923	15.2	.170	.48	.6194	.1295	.031	0.004
MW 125/Kaolin	37.8	36.58	32.1	12.923	15.2	.170	.48	.6194	.1295	.031	0.004
MW 125/Kaolin 121W	37.8	36.58	32.1	12.923	15.2	.170	.48	.6194	.1295	.031	0.004
MW 125/Kaolin PX	37.8	36.58	32.1	12.923	15.2	.170	.48	.6194	.1295	.031	0.004
Dolomite/Kaolin FD	22.27	21.8	38.5	10.20	12.33	.294	.373	14.92	.136	.08	.20
Dolomite/Kaolin 121S	21.0	19.6	36.0	12.96	15.63	.294	.48	13.42	.149	.0759	.18

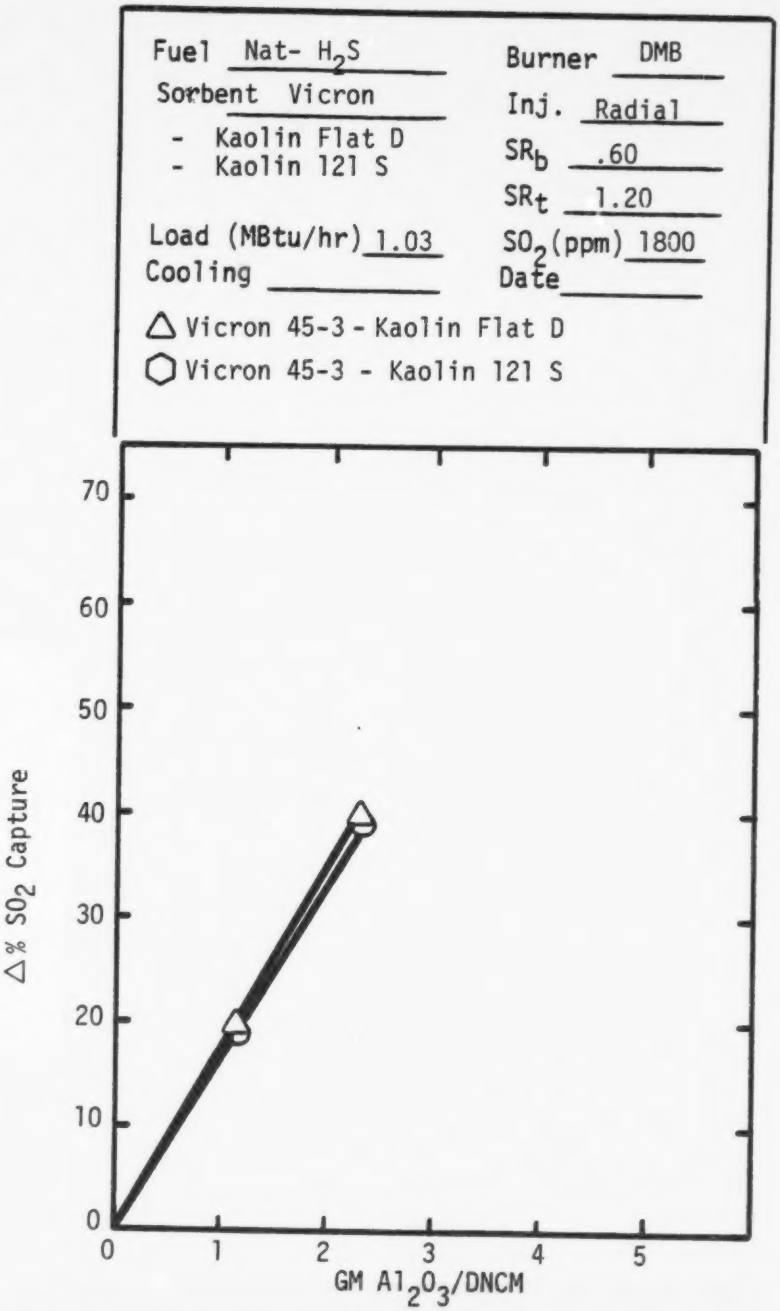

Fuel Nat- H_2S

Sorbent Vicron

- Kaolin Flat D
- Kaolin 121 S

Load (MBtu/hr) 1.03

Cooling

Burner DMB

Inj. Radial

SR_b .60

SR_t 1.20

SO_2(ppm) 1800

Date

△ Vicron 45-3 - Kaolin Flat D

⬡ Vicron 45-3 - Kaolin 121 S

Figure 6-8. Effect of mineral matter concentration on decrease in SO_2 capture with Vicron 45-3.

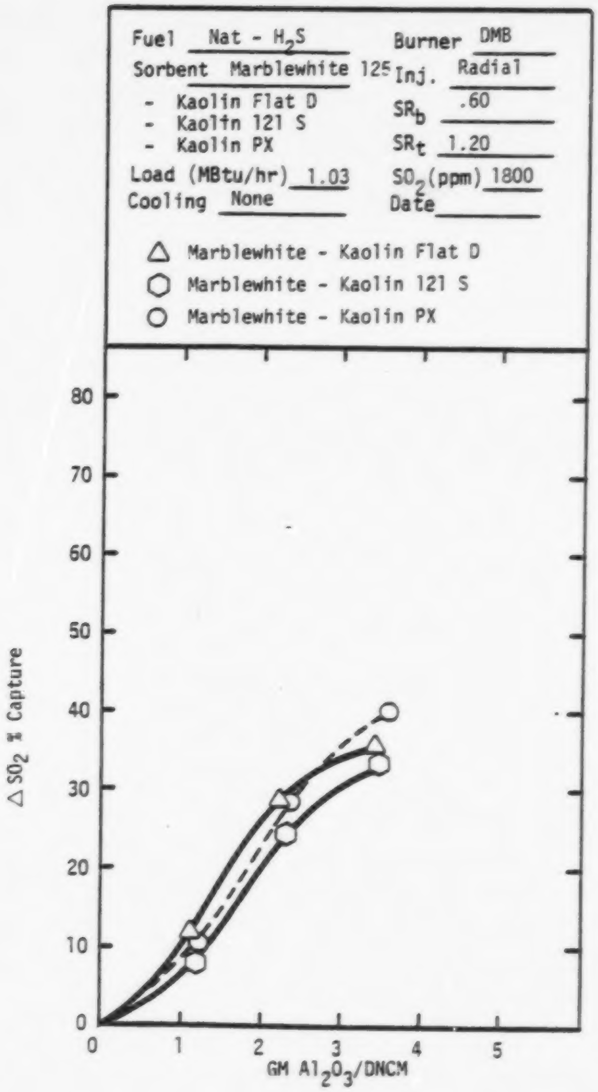

Figure 6-9. Effect of mineral matter concentration on decrease SO_2 capture for Marblewhite 125.

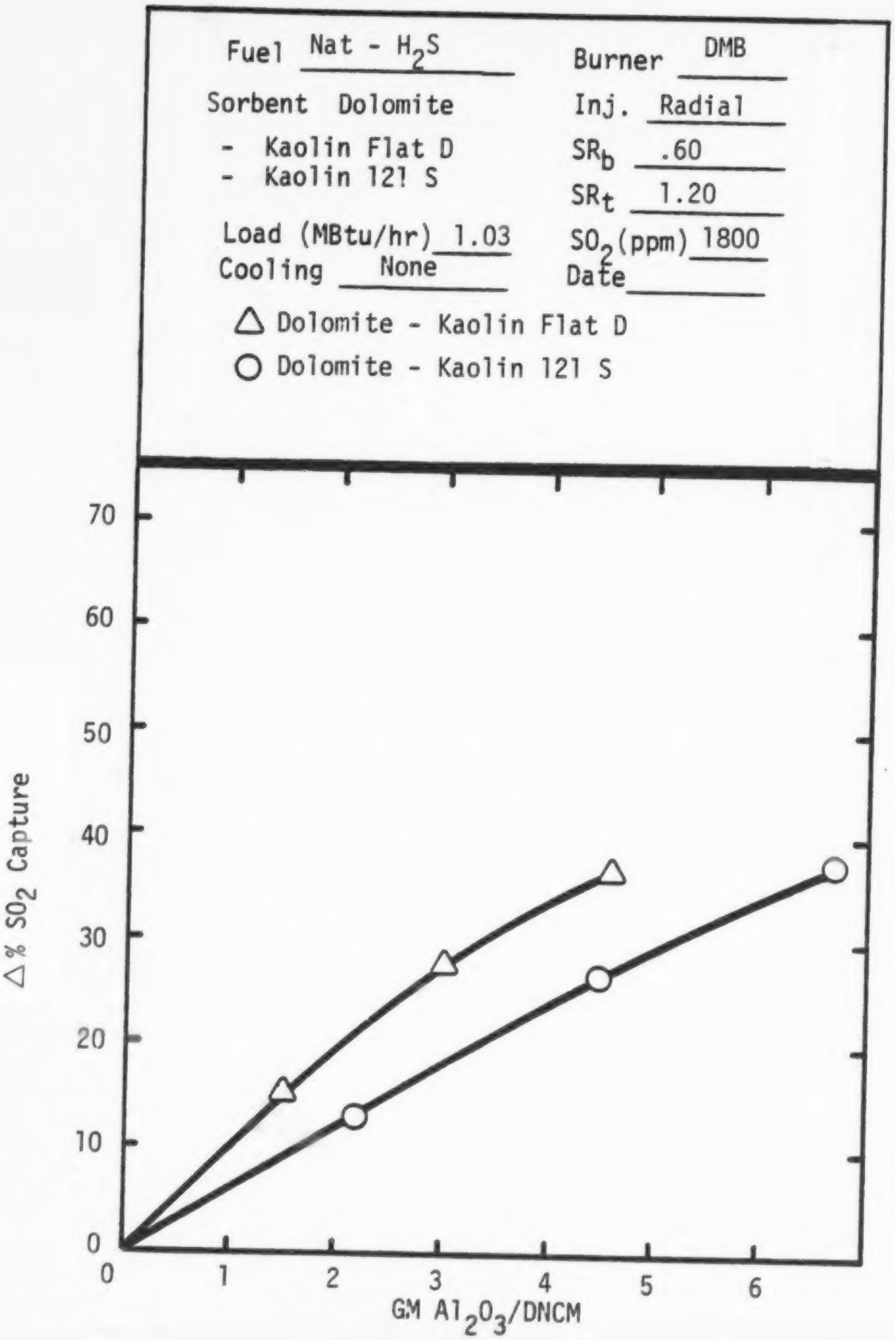

Figure 6-10. Effect of mineral matter concentration on SO_2 capture for Dolomite.

The effect of two kaolins on sulfur cpature by Vicron 45-3 is summarized in Figure 6-8. The change in SO_2 capture from the pure sorbent case ($\%SO_2$ capture) is plotted as a function of the Al_2O_3 loading in the furnace. The decrease in SO_2 capture observed with both kaolins was equivalent. Some care in interpreting this data should be made. The particle size distribution measurements for the Kaolin Flat D and the Kaolin 121S indicate that the 121S is much finer material than the Flat D. This is certainly the case when the two clays are suspended in a liquid (as is done for the particle size measurements). The raw material, however, is different. The Kaolin 121S is a hydrated Kaolin which is spray-dried after hydration. The spray drying yields a fluffy powder which, when suspended in water (or presumably other liquids), breaks up into its component grains. These grains have a mean size of about 1.0 μm, as shown by the sedimentation size data in Figure 6-6a. It is not at all clear if the 121S Kaolin powder breaks up into its component grains when injected into the furnace.

The sulfur capture data indicate that the Kaolin particle size for the small Kaolin particles has no effect on sorbent reactivity, but this conclusion is clouded by the uncertainty about the in-situ size of the Kaolin 121S.

A large particle size limestone, from the same mine as the vicron and with the same characteristic composition and grain size was mixed with three kaolins. The basic data for this sorbent (Marblewhite 125) are discussed in Chapter 7. The effect of the Kaolin on sulfur capture - again using a natural gas/H_2S flame sorbent with the fuel - was investigated. The decrease in SO_2 capture as a function of Al_2O_3 loading in the furnace is plotted for three Marblewhite 125 kaolin mixtures in Figure 6-9. Again, the Kaolin size had little effect on the decrease in SO_2 capture. The impact of the Kaolin on capture by the large Vicron (Marblewhite) sorbent was somewhat less than that observed with Vicron 45-3.

Dolomite was also mixed with two sizes of Kaolin (a mixture of dolomite and Kaolin px was too fine to feed accurately). The effect of the Kaolins on capture by dolomite is summarized by the data in Figure 6-10. Kaolin had a less pronounced effect on dolomite sulfur capture than capture by Vicron. The Kaolin used also influenced the degree of sorbent deactivation; the Kaolin 121S did not decrease capture as much as the kaolin Flat D. The interpretation of these data is not straightforward. It appears that the dolomite is less subject to deactivation than the Vicron 45-3, perhaps partly because of its large particle size. Particle size alone probably cannot account for the difference since the Marblewhite was almost as coarse as the dolomite and showed high deactivation by the Kaolin. Why the Kaolin size would affect dolomite deactivation and not Vicron deactivation is not at all apparent.

6.2 SO_2 and Mineral Matter Concentration Effects

Earlier limestone injection studies have indicated some effect of fuel sulfur content, and gas-phase SO_2 concentration on sulfur capture. The effect of fuel sulfur content on capture by a given sorbent has been reported to be 1/2 order in one system (Payne, 1982) somewhere between first and 1/2 order in another system (Flamet,1981) and first or 1/2 order in some early fundamental studies (Ishihara, 1970, Coutant, 1970). SO_2 concentration and fuel sulfur effects have also been observed in the BSF (Case, 1983), but a clear SO_2 reaction order has not been apparent (these data are discussed in Chapter 7). One possible source for the differences in effect of fuel sulfur content is the coal mineral matter interference. Changes in fuel sulfur change required sorbent injection rate for equivalent Ca/S mole ratios, and therefore, the sorbent/mineral matter ratio also changes with fuel for a given Ca/S concentration.

An attempt to clarify the relative effects of the sulfur content and the mineral matter content was made. H_2S-doped natural gas flames in the BSF were used. The flames were doped to three SO_2 levels. Sorbent Kaolin mixtures which contained 0, 10 and 20 percent Al_2O_3 were prepared. The sorbent mixture was injected with the fuel using the DMB under standard conditions. Sulfur capture was measured at Port 2 for Ca/S ratios of 1,2 and 3 for all three SO_2 levels using all three sorbent Kaolin mixtures. The results of these tests are summarized in Table 6-5.

TABLE 6.5 SULFUR CAPTURE FOR VARIOUS Al_2O_3, SO_2 CONCENTRATION

Run	SO_2 ppm	Al_2O_3%	Ca/S Mole Ratio	% Capture (Port 2)
1	500	0	1	13, 14
	500	0	2	28, 25
	500	0	3	41, 43
	500	10	1	13
	500	10	2	19
	500	10	3	23
	500	20	1	8
	500	20	2	11
	500	20	3	12
2	1800	0	1	15
	1800	0	2	33
	1800	0	3	50
	1800	10	1	8
	1800	10	2	12
	1800	10	3	17
	1800	20	1	4
	1800	20	2	7
	1800	20	3	10
3	3500	0	1	21
	3500	0	2	40
	3500	0	3	57
	3500	10	1	12
	3500	10	2	22
	3500	10	3	26
	3500	20	1	6
	3500	20	2	9*
	3500	20	3	11*

* Extrapolated from data at Ca/S = 1.0, 1.6

The mineral matter concentration in the furnace was calculated from the solids feed rate and gas flow. Figures 6-11, 6-12 and 6-13 show sulfur capture as a function of Al_2O_3 in the furnace at three concentrations. Each figure shows data at one calcium-to-sulfur ratio. It is clear from this data that SO_2 concentration has a slight influence on sulfur capture under these conditions and that even small amounts of Al_2O_3 (or coal mineral matter) have a detrimental effect on sulfur capture. The data imply that a high SO_2 concentration system (which requires high sorbent feed rates) is less strongly affected by the presence of mineral material than a low SO_2 concentration system. This may account for some of the observed dependence of sulfur capture on fuel sulfur content with coal.

6.3 Morphological Characteristics of Ash/Sorbent Mixtures

Samples of the sorbent ash mixtures were collected from the furnace at various locations. The surface area of these flame calcined samples was measured and compared to samples calcined at 1000°C in a crucible. Table 6-6 summarizes the measured surface areas. The addition of Kaolin or bentonite to either sorbent decreased the calcine surface area of both sorbents; the Kaolin had the greatest effect on surface area.

Scanning electron micrographs of raw sorbent mineral mixtures and of flame-calcined materials were taken. There are dramatic changes in the solids characteristics when flame calcined. Figure 6-14 shows electron micorgraphs of a Vicron/Kaolin mixture which was injected with the fuel and sampled from the furnace. The particles are spherical and analysis of individual particles show various Ca/Al/Si ratios. None of the particles analyzed were made up of only calcium or aluminum/silicon (Kaolin). A high-resolution, high-magnification photograph of one of the smooth, spherical, mixed-composition particles (Figure 6-14b) shows a smooth surface "littered" with tiny lumpy grains.

The available analytical technique could not provide a resolution of composition differences between the sphere and the grains stack on it. The physical appearance of the material does, however, suggest a mechanism for

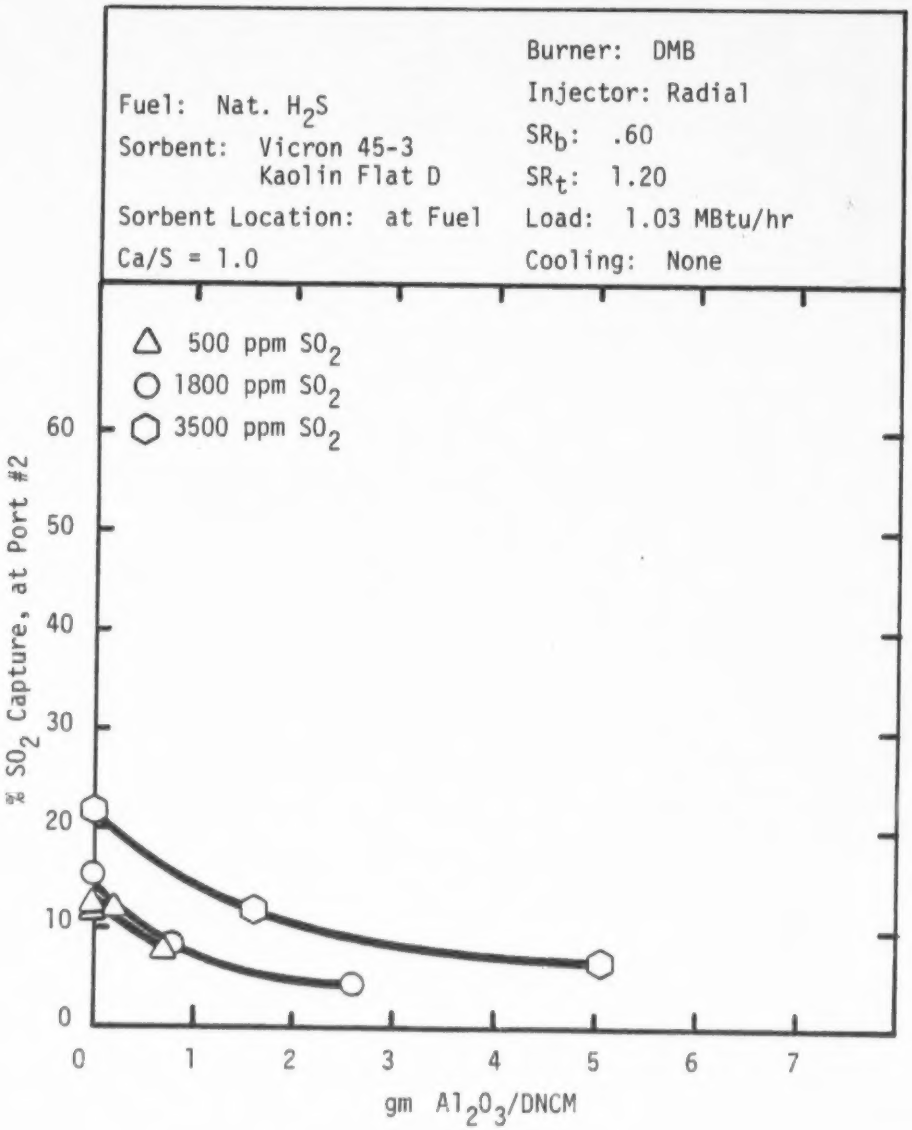

Figure 6-11. Effect of Al_2O_3 and SO_2 concentration on SO_2 capture, natural gas + H_2S, Vicron 45-3/Kaolin, Ca/S = 1.0.

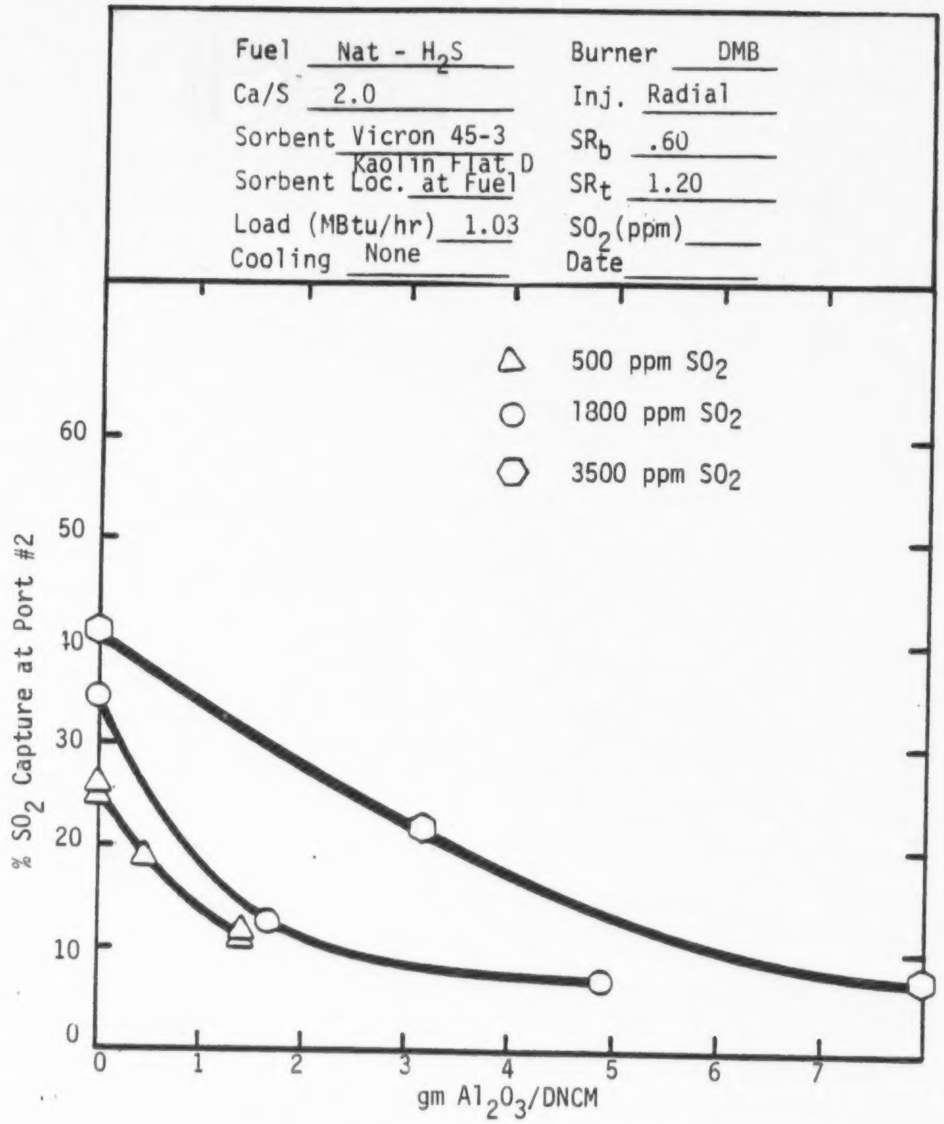

Figure 6-12. Effect of Al_2O_3 and SO_2 concentration on SO_2 capture, natural gas + H_2S, Vicron 45-3/Kaolin, Ca/S = 2.0.

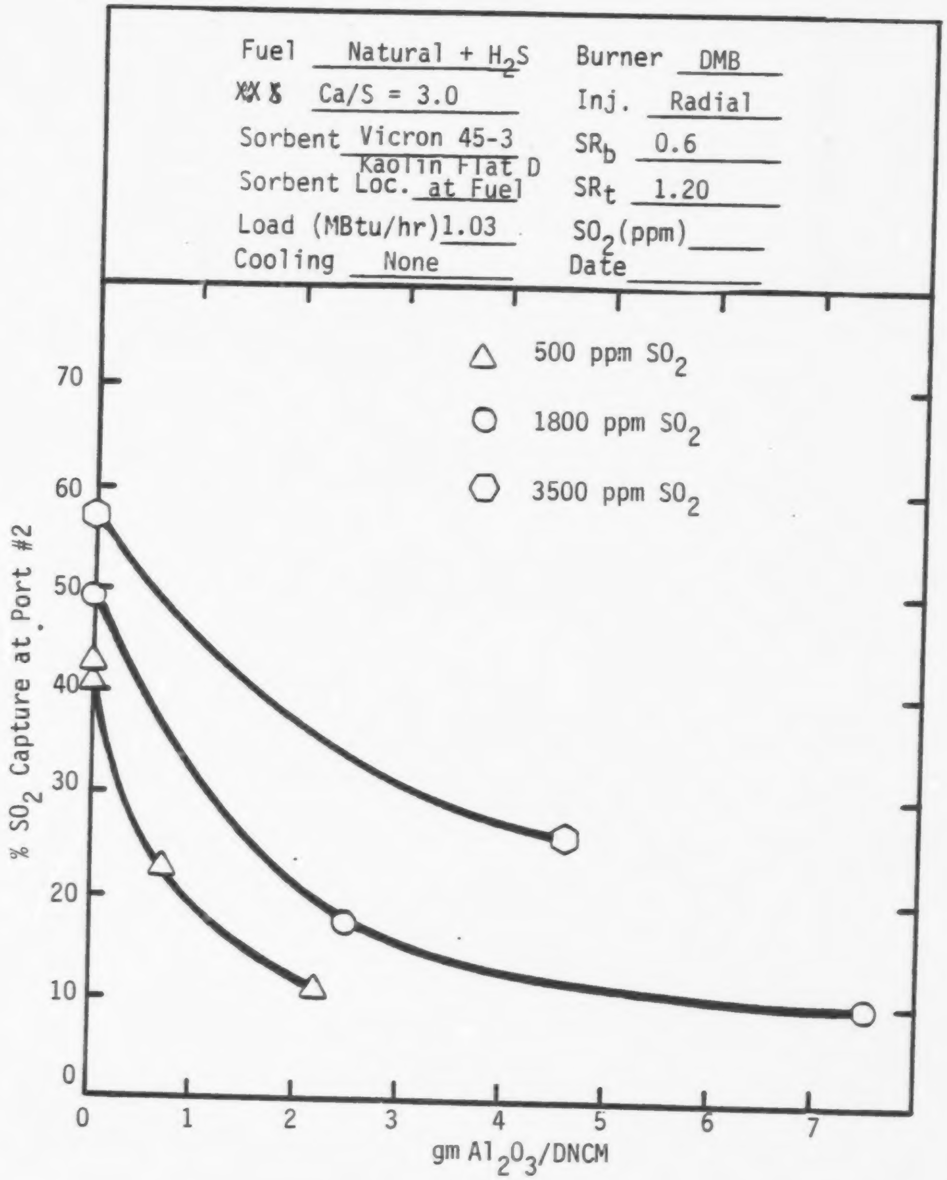

Fuel Natural + H_2S
XX X Ca/S = 3.0
Sorbent Vicron 45-3 Kaolin Flat D
Sorbent Loc. at Fuel
Load (MBtu/hr) 1.03
Cooling None
Burner DMB
Inj. Radial
SR_b 0.6
SR_t 1.20
SO_2(ppm)
Date

Figure 6.13 Effect of Al_2O_3 and SO_2 concentration on SO_2 capture, natural gas + H_2S, Vicron 45-3/Kaolin Ca/S = 3.0.

TABLE 6-6. EFFECT OF MINERAL ADDITION ON SURFACE AREA

Sample	Calcined Sample Surface Area (m^2/gm)		
	Crucible at 1000°C	Flame, at Port 1	Flame, at Port 2
Dolomite	9.17	2.60	2.72
Dolomite/ Bentonite, 1:2	0.89	0.79	0.94
Dolomite/ Kaolin, 1:1	6.49	0.88	2.35
Vicron 45-3	6.79	---	2.97
Vicron 45-3/ Bentonite, 1:2	0.40	1.37	1.55
Vicron 45-3/ Kaolin, 1:1	2.37	1.34	1.41

Reproduced from
best available copy.

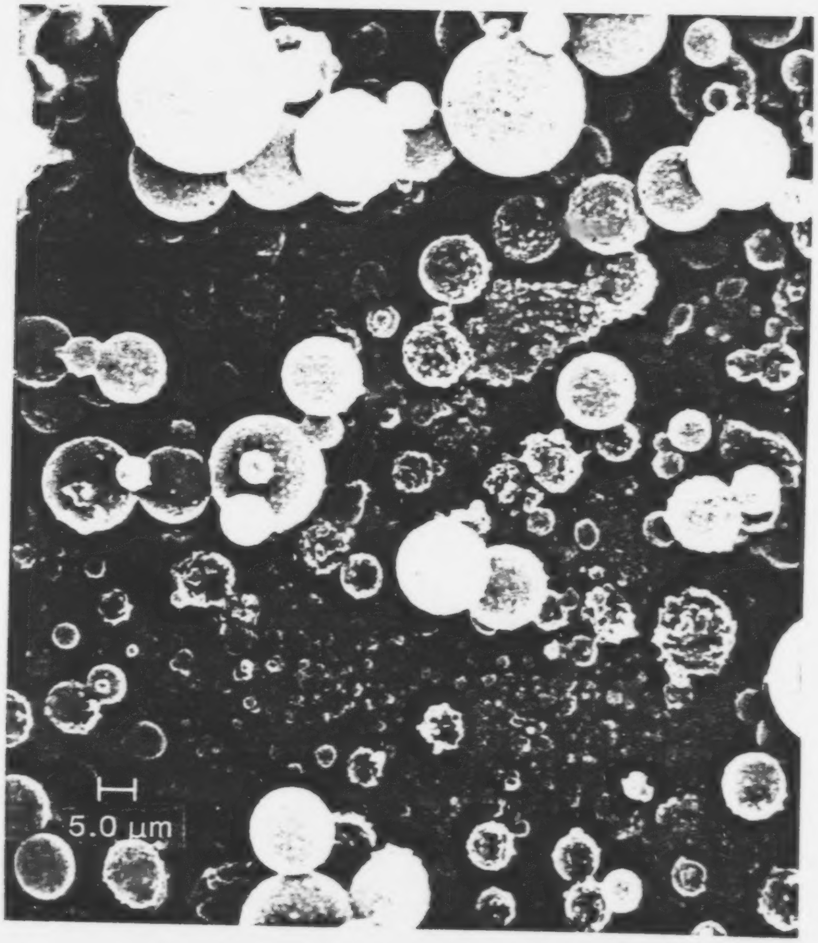

Figure 6-14a. Vicron/Kaolin mixture injected at fuel.

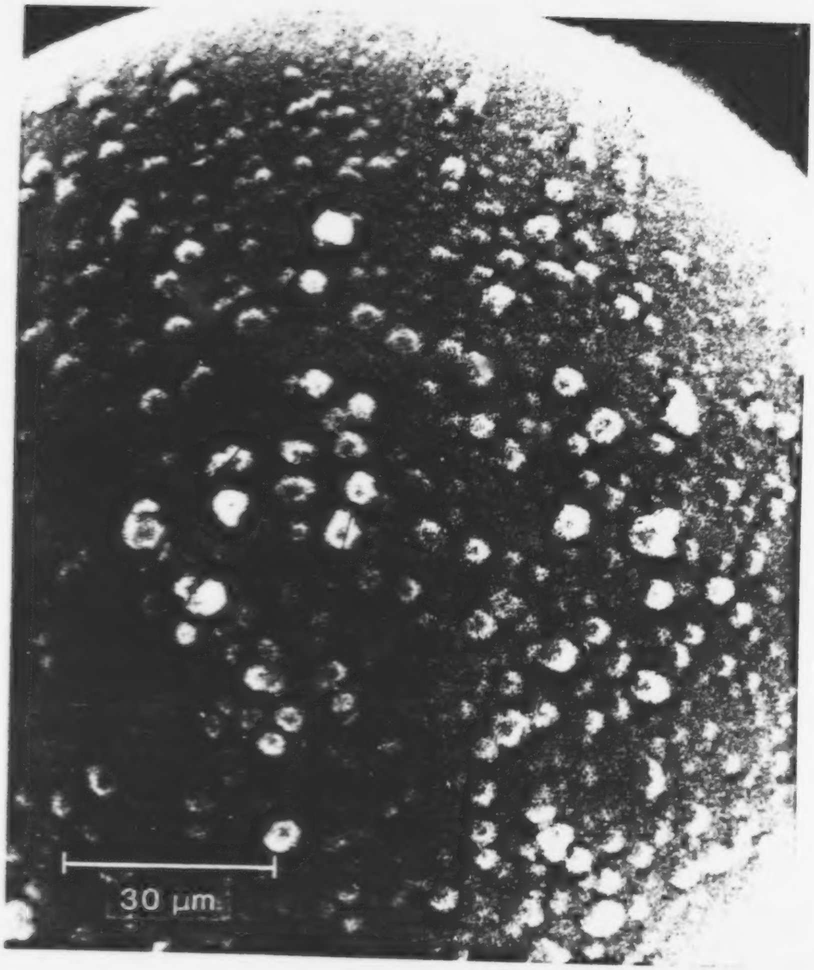

Figure 6-14b. High magnification mixed-composition particle.

sorbent deactivation. The spheres have obviously been molten. It is possible either that the Kaolin melted at flame temperatures and fine sorbent particles stack to it accounting for the littered appearance of the spherical particles, or that sorbent and Kaolin particles, in contact with each other, form a low melting eutectic which melts to give the smooth spherical particles. The CaO/ Al_2O_3/SiO system can form several low-melting eutectics. Figure 6-15 shows a three-phase diagram of the oxide system. The compositions of several particles from the flame-calcined mixture are indicated on the figure. (The analysis only gives metals content, it was assumed that all Ca was CaO, all Al was Al_2O_3 and all Si was SiO_2.) The melting points of these mixtures is considerably lower than that of kaolin or pure CaO, implying that a low melting complex may indeed have caused the sorbent deactivation.

6.4 Conclusions - Mineral Matter Effects

The addition of coal fly ash to vicron 45-3 (limestone) caused a dramatic reduction in sulfur capture by the sorbent in a natural-gas/H_2S flame. Fly ash from a pf-fired furnace is not necessarily the same as the original mineral matter in the coal so two clay minerals were mixed with two sorbents. The addition of kaolin had a strong effect on vicron utilization and a similar effect on dolomite. Bentonite, a different clay material, also decreased sulfur capture by the two sorbents, but not as dramatically as the Kaolin. There was a reasonably good inverse correlation between the alumina (Al_2O_3) content of the sorbent mixture and the sulfur capture with that mixture using either Vicron 45-3 or dolomite.

The relative size of the sorbent and Kaolin particles was investigated using two sizes of Vicron limestone and dolomite. Changing the added mineral size had little effect on the decrease in sulfur capture due to mineral material addition for either limestone. The greatest difference due to different Kaolin size observed with the dolomite where the finer Kaolin caused about a 10 percent greater difference in SO_2 capture than the coarse kaolin (see figure 6-10).

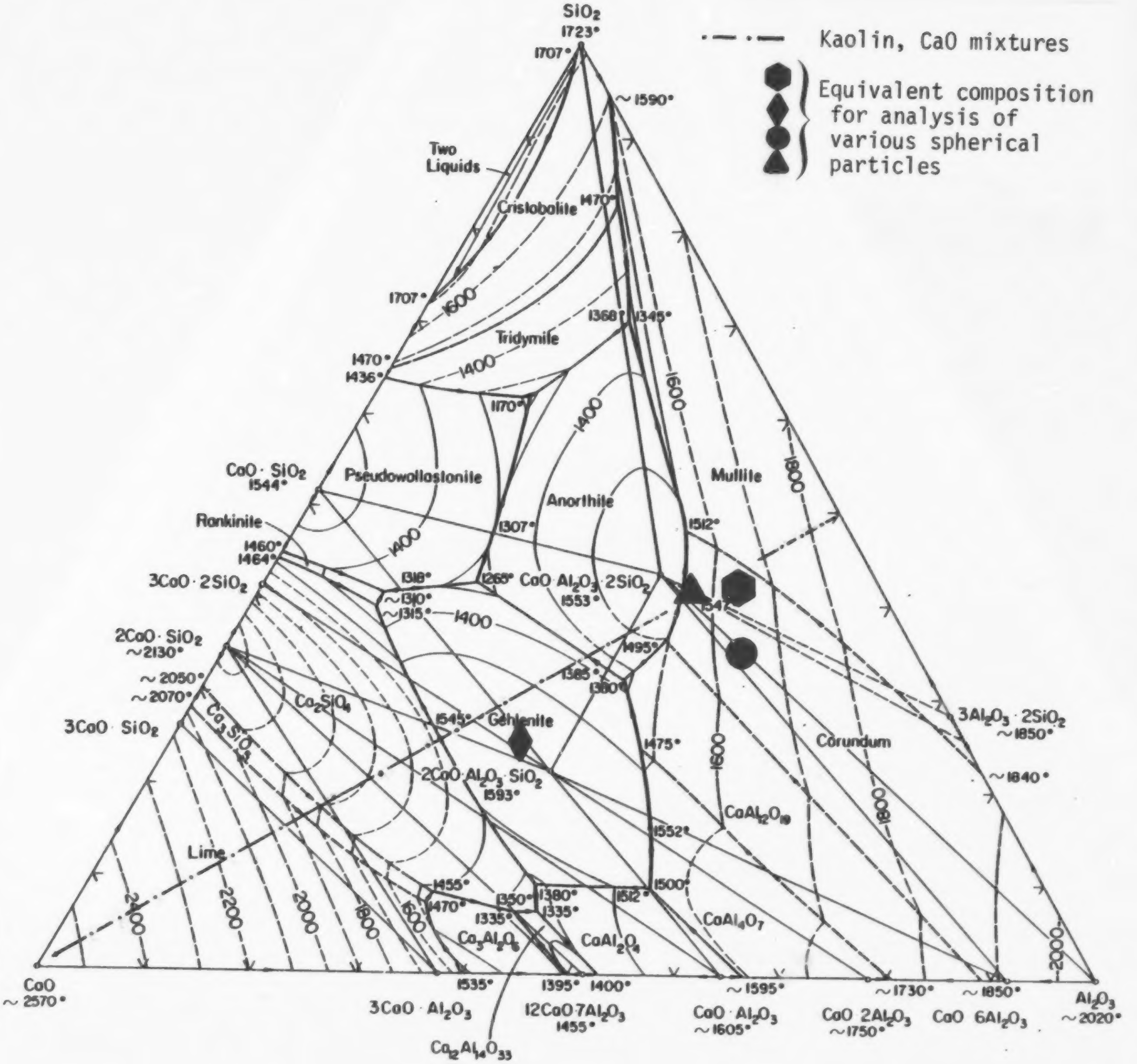
Kaolin, CaO mixtures
Equivalent composition for analysis of various spherical particles
SiO2
1723°
1707°
~1590°
Two Liquids
Cristobalite
1470°
1707°
1600
1368°
1345°
Tridymite
1470°
1436°
1400
1170°
1400
1600
CaO · SiO2
1544°
Pseudowollastonite
Mullite
1800
Anorthite
Rankinite
1307°
1512°
1460°
1464°
1400
3CaO · 2SiO2
1318°
1265°
CaO · Al2O3 · 2SiO2
1553°
~1310°
~1315°
1400
1547°
2CaO · SiO2
~2130°
1495°
~2050°
~2070°
Ca2SiO4
1385°
1380°
3Al2O3 · 2SiO2
~1850°
3CaO · SiO2
Ca3SiO5
1545°
Gehlenite
1475°
1600
Corundum
2CaO · Al2O3 · SiO2
1593°
~1840°
1800
CaAl12O19
1552°
Lime
1455°
1500°
1350°
1380°
1512°
1470°
1335°
1335°
CaAl4O7
2400
2200
2000
1800
1600
Ca3Al2O6
CaAl2O4
2000
CaO
~2570°
1535°
1395°
1400°
~1595°
~1730°
~1850°
Al2O3
~2020°
3CaO · Al2O3
12CaO·7Al2O3
1455°
CaO · Al2O3
~1605°
CaO 2Al2O3
~1750°
CaO 6Al2O3
Ca12Al14O33

Figure 6-15. Phase Diagram for CaO - Al_2O_3 - SiO_2 System.

The concentration of SO_2 in the natural gas-fired tests had a slight effect on sulfur capture, increasing capture at Ca/S = 2 from 26 percent at 500 ppm to 40 percent at 3500 ppm SO_2. The concentration of mineral matter (correlated as gm Al_2O_3 per dry normal cubic meter of flue gas) in the system had a very strong impact on capture at all of the SO_2 concentration levels and Ca/S ratios tested. At a calcium-to-sulfur mole ratio of 2 and 3500 ppm SO_2 the capture went from 40 percent with no mineral material to 8 percent with 7 gm/DNCM Al_2O_3 in the flue gas.

The effect of certain common coal mineral constituents on sulfur capture can be profound. Electron micrographs of sorbent mineral samples taken from the BSF show particles composed of a mixture of Al_2O_3 and CaO. The particles are spherical and have apparently been molten at some point in the furnace. It appears the sorbent/mineral interaction accounts for the observed effect of coal ash on sulfur capture. The mechanism of mineral deactivation is not clear and will be the subject of further investigation.

7.0 FUEL AND SORBENT INTERACTIONS

Experiments investigating the injection of sorbents for SO_2 emission control from pulverized coal flames have been performed in a number of systems, at various scales using different fuels and sorbents. Significant differences on SO_2 capture from the same fuel by different sorbents - and by the same sorbent with different fuels have been observed. In addition, the effect of fuel or sorbent type on sulfur capture has been observed to depend on the firing system and scale.

The purpose of this portion of the project was to provide a systematic data base on the effect of fuel and sorbent type on sulfure capture. Fuel sorbent pairs were tested at the same firing conditions in the BSF. All of the fuels and sorbents scheduled for pilot-scale testing at EER under various other contracts were included in the range of BSF tests. Using the same fuels and sorbents in different systems which are well characterized allows some assessment of particular system effects on sulfur capture. Figure 7-1 summarizes the fuel-sorbent pairs tested.

In addition to the effect of sorbent type on sulfur capture, the effect of sorbent particles size was investigated. Various size of two calcites (Vicron and Fredonia) were tested, two sizes of dolomite were also tested. Two fuels (natural gas and Indiana coal) were used. The sorbent particles size test matrix is shown in Figure 7-2.

7.1 Sorbent Effects

The sorbents tested included limestones, hydrated limes, and dolomite. Calcium carbonate is commonly called limestone and may be one of several mineral types. The limestones used, Vicron (also called Marblewhite depending on the color of the formation) is mined in the California Lucern Valley. The Fredonia is mined in Kentucky and used at the TVA Shawnee power plant wet-scrubber. The Vicron is a very coarse-grained (500-700 μm) limestone while the Fredonia is fine-grained (1-2 μm grain-size). Particle size distributions of the pulverized sorbents are summarized in Appendix C (Volume II).

	Vicron 45-3	Dolomite	$Ca(OH)_2$ Colton	$Ca(OH)_2$ SM	$CaCO_3$ SM	Fredonia C	Fredonia F
Natural Gas/H_2S 1800 ppm SO_2	✓ #9	✓ #10	✓ #10	✓ #9	✓ #10	✓ #9	✓ #9
Indiana L3 (1.2% S BSF)	✓ #8	✓ #8	✓ #10	✓ #8	✓ #10	✓ #8	✓ #10
Indiana L4 (1.5% S, SM)	✓ #8 #9(rep)	✓ #8		✓ #9		✓ #9	
Illinois (3.5% S, Riley)	✓ #8	✓ #8					
Utah (0.9% S, SM)	✓ #8	✓ #8	✓ #8		✓ #8	✓ #8	
Saar (0.76% S, SM)	✓ #10						

- Sorbent with Fuel
- DMB, 1.0 MBtu/hr

= Number of monthly report containing base data.

Figure 7-1. Fuel/sorbent interactions test matrix.

	Vicron 45-3	Vicron 200	MW 125	Fredonia C	Fredonia F	Dolomite A	Dolomite B	Dolomite C
Natural Gas + H_2S	✓	✓	✓	✓	✓	✓	✓	✓
Indiana L3	✓	✓	✓	✓	✓	✓	✓	✓

- Sorbent with Fuel
- DMB, 1.0 MBtu/hr, uncooled

Figure 7-2. Test matrix for sorbent particle size effect.

Dolomite, or dolomite limestone is a mixed calcium carbonate/magnesium carbonate mineral. The dolomite used is a high magnesium dolomite approximately half (on a molar basis) calcium and half-magnesium carbonate mined in the mid-west (Gibsonberg, Ohio). Hydrated lime (or commonly just lime) is produced by calcining limestone and rehydrating or slaking the calcite. The characteristics of a lime depend on both the parent limestone and the calcination and slaking processes. Two hydrated limes were used, one produced in the western U.S. (Colton lime) and the other a European stone used for LIMB tests performed for the IFRF and Steinmuller Company (SM $Ca(OH)_2$).

Physical and chemical characteristics of the sorbents used are summarized in Table 7-1. The oil absorbtion figures, where given, are from manufacturers specifications. Other information is from samples analyzed in-house (methods are described in Appendix B) or, in the case of chemical composition, analysis by an outside laboratory. Complete particle size distributions (measured by sedimentation) of all of the sorbents tested are included in Appendix C.

7.1.1 Effect of Sorbent Type

Sulfur capture by six sorbents injected into a natural gas/H_2S flame in the BSF is summarized by the data in Figure 7-3. Dolomite gave the highest capture, the Colton hydrated lime gave the lowest capture. Similar data for the baseline Indiana coal (lot 3) is shown in Figure 7-4, again dolomite gave the highest capture and the Colton lime the lowest. Capture for all of the sorbent was lower than with the natural gas H_2S flame. The Indiana coal used in various tests at EER has been purchased in several batches. These lots varied considerably in sulfur content - from .9 to 2.5 percent sulfur. The main batches used in current BSF and pilot-scale testing were Indiana Lot 3 the BSF baseline coals, Indiana Lot 4 (1.4-1.5 percent S) used for one set of pilot-scale burner tests as well as in the BSF. The effect of sorbent type on sulfur capture for the higher sulfur Indiana L4 coal is shown in Figure 7-5. The ranking of sorbents in terms of SO_2 capture remained unchanged for the two batches.

TABLE 7-1. SORBENT CHARACTERISTICS

SORBENT	Vicron 45-3 ⬡	Vicron 15-15 ◊	Colton Lime ◇
Petrographic Charact.			
Type	Calcite	Calcite	Hydrated Lime
Composition	$CaCO_3$	$CaCO_3$	$Ca(OH)_2$
Grain Size μm	500-700	500-700	N.A.
Top Size μm	45, 40	15	80
Mean Size μm	11, 12	3	12.5
Bottom Size μm	.3, .8	.15	.7, 4
Density gm/cm^3	2.757	2.757	2.353
Oil Absorption	14	21	
Surface Area	0.9, .6	2.73	10.4,13.8
Ignition Wt. Loss %			
1000°C	44.0,41.0	44.0	26.4,26.0
SA (1000°C) m^2/gm	6.7, 3.7		1.86
Hydration wt. gain (1000°C)	33.08	34.26	33.25
Chemical Comp. (%)			
Ca	39.2	39.3	48.9
Al	0.07	0.08	0.28
Si	0.07	0.07	1.08
Fe	0.037	0.071	0.164
Na	0.022	0.017	0.034
Mg	0.485	0.422	0.255
K	0.011	0.010	0.129
Cr	0.006	0.009	0.005
Cl			
S			

TABLE 7-1. SORBENT CHARACTERISTICS (Continued)

SORBENT	Dolomite ◗	SM Carbonate ○	Fredonia C ◺	SM $Ca(OH)_2$ ⌂
Petrographic Charact.				
Type	Dolomite		Calcite	Hydrated Lime
Composition	$CaCO_3$ $MgCO_3$	$CaCO_3$	$CaCO_3$	$Ca(OH)_2$
Grain Size µm			fine	
Top Size µm	<100	>100	>100	30
Mean Size µm	34.0, 40.	16	10	3.5
Bottom Size µm	1.0	1.5	0.4	0.3
Density gm/cc	2.855	2.76	2.76	2.35
Oil Absorption				
Surface Area	.64, .60	3.42	5.06	13.5, 12.1
Ignition Wt. Loss				
1000°C	47.1, 44.2		43.3	25.3
SA (1000°C) m^2/gm	9.17		1.34	1.64
Hydration Wt. Gain (1000°C)	67.5		31.6	
Chemical Comp. (%)				
Ca	21.0	38.9	40.0	51.0
Al	0.09	0.09		0.26
Si	0.37	0.76		0.80
Fe	0.102	.09		0.22
Na	0.033			
Mg	12.1	0.35	.74	
K	0.039			0.51
Cr	0.27			
P				
Cl				
S				

TABLE 7-1. SORBENT CHARACTERISTICS (Continued)

SORBENT	Fredonia Fine ◣	MW 125 ⬢	Vicron 200 ◑
Petrographic Charact.			
Type	Calcite	Calcite	Calcite
Composition	$CaCO_3$	$CaCO_3$	$CaCO_3$
Grain Size µm	fine	500-700	500-700
Top Size µm	∿50	>100	∿100
Mean Size µm	4	30	17
Bottom Size µm	.3	.7	∿.4
Density gm/cc	2.76	2.76	2.76
Oil Absorption			
Surface Area	2.34	0.42	0.8
Ignition Wt. Loss			
1000°C	42.8	41.2	43.7
SA (1000°C) m^2/gm	1.56	3.58	4.27
Hydration Wt. Gain (1000°C)			
Chemical Comp. (%)			
Ca			
Al			
Si			
Fe			
Na			
Mg			
K			
Cr			
P			
Cl			
S			

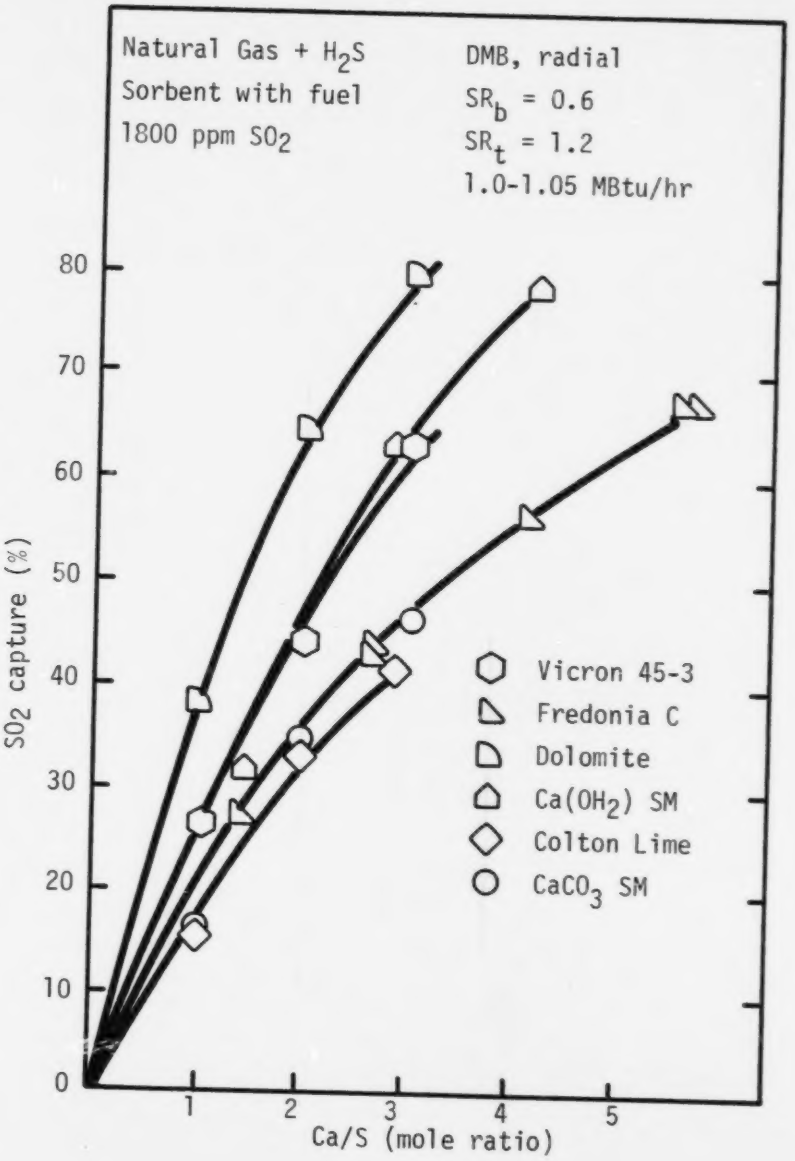

Figure 7-3. Effect of sorbent type, natural gas flame.

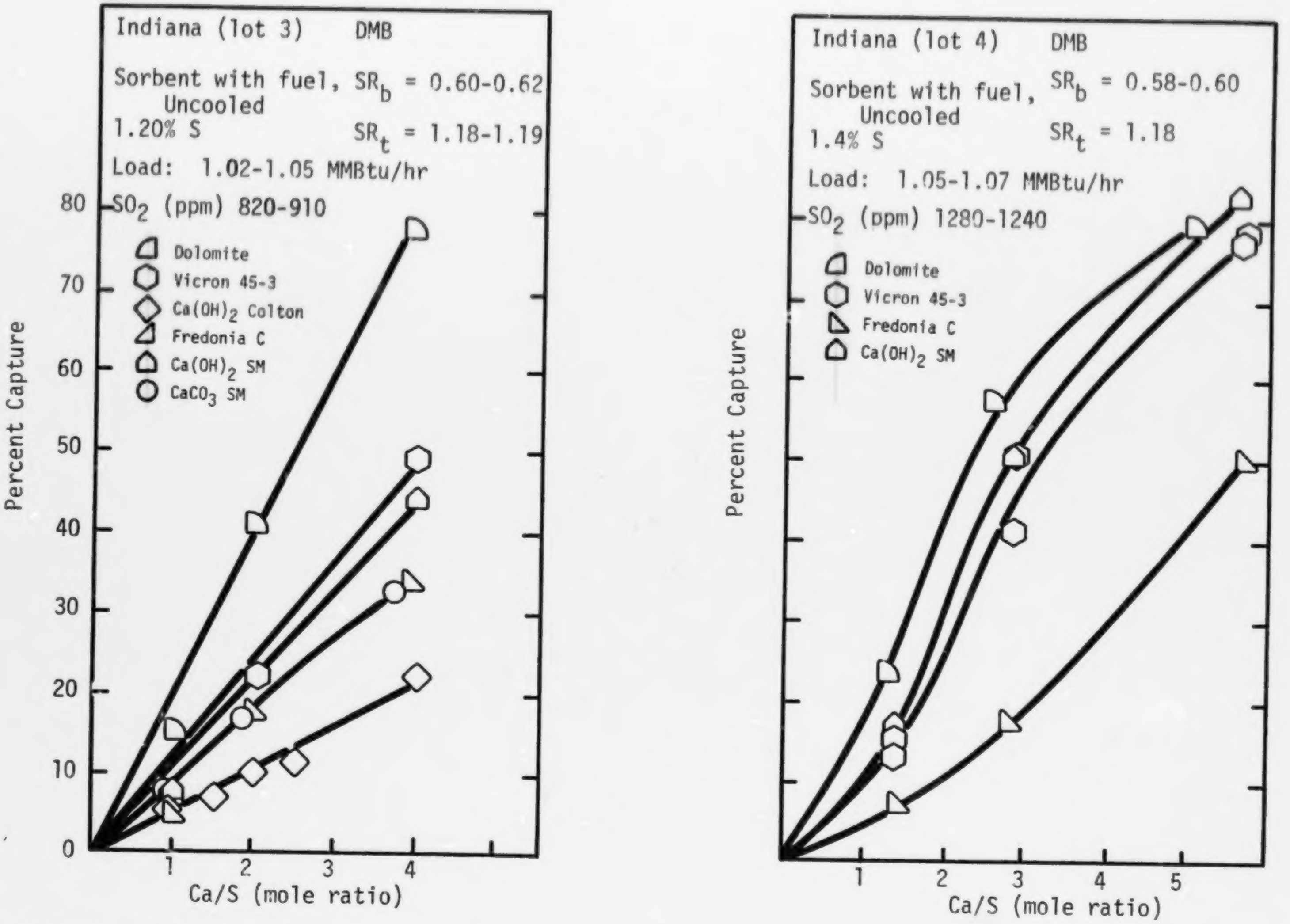

Figures 7-4 and 7-5. Effect of sorbent type on sulfur capture, Indiana Lot 3 and Lot 4 coals.

Two other fuels, Utah (a western low-sulfur, sub-bituminous coal) and Illinois (an eastern high-sulfur, bituminous coal) were tested. Dolomite gave the highest capture with these fuels also, and again with the Utah coal the Colton lime gave the least capture (see Figures 7-6 and 7-7).

A direct comparison of the three limestones (Vicron, Fredonia, and the German [SM] carbonate) shows little difference between in the Fredonia and SM carbonates with slightly better capture by the Vicron. The difference between in the two hydroxides (Colton lime and $Ca(OH)_2$ SM) is more striking. Figures 7-8 and 7-9 summarize SO_2 captures measured for the two limes in gas and Indiana coal flames. Included is data from an earlier test of the Colton Lime with Indiana coal (2667 data). The German hydroxide gave considerably higher capture than the Colton lime with both fuels. Particle size distributions for the two sorbents are shown in Figure 7-10. The German (Steinmuller) hydroxide is finer than the Colton lime and does not exihibit the bimodal size distribution of the Colton hydroxide. It is not clear if the difference in size is the cause of the difference (such as mode of production or calcination) in the two sorbents is responsible for the higher capture measured with the German hydroxide.

7.1.2 Effect of Sorbent Particle Size

The effect of sorbent particle size on sulfur capture was tested with natural gas and Indiana (lot 3) coal. Three sorbents were tested - two limestones and a dolomite. Vicron is a large-grained limestone, which, when pulverized to the sizes tested is "over-ground" meaning that the particles are smaller than the original grain size. Fredonia white is a fine-grained limestone; particles of the pulverized stone are made up of many fine grains. Particle size distributions of the limestones tested are shown in Figures 7-11a and 7-11b. Three samples of dolomite (from the same mid-western mine, producer) were also tested. The dolomite size distributions are shown in Figure 7-12.

The effect of the Vicron particle size on sulfur capture with Indiana coal and natural gas is summarized in Figure 7-13. Increased sorbent particle

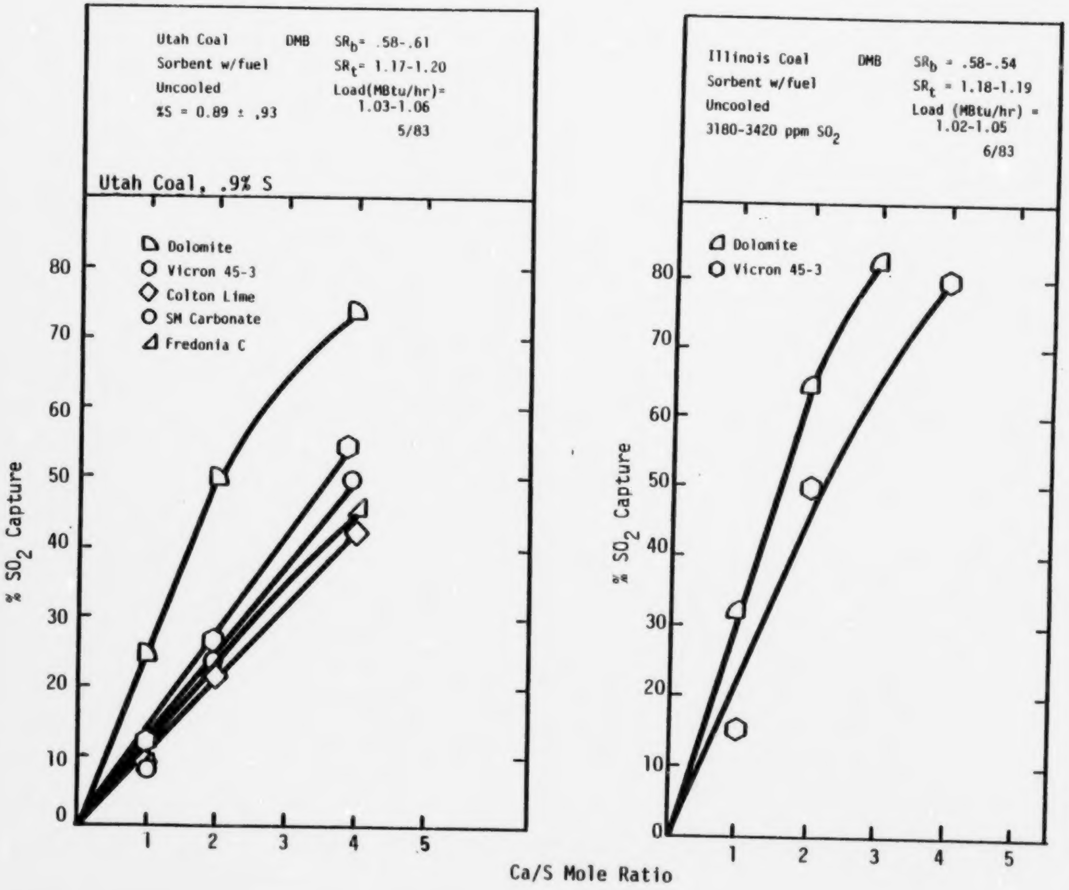

Figures 7-6, 7-7. Effect of Sorbent on Sulfur Capture, Utah and Illinois Coals.

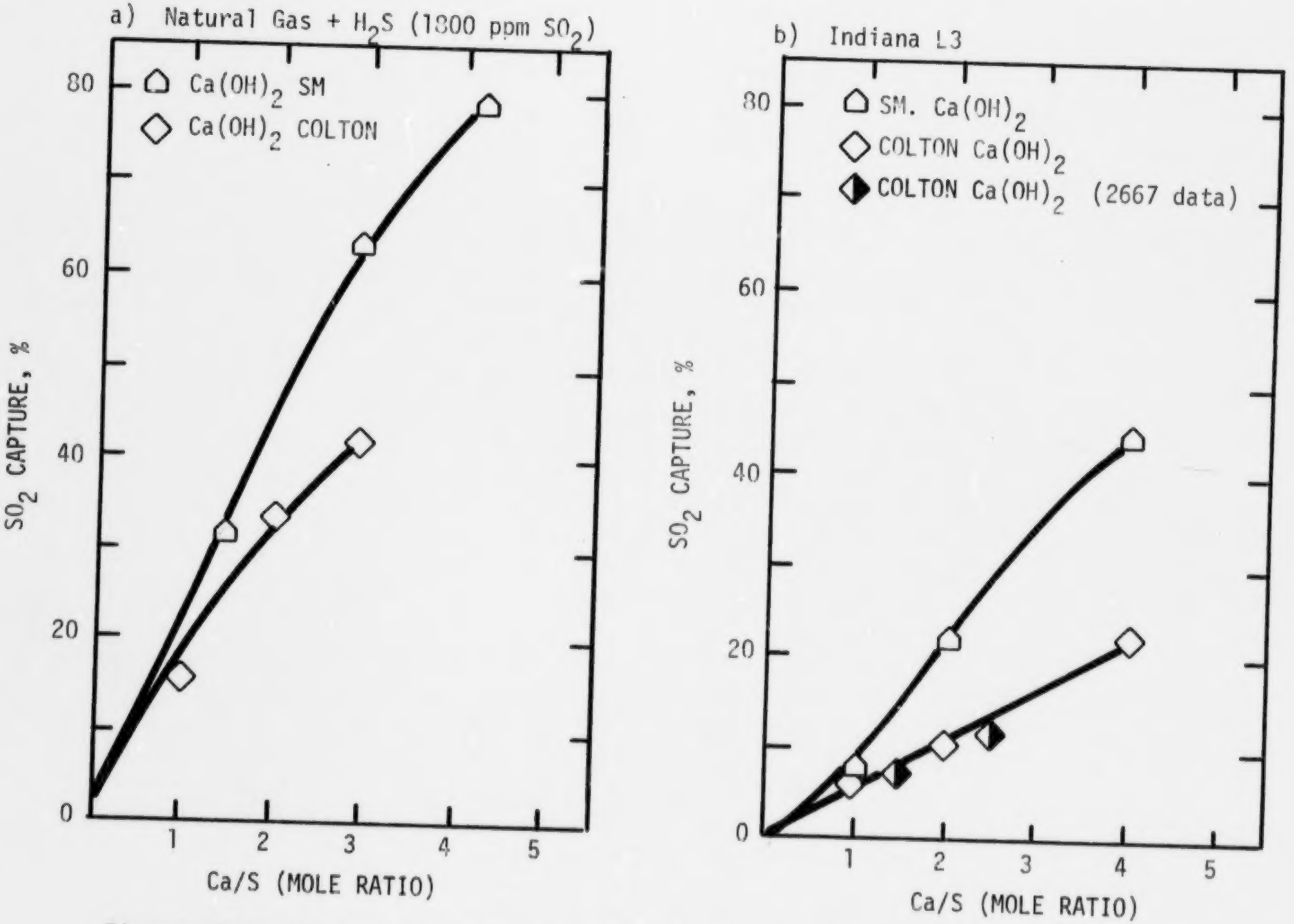

Figures 7-8 and 7-9. Effect of hydrated lime type, Colton and German, on Sulfur Capture. Sorbent with fuel, DMB, uncooled.

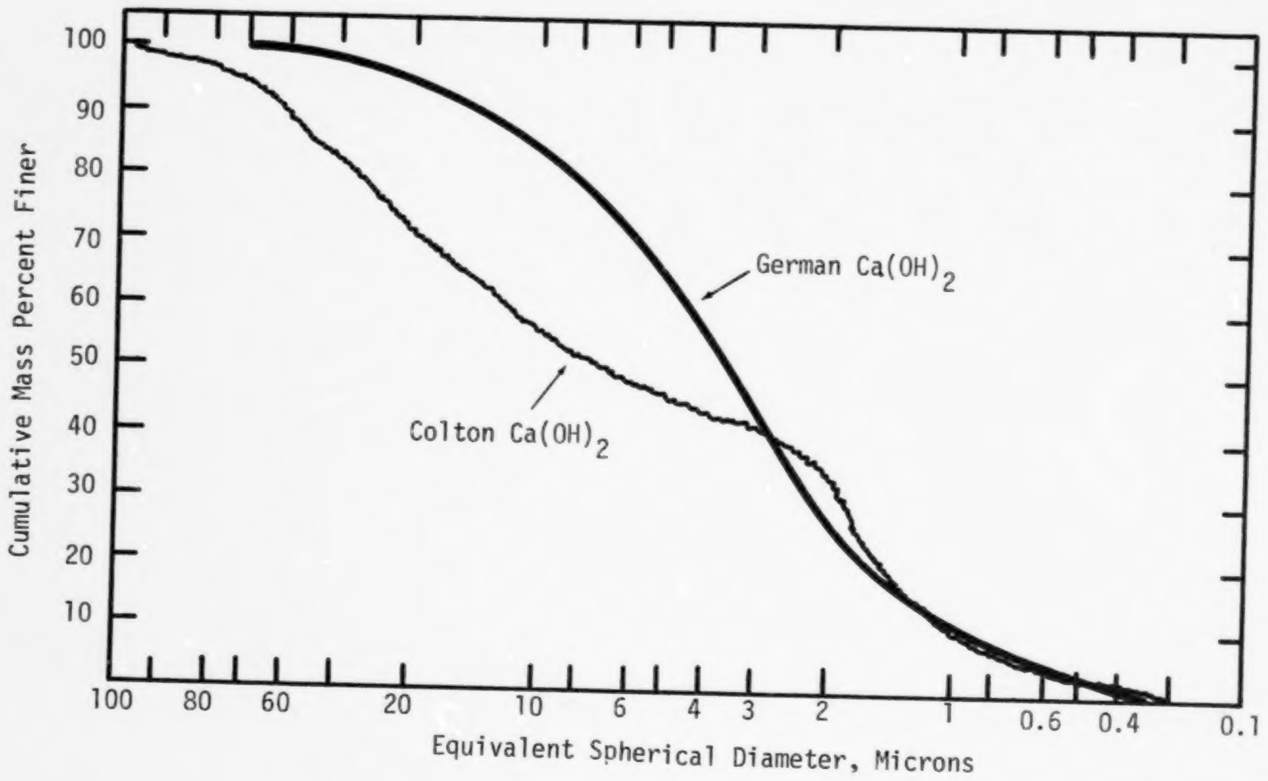

Figure 7-10. Relative particle size distributions, Colton and "Steinmuller" calcium hydroxides.

(a) Vicron

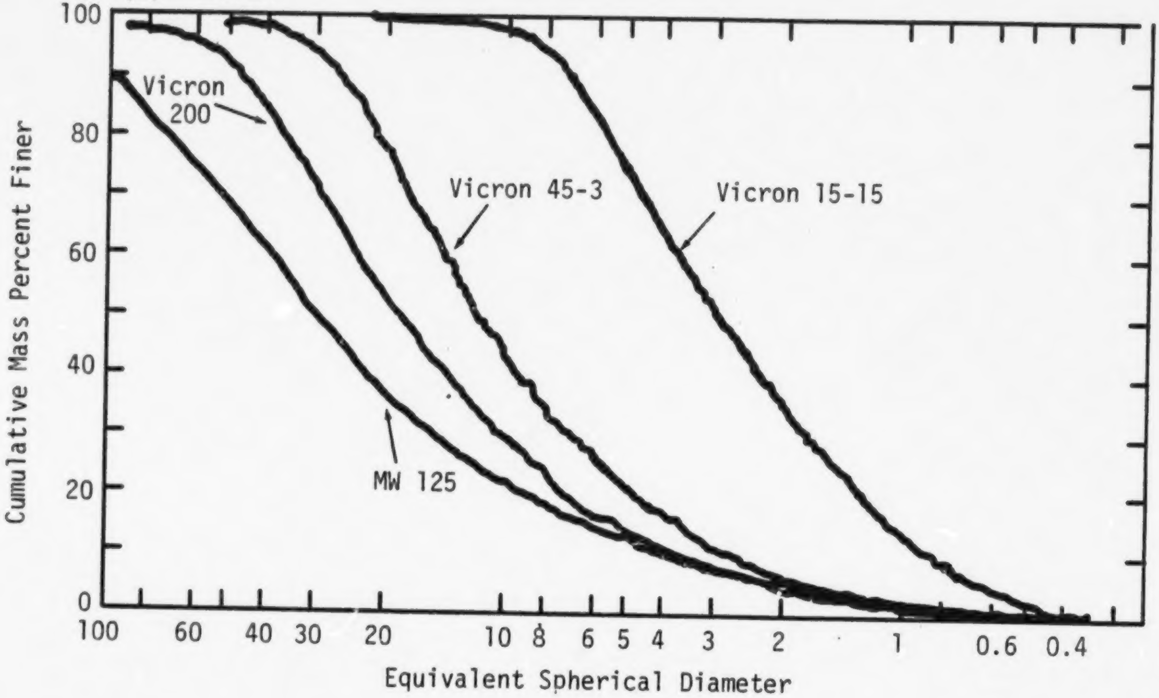

(b) Fredonia

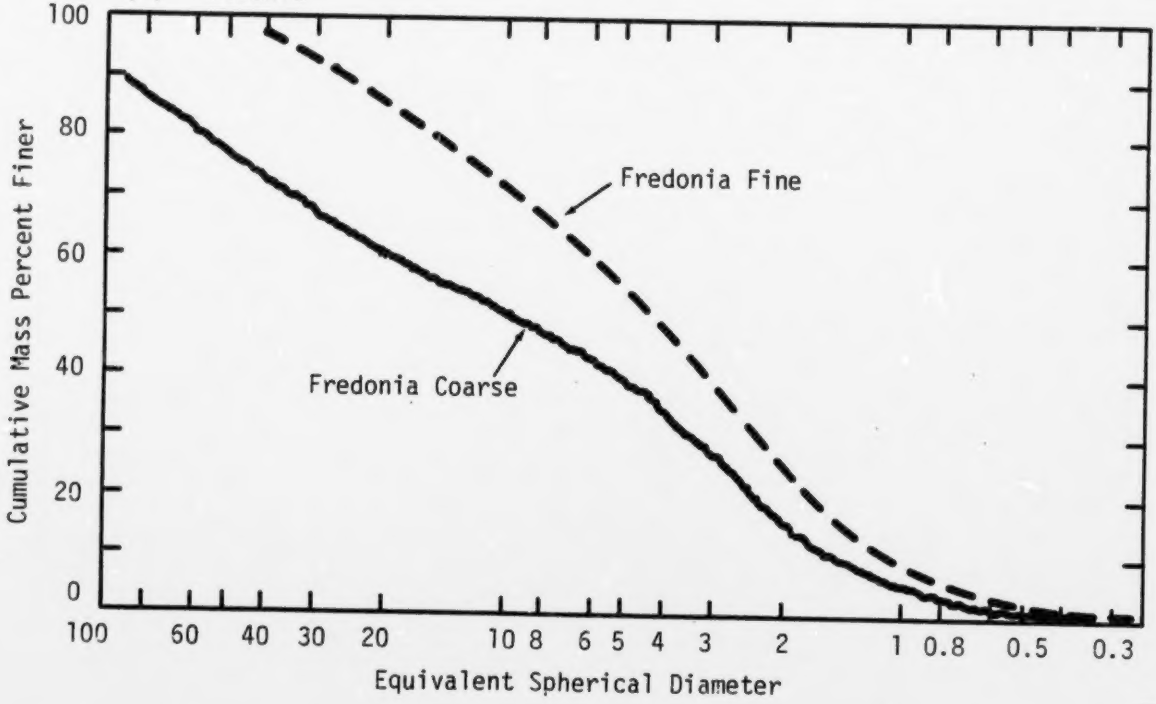

Figure 7-11. Particle size distributions for Vicron and Fredonia sorbents.

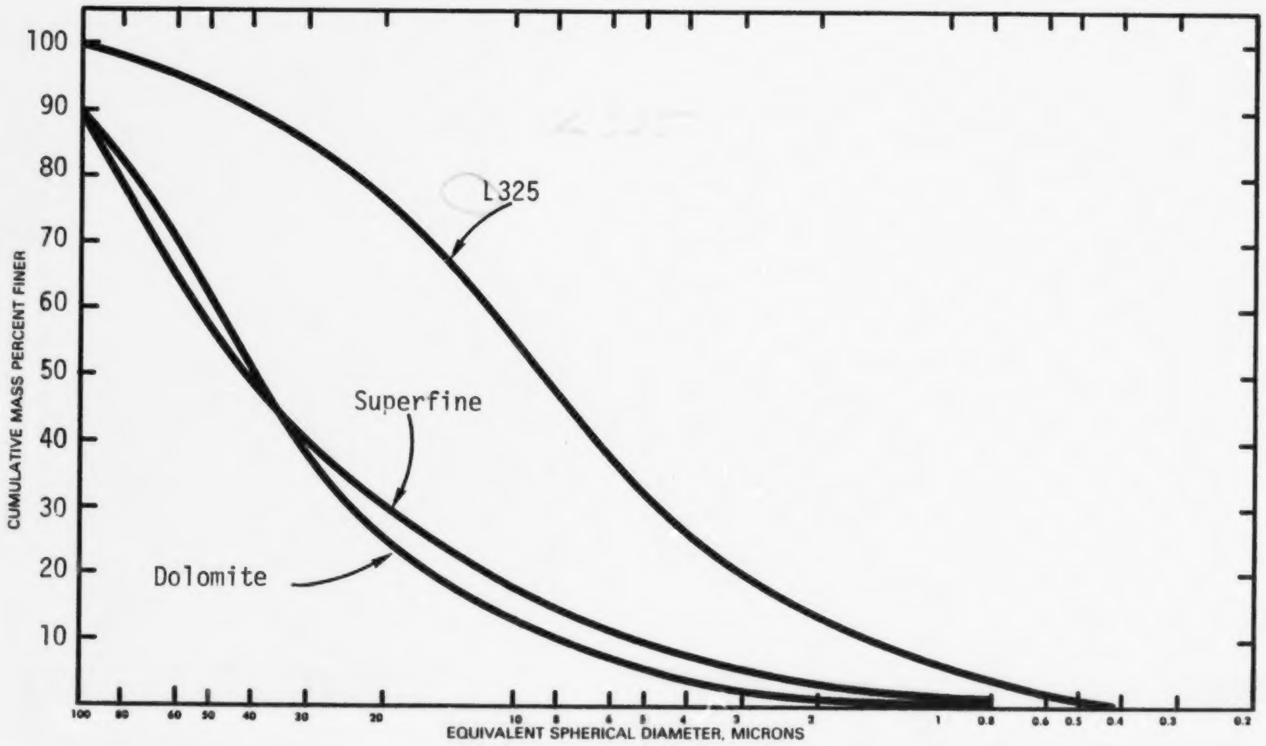

Figure 7-12. Particle size distributions for Dolomite sorbents.

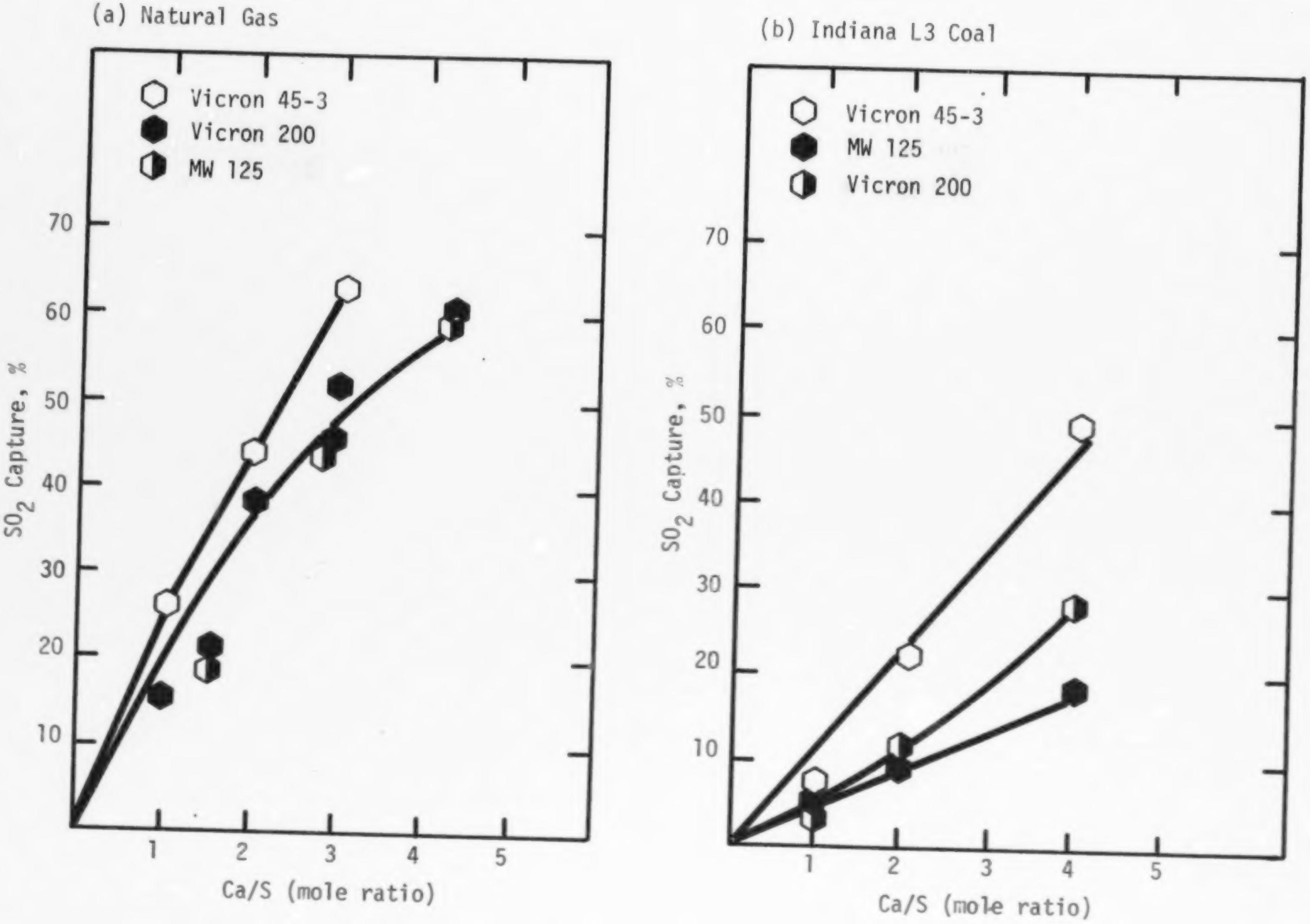

Figure 7-13. Effect of input Vicron particle size on sulfur capture, natural gas and Indiana L3 coal.

size slightly reduced capture with natural gas. The effect of sorbent size was slightly greater with the Indiana coal.

The expected effect of particle size on sulfur capture was determined using the sulfation model. Figure 7-14 shows the calculated effect of sorbent particle size and the measured effect with the gas and coal flames. (Data from earlier tests (2667) with Vicron 15-15 were added to extend the data base.) The calculated values are based on in-situ sorbent size, which is not necessarily the injected sorbent size. Vicron has been demonstrated to fragment when flame calcined. It is very difficult to estimate in-flame particle sizes for the vicrons except to say they are probably smaller than the injected size. The model predicts that particle size has little effect with fine (<10 μm) particles. The natural gas and coal data show the same trend though not as clearly, perhaps in the coal case because of an interaction with the coal mineral matter.

Two sizes of the Fredonia sorbent, sampled from the TVA wet-scrubber limestone feed, were tested with both fuels. These results are shown in Figure 7-15. The Fredonia particle size had little effect in the gas flame, but the coarse sorbent gave significantly lower capture in the coal flame.

Three samples of dolomite (size distributions shown in Figure 7-12) were tested with gas and Indiana coal. Sulfur capture as a function of Ca/S ratio for the sorbents with these fuels is summarized in Figures 7-16 and 7-17. Particle size made a slight difference in the gas flame, the difference was more pronounced (and more consistent) in the coal flame. As with the Vicron, the finer sorbent gave higher sulfur capture, though not dramatically higher.

7.2 Fuel Effects

The effect of fuel type and sulfur content on sulfur capture was investigated. Samples of five coals and natural gas were tested with Vicron 45-3, dolomite and a calcium hydroxide (see Figure 7-1) under the same general firing and sampling conditions. The fuels used were all fuels scheduled for pilot-scale (10-100 MBtu/hr) testing at EER under various other contracts.

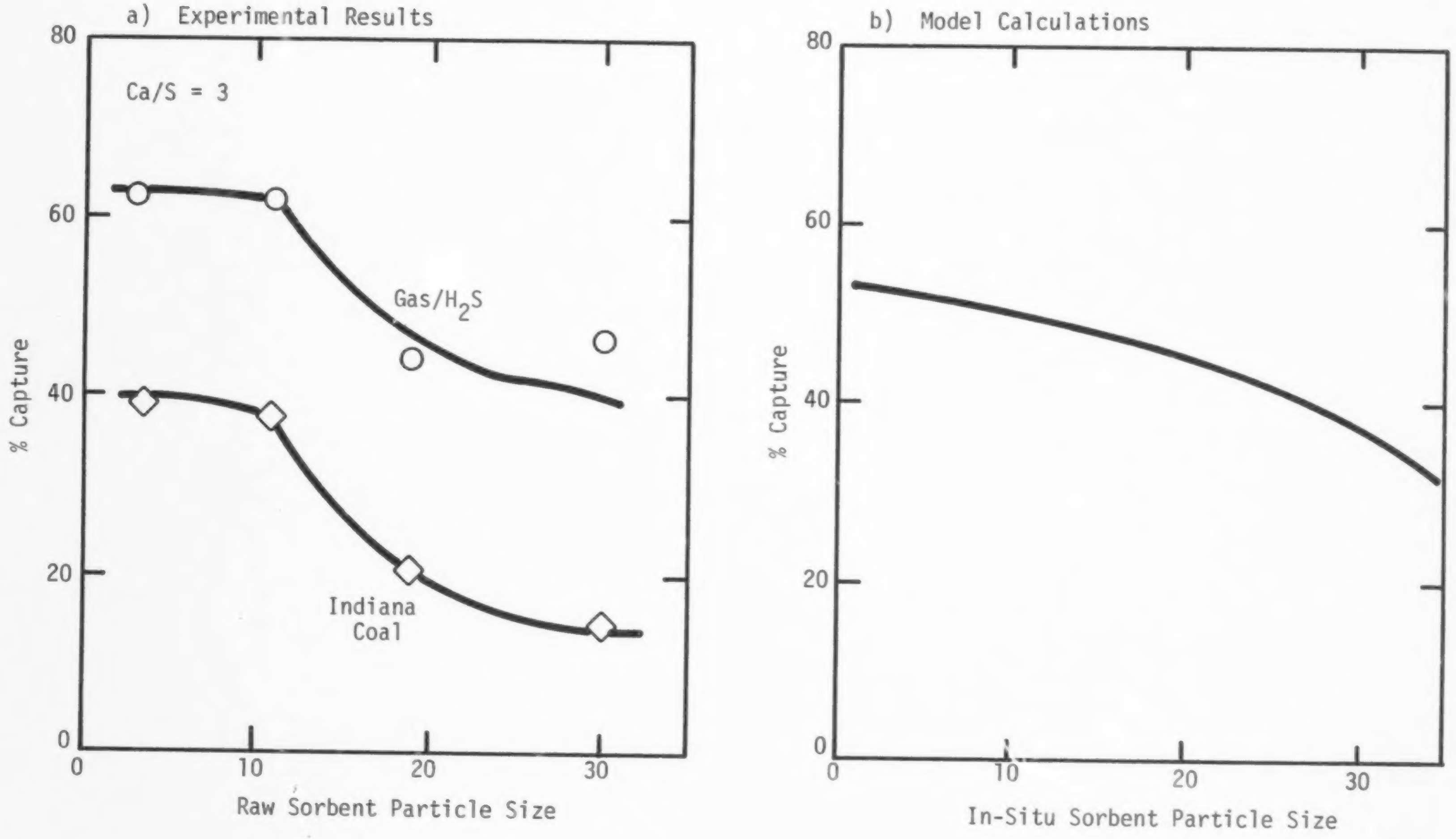

Figure 7-14. Effect of input Vicron particle size on SO_2 capture, comparison of BSF data with model.

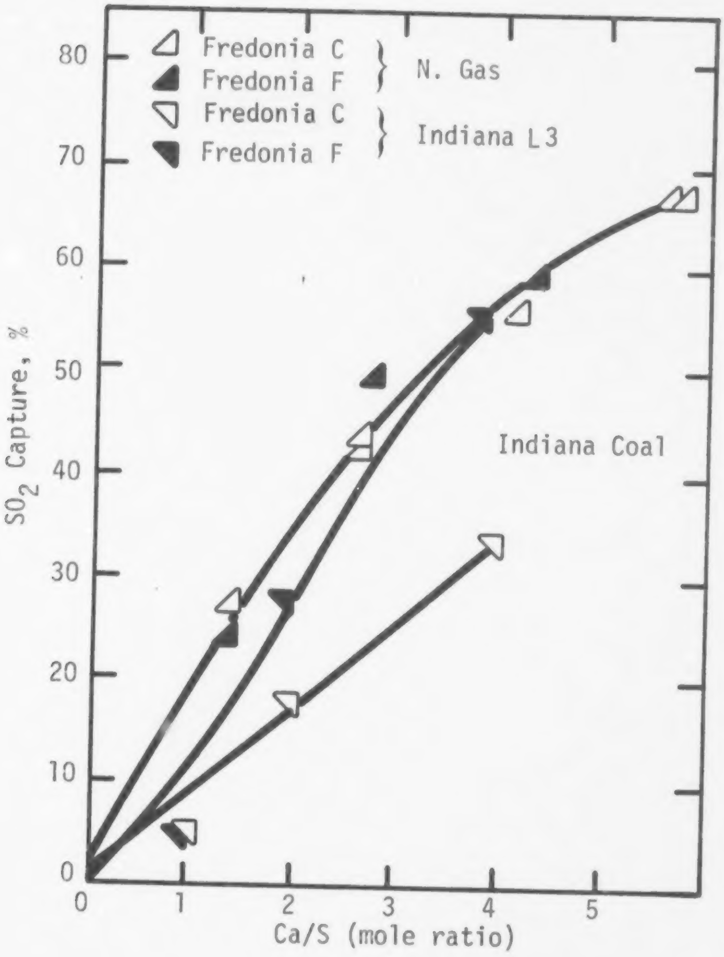

Figure 7-15. Effect of Fredonia sorbent particle size on SO_2 capture, natural gas and Indiana L3 coal.

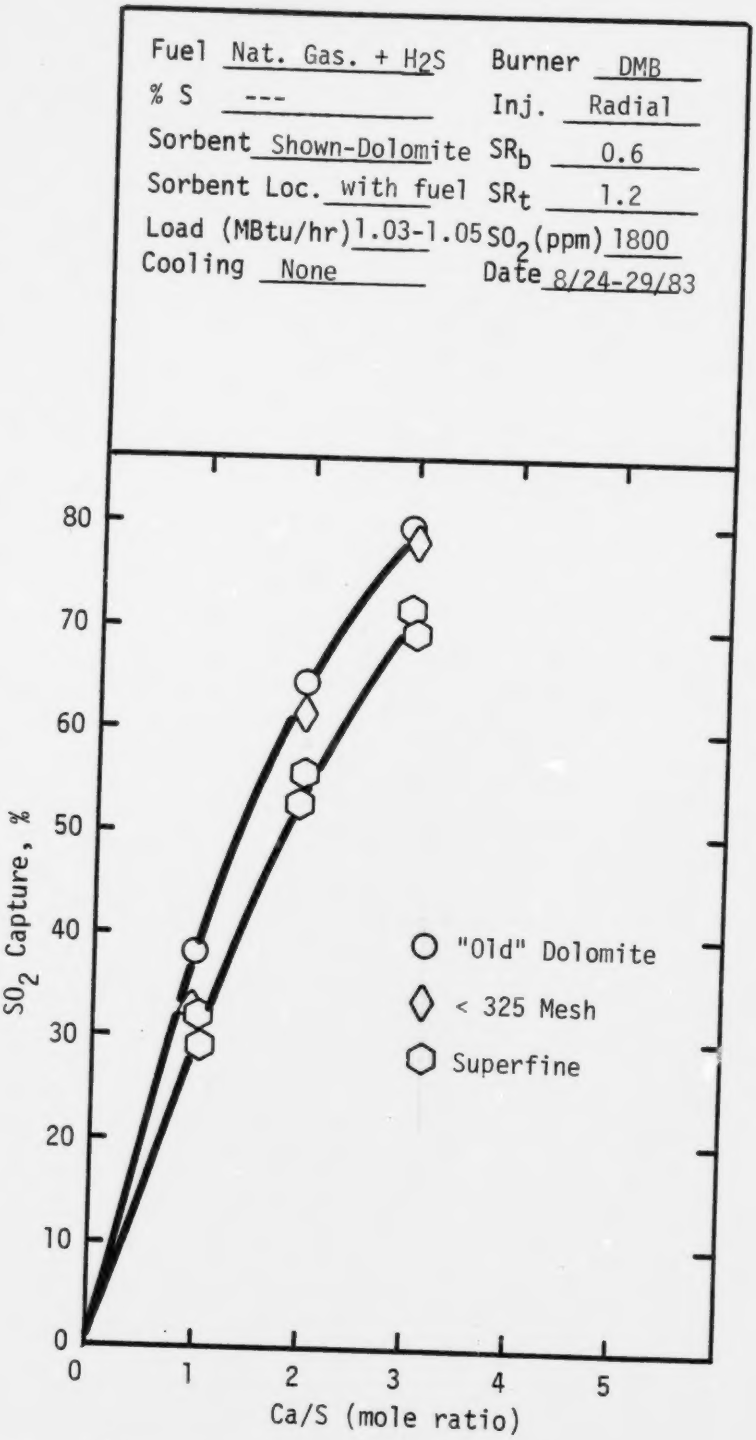

Fuel Nat. Gas. + H_2S
% S ---
Sorbent Shown-Dolomite
Sorbent Loc. with fuel
Load (MBtu/hr) 1.03-1.05
Cooling None
Burner DMB
Inj. Radial
SR_b 0.6
SR_t 1.2
SO_2 (ppm) 1800
Date 8/24-29/83

Figure 7-16. Effect of Dolomite particle size on sulfur capture, gas flame.

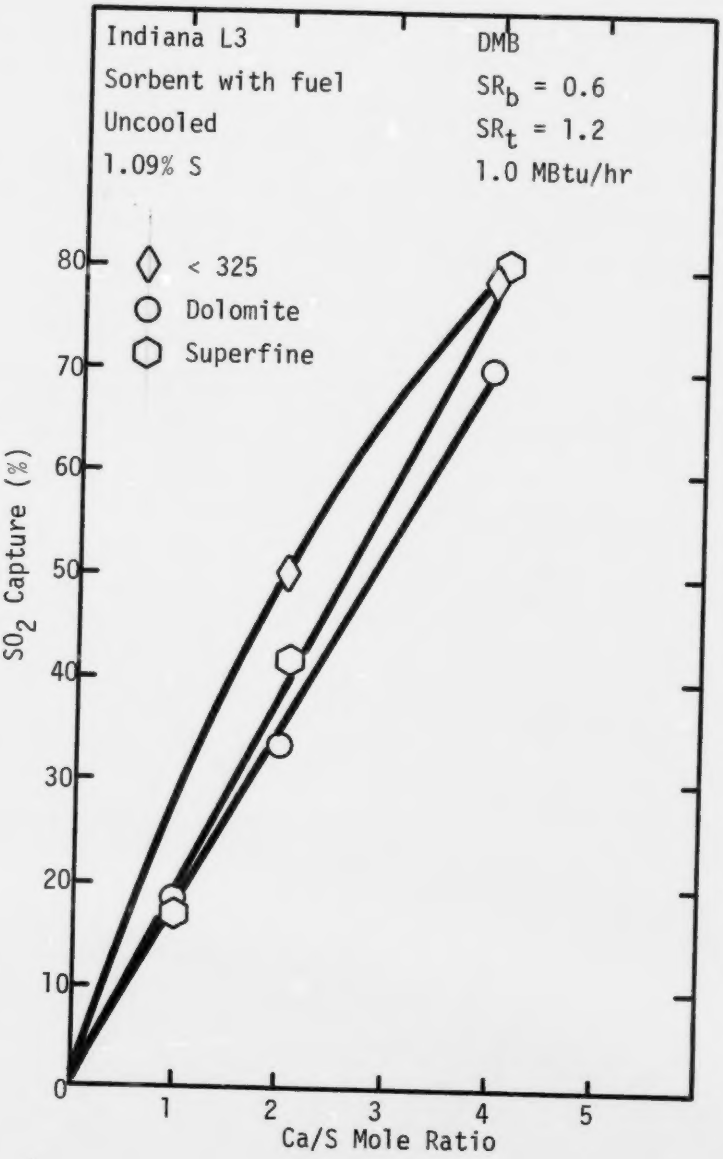

Figure 7-17. Effect of Dolomite particle size on sulfur capture, Indiana (lot 3) coal.

Two batches of Indiana coal (which is characteristically highly variable) were used, a high sulfur eastern bituminous coal (Illinois) and a low sulfur western (Utah) coal were tested. The Sarr coal is a West German black coal used in pilot-scale tests at EER and scheduled for use in a full-scale demonstration at a German power plant. The fuels were sampled when pulverized and during testing. Fuel analysis included determination of proximate and ultimate composition, forms of sulfur, ash composition and ash melting characteristics. Table 7-2 summarizes fuel characteristics and indicates measured variation in composition of the fuels used during these tests.

Vicron 45-3 was tested with four coals, the results of these tests are summarized in Figure 7-18. The figure shows sulfur capture as a function of Ca/S ratio, based on fuel sulfur content and sorbent feed rate. The Utah coal has considerable calcium in the ash so the Ca/S mole ratio including the fuel calcium is also shown. The high sulfur Illinois coal gave the highest capture while Utah and Indiana (lot 3) gave the lowest. Firing the different coals in the BSF gave somewhat different temperature profiles, as shown by the data in Figure 7-18b. Sulfur capture at three furnace locations (residence times) is shown with the temperature profile for each fuel. Clearly, capture took place in the 2200 to 1500°F temperature range with all of the fuels. Major differences in capture were evident only at times (or temperatures) in this sulfation zone; capture at the first sample location was essentially the same for all of the fuels while capture at the furnace exit was considerably higher with the Illinois coal.

Sulfur capture and temperature profile data for dolomite with the same four fuels is shown in Figure 7-19. Again, the high sulfur Illinois coal gave the highest capture, though the difference was not as striking as with the Vicron 45-3. Figures 7-20 and 7-21 show sulfur capture data for Fredonia and Colton lime with several fuels. These two sorbents did not exhibit the same increase in sulfur capture with the higher sulfur fuel. In fact, sulfur capture for Indiana (L3) coal with Colton lime was lower than the Utah with lime even though the Indiana coal had a higher sulfur content. This data is anomalous, with no clear explanation.

TABLE 7-2. FUEL CHARACTERISTICS

Fuel	Indiana L3 ○	Illinois ◇	Utah △	Indiana L4 ◊	Saar ⌂
Proximate (a.r., %)					
Volatiles	29.98	38.22	40.0	32.93	31.37
Fixed C	54.99	46.07	48.48	53.0	59.38
Ash	9.96	9.52	7.62	8.81	7.25
H_2O	5.07	6.19	3.90	5.26	2.0
Ultimate (dry %)					
C	69.65	64.85	69.92	71.65	74.8
H	4.43	4.53	5.07	4.63	4.77
N	1.41	1.23	1.41	1.4	1.21
S	1.15	3.70	0.88	1.37	0.79
O (diff)	12.88	15.54	14.79	12.03	10.55
Btu/lb (dry)	12,721	11,947	12,740	12,188	13,374
Ash Composition (%)					
SiO_2	58.63	52.58	64.06	57.6	44.99
Al_2O_3	23.56	17.62	18.89	23.82	25.0
TiO_2	0.99	0.59	0.78	0.91	0.77
Fe_2O_3	10.26	15.83	4.78	10.28	10.49
CaO	0.95	4.40	5.21	1.37	4.7
MgO	0.36	1.22	0.71	0.73	3.06
K_2O	1.49	2.21	1.16	2.4	3.27
Na_2O	0.22	1.18	0.77	0.45	0.485
SO_3	0.43	4.51	4.95	0.80	5.615
P_2O_5	0.47	0.28	0.43	0.29	0.175
Ash Melting pts					
(°F, red.) IDT	2360	2035	2240	2400	2235
AFT	2590	2070	2380	2540	2360
HT	2615	2240	2480	2630	2450
FT	>2700	2380	2700	>2700	2555
(°F, oxi.) IDT	2600	2250	2320	2520	2317
AFT	>2700	2340	2440	2680	2405
HT		2460	2520	>2700	2490
FT		2540	2700	>2700	2600
Forms of Sulfur (a.r.)					
Pyrite	0.3	0.5	0.1	0.3	0.37
Sulfate	0.41	2.3	0.6	0.4	0.46
Organic	0.33	0.6	0.1	0.5	0.02
Total	1.09	3.4	0.8	1.2	0.78

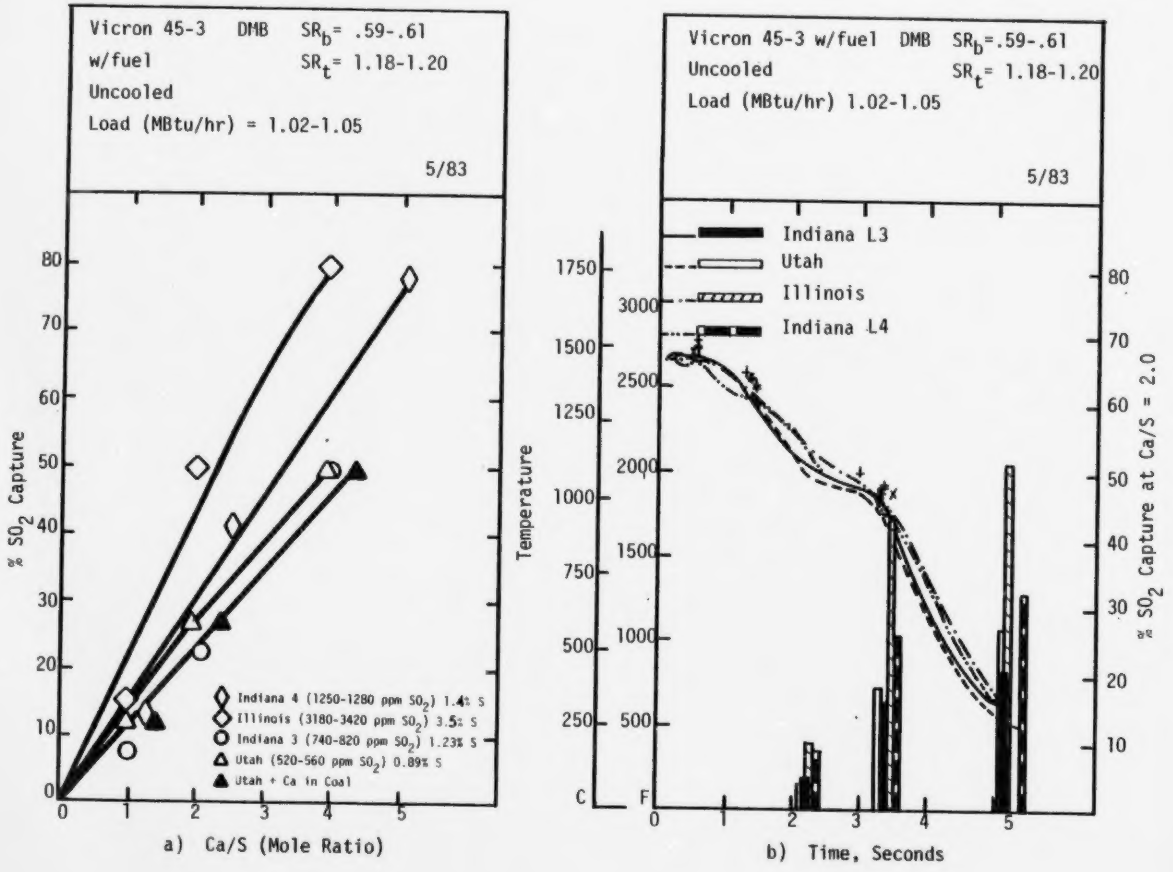

Figure 7-18. Effect of fuel on sulfur capture and thermal history of Vicron 45-3 w/fuel.

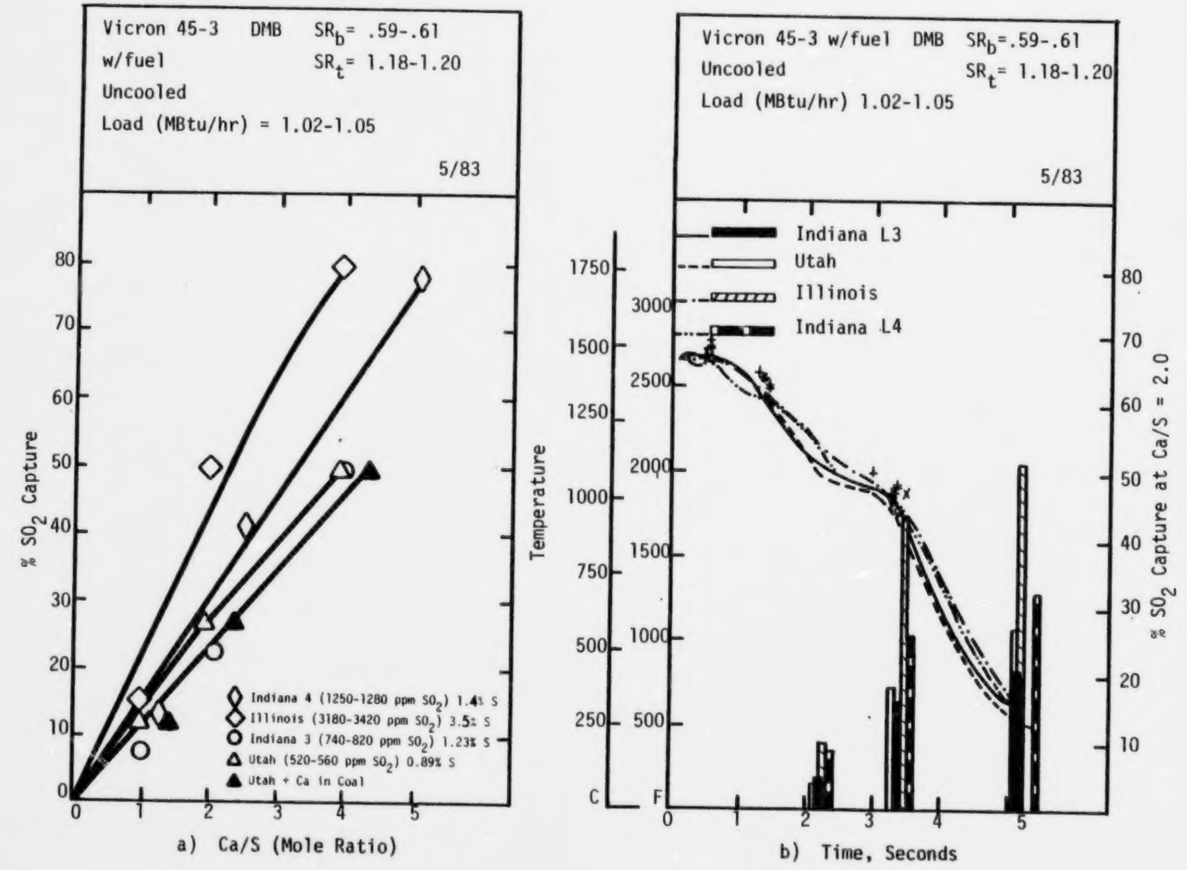

Figure 7-18. Effect of fuel on sulfur capture and thermal history of Vicron 45-3 w/fuel.

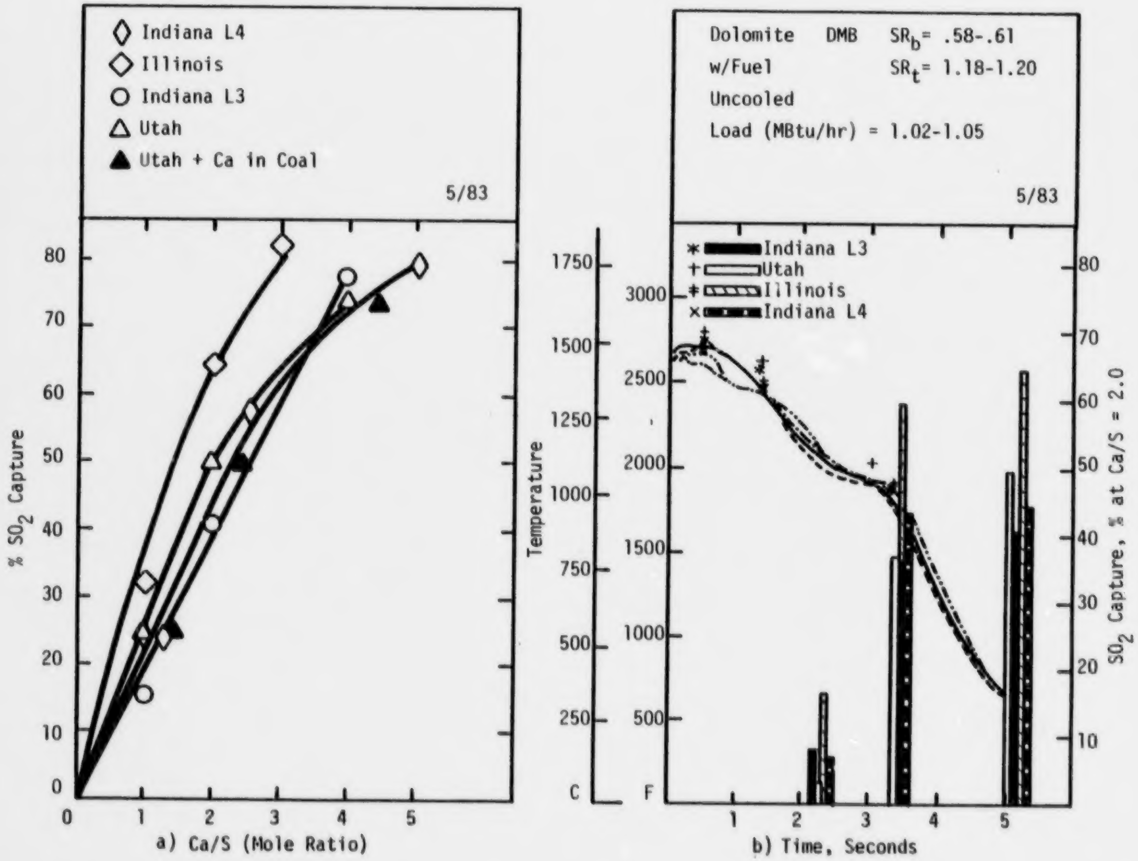

Figure 7-19. Effect of fuel on sulfur capture and thermal history of dolomite, sorbent w/fuel.

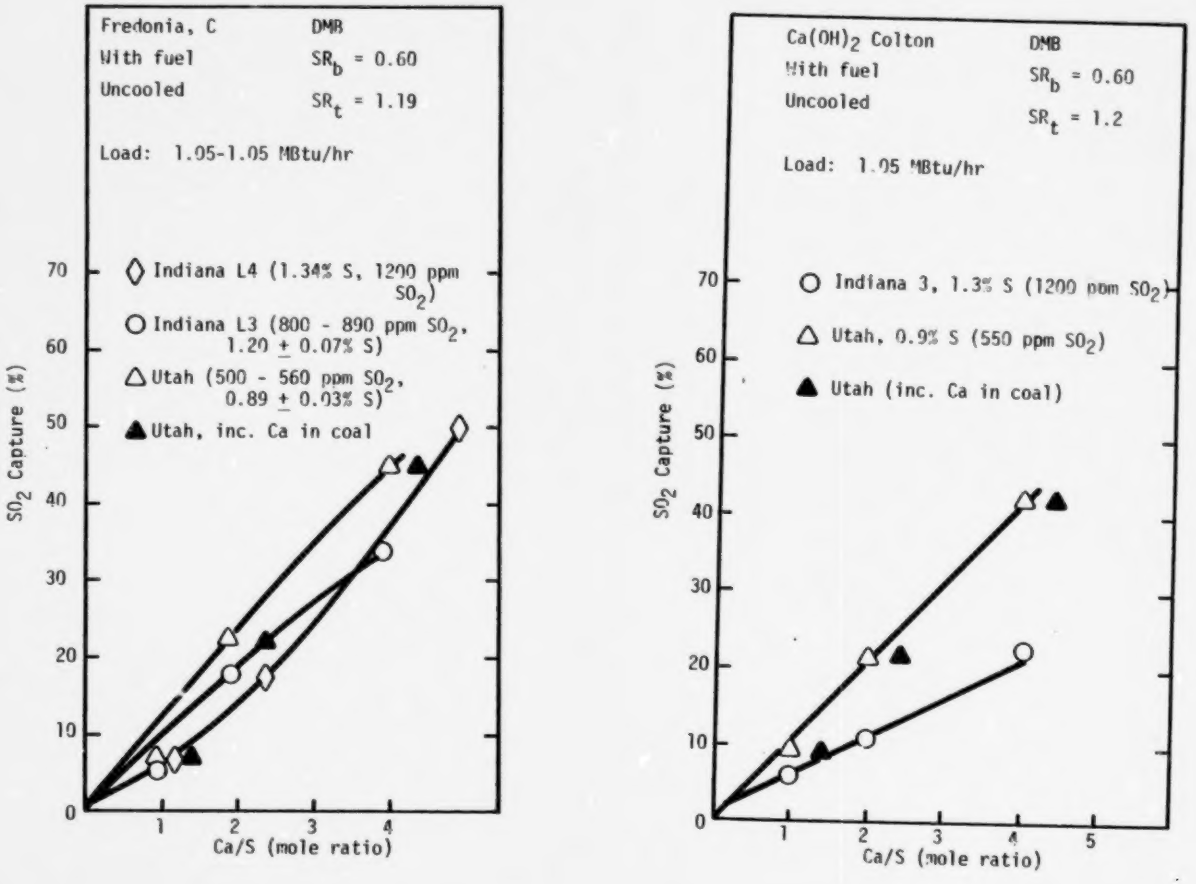

Figures 7-20, 7-21. Effect of fuel on sulfur capture for Fredonia (coarse) and lime (Colton).

Earlier fundamental work (Coutant, 1969) and some pilot-scale results from work performed at EER (Payne, et al., 1982) have indicated that sulfur capture by dry sorbents is proportional to the half order of the SO_2 (or S) present. The data in Figures 7-22 and 7-23 show the application of the correlation to results from Vicron 45-3 and dolomite injection studies. The $\sqrt{S}$ correlation helps remove some of the data spread for these two sorbents although there appear to be other significant fuel effects which result in differences in capture for two fuels at the same Ca/S $\sqrt{S}$.

One possible reason for the different captures by the different fuels at a given $\sqrt{s}$ x Ca/S is the coal mineral matter interference discussed earlier. Table 7-3 summarizes the expected sorbent ash composition (based on the fuel and ash analysis and the sorbent composition) for the coals with either Vicron 45-3 or dolomite added to give a Ca/S ratio of 2.0. (The calculation was based on adding enough sorbent to give a Ca/S ratio of 2.0, based only on the fuel sulfur content and neglected the Ca in the ash). The correlation of the SO_2 capture with aluminum in the solid which was used for the gas fired data was applied to the fuel data. Figure 7-24 shows SO_2 capture as a function of % Al_2O_3 in the solid for the fuels tested, using both dolomite and Vicron data. The correlation is reasonable good, implying that fuel ash composition will affect sulfur capture by injected sorbents.

7.3 Conclusions, Fuel and Sorbent Interactions

A fairly extensive data base of sulfur capture in the BSF for various fuel-sorbent pairs was established. Six fuels and five sorbents were tested (not all possible combinations of fuel-sorbent pairs were included). The fuels were natural gas doped with H_2S, two different lots of Indiana coal (1.2 and 1.5 percent S) Utah coal, Saar (a blended German bituminous coal) and Illinois #6. The sorbents included: two hydrated limes, Colton (a U.S. lime) and a German hydrated lime; two limestones - a coarse-grained western stone - Vicron, and a fine-grained eastern stone - Fredonia; and a mid-western dolomite.

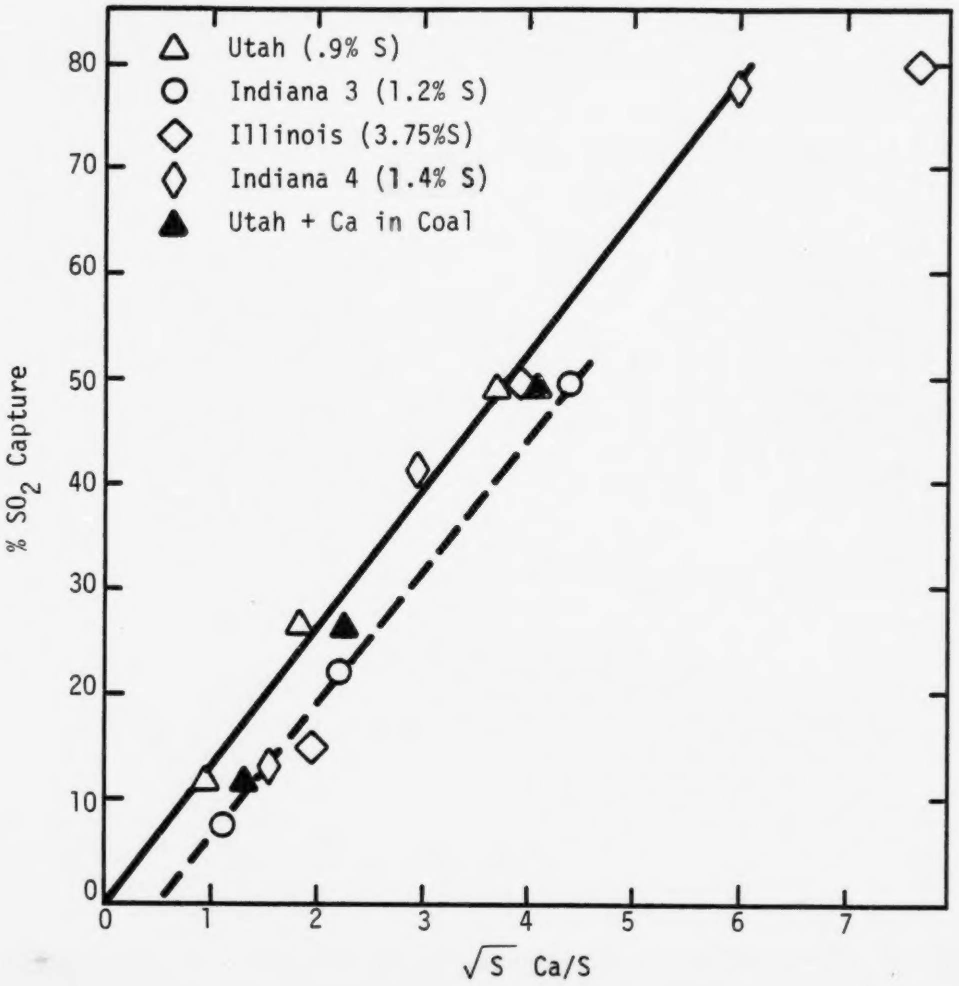

Figure 7-22. Effect of fuel sulfur content on sulfur capture, Vicron 45-3.

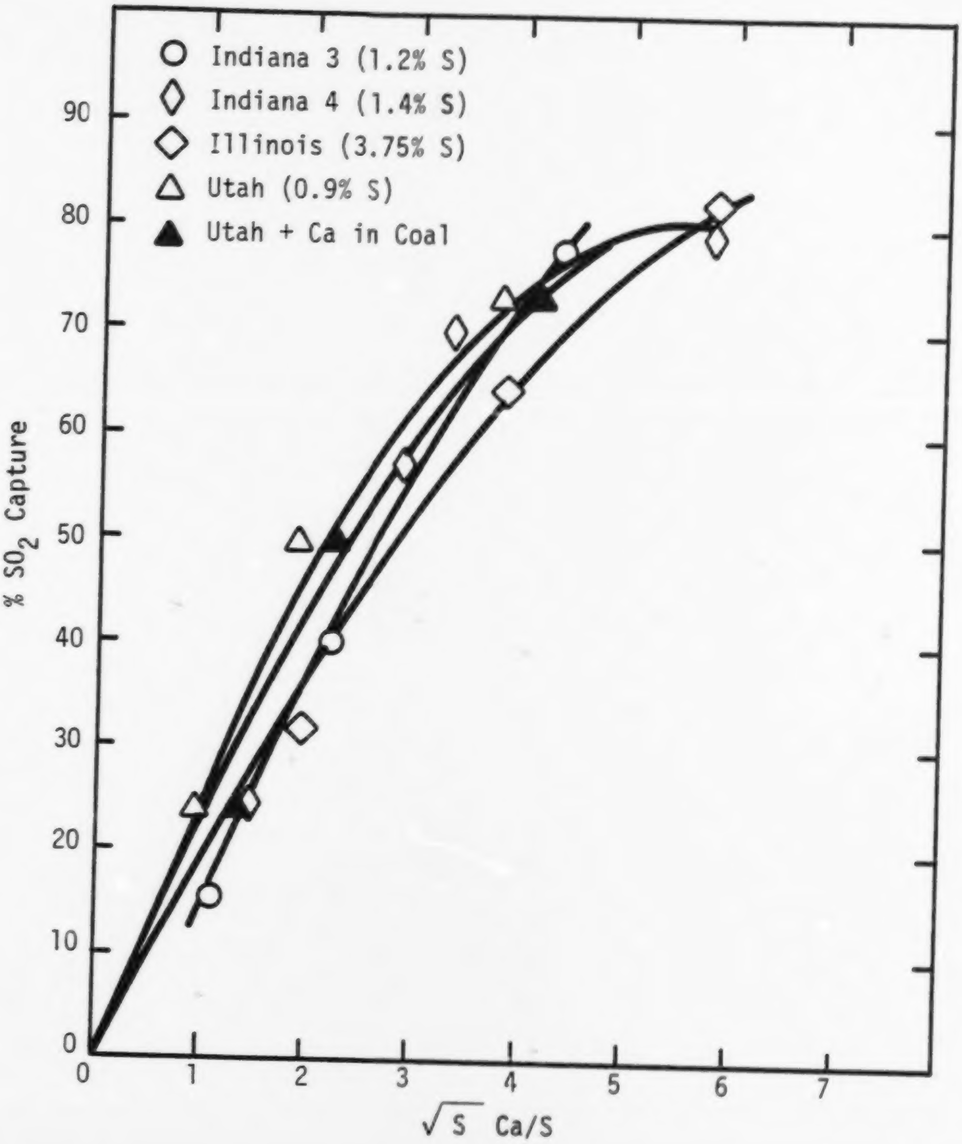

Figure 7-23. Effect of fuel sulfur content on sulfur capture - Dolomite.

TABLE 7-3. COAL (ASH) SORBENT MIXTURE CHARACTERISTICS
(Equivalent Ca/S = 2.0)

Sorbent Mineral	1000°C Ig. Loss	S.A. 1000°C	Chemical Composition (Ignited Sample) Weight, %										
			CaO	SiO_2	Al_2O_3	Fe_2O_3	Na_2O	K_2O	MgO	TiO_2	P_2O_5	CRO_2	SO_3
Indiana 3-Vicron 45-3	19.0		29.26	41.26	17.23	8.81	0.16	0.86	0.85	0.67	0.36	0.005	0.52
Utah-Vicron 45-3	19.3		28.73	48.72	13.54	2.91	0.607	0.71	0.77	0.59	0.34	0.004	3.7
Illinois 6 - Vicron 45-3	27.36		50.12	26.79	9.0	7.86	0.53	1.11	1.77	0.246	0.17		2.4
Saar-Vicron 45-3	17.68		28.26	34.1	19.27	7.75	0.407	2.51	2.6	0.503	0.129		4.47
Indiana 4 - Vicron 45-3	19.17		30.9	39.85	17.51	6.84	0.29	1.70	0.95	0.64	0.18	0.54	0.58
Beulah-Vicron 45-3	8.5		20.61	37.57	13.68	6.04	4.62	1.27	4.0	1.08	0.59		10.52
Indiana 5 - Vicron 45-3	26.88		45.1	25.18	13.76	13.18	0.16	0.7	0.83	0.37	0.11	0.0	0.48
Indiana 3 - Dolomite	28.3		24.28	34.80	14.41	7.47	0.178	0.78	16.42	0.56	0.30	0.35	0.43
Indiana 4 - Dolomite	29.17		25.49	33.49	14.57	5.84	0.29	1.47	17.32	0.53	0.15	0.36	0.48
Utah-Dolomite	25.61		24.36	41.81	11.59	2.63	0.55	0.66	14.48	0.5	0.29	0.36	3.10
Illinois-Dolomite	36.88		37.18	20.74	6.85	6.11	0.46	0.92	25.1	0.18	0.12	0.53	1.78

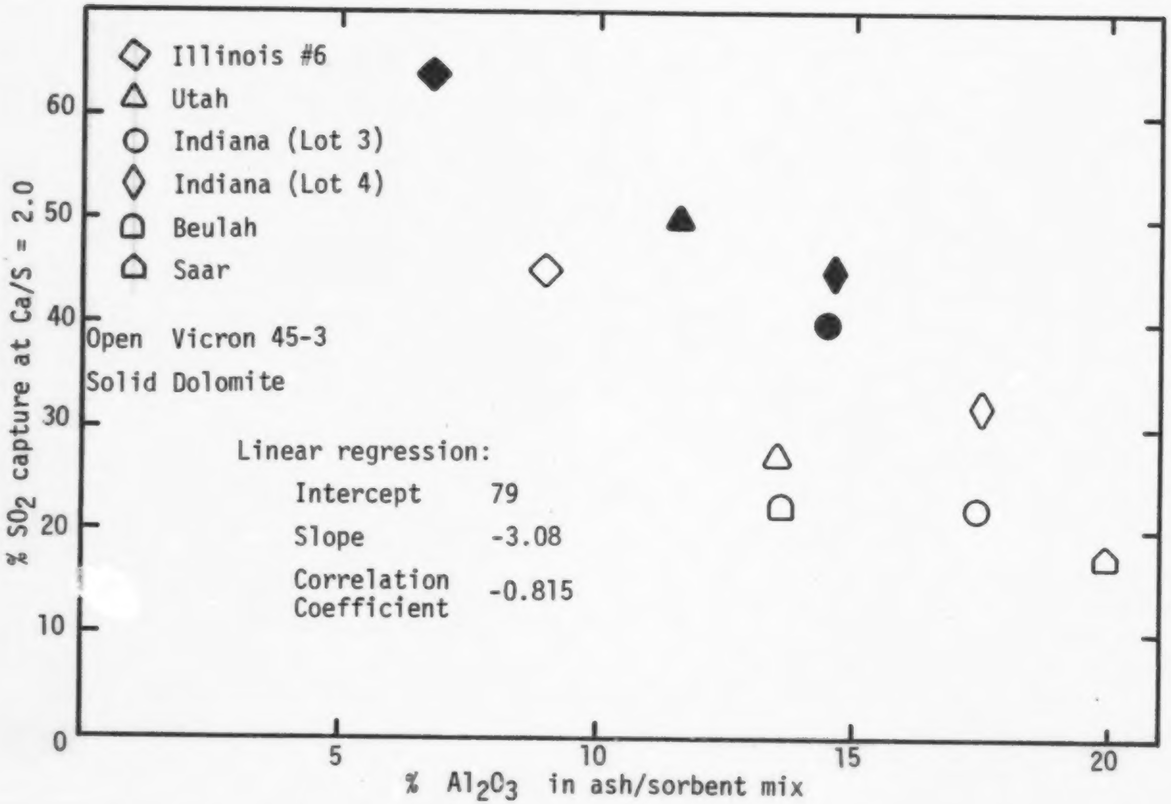

Figure 7-24. Correlation of ash/sorbent Alumina content with sulfur capture.

The effect of sorbent type on capture with a given fuel was dependent on the firing conditions - including sorbent injection location and thermal conditions. The hydrated limes seemed to be most sensitive to thermal conditions and the Vicron least sensitive. The German hydroxide gave better capture than the Colton hydroxide - it was not clear why the two stones had different captures. Dolomite gave the highest capture with all of the fuels tested.

The effect of fuel type on capture with a given sorbent (injection method, firing characteristics and thermal conditions) was also system-dependent. Capture with natural gas was higher for all of the sorbents than with coal - due, in part, to deactivation of the sorbent by coal mineral matter. Sulfur capture for the fuels tested with Vicron 45-3 and dolomite showed a fairly consistant inverse correlation with the calculated Al_2O_3 content of the ash sorbent mixture (at a Ca/S=2.0).

The effect of sorbent particle size on capture using Vicron, Fredonia, and dolomite with natural gas and coal was tested. In general, sorbent size affected capture only for large particles, at mean sizes less than 10 μm particle size had little effect on sulfur capture. The effect of particle size was greater when firing Indiana coal than when firing natural gas. A comparison of the predicted effect of particle size (using the sulfation model described in Section 5.0) and the observed effect using various sizes of Vicron was in good agreement.

8.0 DOWNSTREAM SORBENT INJECTION

One of the most interesting results of earlier experiments (2667) in the BSF was the effect of physical staging on sulfur capture. The BSF can be fired in two general modes; internally staged or DMB (Distributed Mixing Burner) where all of the combustion air is added at the burner face, through the main burner and the tertiary air ports; and physically or externally staged where part of the combustion air is added downstream of the base of the post-flame section. A schematic of the BSF is shown in Figure 8-1. Staging air addition at location A is internal staging, air addition at location B is physical staging.

When the furnace was fired in the internally staged mode, there was considerable difference in SO_2 capture by the same sorbent when injected with coal or natural gas captures for Indiana coal firing. Figure 8-2 summarizes the results of internal and physical staging experiments using Vicron 45-3 and dolomite as the sorbents. The change from fuel injection to downstream injection of the sorbent gave considerable improvement in sulfur capture for both sorbents.

The increase in sulfur capture with downstream sorbent injection could be due to the different thermal environment experienced by the sorbent or to a decrease in the effect of coal ash on the sorbent. In order to further explore downstream injection and to assess the effect of fuel sorbent interactions in this firing configuration, a set of experiments was planned. Table 8-1 shows the test matrix for the downstream injection studies. The furnace was fired at the same load and fuel-air stoichiometries for all of the tests.

8.1 Downstream Injection: Fuel/Sorbent Effects

Downstream injection tests of four sorbents with Indiana (lot 3) coal were performed. Three of the sorbents had been used earlier in physically staged experiments. The results of the sorbent injection tests are summarized in Figure 8-3. The figure also shows the earlier data for comparison. In

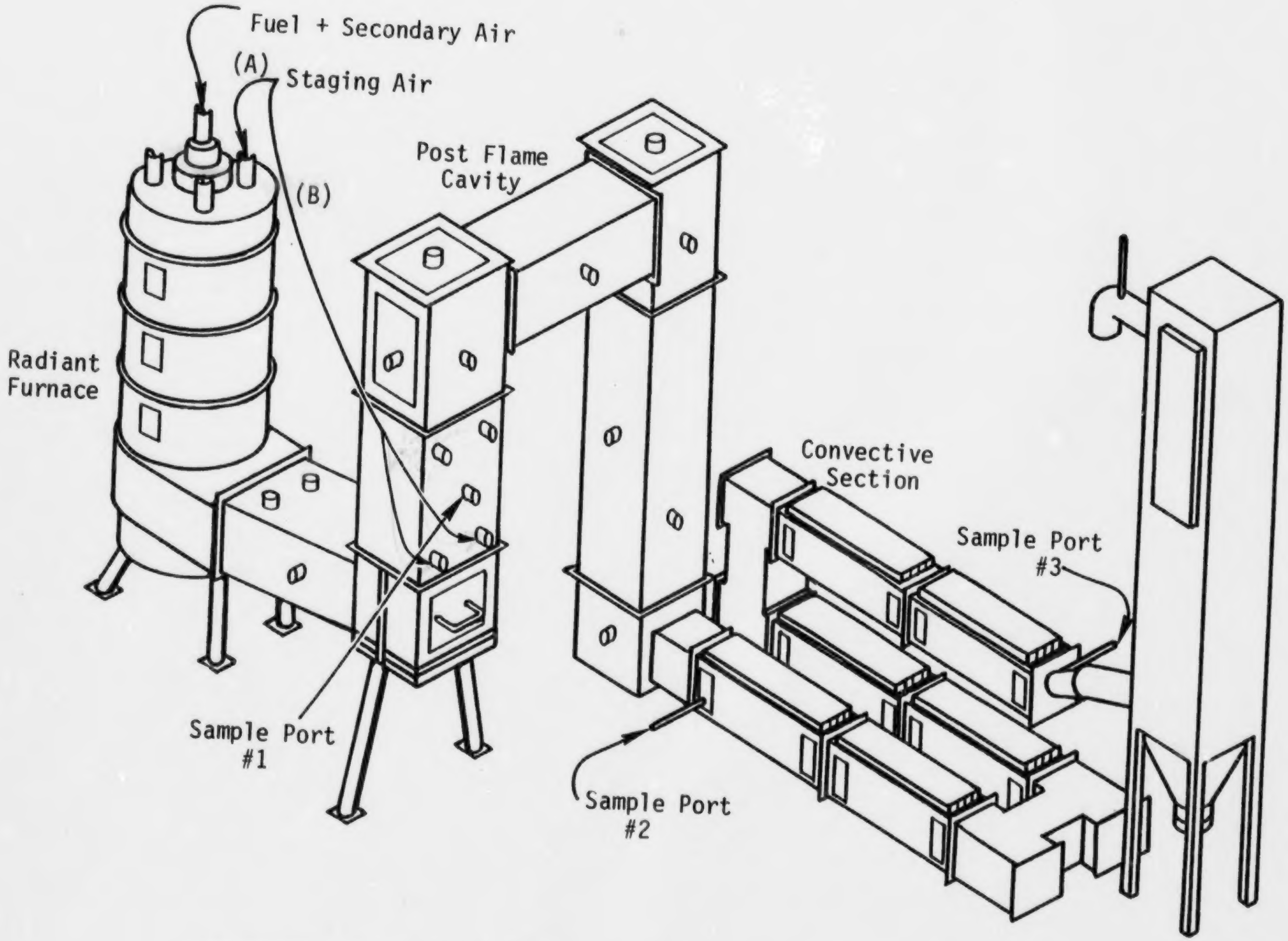
Fuel + Secondary Air
(A)
Staging Air
(B)
Post Flame Cavity
Radiant Furnace
Convective Section
Sample Port #3
Sample Port #1
Sample Port #2

Figure 8-1. Boiler simulator furnace.

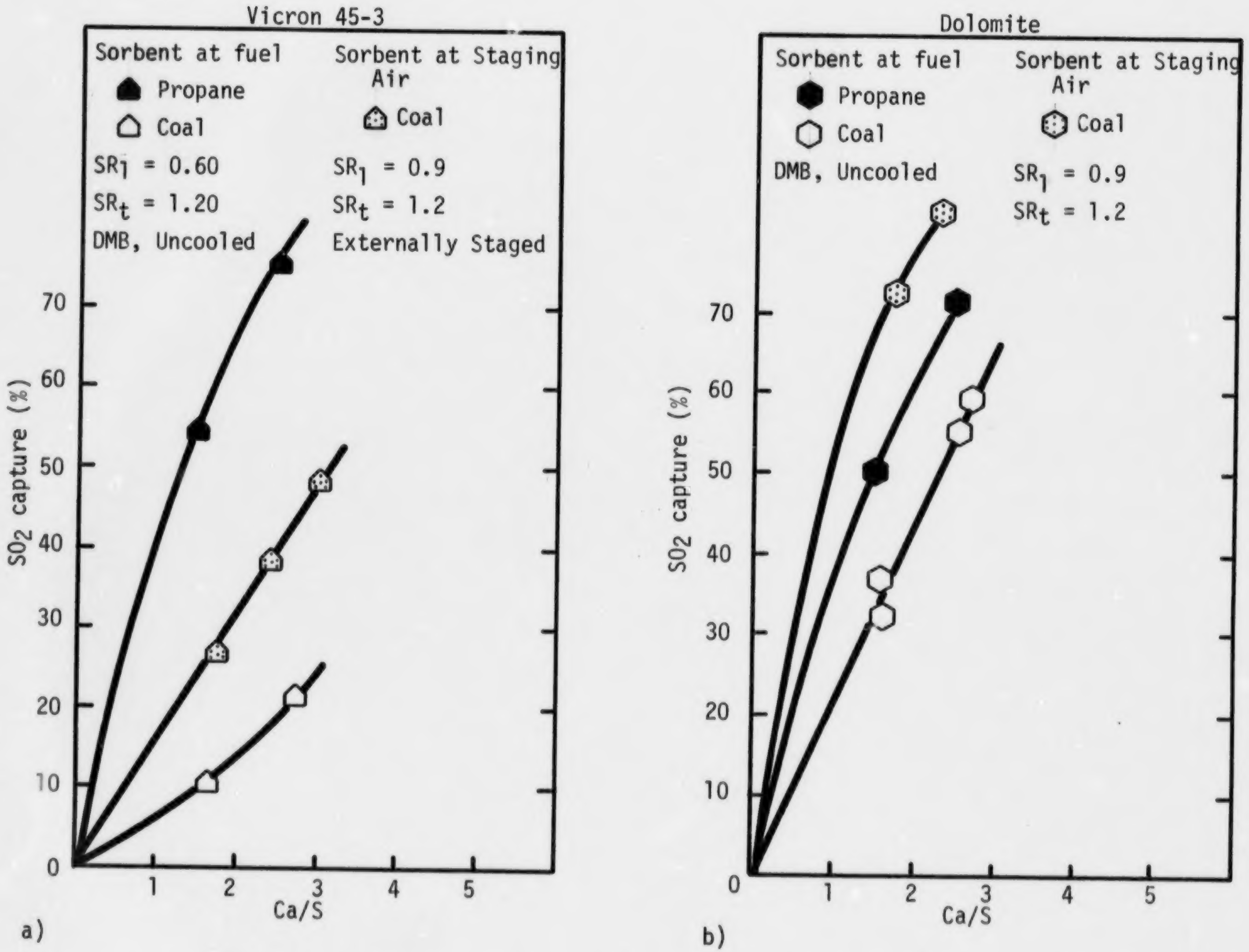

Figure 8-2. Effect of sorbent location on sulfur capture - fuel and downstream injection.

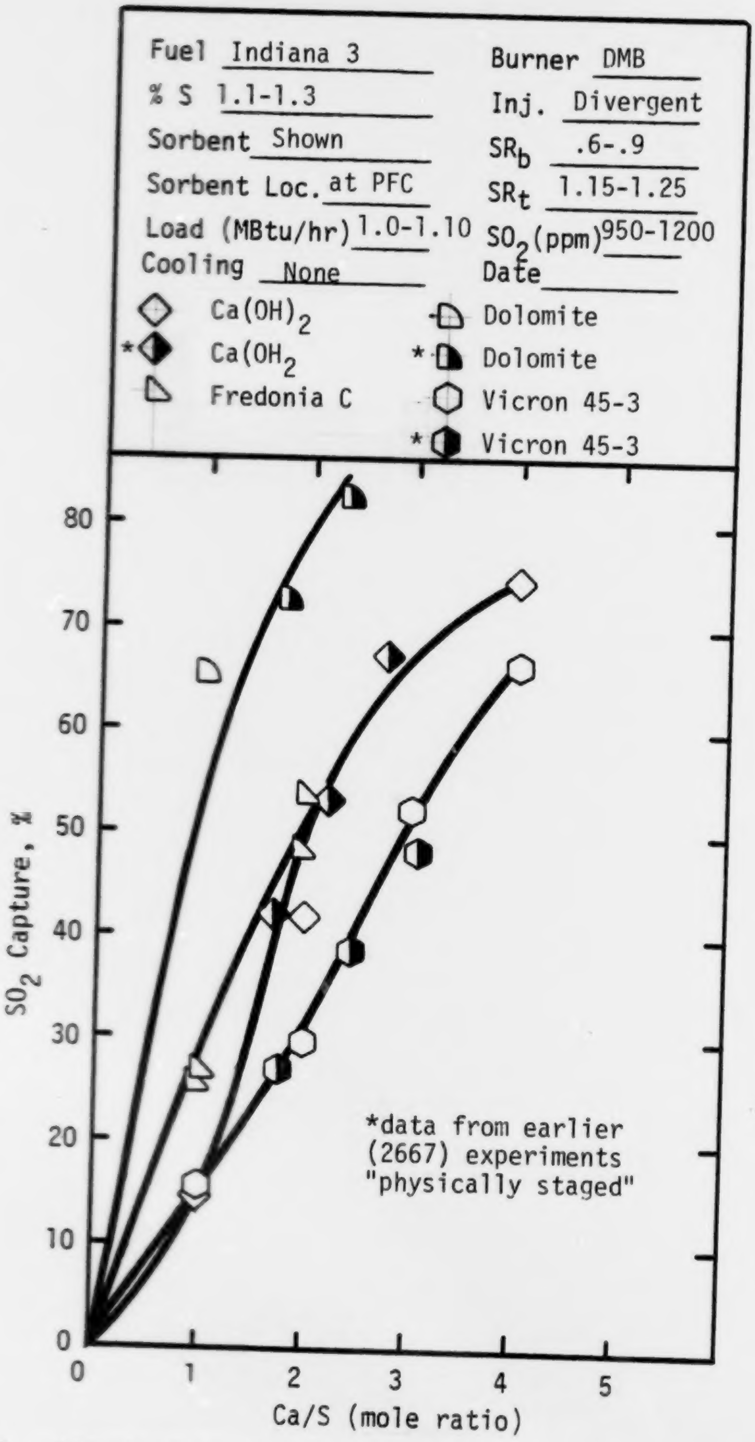

Figure 8-3. Effect of sorbent type on sulfur capture - downstream injection, Indiana L3 coal.

TABLE 8-1. DOWNSTREAM SORBENT INJECTION TESTS

Conditions: DMB, $SR_b = 0.6$, $SR_1 = 1.05$, $SR_t = 1.25$
Uncooled; Sorbent at base of pfc

	Vicron 45-3	Dolomite	$Ca(OH)_2$ Colton	Fredonia Coarse
Natural Gas/H_2S 1800 ppm	X	X	X	X
Indiana L3 1.2% S	X	X	X	X
Indiana L5 2.3% S (Riley)	X	X	X	X
Illinois 3.7%	X	X	X	
Sarr 0.8%	X	X		
Utah .9% S	X	X	X	

general, the data was repeatable and captures were higher than fuel injection for all of the sorbents.

Injecting the sorbent at the base of the post-flame section results in a different thermal history for the particles and in a slightly different furnace temperature profile. The furnace temperature profile for Indiana (lot 5) firing capture using Vicron 45-3 are shown in Figure 8-4. The Vicron was injected at about 2200°F gas temperature and gave approximately 40 percent sulfur capture (at a Ca/S of 2.0) in 1.5 seconds residence time. Figure 8-5 shows capture for Vicron, dolomite, Fredonia (coarse) and Colton lime. Dolomite gave the highest capture and Vicron the lowest. The lime gave better capture than the limestones when injected downstream while, when injected with the fuel the limestones gave better capture. Calcium hydroxide (lime) calcines at a lower temperature than limestone and is likely to be more sensitive to furnace temperature. The high captures when injected downstream may be due to the lower injection temperatures (which give more reactive sorbent).

Similar data are shown for Illinois coal in Figures 8-6 and 8-7. The temperature at the sorbent injection point was 2000°F and the Fredonia sorbent gave approximately 40 percent utilization in just over 1-second residence time. Again, the dolomite gave the highest captures, but there was no difference in the lime and limestone captures. Downstream injection of Vicron 45-3 with Utah coal gave much lower capture than with the other fuels. The sorbent injection temperature was approximately 2000°F and capture at 1-second was only 20 percent for a Ca/S ratio of 2.0 (see Figure 8-8). The different sorbents gave considerably different captures with this fuel, Colton lime was much better than the Vicron (Figure 8-9). Why there was no difference in captures for the lime and limestone with Illinois coal and there was with Utah is not clear. A possible explanation may be that the high sulfur fuel and resulting high SO_2 concentrations gave captures great enough for all of the sorbents that differences in sorbent reactivity were masked by the extent of the sulfation reaction.

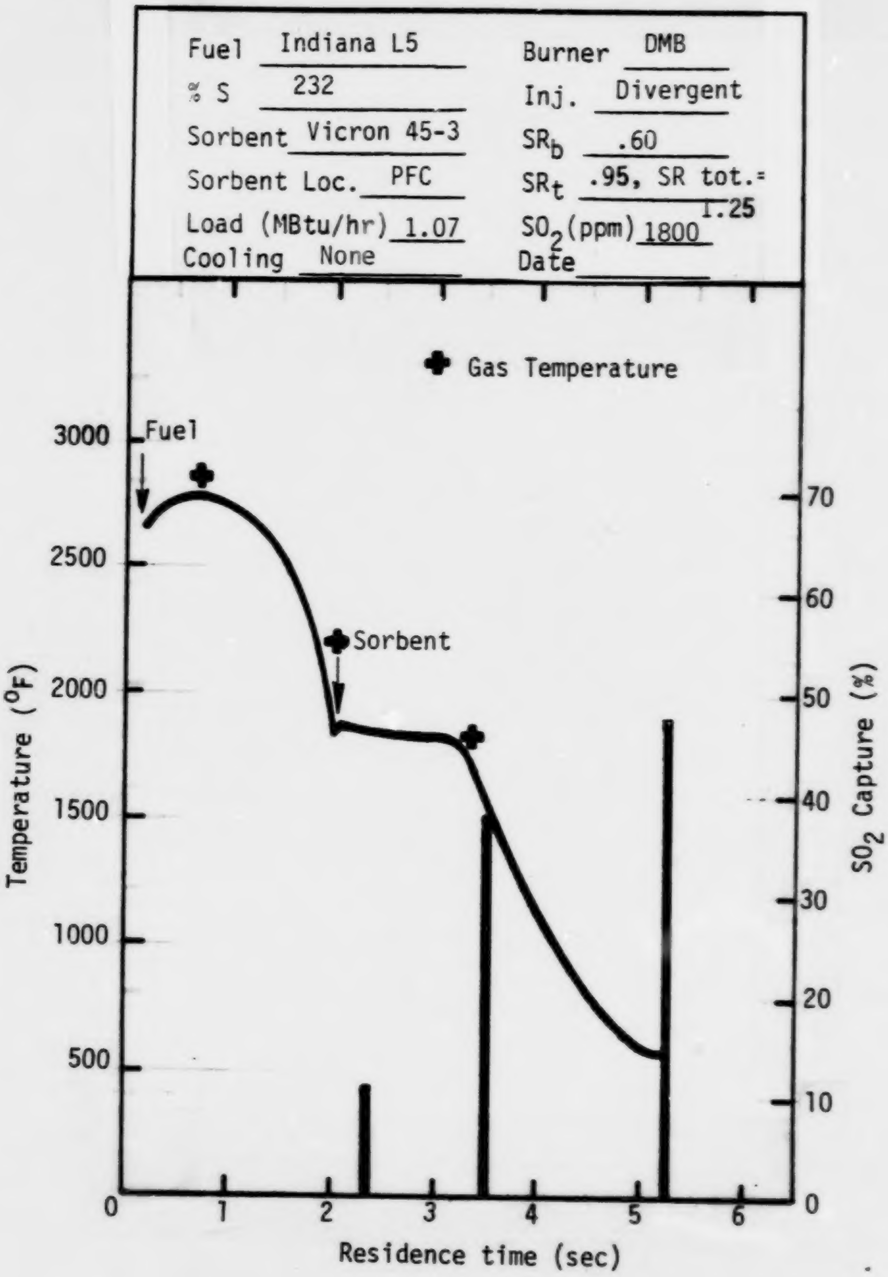

Fuel Indiana L5

% S 232

Sorbent Vicron 45-3

Sorbent Loc. PFC

Load (MBtu/hr) 1.07

Cooling None

Burner DMB

Inj. Divergent

SR_b .60

SR_t .95, SR tot.= 1.25

SO_2(ppm) 1800

Date

Figure 8-4. Temperature profile for downstream injection, Indiana (lot 5) coal.

TABLE 8-2. SORBENT SURFACE AREA RESULTS

Sorbent, Sample #		Injection Location	Sample Location	Peak (or injection) Temp, °F	Sample Location Temp, °F	Residence Time, Sec.	Surface Area m^2/gm	% Calcined	Typical SO$_2$ (Ca/S=2) Capture (Port 3)
Vicron 45-3	1426	With Fuel	#1	2840	2560	1.26	6.98*	91.5	46-52
	1427	With Fuel	#1	2840	2560	1.26	3.90	96	46-52
Vicron 45-3	1433	With Fuel	#2	2860	2150	2.10	2.96	95.5	46-52
	1434	With Fuel	#2	2860	2150	2.10	3.56	94	46.52
Vicron 45-3	1439	At PFC	#2	2060	2000	.3	7.14	93.5	48
	1440	At PFC	#2	2060	2000	.3	6.84	92.8	48
Dolomite	1446	With Fuel	#1	2920	2550	1.25	3.33	98.2	60
Dolomite	1435	With Fuel	#2	2860	2150	2.1	2.7	96.8	60
	1436	With Fuel	#2	2860	2150	2.1	2.59	97.5	60
Dolomite	1437	At PFC	#2	2060	2000	.3	20.38	88.1	82
	1438	At PFC	#2	2060	2000	.3	17.77	88.4	82
Colton Lime	1428	With Fuel	#1	2920	2600	1.26	3.19	97	32
	1429	With Fuel	#1	2920	2600	1.26	2.99	97.5	32
Colton Lime	1430	With Fuel	#2	2880	2150	2.05	2.96	96.8	32
	1431	With Fuel	#2	2880	2150	2.05	2.73	96.9	32
Colton Lime	1441	At PFC	#2	2040	2000	.3	7.22	95.2	38
	1442	At PFC	#2	2040	2000	.3	7.51	91.8	38

* Sample appeared wet when removed from filter.

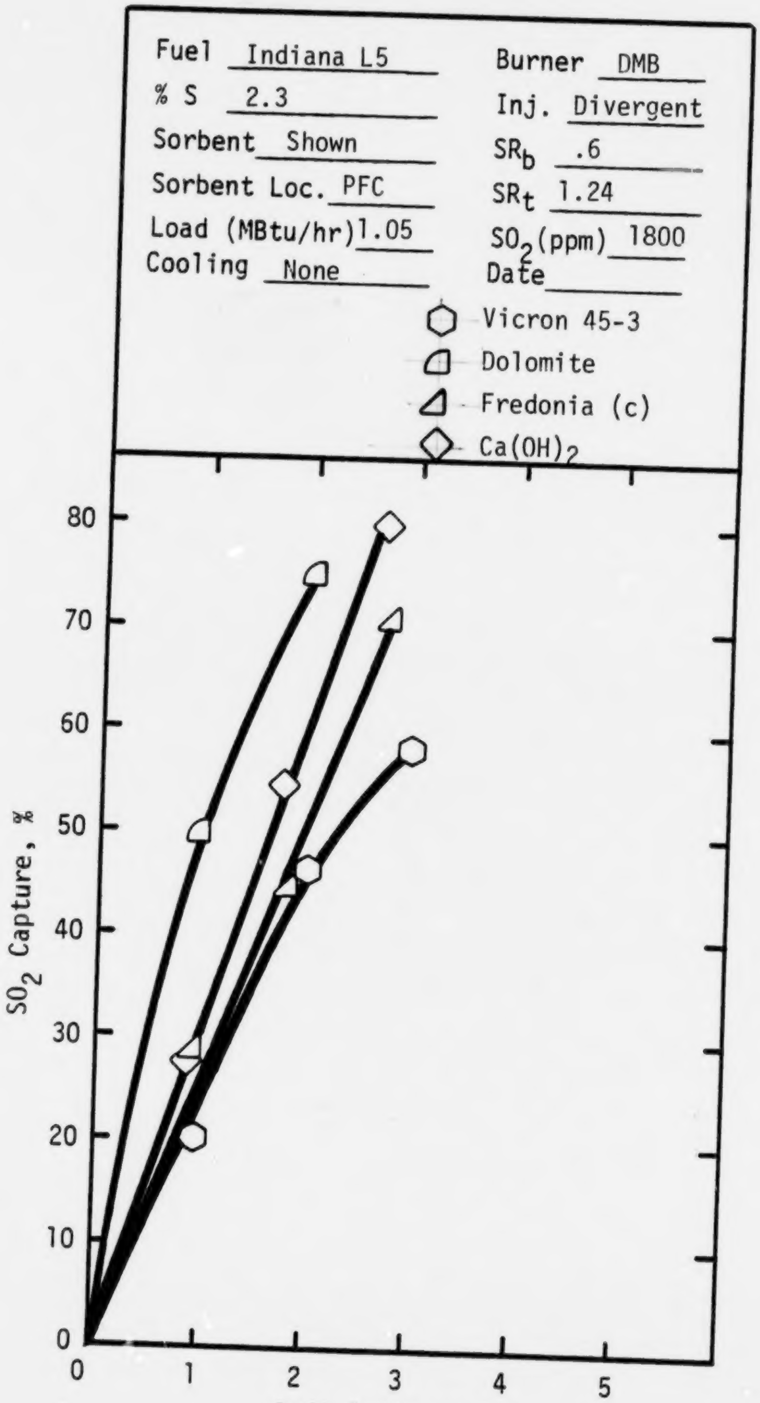

Figure 8-5. Effect of sorbent type on sulfur capture, downstream injection, Indiana L5 coal.

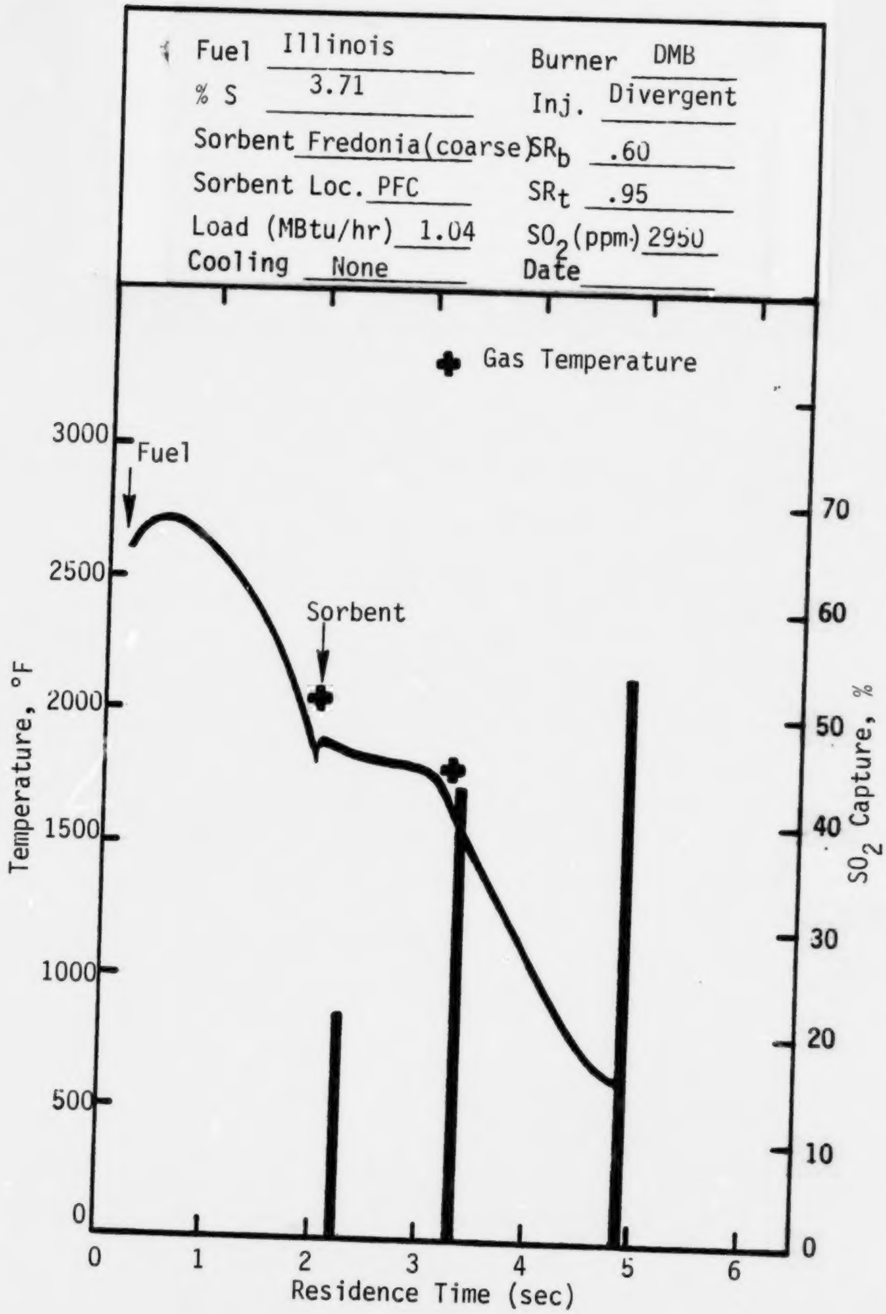

Figure 8-6. Temperature profile for downstream sorbent injection, Illinois coal.

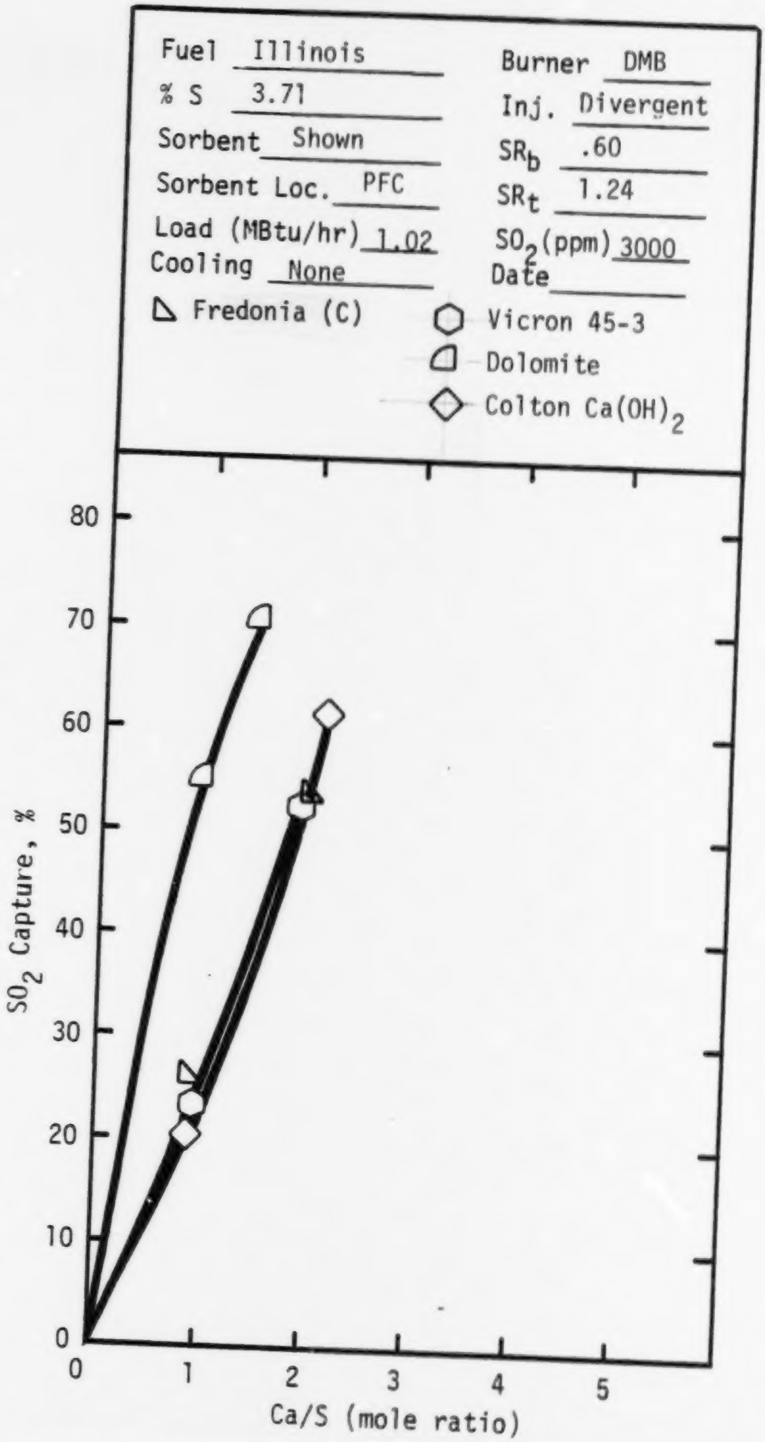

Figure 8-7. Effect of sorbent type on sulfur capture, downstream injection, Illinois coal.

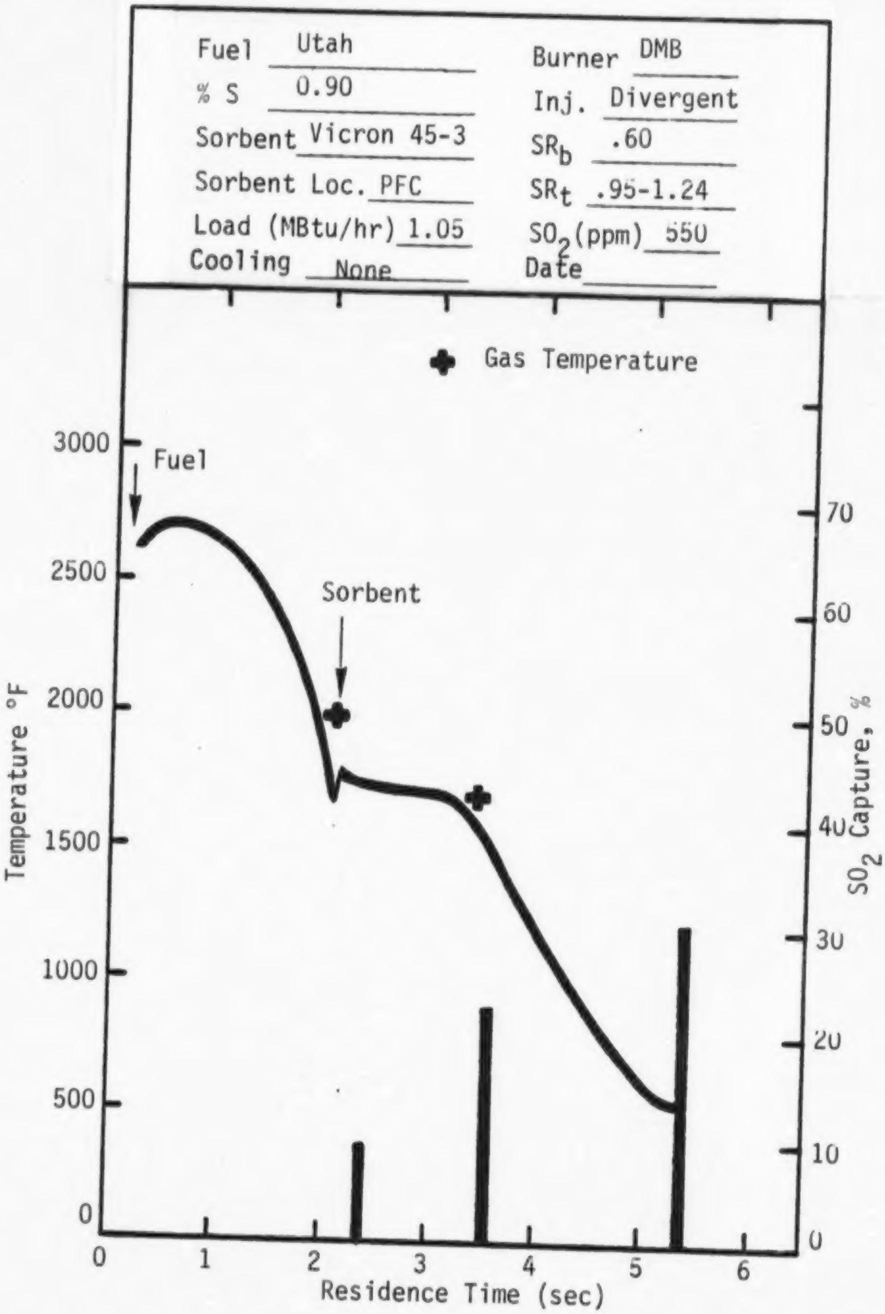

Fuel	Utah	Burner	DMB
% S	0.90	Inj.	Divergent
Sorbent	Vicron 45-3	SR_b	.60
Sorbent Loc.	PFC	SR_t	.95-1.24
Load (MBtu/hr)	1.05	SO_2(ppm)	550
Cooling	None	Date	

Figure 8-8. Temperature Profile for Downstream Sorbent Injection, Utah Coal.

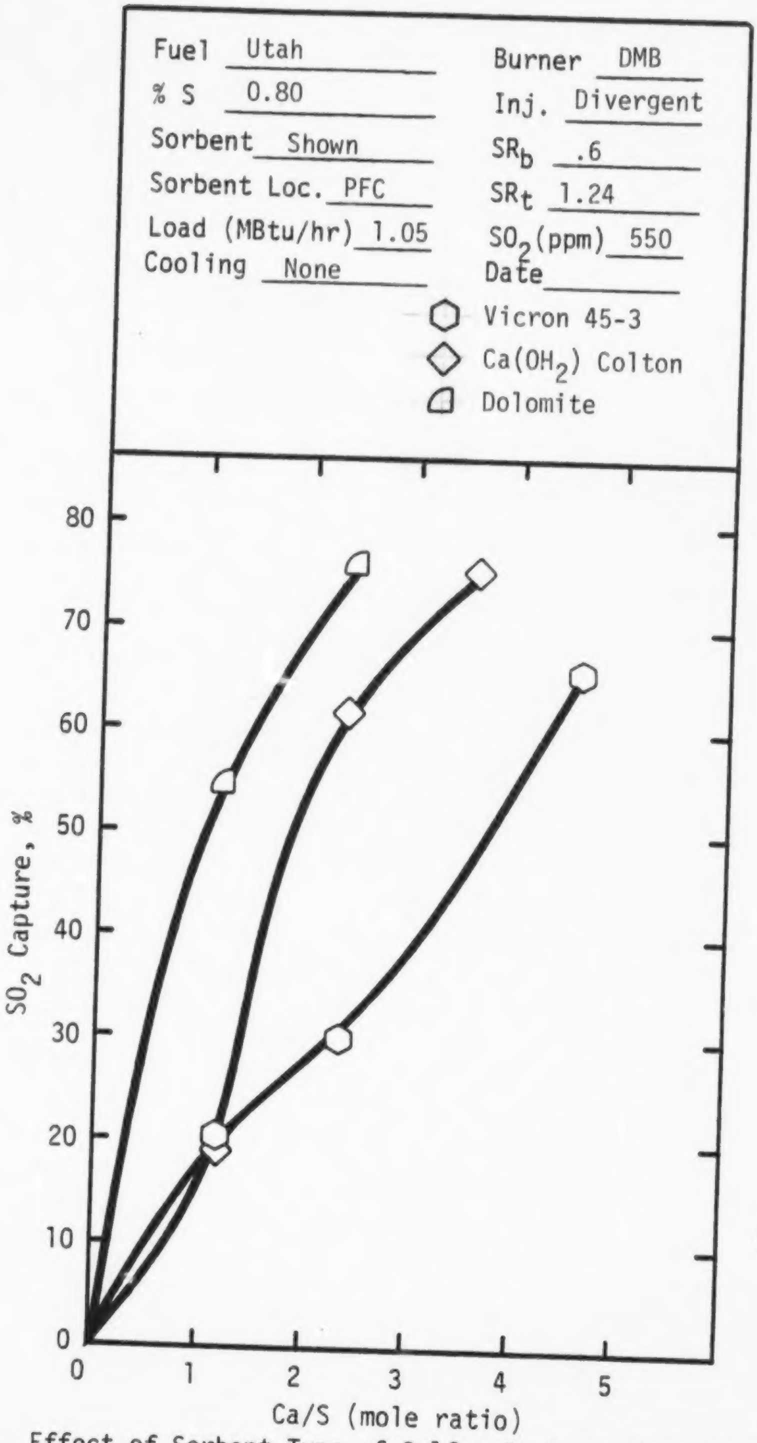

Figure 8-9. Effect of Sorbent Type of Sulfur Capture, Downstream Injection, Utah Coal.

Figure 8-10 shows the temperature profile for Vicron injected downstream with the Saar coal, capture was similar to, but slightly better than, the Utah coal. The dolomite again gave higher captures than the limestone (see Figure 8-11).

Natural gas doped with H_2S was also used as a fuel for the downstream injection tests. The furnace temperature profile and capture for Colton lime injected at the base of the post-flame section (2100°F) are shown in Figure 8-12. Utilization of the Colton lime was high, 70 percent capture at a Ca/S of 2.0 in approximately 1.5 seconds. Captures for the other sorbents are shown in Figure 8-13. As usual, the dolomite gave the highest capture. With the fairly high sulfur captures there was little difference in the lime and limestone effectiveness. This result is similar to the Illinois coal result where the sorbents had high captures with little difference between them.

8.2 Effect of Sorbent Location

Injecting the sorbent downstream of the main radiant (burner) section of the furnace improved sulfur capture, if only marginally, for all of the fuels and sorbents tested. Figure 8-14 summarizes the effect of sorbent location for Vicron 45-3 injected with Utah and Indiana (lot 3) coals. Downsteam injection resulted in improved capture for both fuels; the effect of sorbent location was greater for the Indiana coal. The effect of dolomite injection location for the same two fuels is shown in Figure 8-15. Again, the improvement was greater with the Indiana coal.

The improvement in sorbent effectiveness when injected in the post-flame section may be due to the lower injection temperature or to decreasing the effect of the coal mineral matter. The effect of the mineral matter on sulfur capture by sorbents injected with the fuel and in the post-flame section was studied. Kaolin, a common coal mineral, (see Chapter 6) was used. The furnace was fired with natural gas doped with H_2S. Capture by the sorbent injected with the fuel and by the sorbent mixed with Kaolin and injected with the fuel was measured. Figure 8-16 summarizes the results. The Kaolin/

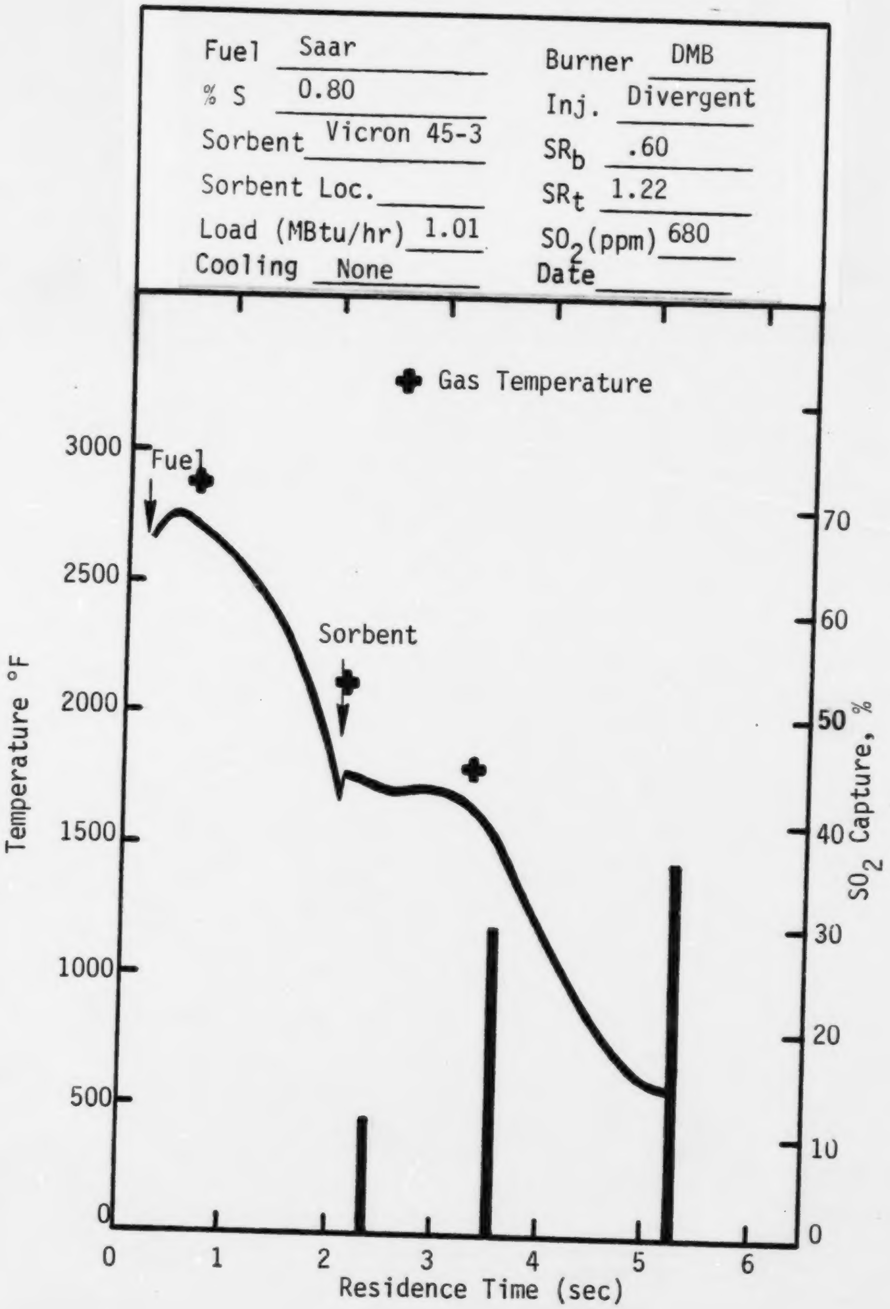

Fuel Saar
% S 0.80
Sorbent Vicron 45-3
Sorbent Loc.
Load (MBtu/hr) 1.01
Cooling None
Burner DMB
Inj. Divergent
SR_b .60
SR_t 1.22
SO_2(ppm) 680
Date

Figure 8-10. Temperature profile for downstream sorbent injection, Saar coal.

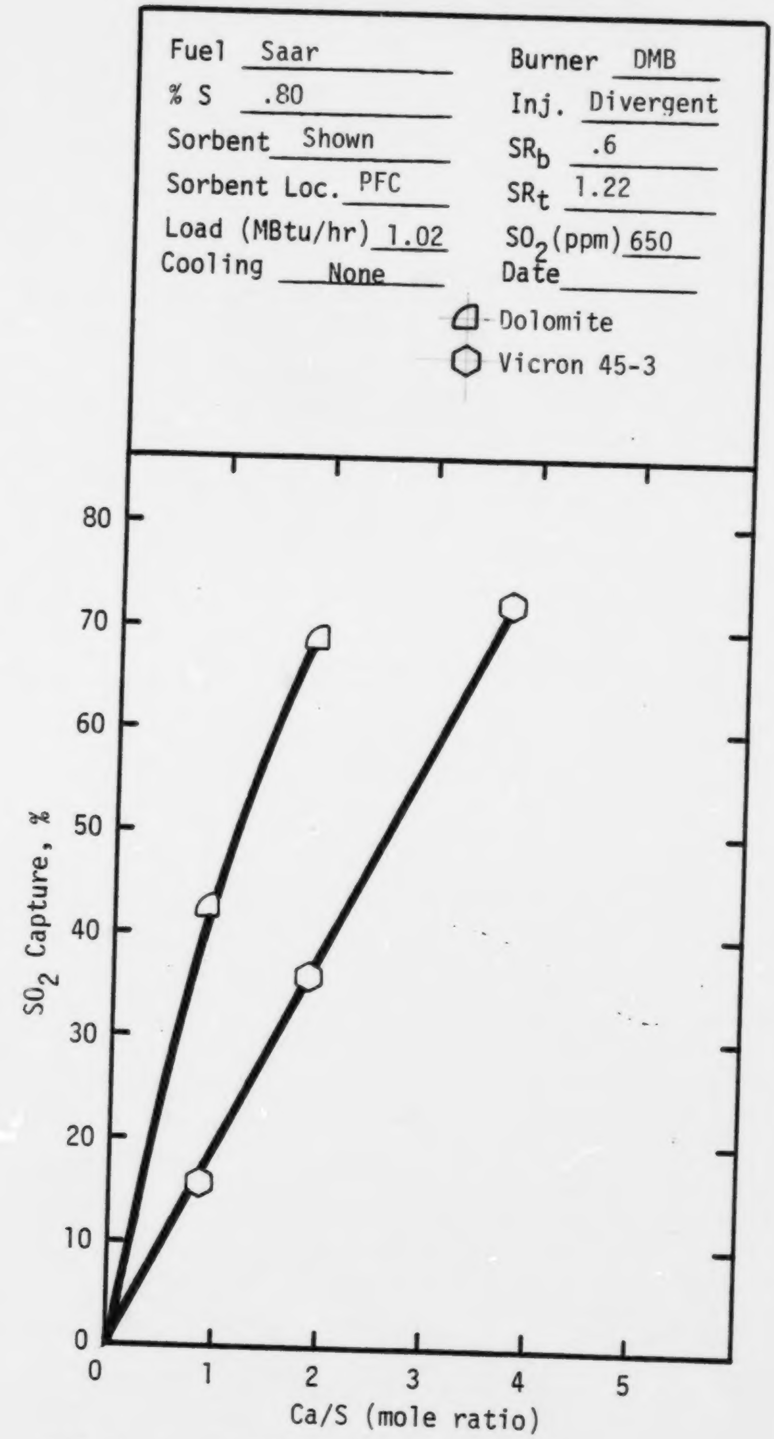

Figure 8-11. Effect of sorbent type on sulfur capture, downstream injection, Saar coal.

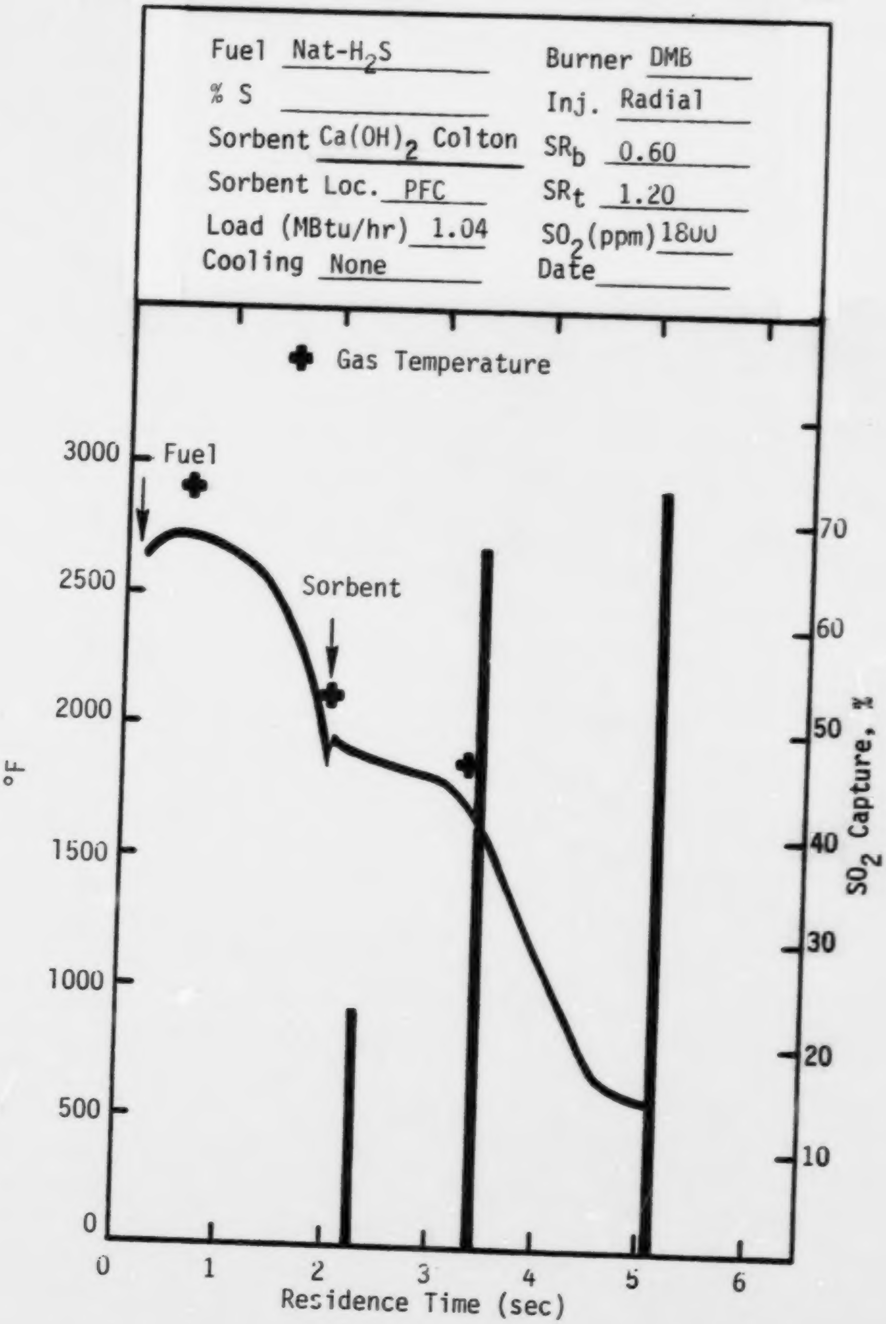
Fuel Nat-H_2S

% S

Sorbent $Ca(OH)_2$ Colton

Sorbent Loc. PFC

Load (MBtu/hr) 1.04

Cooling None

Burner DMB

Inj. Radial

SR_b 0.60

SR_t 1.20

SO_2(ppm) 1800

Date

Figure 8-12. Temperature Profile for Downstream Sorbent Injection, Natural Gas + H_2S.

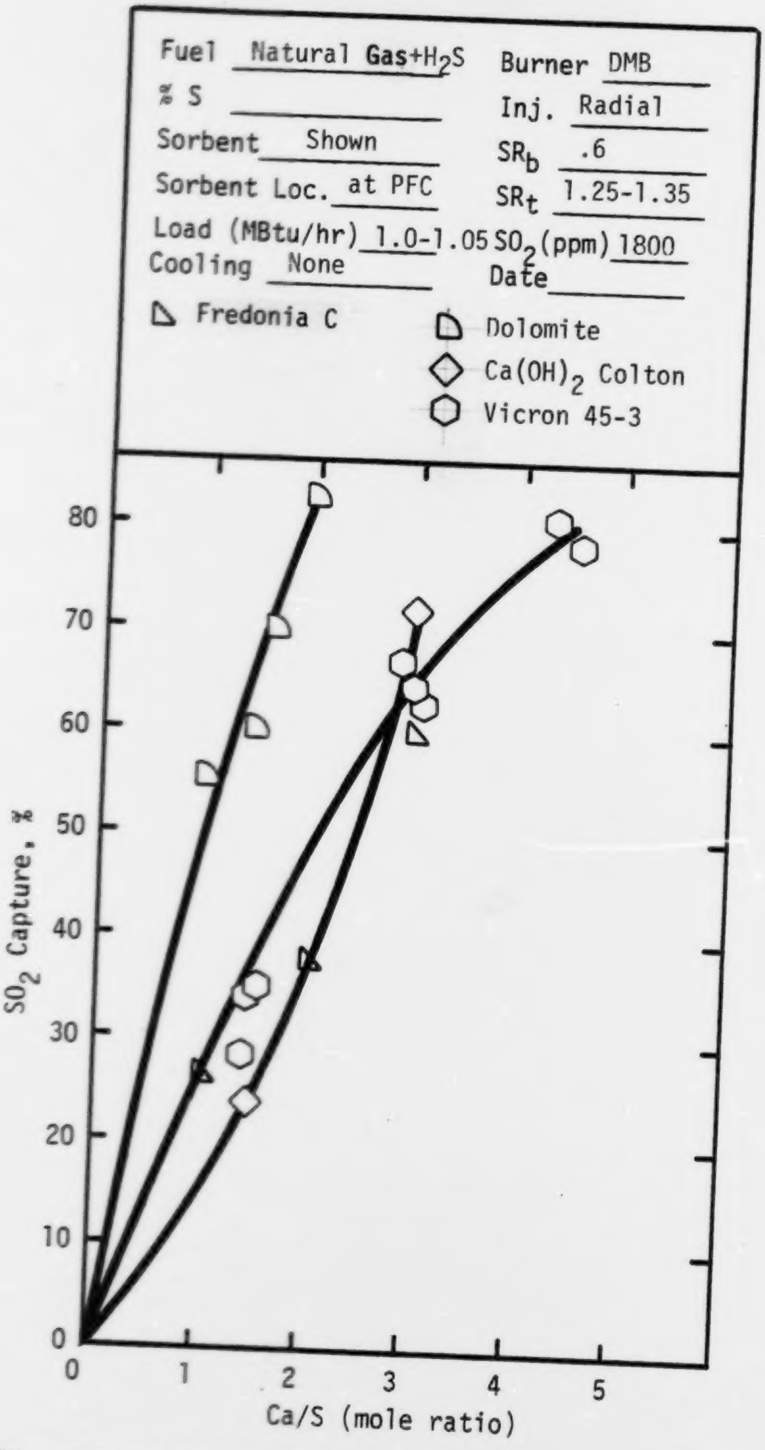

Figure 8-13. Effect of Sorbent Type on Sulfur Capture, Downstream Injection, Natural Gas + H_2S.

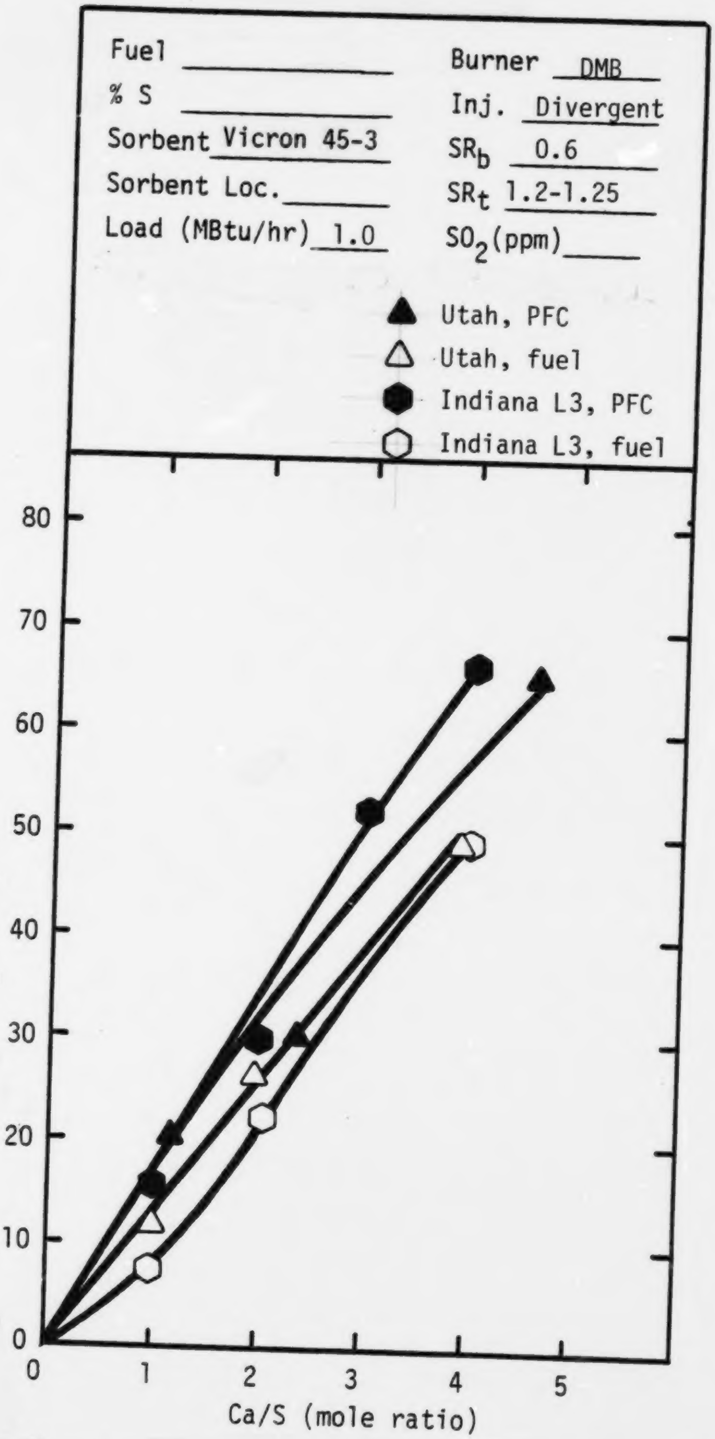

Figure 8-14. Comparison of Sorbent Injection Location, with Utah and Indiana Coal, Vicron 45-3.

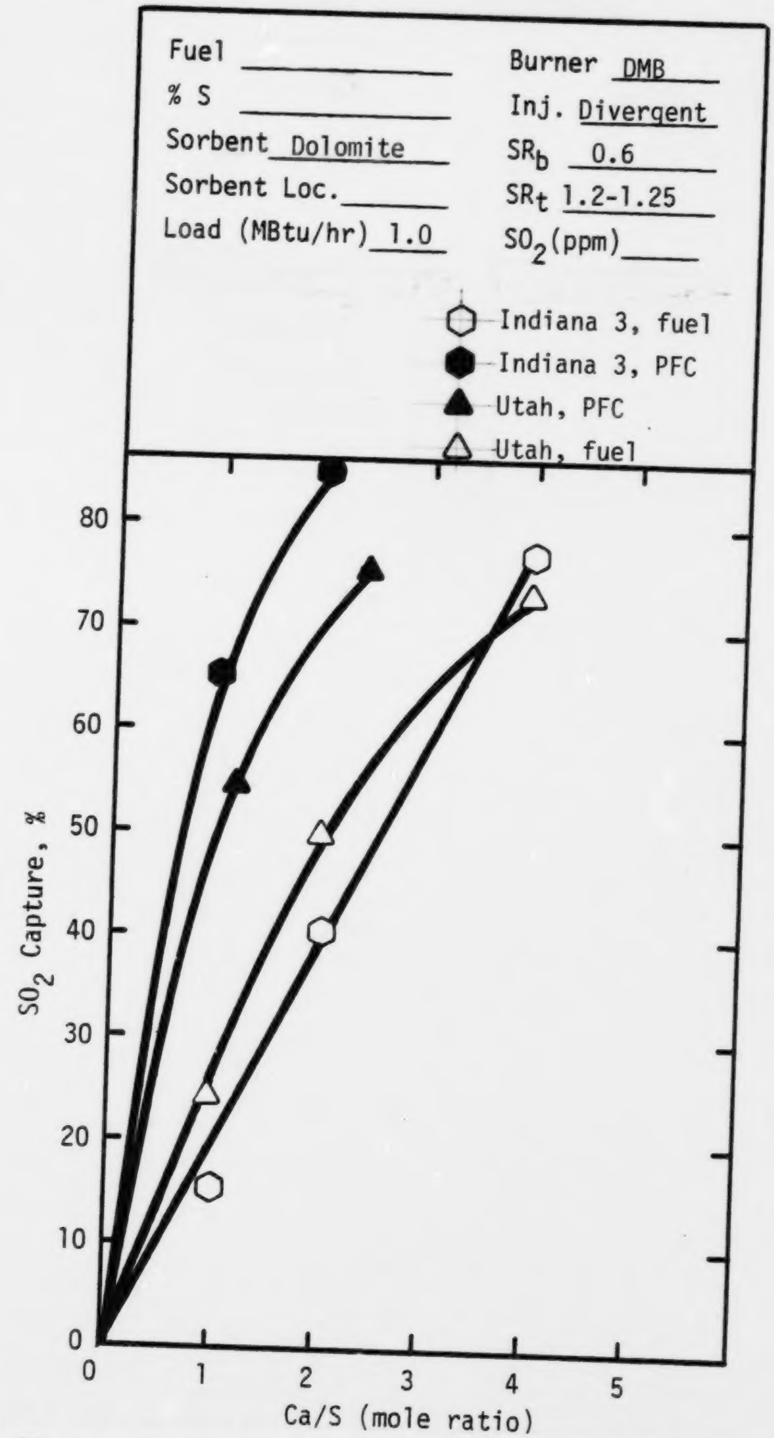

Figure 8-15. Comparison of Sorbent Injection Location, with Utah and Indiana Coals, Dolomite.

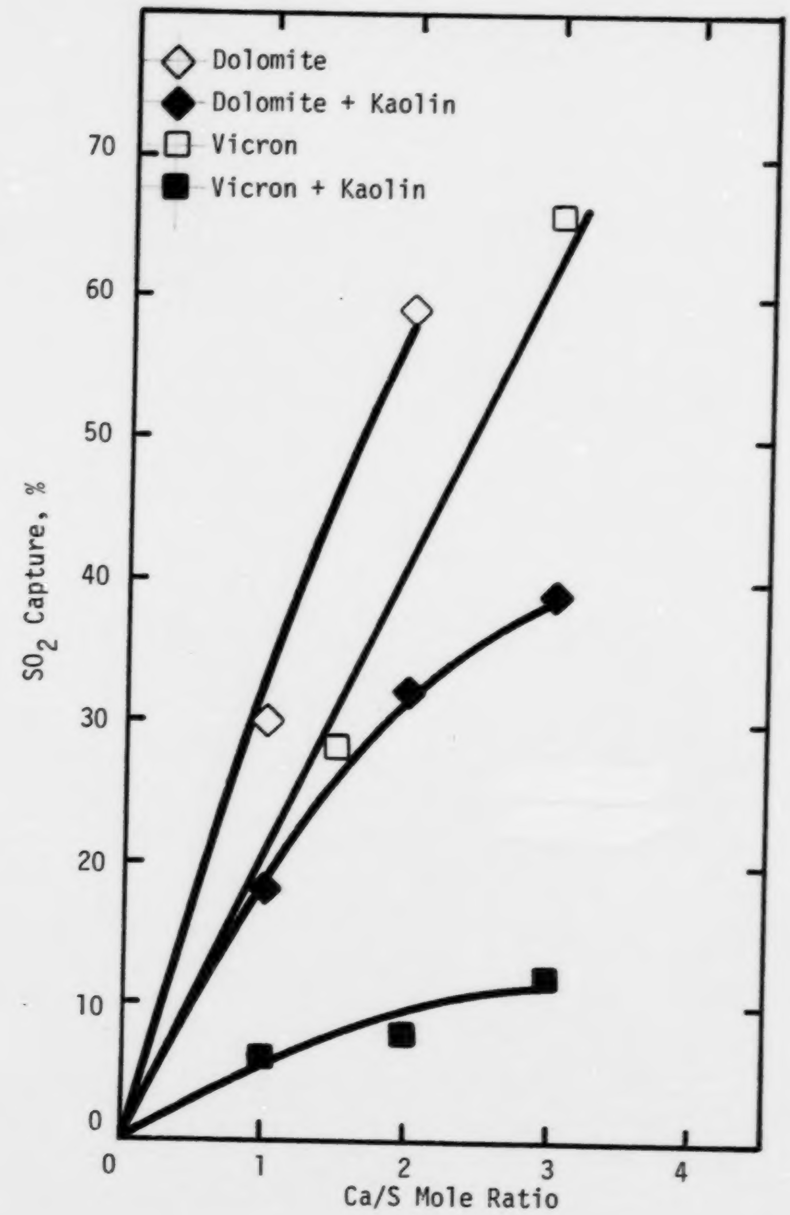

Figure 8-16. Effect of Kaolin addition, sorbent and Kaolin with fuel, natural gas + H_2S-firing.

sorbent mixture was considerably less effective than either the Vicron or dolomite alone.

The coal-fired sytsem was then simulated by injecting sorbent into the post-flame section with and without kaolin injected with the fuel. The kaolin, as a coal ash substitute decreased the capture when mixed with the sorbent. However, when the sorbent was added downstream kaolin addition had little effect on sulfur capture. Figure 8-17 shows sulfur capture for Vicron and dolomite injected in the post-flame section with and without kaolin added in the fuel. The kaolin made a small difference in sorbent effectiveness, much less than the effect when mixed with the sorbent and injected with the fuel.

8.2.1 Sorbent Surface Areas

Samples of three sorbents injected while firing natural gas without H_2S were taken in order to assess the effect of sorbent type and injection location. The sorbents were either injected with the fuel and sampled at two locations downstream or injected at the base of the post-flame cavity and sampled at one downstream location (see Figure 8-18). Temperature profiles for the two types of sorbent injection are shown in Figures 8-19 and 8-20. When injected with the fuel the sorbent may reach the peak gas temperature in the furnace which is approximately 2900°F. When injected downstream in the post-flame cavity, the peak temperature is considerably lower; on the order of 2100°F.

Table 8-2 summarizes the results of these tests. For all of the sorbents tested downsteam-injection gave higher surface areas at samples location 2 than when injected with the fuel. The changes in surface area with sorbent injection location was most pronounced for the dolomite, increasing from 2.7 to about 19 m^2/gm. The increase in sorbent surface area with downstream sorbent injection was accompanied by an increase in sulfur capture, the largest increase in capture also was with the dolomite.

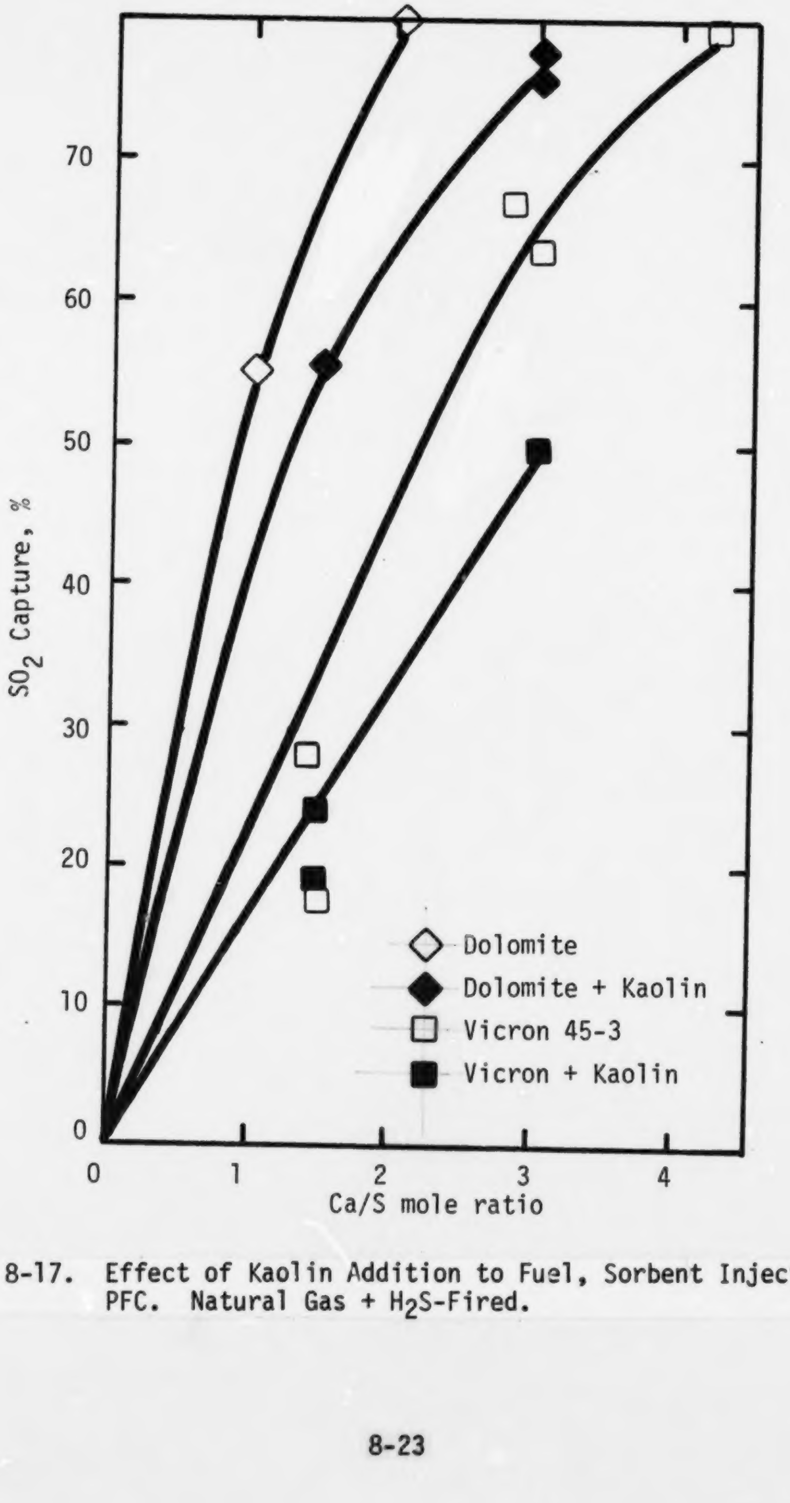

Figure 8-17. Effect of Kaolin Addition to Fuel, Sorbent Injected in PFC. Natural Gas + H_2S-Fired.

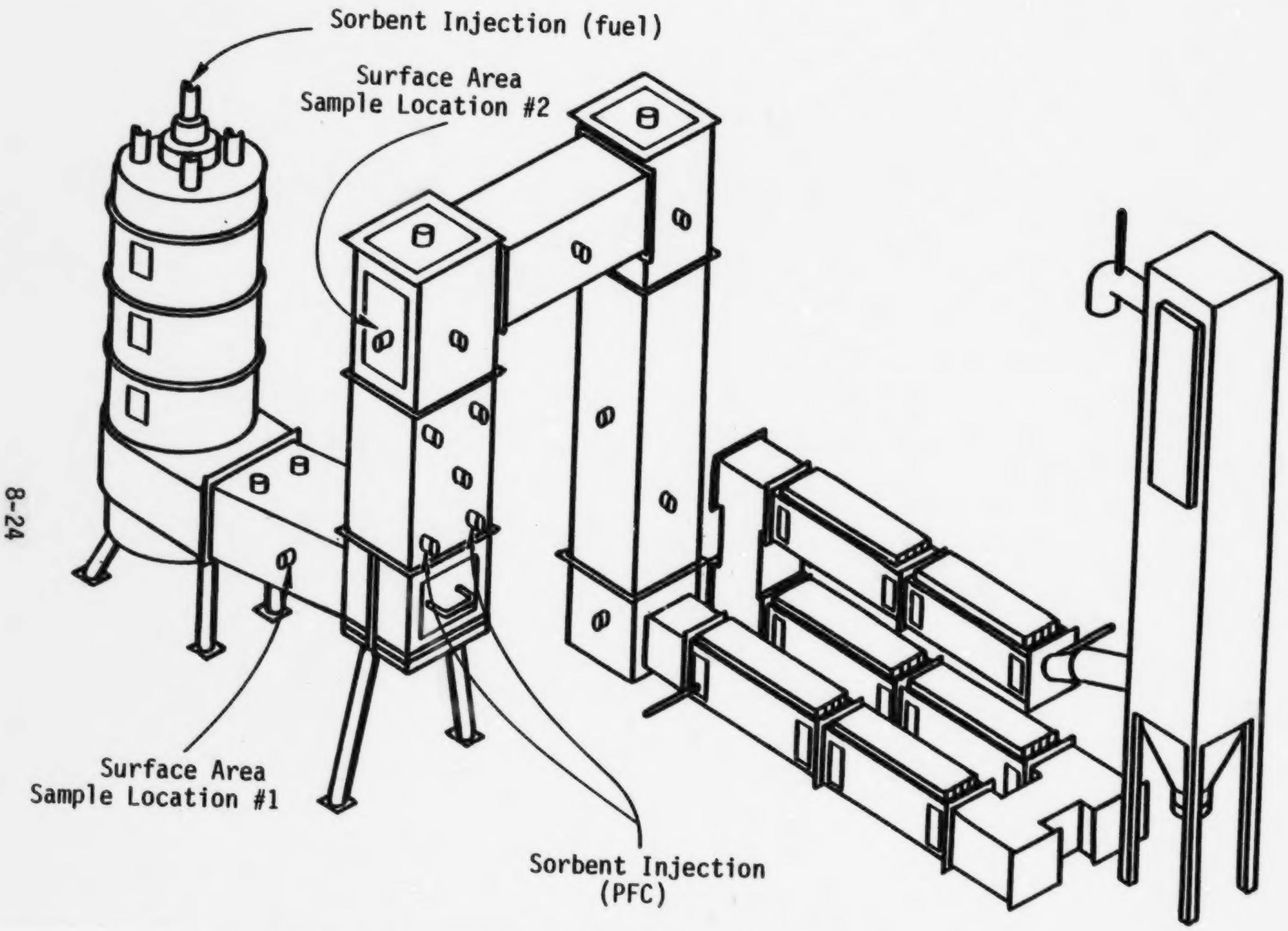
Sorbent Injection (fuel)
Surface Area Sample Location #2
Surface Area Sample Location #1
Sorbent Injection (PFC)

Figure 8-18. Sorbent injection and sample locations for surface area measurements.

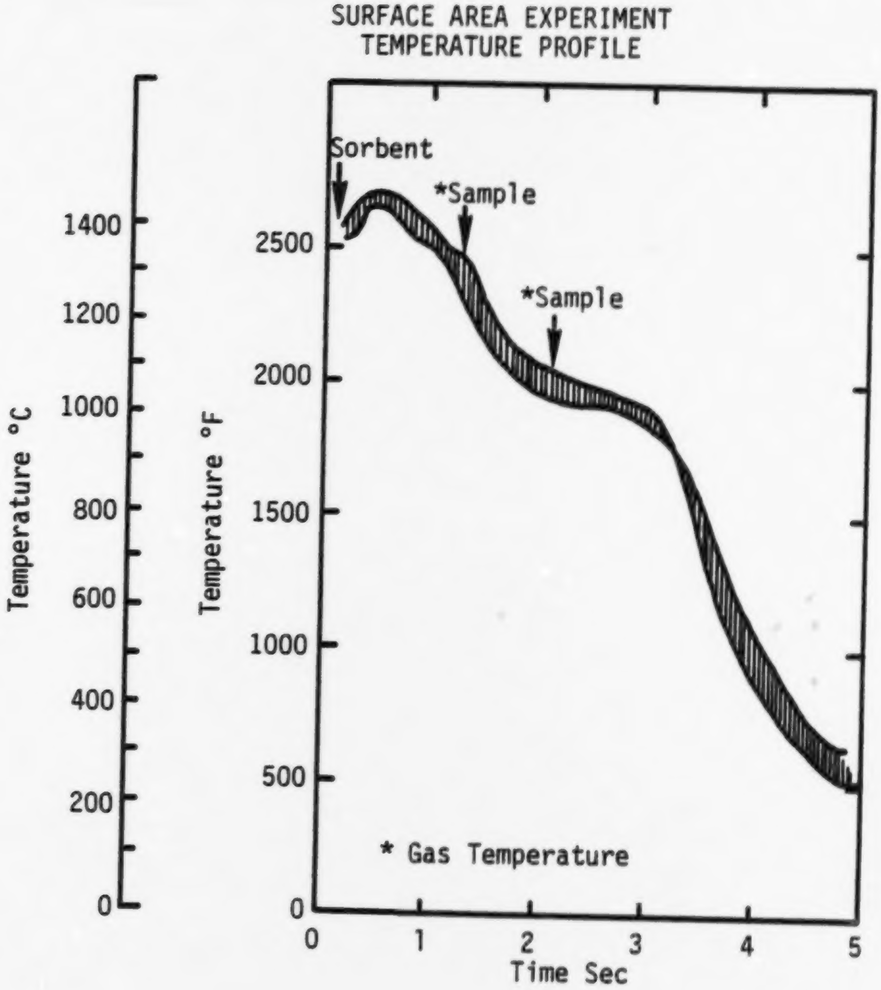

Figure 8-19. Furnace temperature profile, sorbent with fuel.

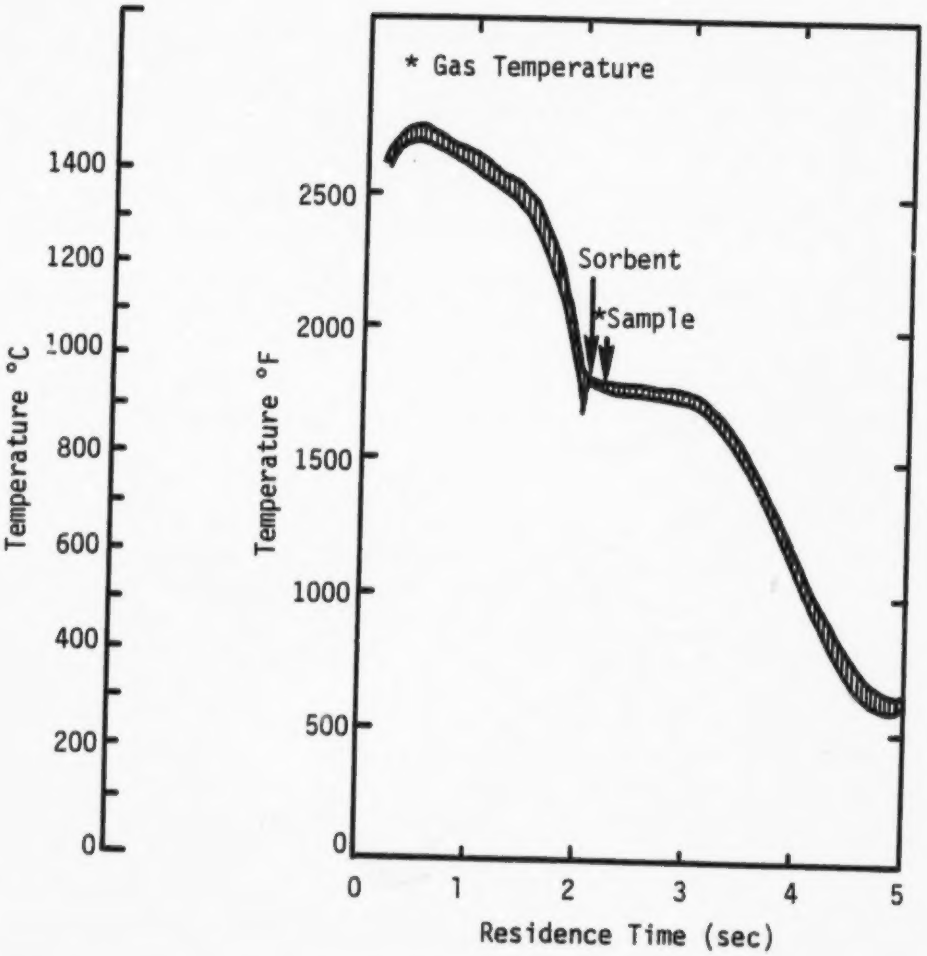

SURFACE AREA EXPERIMENT
TEMPERATURE PROFILE

Figure 8-20. Furnace temperature, sorbent in post-flame cavity.

8.2.2 Electron Micrographs - Sorbent Injection Location

Samples of the sorbent injected at both locations (fuel and pfc) using the natural gas flame with Kaolin addition (the data in Figures 8-16 and 8-17) were taken. Electron micrographs of the sorbent/Kaolin mixtures showed clear differences between sorbent injected with Kaolin at the fuel and sorbent injected downstream. Figure 8-21 shows a high magnification photograph of Vicron mixed with Kaolin and injected with the fuel. As discussed earlier (Section 6.4) the particles are typically spherical and are a mixture of Ca, Al and Si. When the sorbent was injected downstream, discrete irregular sorbent particles mixed with smooth spherical mineral material particles can be easily identified (see Figure 8-22).

Samples of Indiana coal ash with Vicron 45-3 injected with the fuel or downsteam show characteristics similar to the Kaolin/Vicron in natural gas samples. Scanning electron micrographs of the two samples are shown in Figures 8-23 and 8-24. Figure 8-23 shows many fused spherical particles which, when analyzed, are composed of Ca, Al, Si, Fe and other typical ash metals. There are essentially no irregular high surface area sorbent (nearly pure Ca) particles in the field. In contrast, two types of particles can be seen in the micrograph of the "downstream-injection" samples: irregular high-surface area sorbent particles and smooth mineral, ash particles.

The electron micrographs give further substantiation to the coal ash deactivation theory and help to explain the increase in sulfur capture with downstream sorbent injection for coal firing.

8.3 Conclusions Downstream Sorbent Injection

Injecting the sorbent downstream from the main flame resulted in improved utilization in coal flames. Experiments with natural gas flames showed that the sorbents had somewhat higher surface areas in the reaction zone when injected downstream. Gas-fired experiments using mineral matter additives showed that mineral material deactivation of the sorbent could be reduced by injecting the sorbent downstream of the main flame. Electron micrographs of

Reproduced from best available copy.

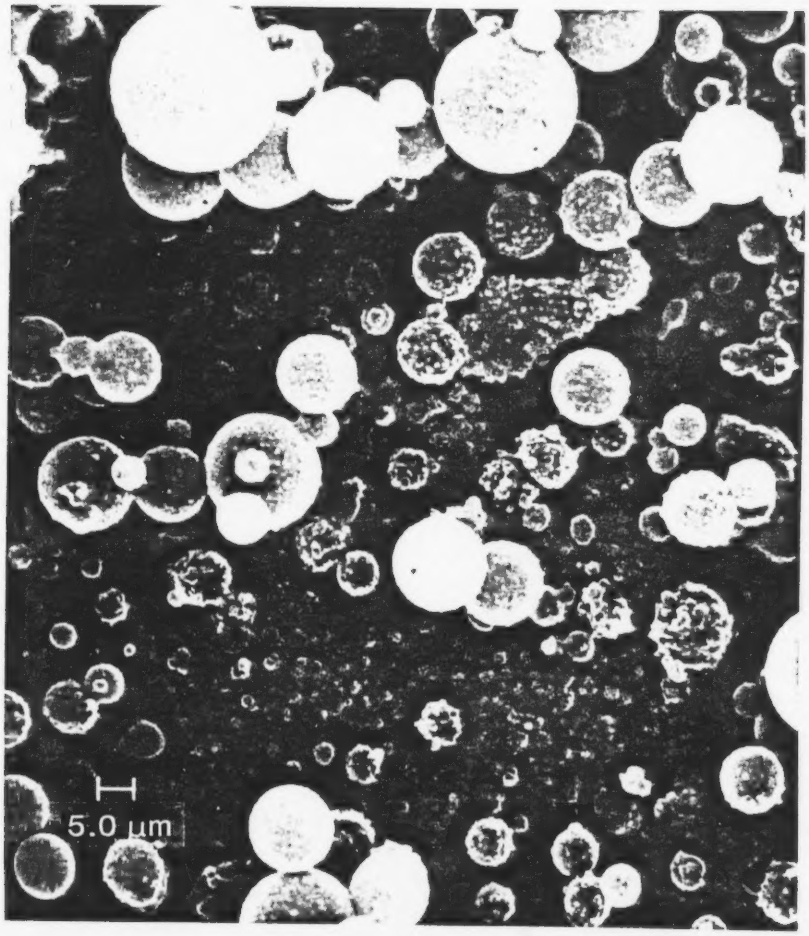

Figure 8-21. Natural gas flame. Vicron and Kaolin injected at fuel.

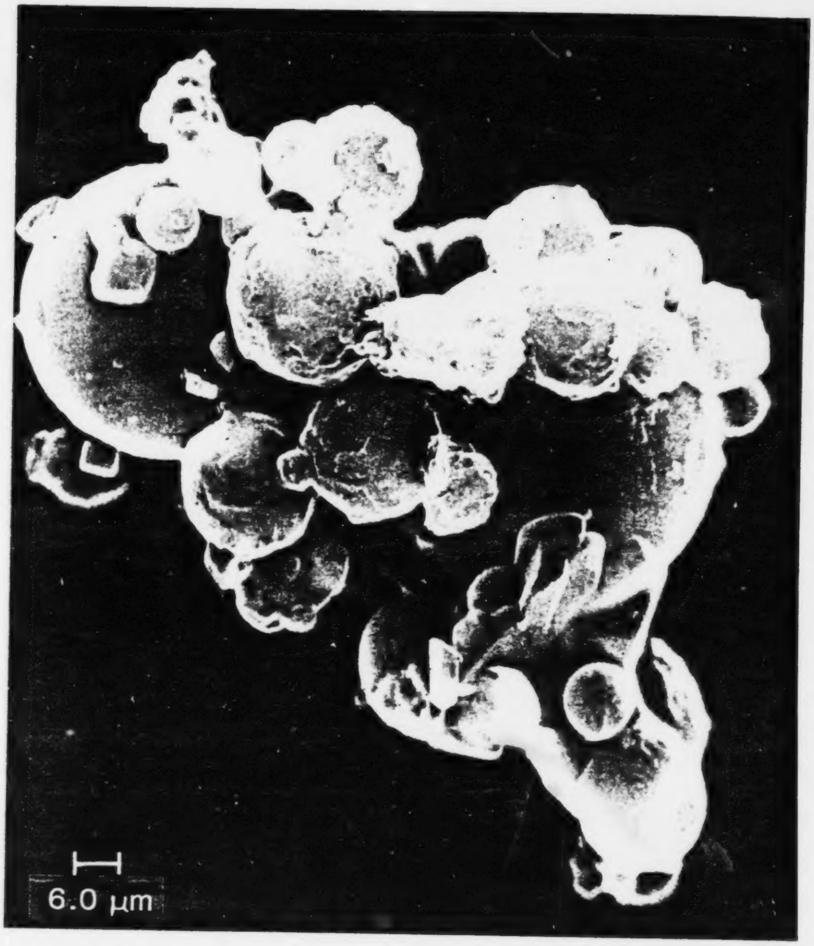

Figure 8-22. Natural gas flame. Kaolin injected at fuel and Vicron injected downstream.

Reproduced from
best available copy.

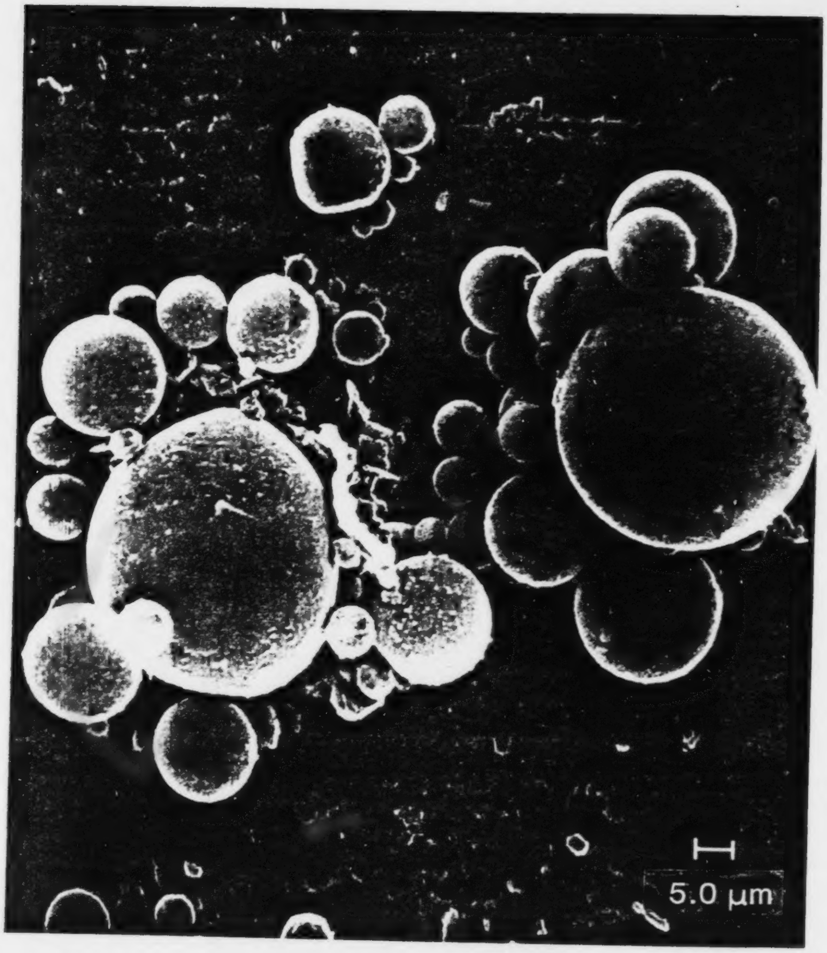

Figure 8-23. Indiana Coal with Vicron injected at fuel.

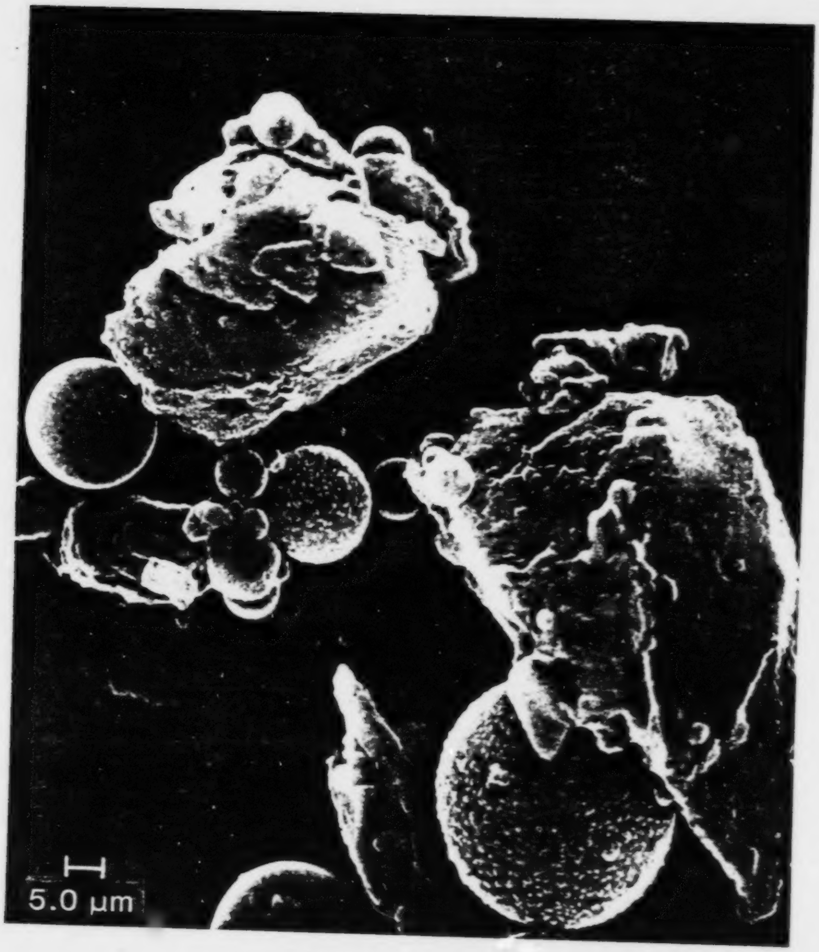

Figure 8-24. Indiana Coal with Vicron injected downstream.

sorbent injected downstream with Kaolin injected with the fuel showed discrete irregular sorbent particles and spherical mineral material particles, implying that improved capture in coal flames with downsteam sorbent injection is due to reduced deactivation of the sorbent by the coal minerals.

9.0 FURNACE MODELING

As part of the Task 3 effort, assessing the effect of scale on SO_2 capture, EER's boiler performance code has been applied to several test furnaces including the SWS, MT, and LWS. This section outlines the objectives for furnace modeling, briefly describes the code, discusses the thermal modeling efforts for two-dimensional furnaces, and reports the results obtained from combining the sulfation model with the furnace models.

9.1 Furnace Modeling Objectives

The primary objective of Task 3 is to investigate scale effects on the performance of systems designed for the simultaneous reduction of NO_x and SO_x emissions. The temperature history of gases and particles is a key factor in the capture of sulfur compounds. However, reliable information on time/temperature profiles in large-scale systems is, at best, fragmentary. Even in experimental systems data is seldom taken in such a manner that comprehensive scale relationships can be observed. A model is necessary to fill in the gaps between data points to obtain the detailed temperature/flow field map necessary to track particles through a furnace. Such a model allows the experimenter to rationalize sulfur capture data, to explain observed trends in terms of the effects of parameters and scale, and to extrapolate data to different and larger-scale systems.

9.2 Boiler Performance Code

The boiler performance code was orignially developed within EER for three-dimensional furnaces such as the LWS. The code has a simplified, less-expensive two-dimensional version. This section discusses the three-dimensional and two-dimensional codes and the modifications necessary to adapt the two-dimensional version of the code to the SWS and MT furnaces.

9.2.1 Three-Dimensional Furnace Heat Transfer Code

The furnace performance code was developed by Wolfgang Richter of EER and allows predictions of local and overall heat transfer and fuel burnout in boiler combustion chambers and industrial furnaces. The results are dependent on furnace geometry and operating conditions, characteristics of fuel and characteristics of wall deposits. The flow pattern within the furnace and the distribution of heat release due to combustion of volatile or gaseous fuel species is prescribed. The three-dimensional predictions of local furnace variables include:

- Gas temperatures;
- Incident and net radiative and total heat fluxes to heat sink surfaces;
- Temperatures of refractory walls and wall deposits;
- Burnout of solid fuel particles of up to ten size classes;
- Equilibrium concentrations of major gaseous species corresponding to the progress of fuel burnout;
- Complete time/temperature histories of real or imaginary tracer particles or material within the furnace;
- Time dependent representation of all considered dependent variables, if requested.

The prediction of overall furnace performance includes:

- total furnace heat absorption of furnace efficiency;
- mean furnace exit temperature;
- burnout of solid fuel particles;
- mean residence times.

A simple model for predictions of temperature distribution along convective passages of boilers can be coupled with the furnace program.

The furnace calculations are based on a zone method. The zone arrangement can have a variable fineness with flexible shape of zones, thus any furnace geometry and firing pattern encountered in practice can be investigated. A typical zone arrange consists of 5 x 5 x 15 zones.

The key part of the furnace code is a Monte Carlo type radiation model which allows an accurate computation of multi-directional radiative exchange between all furnace zones, even for inhomogeneous distribution of absorption coefficients. The modeling of grey or spectral behavior of radiating species like H_2O, CO_2, ash, char and soot particles is based on our own measurements in laboratory and pilot-scale combustion chambers fired wth gas, oil or pulverized fuel. Isotropic or non-isotropic scattering at solid particles can be taken into account. The model of radiative exchange is coupled with a total heat balance for all furnace zones and similar balances for mass concentrations of O_2 and fuel particles of various size classes. Turbulent exchange is simulated by mutual convective mass flow vectors assigned at each non-wall boundary surface of each furnace volume zone. An iterative solution of the combined heat and mass balances is obtained utilizing a combined Newton-Raphson and Gauss-Seidel technique which usually leads to convergence without problems despite a certain statistical error due to the semi-stochastic nature of the radiation model. By an averaging process, the statistical error in the prediction of temperature, heat fluxes and other furnace variables can be minimized at the expense of computing time. Typical calculation times for large pulverized fuel-fired boiler combustion chambers are 500 s on a CDC 7600, however, these times depend very much on special program options chosen, for instance consideration of scattering, etc.

A special program option allows the replacement of the iterative Newton-Raphson and Gauss-Seidel technique with steady solution of dependent furnace variables by an explicity time-dependent scheme yielding non-steady solutions. Another very useful option is a graphical display of isolines of furnace variables in each horizontal or vertical cross-section of the furnace and at each section of the furnace walls including inclined surfaces.

The boiler performance code has successfully been applied for solution of fundamental problems of furnace heat transfer as well as for solution of practical problems experienced by boiler manufacturers, fuel producers and utilities. Full-scale verification of the code has been carried out for gas, oil and large pulverized-fuel-fired boilers yielding satisfying agreement between measured and predicted values of furnace unit temperature profiles as well as of local heat fluxes and other furnace variables.

9.2.2 Two-Dimensional Furnace Heat Transfer Code

The two-dimensional furnace heat transfer code is a simplified version of the three-dimensional model. The 2-D code is written for computation of heat transfer and solid fuel burn-out in cylindrical furnaces fired along the axis by single flames. With exceptions of the pecularities of the geometry of the axisymetric system, the code includes all options described in the summary for the three-dimensional code.

The arrangement of concentric cylindrical furnace zones is quite flexible. A typical fine arrangement of zones would consist of five radial and ten axial volume zones. With such an arrangement, details of the near-burner flow and mixing pattern can be incorporated easily. Those patterns may be obtained from empirical Thring-Newby entrainment theory, from isothermal physical models or from numerical fluid dynamics codes.

A specially useful feature of the code is that it can be run for coarse zone arrangements on smaller computers such as PDP 11/23. Thus, this code can easily be used for a first overall evaluation of heat transfer behavior of various fuels studied in a particular furnace. A typical computing time on a PDP 11 would be 1 hr for 20 iterations. This number applies for a cylindrical pulverized-coal-fired combustor with 10 axial "plug flow" zones and a reasonable reduction of the statistical error of the radiataive heat transfer calculations. Running times on a CDC 7600 would be much shorter, making this code a candidate for coupling with a detailed chemistry model.

9.2.3 Model Modifications

The original version of the two-dimensional furnace model allowed for only a single type of side-wall surface. The SWS and the MT have two types of inside surfaces. A portion of each furnace has water-cooled walls covered only with a thin layer of slag, and the remainder of each furnace has water-cooled walls covered with a thick layer of insulation. The program has been modified to utilize an effective wall with heat-balance averaged properties of the two walls.

The exit duct of the SWS is on one side of the rear of the furnace. In the axisymmetric model, the exit has been approximated as a porous wall on the outer radial side of the outermost rear zone. The MT exits axisymmetrically at the rear. In modeling, the exit has been approximated as a black hole at a specified temperature on the rear axial side of the two innermost rear zones.

9.3 Two-Dimensional Furnace Modeling

The two-dimensional furnace heat transfer code was utilized to model the SWS and the MT furnaces. The technique for applying the model was perfected by matching predicted results with detailed measurements taken on the SWS. This technique was then applied to the MT where fewer measurements were available. (Making complete verification of the MT case impossible.)

9.3.1 Detailed SWS Modeling

This section describes the SWS model including fuel, burner, and flow and heat release patterns; outlines the tuning procedure used to match model predictions with detailed data for the baseline case and discusses the results.

Utah coal has been chosen as the baseline fuel. Proximate and ultimate analyses are shown in Table 9-1. The size distribution of the ground coal approximates a Rosin-Rammler distribution.

TABLE 9-1. UTAH COAL ANALYSIS

Proximate: Mass Fraction Wet

H_2O	0.0372	Higher Heating Value = 29198 KJ/Kg wet
Volatiles	0.4537	
Ash	0.0763	
Fixed Carbon	0.4328	
	1.0000	

Ultimate: Mass Fraction Wet

C	0.6847
H	0.0504
N	0.0146
S	0.0091
O	0.1357
Moisture	0.0321
Ash	0.0734
	1.0000

$$R = \exp\left[-(54.5\ \mu m)^{1.33}\right]$$

where R is the mass fraction of particles larger than diameter D. The fly ash size distribution has been calculated from the coal size distribution assuming that each coal particle produces two fly ash particles, and the absorption efficiency of fly ash has been assumed to be 0.6.

The Distributed Mixing Burner (DMB) has been chosen as the baseline burner. The dimensions of the DMB are listed in Table 9-2. In typical operation, all of the fuel and 20 percent of stoichiometric air goes to the primary, 50 percent of stoichiometric air goes to the secondary, and 50 percent of stoichiometric air goes to the tertiary. Effective burner radii have been calculated according to Field, et al. (1967).

$$r'o = \frac{\dot{m}}{\left(\pi \rho_0\ \dot{G}\right)^{1/2}} \left(\frac{T_f}{T_o}\right)^{1/2}$$

where m is mass flux

$\dot{G}$ is momentum flux
ρ_0 is jet fluid density
T_f is ambient temperature
T_o is jet temperature

At standard input conditions, these calculations yield an effective primary burner radius of 0.11 m and an effective combined primary-secondary-tertiary burner radius of 0.36 m.

The dimensions and the flow and heat release patterns of the SWS furnace model in its present state are shown in Figure 9-1. The furnace is divided into five radial zones by ten axial zones. The radial dimensions of the inner two zones are defined by the effective radii of the primary burner and the combined primary-secondary-tertiary burner. The outer radius of the third zone coincides with the point in the confined jet where entrainment stops and recirculation begins. The outer two radial zones equally divide the remaining volume.

Mass flow patterns have been calculated from the swirling jet entrainment theory of Kerr and Fraser (1965).

$$\frac{\dot{m}}{\dot{m}_o} = \frac{x}{d_o} (K_1 + K_2 S)$$

where

$\dot{m}$ = mass flow in the jet at axial distance x
$\dot{m}_o$ = initial mass flow in the jet
x = distance from burner exit
d_o = effective burner diameter
K_1 = 0.35
K_2 = 1.4

S, the swirl number was calculated from

$$\tan \emptyset = (1 + K_3) S \tan \emptyset_o$$

where

$\emptyset$ = jet half-angle (35^o based on measured CO profiles)
K_3 = 5.68
$\emptyset_o$ = jet half-angle in the absence of swirl, typically 4.85^o

TABLE 9-2. VERSATILE BURNER DIMENSIONS

CORE:

ID = 2.25 in
OD = 2.75 in

PRIMARY:

Diameter of inner boundary = 2.75 in
Diameter of outer boundary = 5.25 in
Area blocked by vane cross-section = 1.0 in^2
Flow area: 14.71 in^2

INNER SEC:

Diameter of inner boundary = 6.0 in
Diameter of outer boundary = 9.25 in
Flow area = 38.93 in^2

OUTER SEC:

Diameter of inner boundary = 10.0 in
Diameter of outer boundary = 12.75 in
Flow area = 49.14 in^2

TERTIARY:

Inner diameter = 5.5 in
Flow area/tertiary port = 23.76 in^2

Vectors: Mass flow (fraction of input mass flow)

Circles: Volatile heat release (fraction of total volatile heat release)

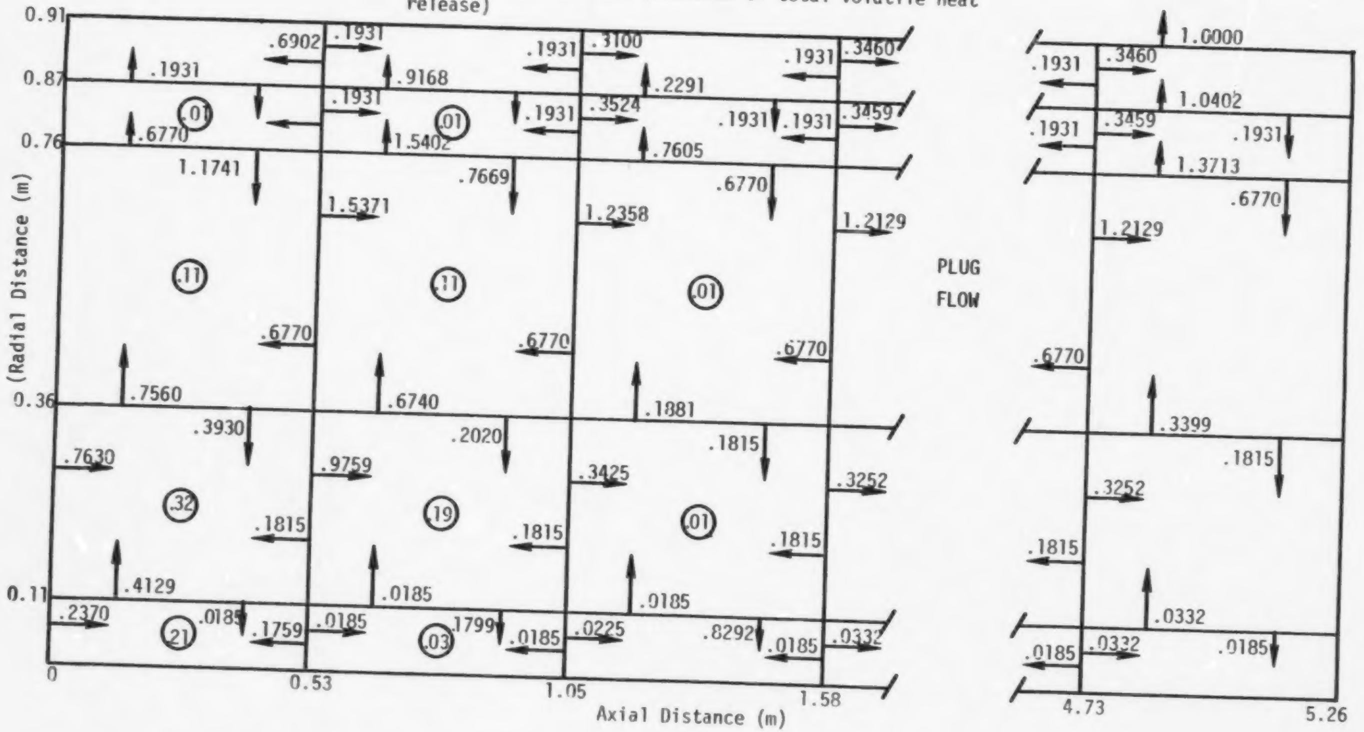
0.91
0.87
0.76
0.36
0.11
0
(Radial Distance (m)
0.53
1.05
1.58
4.73
5.26
Axial Distance (m)
PLUG FLOW
.1931
.6902
.1931
.9168
.1931
.3100
.2291
.1931
.3460
.01
.6770
.1931
.01
1.5402
.1931
.3524
.7605
.1931
.1931
.3459
1.1741
1.5371
.7669
1.2358
.6770
1.2129
.11
.11
.01
.6770
.6770
.6770
.7560
.6740
.1881
.3930
.2020
.1815
.7630
.9759
.3425
.3252
.32
.19
.01
.1815
.1815
.1815
.4129
.0185
.0185
.2370
.0185
.1759
.0185
.1799
.0185
.0225
.8292
.0185
.0332
.21
.03
1.0000
.1931
.3460
1.0402
.1931
.3459
.1931
1.3713
.6770
1.2129
.6770
.3399
.1815
.3252
.1815
.0332
.0185
.0332
.0185

Figure 9-1. SWS flow and heat release patterns.

Entrainment was applied to the confined jet using the approach of Field et al. (1967). Entrainment is assumed to occur according to the above formula from the point of zero entrainment (where $\dot{m} = \dot{m}_0$) to the point halfway between the point of zero entrainment and the point where the jet impinges on the wall. Recirculation (equal to the above entrainment) occurs between the halfway point and the impingement point. Plug flow is assumed beyond the impingement point. Reverse primary entrainment (not included in Kerr and Fraser) equal to the primary flow, and turbulence equal to a fifth of the input flow times the ratio of the cross-sectional area of each zone to the area of the effective burner, have been superimposed on the original flow pattern.

Volatile heat release has been calculated according to the empirical formula of Faber and Michelfelder (1978).

$$\frac{\dot{Q}}{\dot{Q}_o} = \exp\left[-3.2\left(\frac{x}{.709\ L_f}\right)^2\right]$$

where

$\dot{Q}$ = volatile mass flow at axial distance x

$\dot{Q}_o$ = initial volatile mass flow

L_f = flame length (1.8 m based on visual estimate)

The radial distribution of volatiles has been calculated from the mass flow pattern.

A major portion of the modeling effort has been devoted to accurately reproducing SWS baseline measurements. Once a satisfactory model application procedure has been established, it is a relatively simple matter to modify the model to consider alternate fuels, burners, combustion conditions, and furnaces.

The baseline case for the SWS was chosen using Utah coal in the Distributed Mixing Burner at full load (10 MBtu/hr). This case was chosen because a wide variety of experimental data were available for these conditions including:

- Furnace exit temperature;
- Radial and axial gas temperature profiles;
- Radial and axial carbon monoxide concentration profiles;
- Carbon burnout;

The input parameter which has the greatest effect on exit temperature is the ratio of wall conductivity to wall thickness (λ/S). The wall of the SWS (and the MT) is partially covered with insulation. The conductivity of this insulation has been estimated from manufacturer specifications resulting in $(\lambda/S)_i = 0.0075$ KW/m^2. The resistance to heat transfer of the uninsulated portion of the furnace is dominated by its coating of slag of unknown conductivity and thickness. This $(\lambda/S)_u$ has been chosen as 0.10 KW/m^2 to force the predicted furnace exit temperature to agree with the measurement. Utilizing these values, the model accurately predicts the effects of load on furnace exit temperature, as shown in Figure 9-2.

Heat release and flow patterns are inputs to the model which have not been measured in the SWS. These parameters have only a minor effect on furnace efficiency and exit temperature. Initially, theoretical flow patterns were calculated, for non-swirl conditions following the treatment of Field et al., and modified for swirl using the theories of Kerr and Fraser[2]. Volatile fuel was assumed to follow the general flow pattern and volatile heat release was calculated according to an empirical formula developed by Faber and Michelfelder[3]. These inputs yielded gas temeprature profiles shown by the solid lines of Figures 9-3 and 9-4. Figure 9-3 shows that the predicted gas temperature profile 0.5 m off the centerline (representing most of the mass flow) was in fair agreement with the measurement. However, predicted centerline temperatures, as shown in Figure 9-4, were about 400°K too high. Turbulence and reverse entrainment in the primary (not considered in the initial flow pattern) were introduced in an attempt to lower the predicted

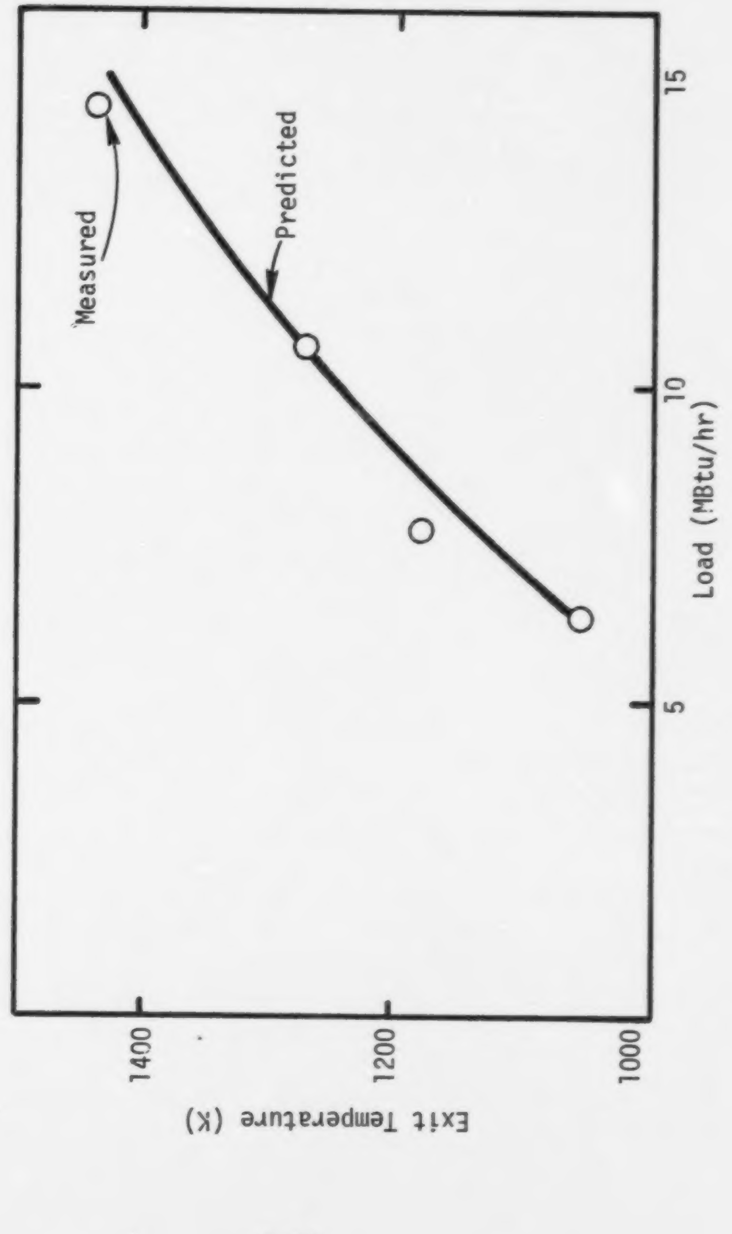

Figure 9-2. Effect of Load on SWS Exit Temperature.

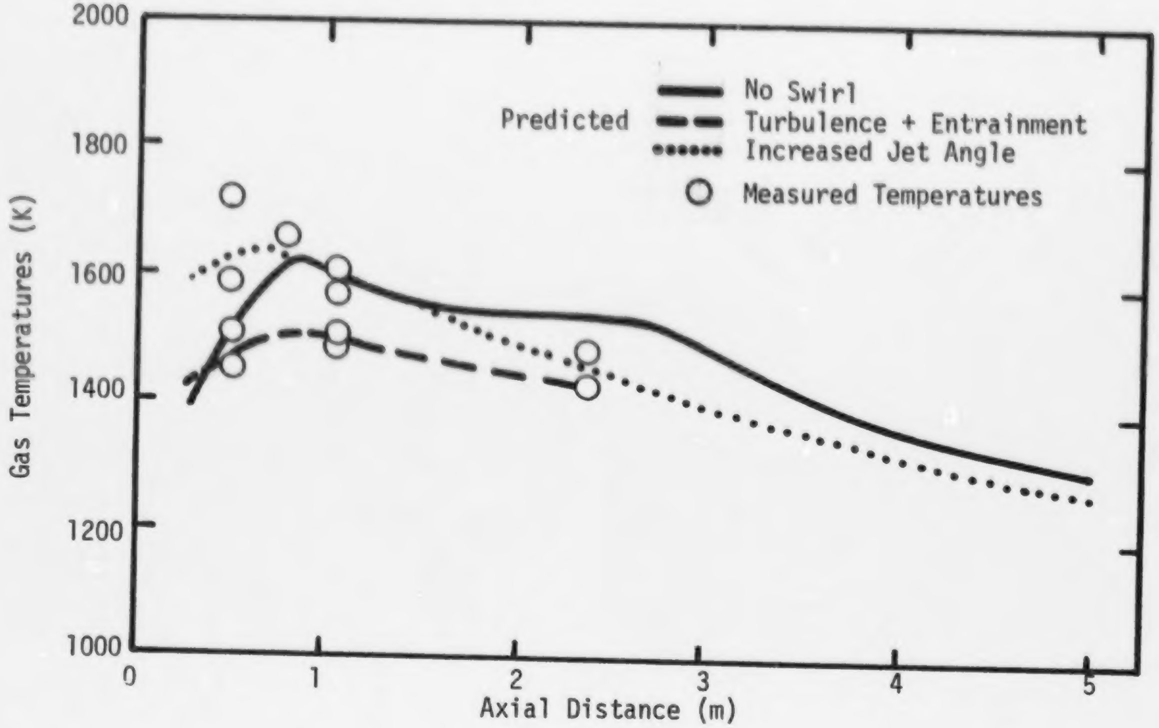

Figure 9-3. 0.5 m off-centerline gas temperatures.

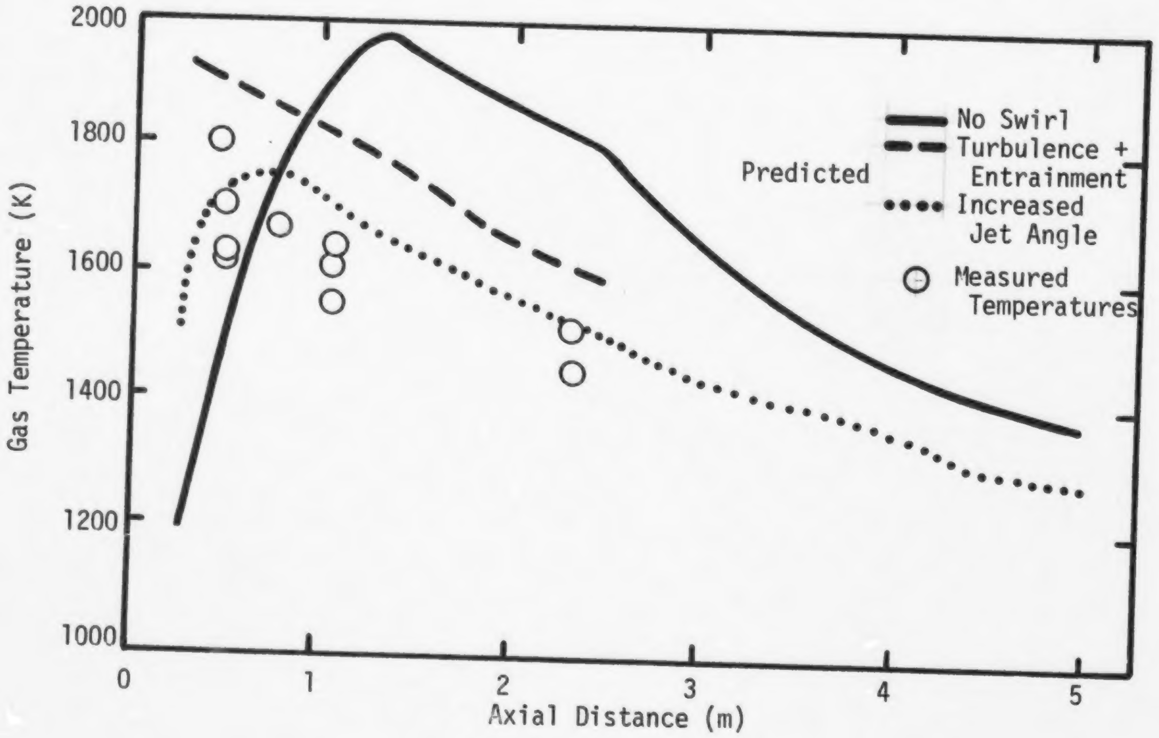

Figure 9-4. Centerline gas temperatures.

centerline temperatures, yielding the dashed lines of Figures 9-3 and 9-4. Finally, the jet angle was increased from the originally calculated one to make volatile fuel concentrations more closely follow measured CO concentrations yielding the dotted lines of Figure 9-3 and 9-4. This final prediciton agrees fairly well with both centerline and off-centerline measurements.

Figure 9-5 shows wall temperatures throughout the furnace. Temperatures of the insulated portion of the furnace are about 2000^{o}K higher than the uninsulated portion and are about 50^{o}K lower than the off-centerline gas temperatures of Figure 9-4. The fluctuations observed in the front and back wall temperatures are likely due to their decreased surface area which makes them more sensitive to random factors in the model. Figure 9-6 shows that heat flux to the walls closely follows gas temperature and that flux to the totally insulated front and back walls is less than a fifth as much as flux through the partially insulated side walls. This indicates that most of the heat is passing through the uninsulated portions and that factors which affect the conductivity of the uninsulated wall (e.g. slag buildup) have a major effect on furnace heat transfer.

In summary, the SWS model accurately predicts the effects of load on exit temperature and reproduces measured temperature profiles. Additional measurements which could be used to improve the model include:

- Wall temperature profile;
- Radiation flux;
- Fly ash size distribution;
- Gas velocity profiles.

9.3.2 MT Modeling

The MT model was developed following the same procedure as the SWS. The same fuel was used. A larger Distributed Mixing Burner was modeled with dimensions listed in Table 9-3. The effective radii of the primary and of the combined primary-secondary-tertiary burner were calculated as 0.23 and 0.67

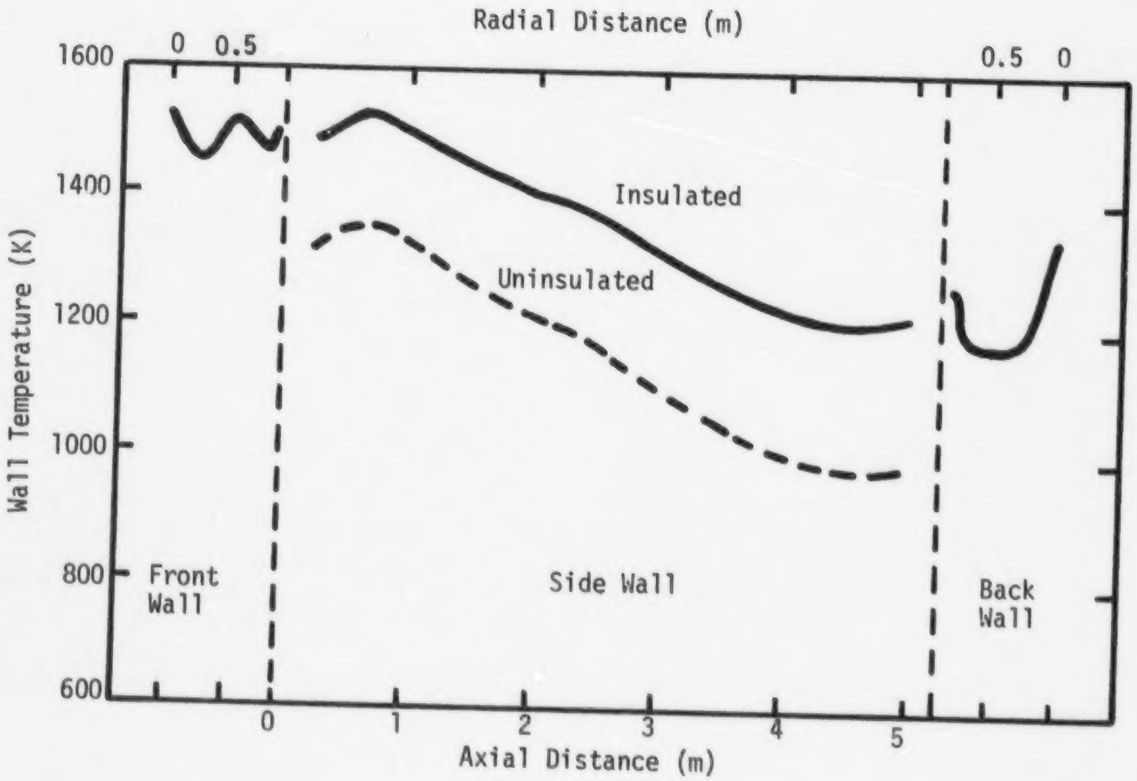

Figure 9-5. SWS wall temperatures.

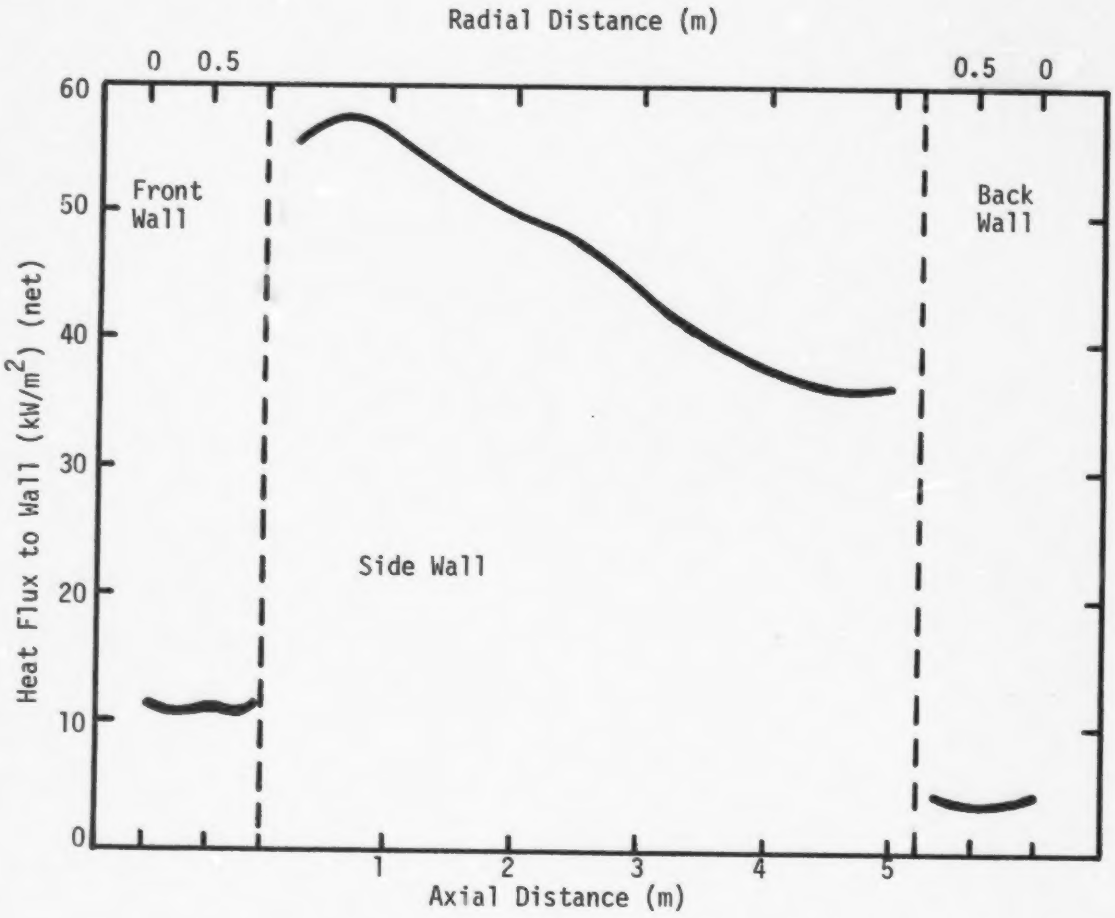

Figure 9-6. SWS Heat flux to walls.

TABLE 9-3. V50 BURNER DIMENSIONS

CORE:

ID = 1.94 in

OD = 2.75 in (at the exit)

PRIMARY:

Diameter of inner boundary: 2.75 in

Diameter of outer boundary: 9.25 in

Area blocked by van cross-section: 1.63 in^2

Flow area: 59.63 in^2

INNER SEC:

Diameter of inner boundary: 10.0 in

Diameter of outer boundary: 16.63 in

Flow area: 138.67 in^2

OUTER SEC:

Diameter of inner boundary: 17.38 in

Diameter of outer boundary: 23.75 in

Flow area: 205.77 in^2

TERTIARY:

4 ports on 52.25 in radius

Inner diameter: 12.0 in

Flow area/tertiary port: 113.1 in^2

respectively; however, the radius of the second innermost zone was chosen as 0.76m to coincide with the dimensions of the furnace exit. CO measuremetns were unavailable, so the jet half-angle was set as 13.5^{0} based on visual observation of the flame. Turbulence and reverse primary entrainment were calculated as in the SWS case. Volatile heat release was calculated based on an observed flame length of 5.2 m. Figure 9-7 shows the dimensions, flow patterns and volatile heat release patterns used in the MT model.

The insulated portion of the MT wall was assumed to have the same conductivity as in the SWS. The slag layer on the MT was varied changing the uninsulated λ/S to 0.12 so that the predicted exit temperature agreed with the 1480^{0}K measurement. Figure 9-8 shows predicted gas temperatures (no measurements were available for comparison). Unlike the SWS prediction, centerline gas temperatures for the MT were considerably higher than bulk-flow temperatures. This was due to the smaller jet angle and to the larger radius of the MT. Except for the centerline, predicted temperatures in the MT were reasonably constant around 1500^{0}K throughout the length of the reactor. Wall temperatures, as shown in Figure 9-9, followed a similar trend with insulated wall temperatures approaching the gas temperature and uninsulated wall temperatures running about 230^{0}K cooler. Figure 9-10 shows that predicted heat flux through the partially insulated side wall of the furnace was fairly constant around 55 Kw/m^2. Heat flux through the uninsulated front wall was much higher although a sharp radial gradient was present due to the low centerline gas temperature (slow ignition) near the burner. Heat flux through the totally insulated outer three zones of the rear wall was again less than a fifth of the flux through the side wall, indicating that most of the heat passed through the uninsulated portion of the side wall. Heat flux through the inner two zones of the rear wall, which comprised the exit, was more than double the flux through the outer three zones, but still much less than flux through the side wall due to the low effective radiating temperature (1000^{0}K) assumed for the exit.

In summary, the MT model accurately predicts the exit temperature, however, no measurements are available to compare with predicted gas temperature profiles. These measurements, along with CO concentration

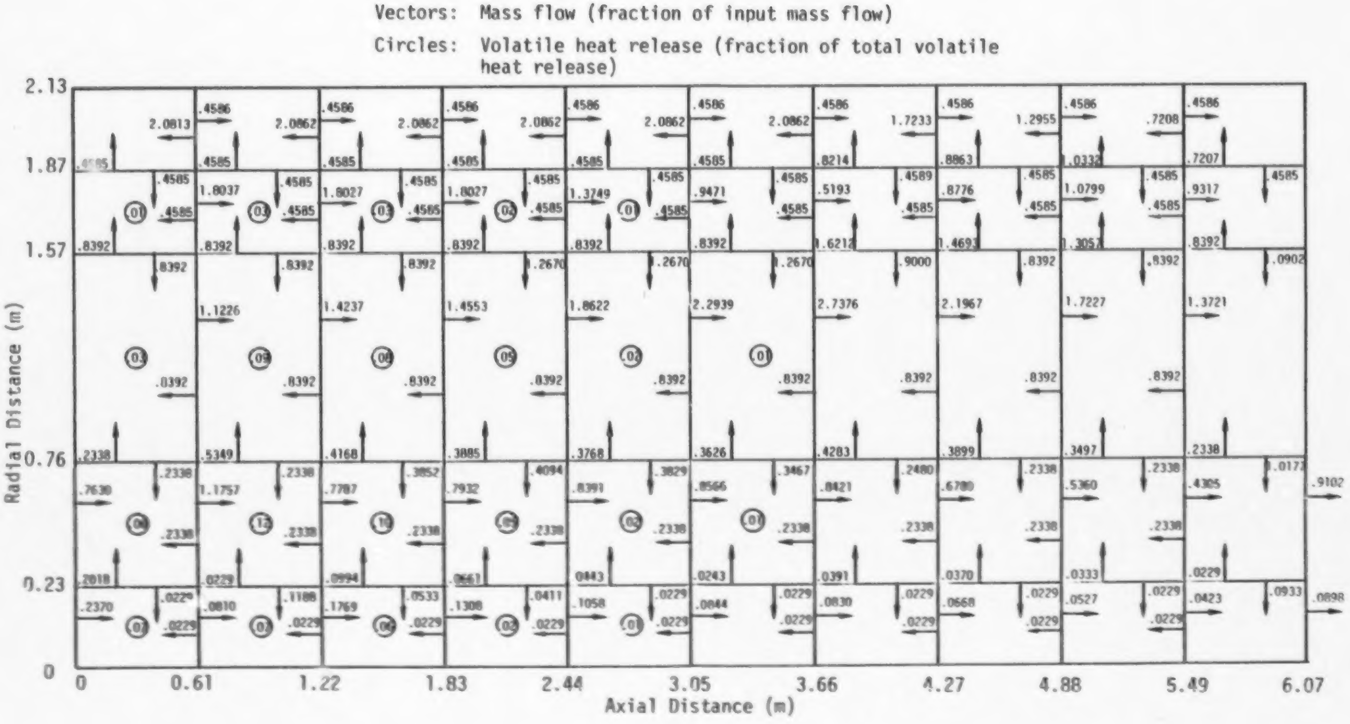
Vectors: Mass flow (fraction of input mass flow)
Circles: Volatile heat release (fraction of total volatile heat release)
2.13
1.87
1.57
0.76
0.23
0
Radial Distance (m)
.4585
2.0813
.4586
.4585
2.0862
.4586
.4585
2.0862
.4586
.4585
2.0862
.4586
.4585
2.0862
.4586
.4585
2.0862
.4586
.8214
1.7233
.4586
.8863
1.2955
.4586
1.0332
.7208
.4586
.7207
.4585
01
.4585
.8392
1.8037
.4585
03
.4585
.8392
1.8027
.4585
03
.4585
.8392
1.8027
.4585
02
.4585
.8392
1.3749
.4585
01
.4585
.8392
.9471
.4585
.4585
.8392
.5193
.4589
.4585
1.6212
.8776
.4585
.4585
1.4693
1.0799
.4585
.4585
1.3057
.9317
.4585
.8392
.8392
03
.0392
.2338
1.1226
.8392
09
.8392
.5349
1.4237
.8392
08
.8392
.4168
1.4553
.2670
05
.8392
.3885
1.8622
.2670
02
.8392
.3768
2.2939
.2670
01
.8392
.3626
2.7376
.9000
.8392
.4283
2.1967
.8392
.8392
.3899
1.7227
.8392
.8392
.3497
1.3721
.0902
.2338
.7630
.2338
04
.2338
.2018
1.1757
.2338
12
.2338
.0229
.7707
.3852
10
.2338
.0994
.7932
.4094
09
.2338
.0661
.8391
.3829
03
.2338
.0443
.8566
.3467
01
.2338
.0243
.8421
.2480
.2338
.0391
.6700
.2338
.2338
.0370
.5360
.2338
.2338
.0333
.4305
.0177
.9102
.0229
.2370
.0229
07
.0229
.0810
.1188
02
.0229
.1769
.0533
06
.0229
.1308
.0411
02
.0229
.1058
.0229
01
.0229
.0844
.0229
.0229
.0830
.0229
.0229
.0668
.0229
.0229
.0527
.0229
.0229
.0423
.0933
.0898
0
0.61
1.22
1.83
2.44
3.05
3.66
4.27
4.88
5.49
6.07
Axial Distance (m)

Figure 9-7. MT flow and heat release patterns

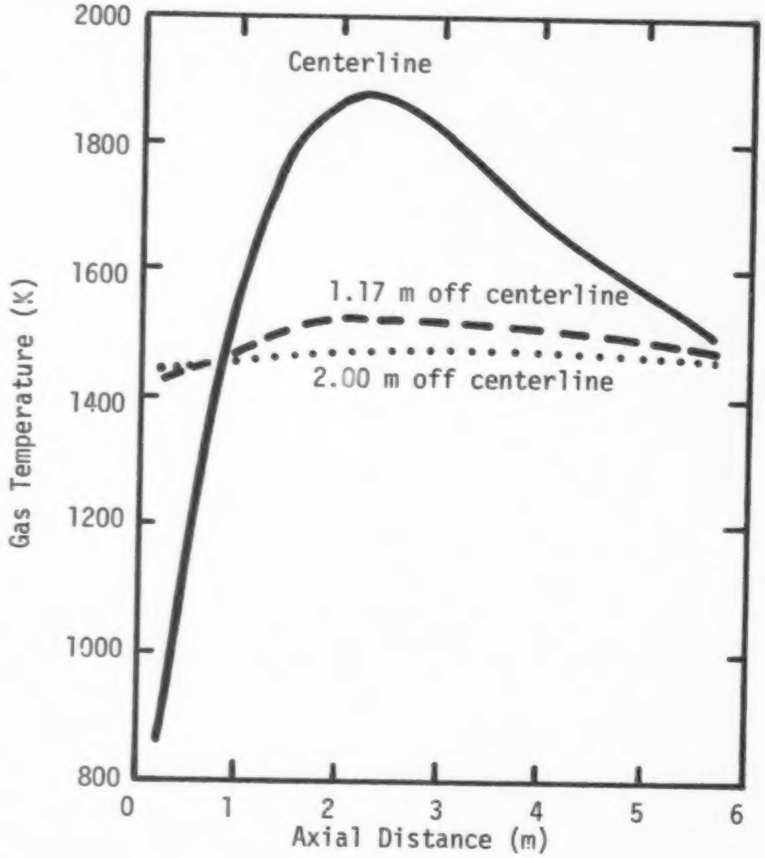

Figure 9-8. MT gas temperatures.

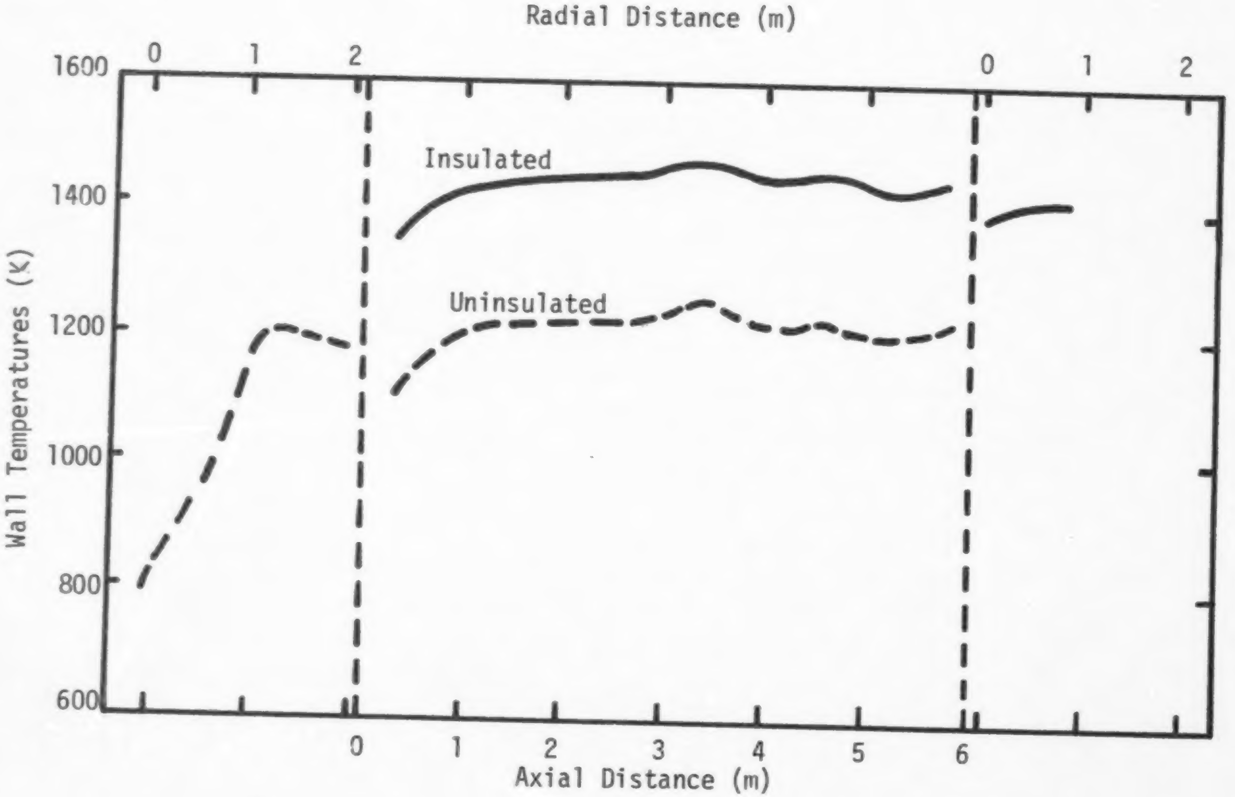

Figure 9-9. MT wall temperatures.

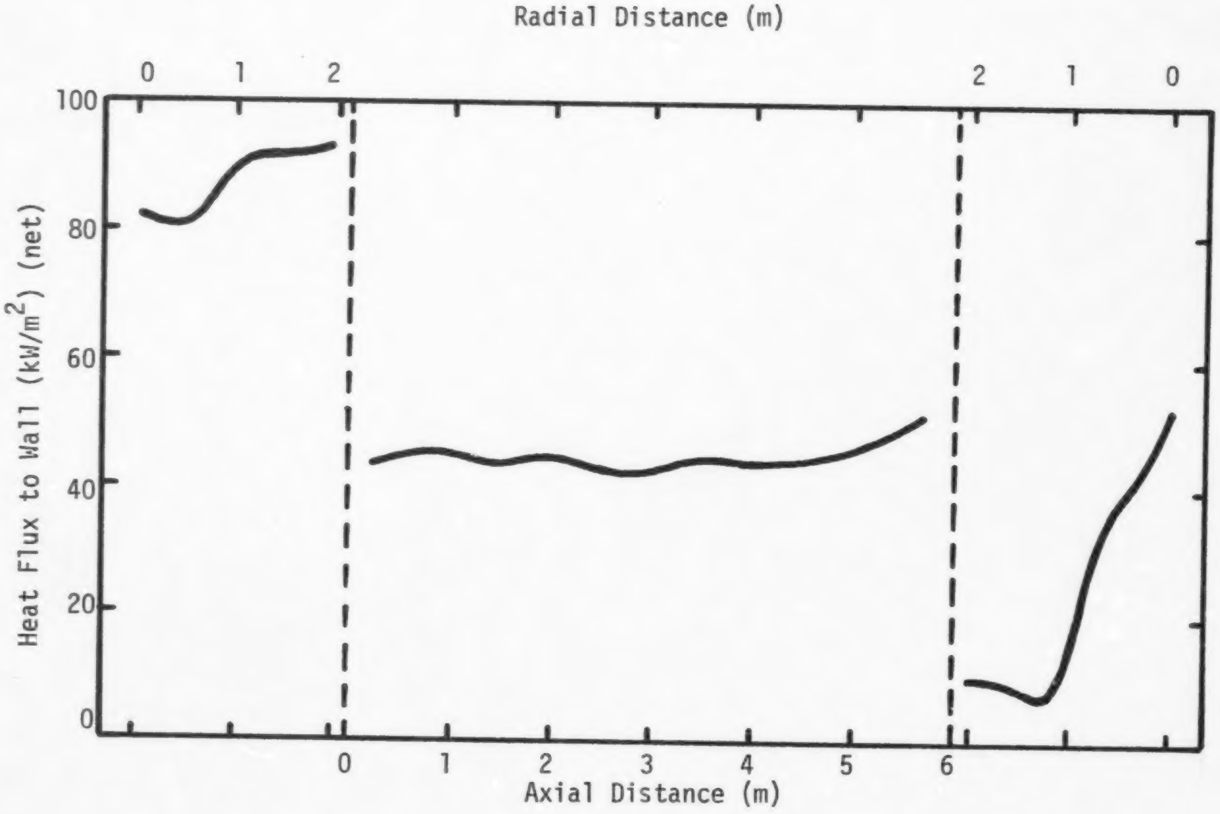

Figure 9-10. MT heat flux to wall.

profiles to allow better calculation of the jet angle and flow heat release patterns are needed in order to be confident of temperature history predictions.

9.4 Three-Dimensional Furnace Modeling

Three-dimensional modeling was undertaken in order to expand the predictions to a larger scale, geometrically irregular furnace. Due to the added expenses involved in modeling a larger furnace, the three-dimensional modeling was not carried out to the same degree of completion as the two-dimensional modeling. The emphasis was on demonstrating the effects of scale on thermal performance and sulfur capture rather than on accurately reproducing actual data points.

The LWS was modeled using Utah coal in a 5 x 5 x 11 zone arrangement as shown in Figure 9-11. Inputs to the model were taken from a number of sources. The flow field was estimated from observation of a 1/15 linear scale isothermal model run with a simulated DMB burner scaled according to Thring-Newby criteria with air flows corresponding to 21 percent primary, 51.3 percent secondary and 55.7 percent tertiary, or an overall stoichiometry of 128 percent theoretical air. Turbulent exchange between zones was estimated as a constant times the local mass flux plus a constant times the total mass flux. A measured size distribution of 72 percent through 200 mesh (74 micron) was used for the coal, and a typical size distribution measured from Utah coal combustion particulate in a bench-scale reactor was used for the fly ash. The absorption efficiency of fly ash was assumed to be 0.5. Portions of the LWS walls were covered with refractory as shown by the bold lines in Figure 9-11. Uninsulated portions of the wall were assumed to be coated with 5 mm ash. The conductivity to thickness ratio used was 0.8 $KW/^{o}K-m^2$ for the ash-coated walls, 0.01577 for the vertical insulated walls, and 0.008 for the slanted insulated walls.

The LWS was modeled in two runs. The first run was used to produce the detailed thermal contours of the following figures. In this run, volatile heat release was fixed in the vicinity of the burner. The second run was used

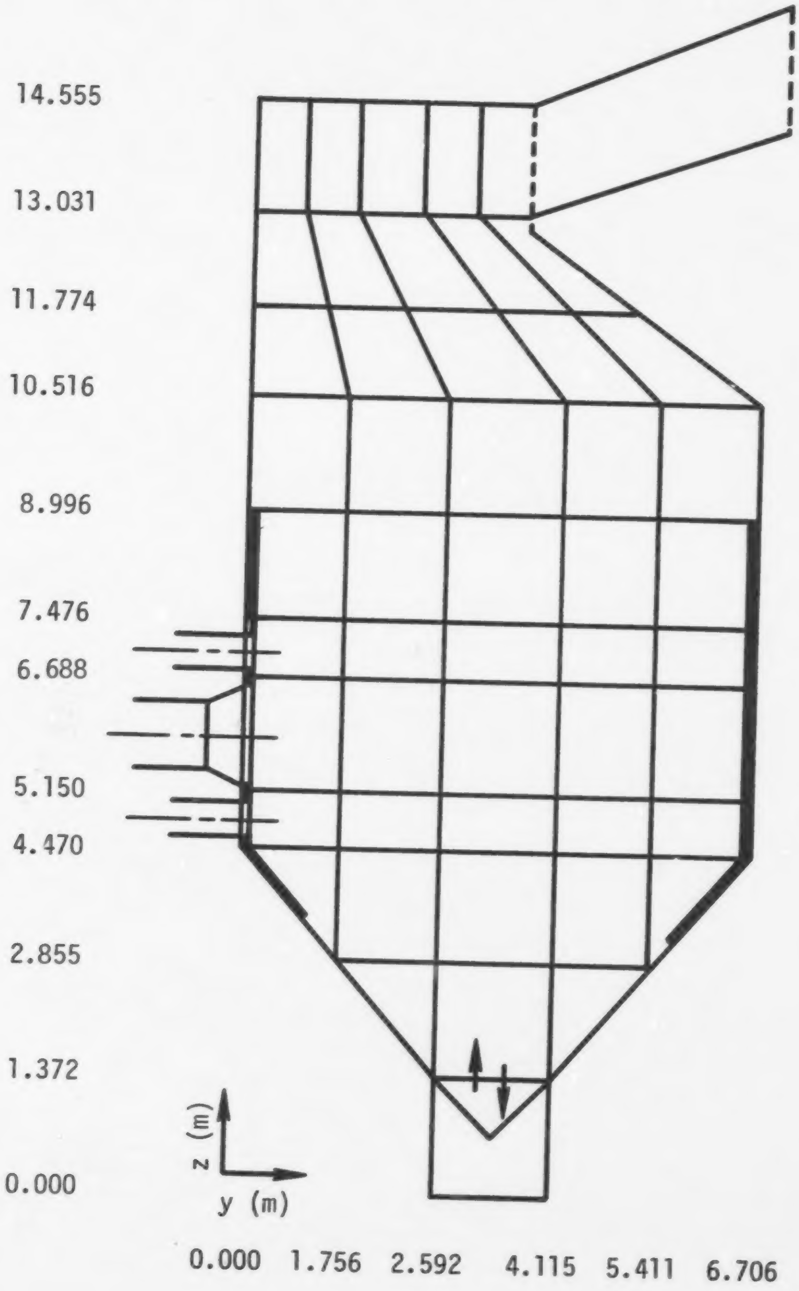
14.555
13.031
11.774
10.516
8.996
7.476
6.688
5.150
4.470
2.855
1.372
0.000
z (m)
y (m)
0.000
1.756
2.592
4.115
5.411
6.706

Figure 9-11. LWS Zoning.

to produce the temperature profiles used as input to the sulfation model as discussed in Section 9.5. In this latter run, several minor adjustments were made including the improvement that volatile heat release was calculated based on visual observation of the flame such that 0.1 percent of the volatiles remained unburned after 0.7 seconds.

The predicted exit temperature of 1182°K was within 35 degrees of a measured exit temperature of 1217°K taken under different, but similar, operating conditions to those of the model. Although the agreement indicates that the model produces reasonable results and probably accurately reflects trends, due to the differences in operating conditions it does not necessarily verify the actual predicted temperature profiles. Figure 9-12 shows the effect of load on LWS exit temperature. A load decrease from 100 MBtu/hr to 70 MBtu/hr dropped the mean exit temperature from 1182 to 1061°K. Gas temperature profiles for the full-load and seventy percent load cases are shown in Figures 9-13 and 9-14. Peak flame temperatures around 1800°K were predicted for both cases, but the low-load case had sharper temperature gradients resulting in the lower exit temperature.

In summary, the LWS model is adequate for predicting effects of scale and of changing parameters on furnace temperatures, but more detailed modeling is necessary to produce accurate profiles of absolute temperatures for a given operating point.

9.5 Combined Thermal/Sulfation Modeling

The flow field and temperature maps from the furnace heat transfer models have been used to supply temperature histories as inputs to the sulfation model. This section outlines the statistical approach to the problem of choosing particle paths through the furnace and discusses the results including the effects of scale on sulfation in four furnaces.

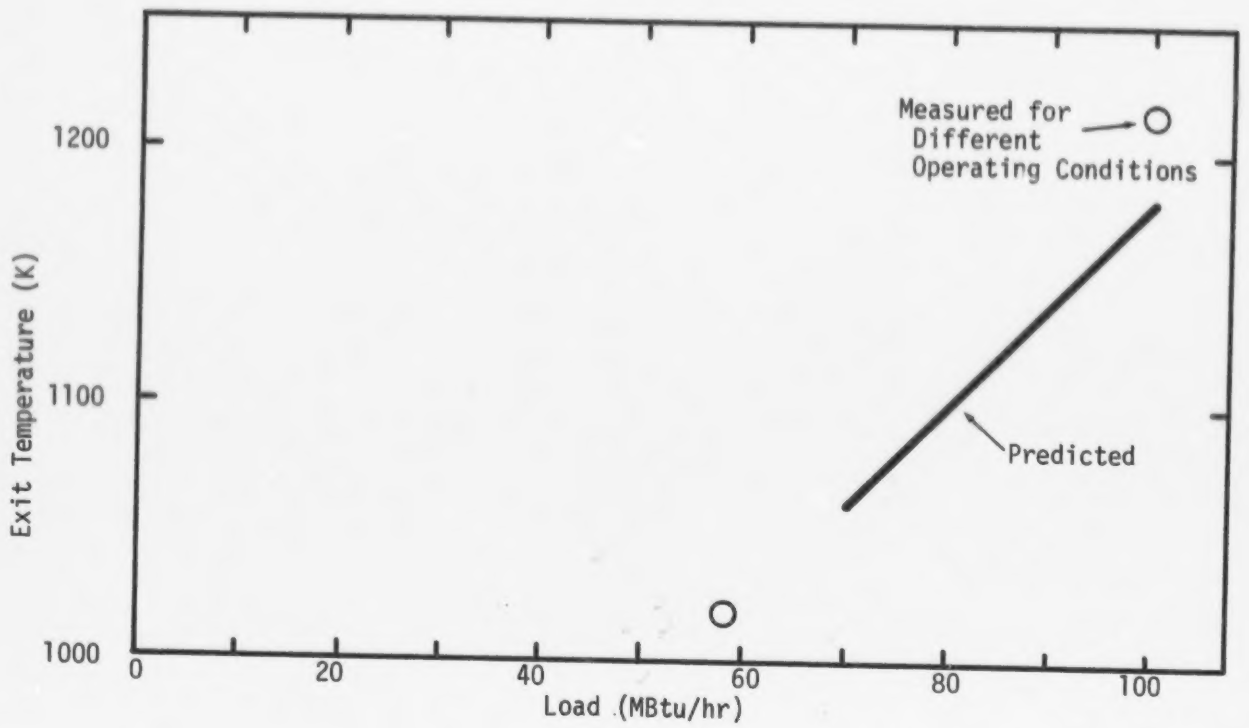

Figure 9-12. Effect of Load on LWS Exit Temperature.

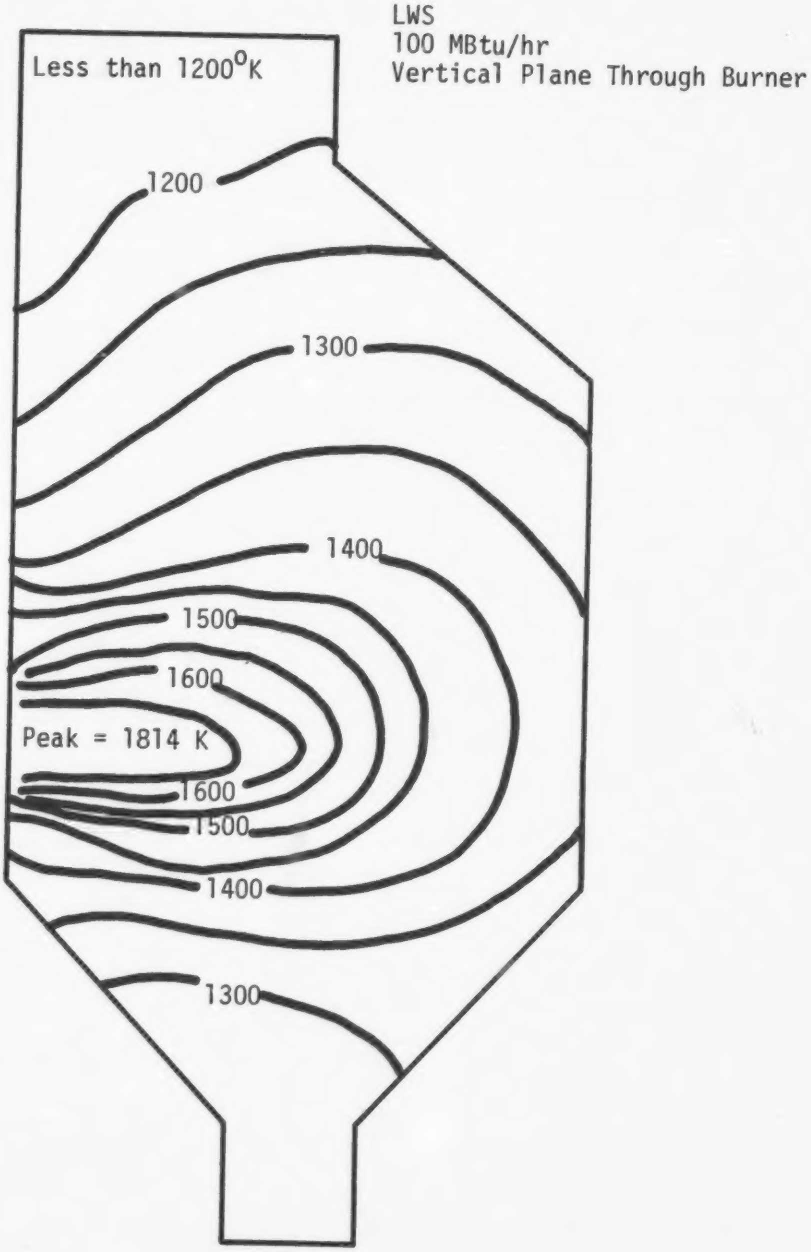
LWS
100 MBtu/hr
Vertical Plane Through Burner
Less than 1200°K
1200
1300
1400
1500
1600
Peak = 1814 K
1600
1500
1400
1300

Figure 9-13. LWS Temperature Profiles.

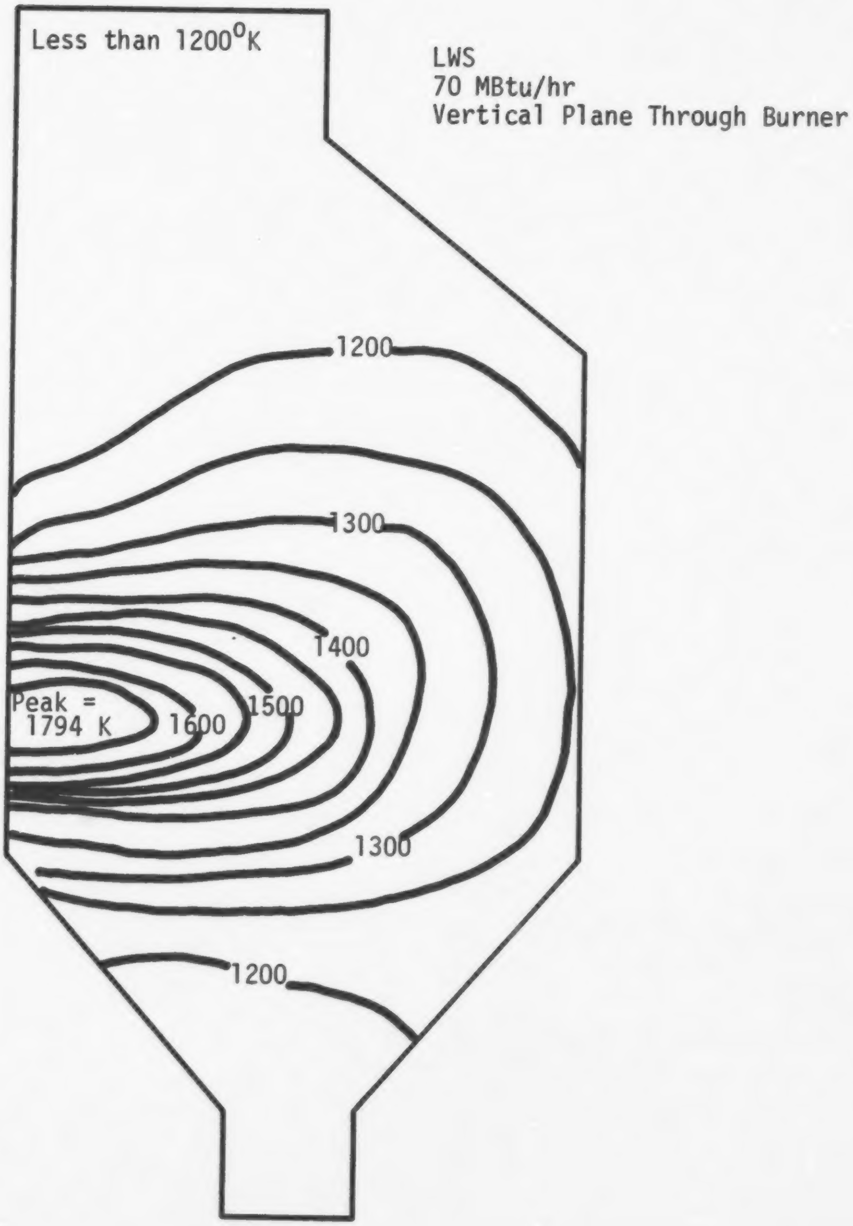
Less than 1200°K
LWS
70 MBtu/hr
Vertical Plane Through Burner
1200
1300
1400
Peak =
1794 K
1600
1500
1300
1200

Figure 9-14. LWS Temperature Profiles.

9.5.1 Approach

There are an infinite number of possible particle paths through a furnace with recirculating flow resulting in an infinite number of possible temperature histories. Selection of a single, or a manageable number, of representative temperature histories is not a simple problem. A statistical approach to the problem was chosen, similar in concept to the semi-stochastic radiative heat transfer model of the boiler performance code. A particle in a furnace zone is assumed to remain in that zone for the mean gas residence time at the mean gas temeprature. When the particle leaves the zone, the path that it takes is chosen at random, weighted by the probability density function for the gas flow vectors. A particle is followed from zone to zone until it exits the furnace. The assumption that the particle follows the gas stream should be fairly accurate for small, typical sorbent-size particles. Distributions of temperatures and residence times within a zone are not taken into account; however, use of a sufficiently fine zone grid should minimize any errors introduced by this approximation.

An idealized example of this technique is shown in Figure 9-15. A particle is injected into zone 1,1 of a 2 x 2 furnace. It remains there for the average residence time (the volume of the zone divided by the total volumetric flow through the zone) of 0.05 seconds at the average temperature of 1500°K. Half of the flow exiting zone 1,1 expands to zone 2,1 and half of the flow passes straight through to zone 1,2. With a 50/50 chance, random numbers determine that the particle follows the straight path to zone 1,2. It remains in zone 1,2 at 1400°K for .06 sec. Following the flow field, there is a 10 percent chance that turbulence will push the particle back into zone 1,1 and a 40 percent chance that the particle will continue straight and pass out of the furnace, but random numbers determine that the particle follows the most probable path and expands into zone 2,2. The particle remains in zone 2,2 at 1300°K for 0.07 seconds. From the probability density function for the exit flows, there is a 10 percent chance that turbulence will push the particle back into zone 1,2 and a 50 percent chance that the particle will follow the recirculation pattern into zone 2,1, but this time the random numbers defy the odds and the particle exits the furnace.

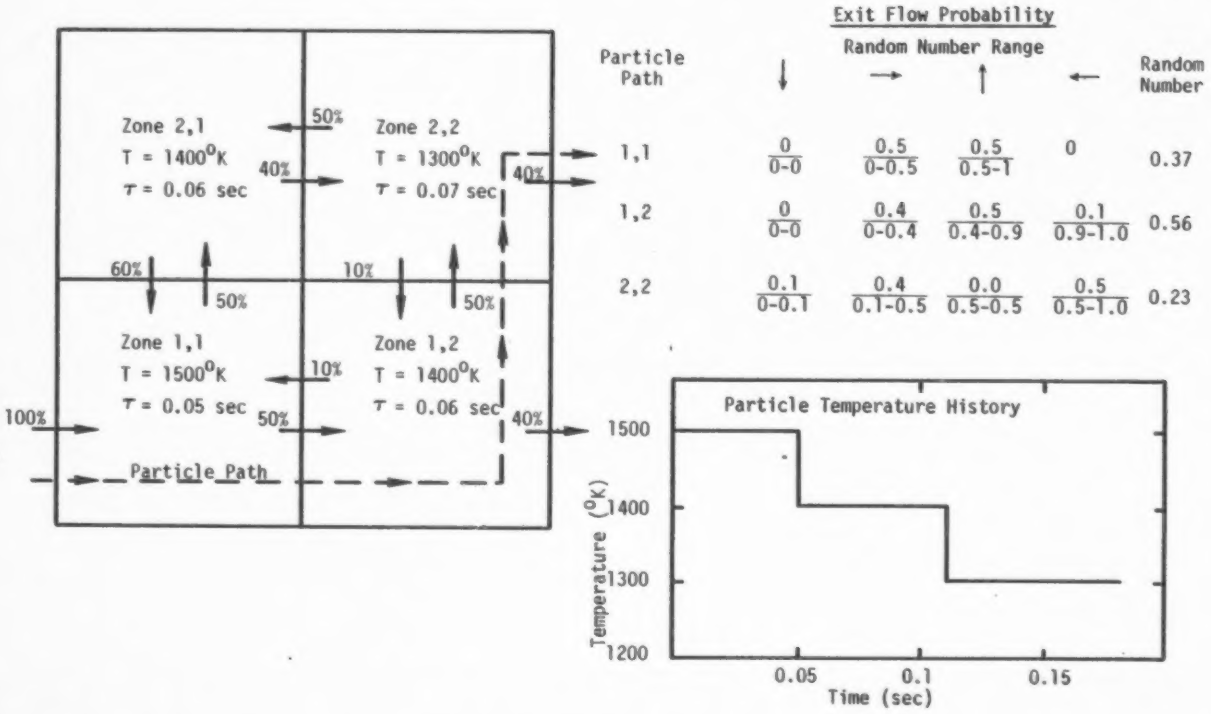
Zone 2,1
T = 1400°K
τ = 0.06 sec
Zone 2,2
T = 1300°K
τ = 0.07 sec
Zone 1,1
T = 1500°K
τ = 0.05 sec
Zone 1,2
T = 1400°K
τ = 0.06 sec
100%
50%
40%
60%
50%
10%
50%
10%
50%
40%
40%
Particle Path
Particle Temperature History
Temperature (°K)
1500
1400
1300
1200
0.05
0.1
0.15
Time (sec)

Exit Flow Probability

Particle Path	↓	→	↑	←	Random Number
	Random Number Range				
1,1	$\frac{0}{0-0}$	$\frac{0.5}{0-0.5}$	$\frac{0.5}{0.5-1}$	0	0.37
1,2	$\frac{0}{0-0}$	$\frac{0.4}{0-0.4}$	$\frac{0.5}{0.4-0.9}$	$\frac{0.1}{0.9-1.0}$	0.56
2,2	$\frac{0.1}{0-0.1}$	$\frac{0.4}{0.1-0.5}$	$\frac{0.0}{0.5-0.5}$	$\frac{0.5}{0.5-1.0}$	0.23

Figure 9-15. Particle Tracking Example.

If a large number of particles are tracked through a furnace, a representative sample of temperature histories is obtained. Unfortunately, the number of trackings required is too large to economically apply the sulfation model to each temperature history. Thus, some sort of statisitical manipulation is necessary.

Ten thousand particles were tracked through the temperature/flow map of the baseline SWS furnace model. The results are plotted in Figures 9-16 through 9-19. Mean particle temperature history is shown in Figure 9-16. The mean particle temperature at a given time is calculated from the local temperatures of all the particles which have been in the furnace for that period of time, independent of the path taken to reach that time/temperature. For the SWS, the average particle temperature reaches a peak of about 1575°K early then declines with time; however, due to the alternate paths which particles can follow, a wide range of possible temperatures exist for a particle at a given time. Thus, the standard deviation about the average temperature ranges from 100-200°K. The mean residence time in the SWS is around 3 seconds; however, due to recirculation and turbulence particle residence times range from 0.3 to 12.5 seconds as shown in Figure 9-17. These ranges in temperatures and residence times make it difficult to choose a single representative temperature history.

The motive for selecting a representative temperature history is to use it as an input to the sulfation model. Sorbent activation depends upon the peak particle temperature. Figure 9-18 shows the distribution of peak particle temperatures in the SWS as a cumulative probability plot. No particles have peak temperatures below 1530°K; half of the particles have peak temperatures below 1600°K; and all of the particles have peak temperatures below 1720°K. This curve can be used with an empirical correlation of surface area vs peak particle temperature such as Figure 5-2 to estimate an average particle surface area for the furnace. Figure 9-18 also plots the average time it takes for a particle to reach its peak temperature. This is of interest because particles which take a long time to reach their peak temperature may have undergone significant sulfation at lower, more active temperatures. Given the initial particle surface area, sorbent sulfation

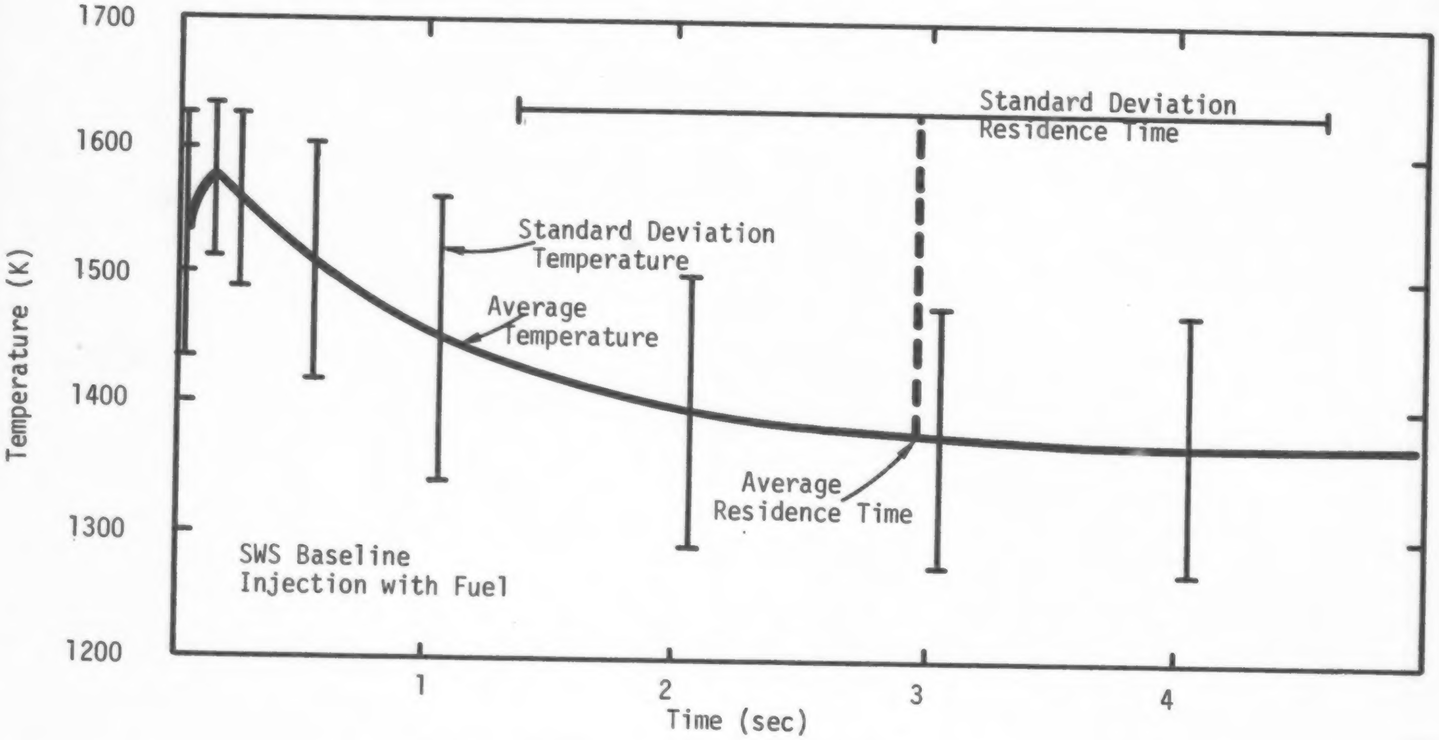

Figure 9-16. SWS Mean Particle Temperature History.

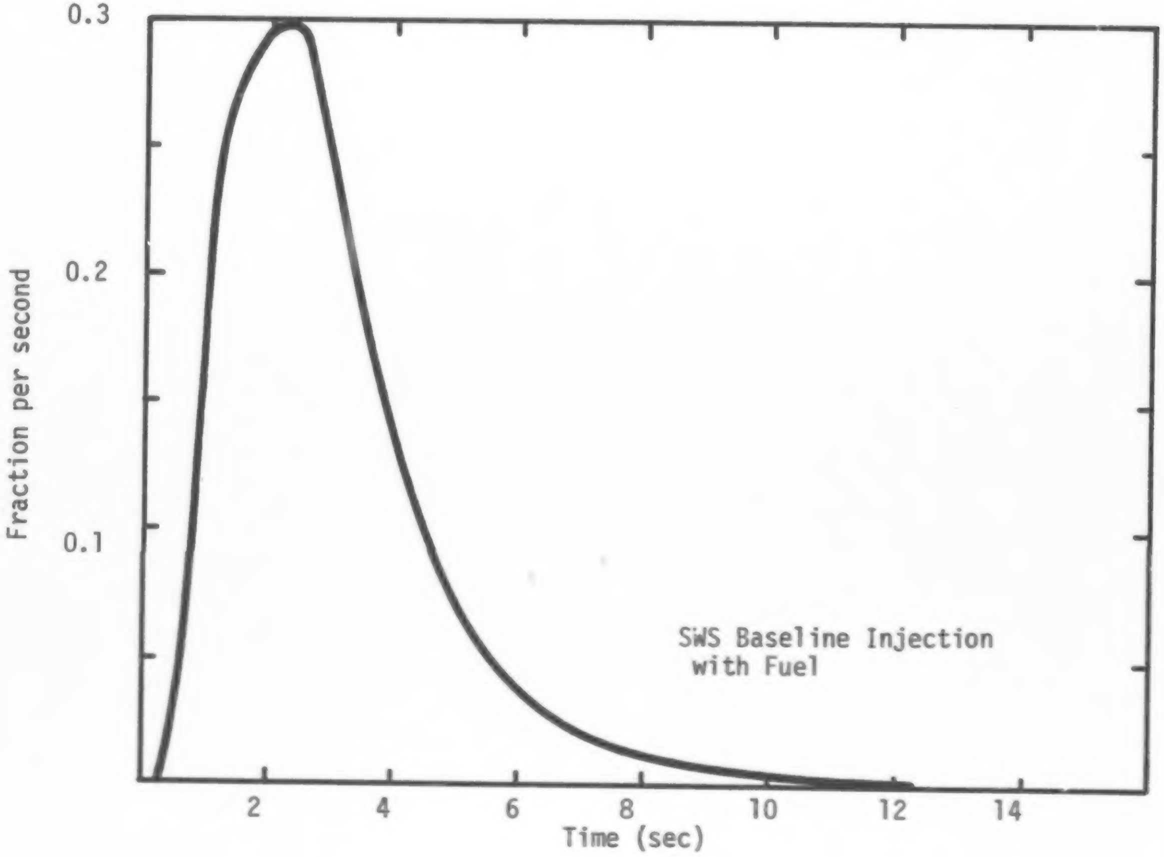

Figure 9-17. SWS Distribution of Particle Residence Times at Exit.

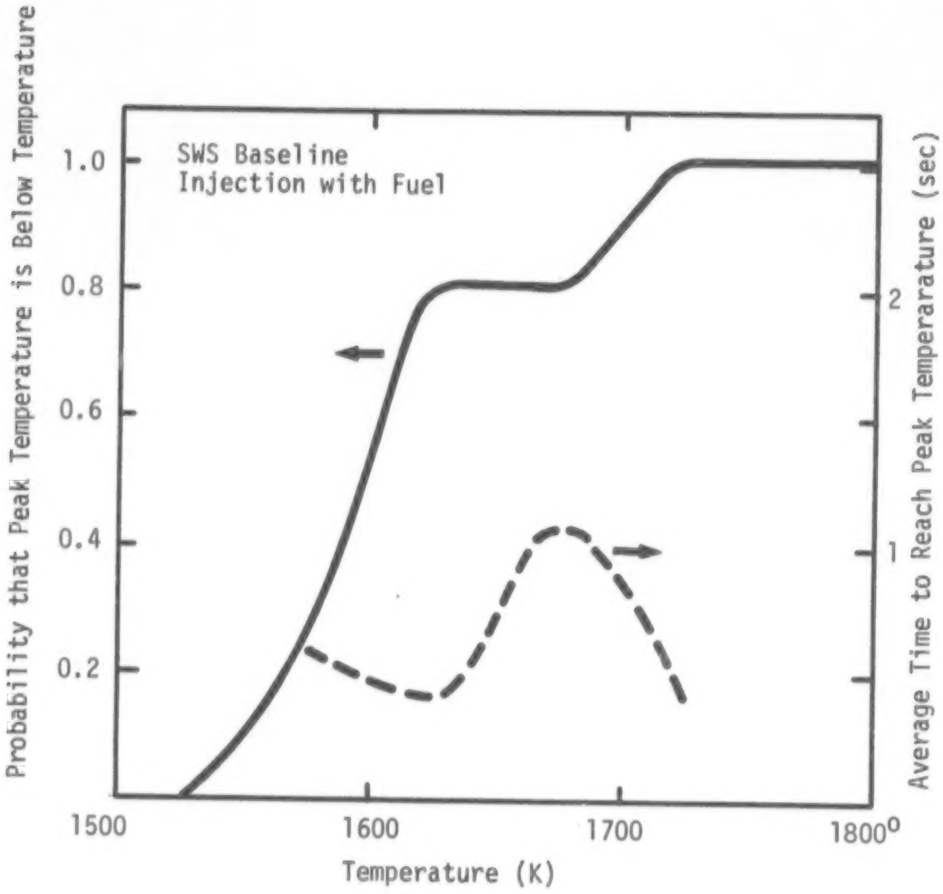

Figure 9-18. SWS Peak Particle Temperature Distribution.

depends upon the average time a particle spends at each temperature, but the actual path the particle takes is relatively unimportant. Thus, a cumulative probability plot of particle temperature distribution as shown in Figure 9-19, can be used to produce a typical temperature history. However, case studies have shown that it is adequate to use single mean particle temperature (below the equilibrium cut-off temperature for the sulfation reaction) over a single mean residence time (below the cut-off temperature).

To summarize the approach to combined thermal/sulfation modeling:

- The furnace heat transfer model is used to produce a temperature/flow map of the furnace.
- A large number of particles are tracked through the furnace, passing from zone to zone at random, weighted by the gas flow.
- The distribution of peak particle temperatures is used to calculate a mean particle surface area according to the sorbent activation correlation.
- The mean temperature and the mean residence time are used to calculate sulfation according to the sorbent sulfation model.

9.5.2 Results

The combined thermal/sulfation modeling approach was used on the SWS, MT, and LWS furnaces. The importance of assumptions inherent to the approach was investigated, and the results from the three furnaces were compared with each other and with results obtained applying the sulfation model to measured temperature profiles on the BSF.

Table 9-4 lists the baseline conditions used for the SWS. Typical temperature and sulfur capture profiles used for the SWS are shown in Figure 9-20. A mean particle surface area of 6.26 cm^2/cm^3 was calculated by applying

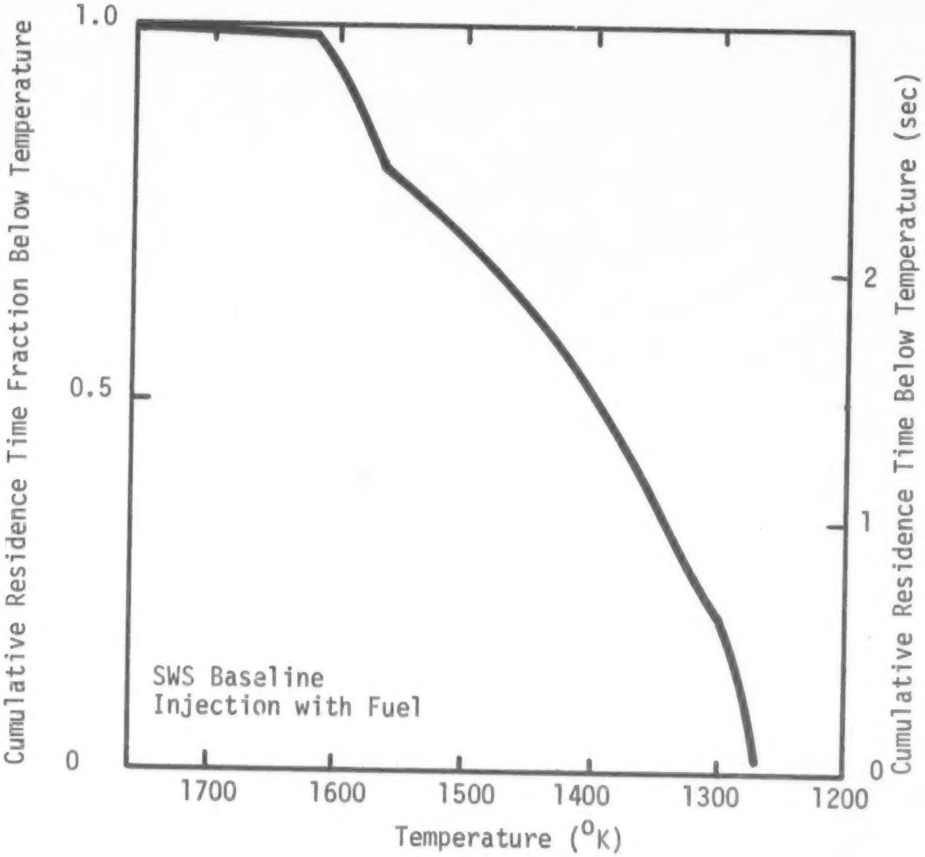

Figure 9-19. SWS Particle Temperature Distribution.

TABLE 9-4. SWS BASELINE CONDITIONS

Load = 10 MBtu/hr
Ca/S = 2.0
$[SO_2]$ = 2500 ppm
Equilibrium Cutoff Temperature = 2300^oF = 1533^oK
Particle Diameter = 5 μm

Furnace Exit Temperature = 1273^oK
Residence Time in Exit Duct = 1.72 sec
Temperature at Sample Port = 898^oK

	Injection with Fuel	Injection with Air
Mean Particle Temperature Below Cutoff Temperature	1372.4^oK	1372.0^oK
Mean Partial Residence Time Below Cutoff Temperature	2.21 sec	2.21 sec

Turbulence Factor = 0.2
Reverse Primary Recirculation = 1.0
Calcination = 97%
Porosity = 0.725
Density = 0.8257 g/cm^3
Sherwood Number = 2.0

Peak Temperature (K)	1575	1625	1675	1725
Fraction (Fuel Injection)	0.32	0.49	0.03	0.16
Fraction (Air Injection)	0.32	0.52	0.03	0.13
Surface Area (10^4 cm^2/cm^3)	7.27	6.11	5.37	4.87
Mean Pore Size (μm)	0.205	0.244	0.277	0.306
Pore Spread (decades)	0.1	0.1	0.1	0.1
Pore Length (10^8 cm/cm^3)	6.12	4.32	3.33	2.75

	Injection with Fuel	Injection with Air
Mean Surface Area (10^4 cm^2/cm^3)	6.26	6.30

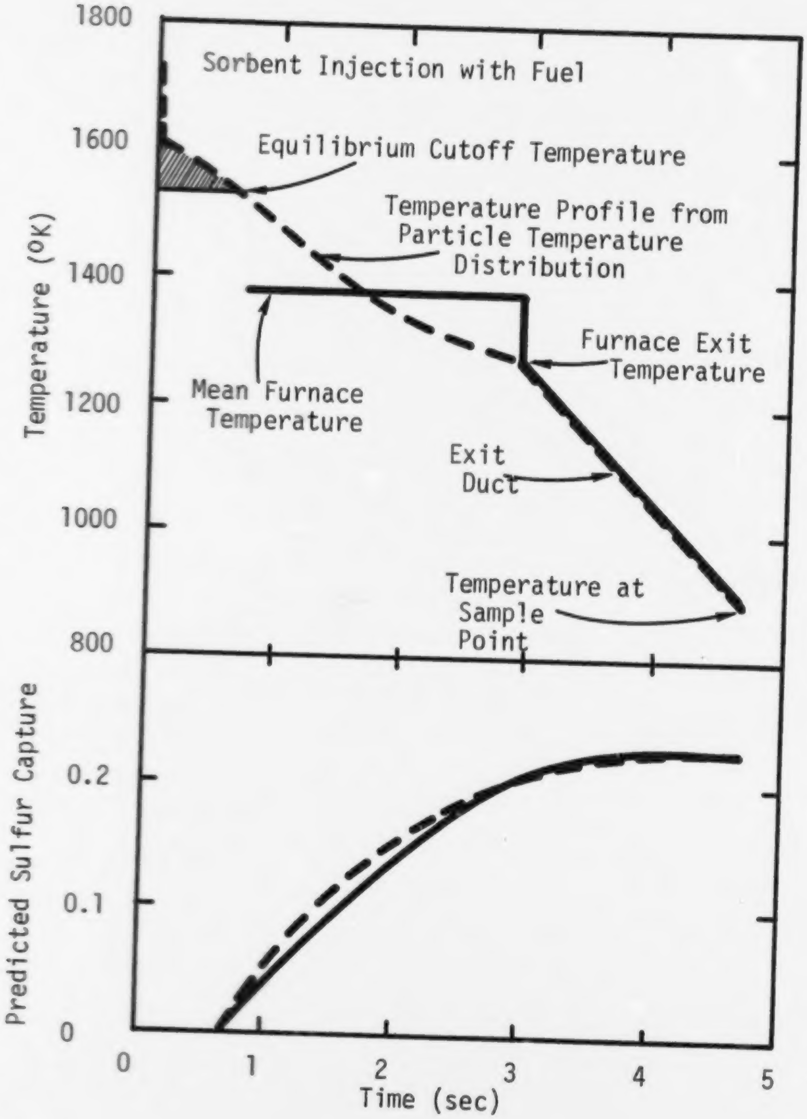

Figure 9-20. Sulfur Capture in SWS.

the peak particle temperature distribution of Figure 9-18 to the surface area vs peak particle temperature correlation of Figure 5-2. Sulfur capture was calculated for two temperature profiles. The solid lines of the figure utilize the mean furnace temperature (the standard approach) and the dotted lines utilize the more representative temperature distribution from Figure 9-19. In both cases, a linear temperature decline was assumed to occur in the exit duct between the measured temperatures at the furnace exit and the sample point. Sulfur capture for the two cases differed by less than 2 percent. Thus, utilizing mean furnace temperature rather than the actual temperature distribution appears to be an acceptable approximation.

Other SWS results are summarized in Table 9-5. Injection of sorbent with the air stream rather than the fuel stream caused an increase in sulfur capture of only 1 percent. The two cases had nearly identical mean furnace temperatures, but injection with the air stream caused a slight shift in peak particle temperature distribution resulting in a slightly higher surface area. Use of a single mean surface area (weighted by the peak particle temperature distribution) was compared with running a distribution of surface areas and weighting the resulting sulfur captures by the peak particle temperature. The results were identical, indicating that use of a single mean surface area is a reasonable approximation. Finally, use of a single mean residence time was compared to use of the distribution of residence times shown in Figure 9-17. Sulfur captures for the two cases were within 3 percent, indicating that the residence time distribution can be adequately replaced by a single mean residence time.

Baseline conditions for the MT calculations are listed in Table 9-6. The point of sorbent injection was more important for the MT than for the SWS. Figure 9-21 shows that an increase of 11 percent in sulfur capture resulted from injecting the sorbent with the tertiary air rather than the fuel. Injection with air resulted in a higher particle surface area because a larger percent of the particles bypassed the hotter zones of the furnace. This was more significant in the MT due to its sharp radial temperature gradient shown in Figure 9-8.

TABLE 9-5. SULFUR CAPTURE IN SWS

INJECTION	SURFACE AREA	RESIDENCE TIME	TEMPERATURE PROFILE	CAPTURE
Fuel	Average	Average	Average	0.232
Fuel	Average	Average	Distribution	0.228
Fuel	Average	Distribution	Average	0.227
Fuel	Distribution	Average	Average	0.232
Air	Average	Average	Average	0.234

TABLE 9-6. MT BASELINE CONDITIONS

Load = 50 MBtu/hr
Ca/S = 2.0
$[SO_2]$ = 2500 ppm
Equilibrium Cutoff Temperature = $2300^{o}F$ = $1533^{o}K$
Particle Diameter = 5 μm

Furnace Exit Temperature = $1478^{o}K$
Residence Time in Exit Duct = 1.94 sec
Temperature at Sample Port = $944^{o}K$

	Injection with Fuel	Injection with Air
Mean Particle Temperature Below Cutoff Temperature	$1469.8^{o}K$	$1471.2^{o}K$
Mean Partial Residence Time Below Cutoff Temperature	3.17 sec	3.26 sec

Turbulence Factor = 0.2
Reverse Primary Recirculation = 1.0
Calcination = 97%
Porosity = 0.725
Density = 0.8257 g/cm^3
Sherwood Number = 2.0

Peak Temperature (K)	1550	1650	1750	1850
Fraction (Fuel Injection)	0.62	0.01	0.19	0.18
Fraction (Air Injection)	0.83	0.02	0.08	0.07
Surface Area (10^4 cm^2/cm^3)	8.09	5.70	4.54	3.88
Mean Pore Size (μm)	0.184	0.261	0.328	0.384
Pore Spread (decades)	0.1	0.1	0.1	0.1
Pore Length (10^8 cm/cm^3)	7.58	3.77	2.38	1.74

	Injection with Fuel	Injection with Air
Mean Surface Area (10^4 cm^2/cm^3)	6.63	7.49

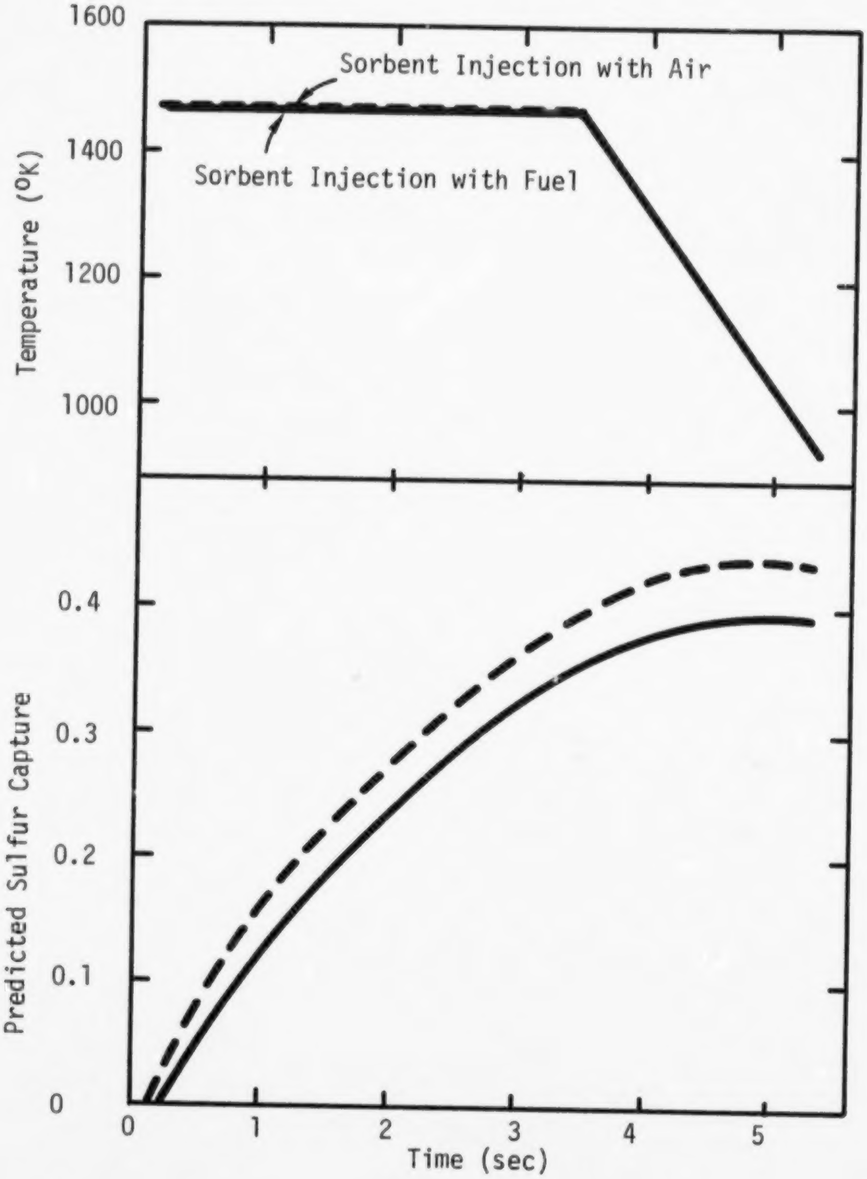

Figure 9-21. Sulfur Capture in MT.

TABLE 9-7. SULFUR CAPTURE IN MT

Injection	Turbulence Factor[*]	Reverse Primary Recirculation Factor[**]	Capture
Fuel	0.2	1.0	0.392
Fuel	0.0	1.0	0.393
Fuel	0.0	0.0	0.391
Air	0.2	1.0	0.435
Air	0.0	1.0	0.446
Air	0.0	0.0	0.445

[*] Turbulent Mass Flow = Total Input Mass Flow x $\frac{\text{Cross Sectional Area of Zone}}{\text{Cross Sectional Area of Burner}}$ x Turbulence Factor

[**] Reverse Primary Recirculation Mass Flow = Reverse Primary Recirculation Factor x Primary Input Mass Flow

TABLE 9-8. LWS BASELINE CONDITIONS

Load = 100 MBtu/hr

Ca/S = 2.0

$[SO_2]$ = 2500 ppm

Equilibrium Cutoff Temperature = $2300^{\circ}F$ = $1533^{\circ}K$

Particle Diameter = 5 μm

Furnace Exit Temperature = $1199^{\circ}K$

Residence Time in Exit Duct = 1.08 sec

Temperature at Sample Port = $1075^{\circ}K$

	Injection with Fuel	Injection with Air
Mean Particle Temperature Below Cutoff Temperature	$1326.3^{\circ}K$	$1323.6^{\circ}K$
Mean Partial Residence Time Below Cutoff Temperature	7.12 sec	7.17 sec

Calcination = 97%

Porosity = 0.725

Density = 0.8257 g/cm^3

Sherwood Number = 2.0

Peak Temperature (K)	1375	1425	1475	1525	1575
Fraction (Fuel Injection)	0.0	0.03	0.07	0.49	0.41
Fraction (Air Injection)	0.03	0.09	0.22	0.45	0.21
Surface Area (10^4 cm^2/cm^3)	20.64	14.37	10.98	8.58	7.27
Mean Pore Size (μm)	0.072	0.104	0.136	0.174	0.205
Pore Spread (decades)	0.1	0.1	0.1	0.1	0.1
Pore Length (10^8 cm/cm^3)	49.29	23.91	13.96	8.52	6.12

	Injection with Fuel	Injection with Air
Mean Surface Area (10^4 cm^2/cm^3)	8.38	9.72
Sulfur Capture	0.486	0.535

Other MT results are summarized in Table 9-7. Turbulence and reverse primary recirculation are two of the major uncertainties in flow field input to the furnace heat transfer model. Both are very simple relations based more on engineering intuition than on theoretical considerations. The effect of these two parameters, independent of temperature, was investigated by changing the flow field input to the particle tracking portion of the combined thermal/sulfation model for the MT. Changing the turbulence factor from the baseline value of 0.2 to 0, representing no turbulence, caused very little change in sulfur capture for sorbent injection with the fuel, and caused less than a 3 percent increase in sulfur capture for sorbent injection with the tertiary air. The increase in capture with decreasing turbulence in the air injection case was due to a slight increase in surface area as turbulent exchange was eliminated between the cooler injection zones and the hotter core of the furnace. However, the increase is small, indicating that, apart from its effect on temperature profiles, turbulence is relatively unimportant. Similarly, elimination of reverse primary recirculation had very little effect on predicted sulfur capture.

Baseline conditions for the LWS calculations are listed in Table 9-8 along with sulfur capture results for fuel and air sorbent injection. The LWS, as shown in Figure 9-13, has sharp temperture gradients around the burner. Thus sorbent particles injected with the tertiary air are likely to reach lower peak temperatures than those injected with the fuel. As a result, 10 percent higher capture was predicted for the tertiary air sorbent injection case as shown in Figure 9-22.

The sulfation model was applied to the BSF for measured temperature profiles under baseline conditions outlined in Table 9-9. These results were compared with results using an average furnace temperature. Ultimate sulfur capture was the same in both cases, also shown in Table 9-9.

Effects of scale were investigated by comparing sulfur capture predictions for the four furnaces under baseline conditions for sorbent injection with the fuel with results shown in Figure 9-23. The three parameters which primarily affect sulfur capture are temperature, surface area

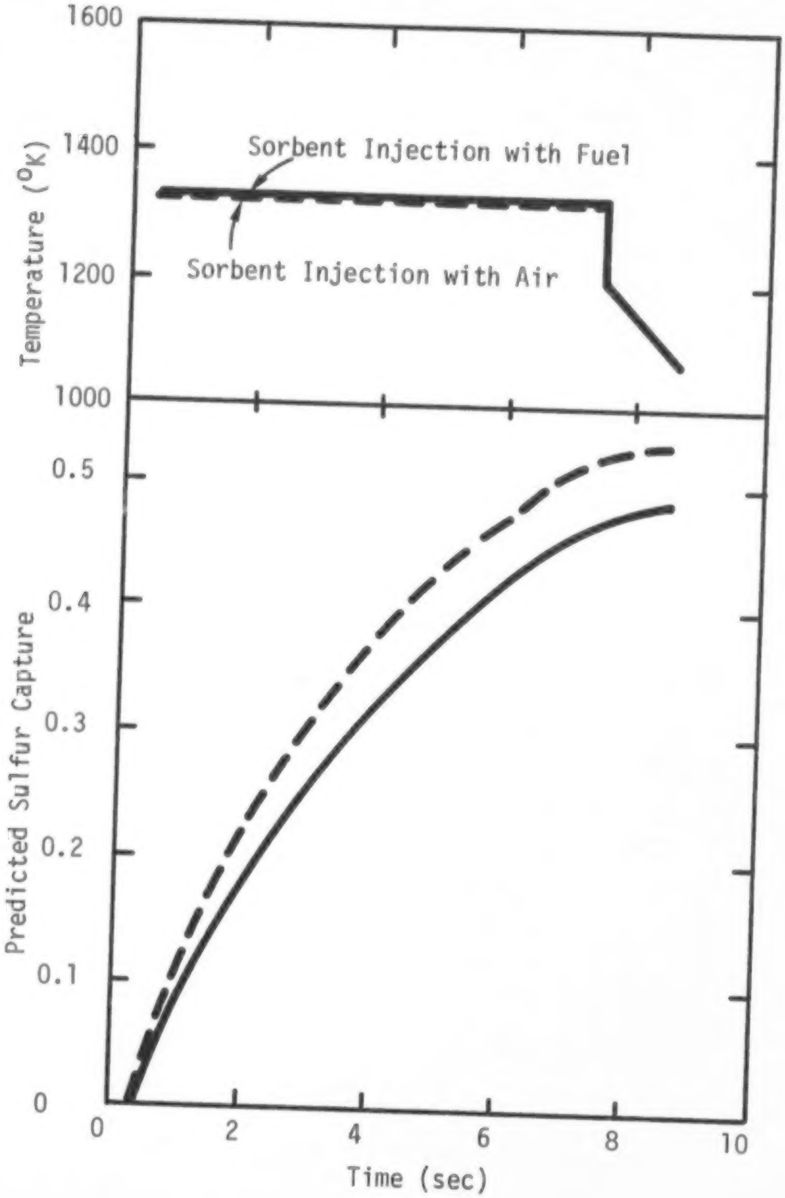

Figure 9-22. Sulfur Capture in LWS.

TABLE 9-9. BSF BASELINE CONDITIONS

Load = 1 MBtu/hr
Ca/S = 2.0
$[SO_2]$ = 2500 ppm
Equilibrium Cutoff Temperature = 1533°K
Particle Diameter = 5 μm
"Furnace" Exit Temperature = 1383°K
Residence Time in 1st Exit Section = 0.8 sec
Temperature at End of 1st Exit Section = 1117°K
Residence Time in 2nd Exit Section = 0.9 sec
Temperature at Sample Port = 656°K
Mean Particle Temperature Below Cutoff Temperature = 1427°K
Mean Particle Residence Time Below Cutoff Temperature = 1.25 sec
Plug Flow Calcination = 97%
Porosity = 0.725
Density = 0.8257 g/cm^3
Sherwood Number = 2.0
Peak Temperature (°K) = 1839
Surface Area (10^4 cm^2/cm^3) = 3.88
Mean Pore Size (μm) = 0.384
Pore Spread (decades) = 0.1
Pore Length (10^8 cm/cm^3) = 1.74

Fractional Sulfur Capture:

Temperature Profile	Capture
Measured	0.126
Average	0.126

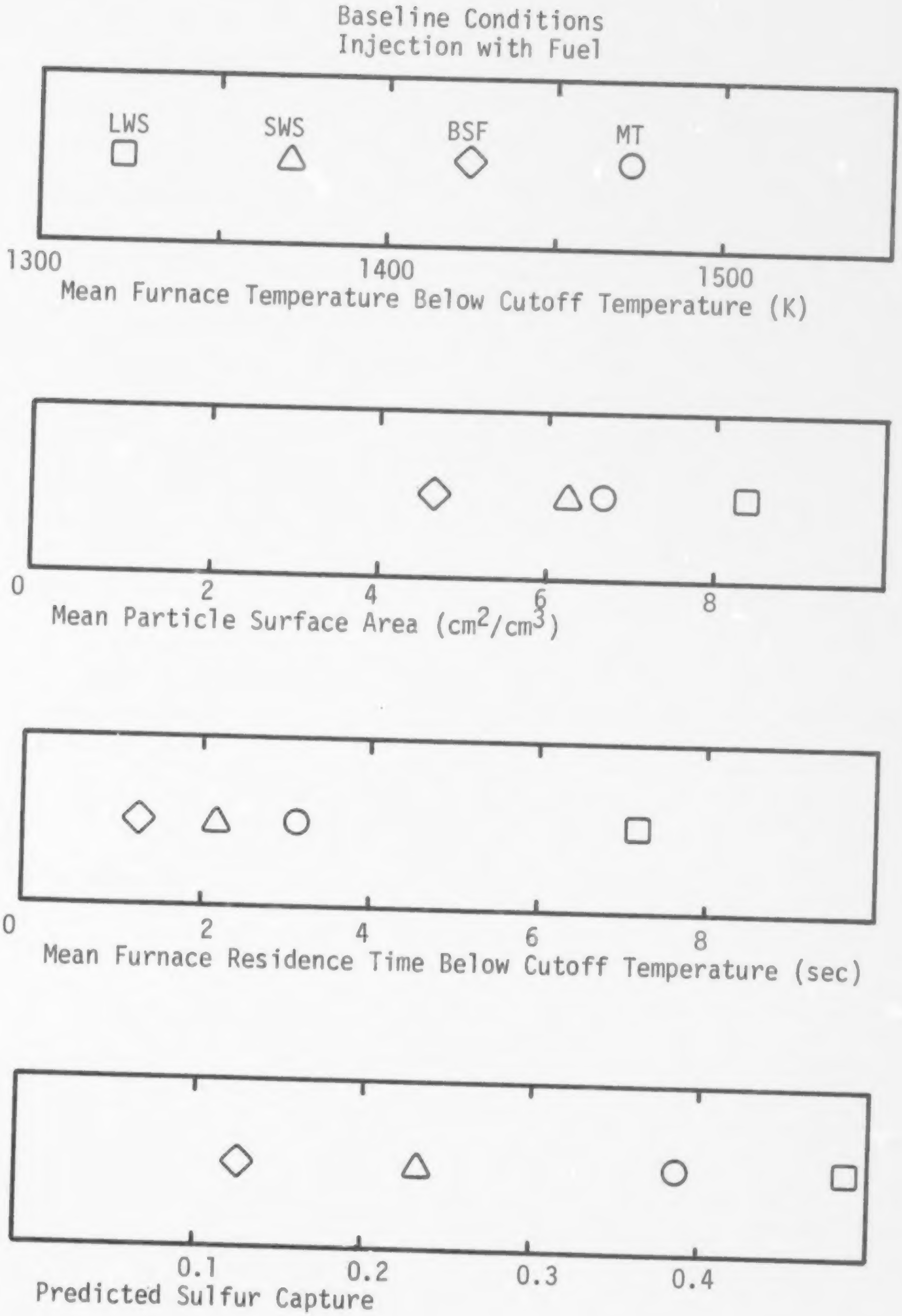

Figure 9-23. Furnace Comparison.

and residence time. Averaging techniques, as previously described, were used for these three parameters for each furnace. The predicted sulfur capture of 44 percent for the LWS was highest due to its long residence time and high surface area which more than offset its low mean temperature. Sulfur capture of 39 percent was predicted for the MT, still fairly high, due to its high mean temperature, but relatively flat temperature profile resulting in a fairly high surface area. The SWS had a predicted sulfur capture of only 23 percent. Its average temperature was cool, but its peak temperatures were not, so its mean surface area was not high. The 13 percent capture predicted for the BSF was the lowest. The BSF had highest peak temperature resulting in the lowest surface area and it had the shortest residence time.

The major conclusion which can be reached on the basis of this furnace comparison is that the optimum conditions for sulfur capture are long residence time and constant temperature low enough so that deadburning is minimized, but not so low that calcination or sulfation is slowed significantly.

10.0 SYSTEM EFFECTS

Although the LIMB process is conceptually simple, sulfur capture can be affected by so many variables that actual analysis of the process and prediction of results is very complex. In addition to the effects due to fuel and sorbent characteristics, sorbent location and injection method and furnace operating conditions (all of which have been discussed in previous chapters) the firing/boiler system itself has an effect on sulfur capture. System effects are due to different thermal, mixing and residence time characteristics of different facilities. The effects of these variables are difficult to separate, although judicious application of modeling procedures (as described in Chapter 9) is of some help in analysis of system effects.

The fuel sorbent pairs tested in the Boiler Simulator Furnance were selected, in part, in order to provide a basis for comparison of various firing systems. Testing of the sorbent injection concept in pilot-scale facilities - including the SWS, LWS and MT with various burners is currently in progress. A comparison of some of the available data is of interest.

The BSF system is described in detail in Appendix A. The pilot-scale facilities are described in other reports primarily: Payne, et al., 1983. The Large Watertube Simulator (LWS) was used for several sets of pilot-scale tests. Figure 10-1 shows a schematic of the LWS and summarizes the facility characteristics.

Two coals commonly used for pilot-scale tests are Indiana and Utah. The Indiana coal is a medium-sulfur eastern bituminous coal which has a characteristically varying sulfur content (from 1.0 - 3.5 percent S) from batch to batch. The Utah coal is considerably more consistant in composition.

A comparison of the LWS and BSF systems can be made by comparing data obtained from similar firing schemes using the same fuel and sorbent. Figure 10-2 a and b shows such a comparison. The LWS was fired at 100 MBtu/hr using a distributed mixing type burner, staged, with Vicron 45-3 injected through the mill with the fuel. The BSF was fired at 1.0 MBtu/hr using the subscale

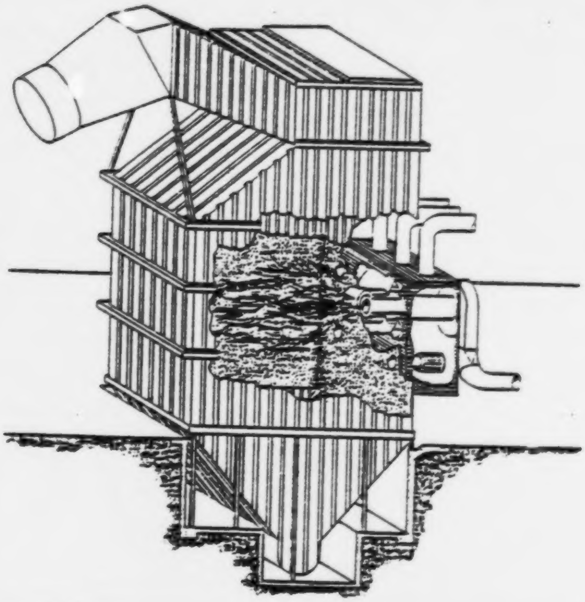

Parameter		Value	
Firing			
Configuration	Primary	Single Wall	
	Optional	Opposed or Corner	
Firing Rate	Minimum	50×10^6 Btu/hr	
	Maximum	150×10^6 Btu/hr	
Dimensions			
Firing Depth		22 ft.	
Width		16 ft.	
Rear Wall Height		20 ft.	
Knuckle-to-Nose Height		27.5 ft.	
Nose Angle		37^o (from horizontal)	
Hopper Angle		52^o (from horizontal)	
Height Above Ground Level		35.7 ft.	
Total Vertical Height		50.5 ft. (pit to top)	
Cooled Surface Area			
Burner Zone		704 ft.^{2}	
Total Furnace		1951 ft.^{2}	
Volume			
Burner Zone		3520 ft.^{3}	
Total Furnace		11,544 ft.^{3} (to nose)	
Insulation		All Sidewalls knuckle-up 16 ft.	
Cooling		Spray-cooled on all surfaces	
Thermal Environment			
Heat Release/Cooled Surface		213,068 Btu/hr ft^2	In burner zone at maximum firing rate
Heat Release/Volume		42,614 Btu/hr ft^3	

Figure 10-1. Characteristics of the LWS Test Furnace.

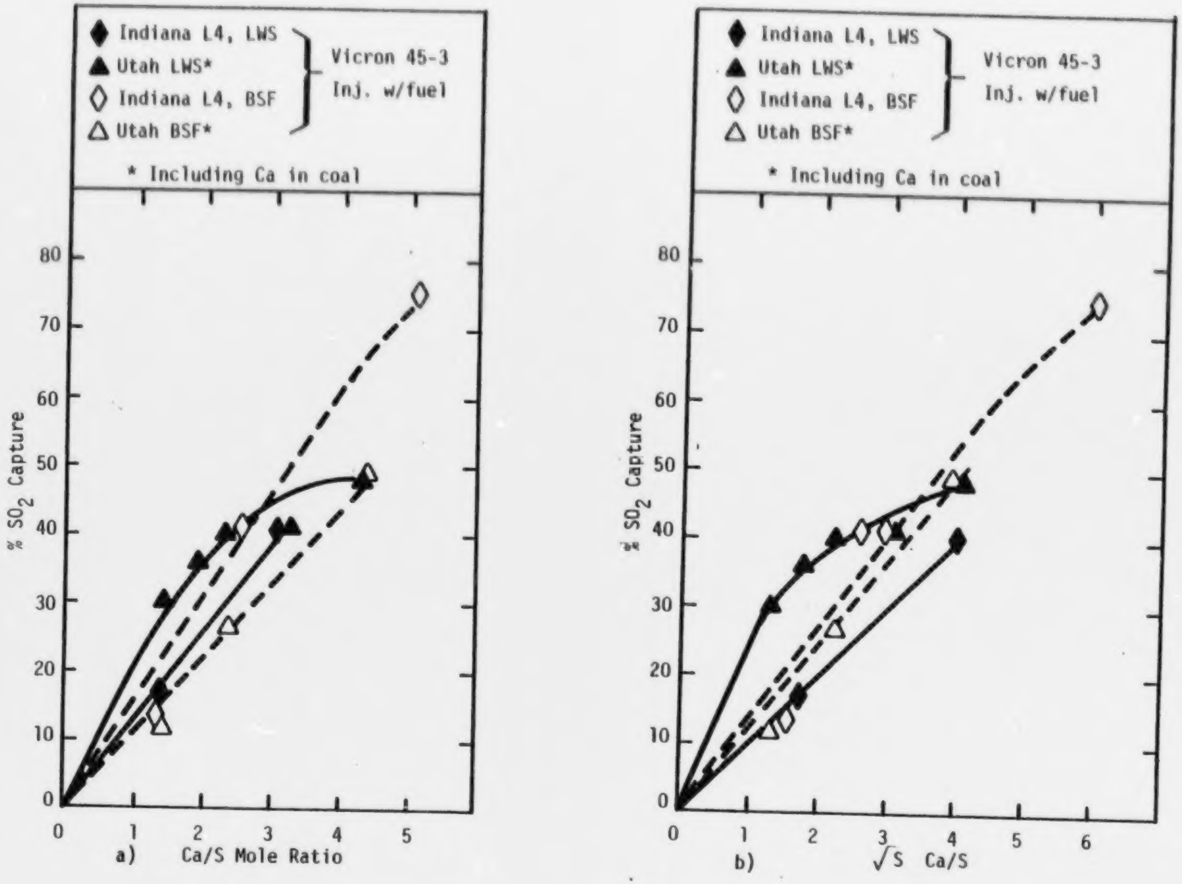

Figure 10-2. Effect of Firing system on sulfur capture, Vicron 45-3 with two fuels in LWS and BSF.

distributed mixing burner, staged with Vicron 45-3 injected with the fuel. Figure 10.2a shows sulfur capture by Vicron 45-3 as a function of Ca/S ratio for two coals in the two furnaces. The Indiana (lot 4) coal had 1.9 percent S and the Utah coal had .9 percent S.

In earlier pilot-scale studies, multiplying the calcium-to-sulfur ratio by the square root of the coal sulfur content was effective in eliminating some of the apparent effect of fuel sulfur content on sulfur capture (Payne, et al. 1982). Figure 10.2b shows this correlation applied to the BSF and LWS data. Data from the BSF with the two fuels becomes very comparable while the fuel effect in the LWS is exaggerated. Clearly some property or set of properties of the two systems, aside from fuel or fuel sulfur content, has an effect on sorbent injection performance.

The analysis performed on the two systems using thermal and sulfation models (Chapter 9) indicated that all other things being equal (fuel sorbent interactions, ash interference, mixing, etc) capture in the LWS was better than in the BSF. This appears to be the case for the Utah coal, but not for the Indiana. The modeling/analysis method cannot take account of ash and /or sorbent distribution effects. This may account for the difference between observed and expected system effects.

11.0 EFFECT OF SORBENT INJECTION ON BOILER OPERATING CHARACTERISTICS

The injection of significant amounts of dry sorbent into a boiler is bound to have an impact on the boiler performance characteristics and may, indeed, affect boiler availability. Information on these "side effects" of sorbent injection is scattered through the documentation of various pilot and demonstration studies, as these effects have not been the primary focus of any investigations. The effect of sorbent addition on furnace heat transfer characteristics, including temperature and emissivity of the flame and furnace walls, as well as changes in slagging and fouling characteristics of the particulate, are of primary interest.

In addition to affecting boiler operational characteristics, sorbent injection will affect the flue-gas cleaning systems associated with the boiler. Sorbent injection will increase solids loading to the particulate removal system and will probably affect the solid particle size distribution and ash resistivity. These changes will have an impact on any electrostatic precipitator associated with the boiler and may affect baghouse and/or scrubber operating characteristics. This section briefly reviews the available data on the effect of sorbent injection on boiler and flue gas cleaning systems. The results of a brief set of experiments addressing LIMB-ash characteristics which were performed in the BSF are described.

11.1 Review: Effects on Boiler Operating Characteristics

11.1.1 Effect on Slagging and Fouling

The effects of sorbent injection on ash slagging and fouling characteristics have been described in reports of several of the larger-scale sorbent injection studies, including: TVA (Shawnee), Babcock and Wilcox, RWE, and Hoot Lake (DOE/Radian). Long-term tests of sorbent injection at TVA resulted in superheater plugging problems. The problems persisted in spite of increased soot blowing, necessitating two outages to clean the reheater tubes after excessive pressure drops across the reheater developed. Excessive, difficult to remove deposits were generally confined to the first rows (6 or so) of tubes in the reheater banks. The close tube spacing and fluxuations in sorbent injection rate were held responsible for much of the plugging problem No problems with waterwall slagging or air heater plugging were reported.

The effect of sorbent addition on ash sinter strength (and therefore, at least qualitatively, difficulty in soot blowing) and ash fusion temperatures was briefly investigated by B & W. For the fuels used, addition of sorbent up to 30-40 percent in coal ash, the sorbent reduced the ash fusion temperatures - higher concentrations may increase fusion temperatures. In most cases sorbent addition was found to reduce ash sinter strength, though the effect was again dependent on ash composition and sorbent concentration. Any wetting of the ash sorbent mixture resulted in catastropic, cement or plaster-like hardening of the deposits.

Lignite-fired power plants are typically designed with larger fire boxes and wider tube spacing because of the lower heating values and fouling tendencies of lignite coals. Reports of studies of sorbent injection with lignite coals indicate higher solids loading and deposition rates, but no plugging of air heater or reheater sections and no increased difficulty in soot blowing and ash removal (RWE, Hoot Lake). In fact, limestone (or other alkali) is occasionally added to high-sodium fouling-prone lignite coals to reduce fouling problems. Alkali addition "softens" the deposits on boiler tubes, making them easier to remove by soot blowing.

11.1.2 Effect on Mill Performance and Power Usage

Limestone was added to the lignite fuel before pulverization in some of the tests at Hoot Lake. An increase in mill power consumption, as high as 11 percent, was observed during the sorbent injection periods. The observed power/capacity requirement increase was judged significant; in fact the problem is likely to be worse for higher sulfur bituminous plants as the mills for lignite-fired plants are generally sized for higher and wider variations in capacity than other plants. It is likely that many power plants will not have sufficient pulverizer capacity to grind coal limestone mixtures. In spite of the observed power increase, and the available capacity of the mills at the Hoot Lake Station, the pulverizers apparently could not adequately grind the limestone to a consistently small particle size. This implies that LIMB may require special pulverizers (or pre-pulverized limestone) for the sorbent.

11.1.3 Effect on Particulate

Possibly the most worrisome impact of sorbent injection on boiler performance is the effect of increased solids loading and changed particulate characteristics. The increase in solids loading is directly dependent on the fuel sulfur level and level of SO_2 removal required. Both affect sorbent injection rate and, therefore, solids loading. The increased solids loading alone would require larger particulate collection and handling capacity, however, sorbent injection affects effluent particulate properties and, therefore, may also affect collector efficiency.

The available information indicates that effluent particle size distribution with added sorbent is only slightly affected by the sorbent and can be reasonably well predicted form the normal ash size distribution and the input sorbent size distribution. Figures 11-1 and 11-2 show size distributions for ash and ash plus sorbent mixtures measured at two sites (TVA and Detroit Edison). Mean size of ash without sorbent addition slightly reduced mean particle size.

Fly ash resistivity is a function of several factors, including flue gas temperature, SO_3 concentration, solids composition, and ash thermal history; therefore, measurements of solids resistivity with and without added alkali sorbents are widely scattered. The only firm conclusion about the effect of sorbent addition on ash resistivity is that added sorbents generally increase resistivity. Figure 11-3 shows collected data on ash resistivity as a function of flue gas temperatures for a range of test conditions in several furnaces. The open area includes resistivities measured with sorbent addition. Figures 11-4 and 11-5 show resistivities measured at TVA for various coal sulfur contents with and without sorbent addition. The data are scattered but generally high sulfur content decreased resistivity and sorbent

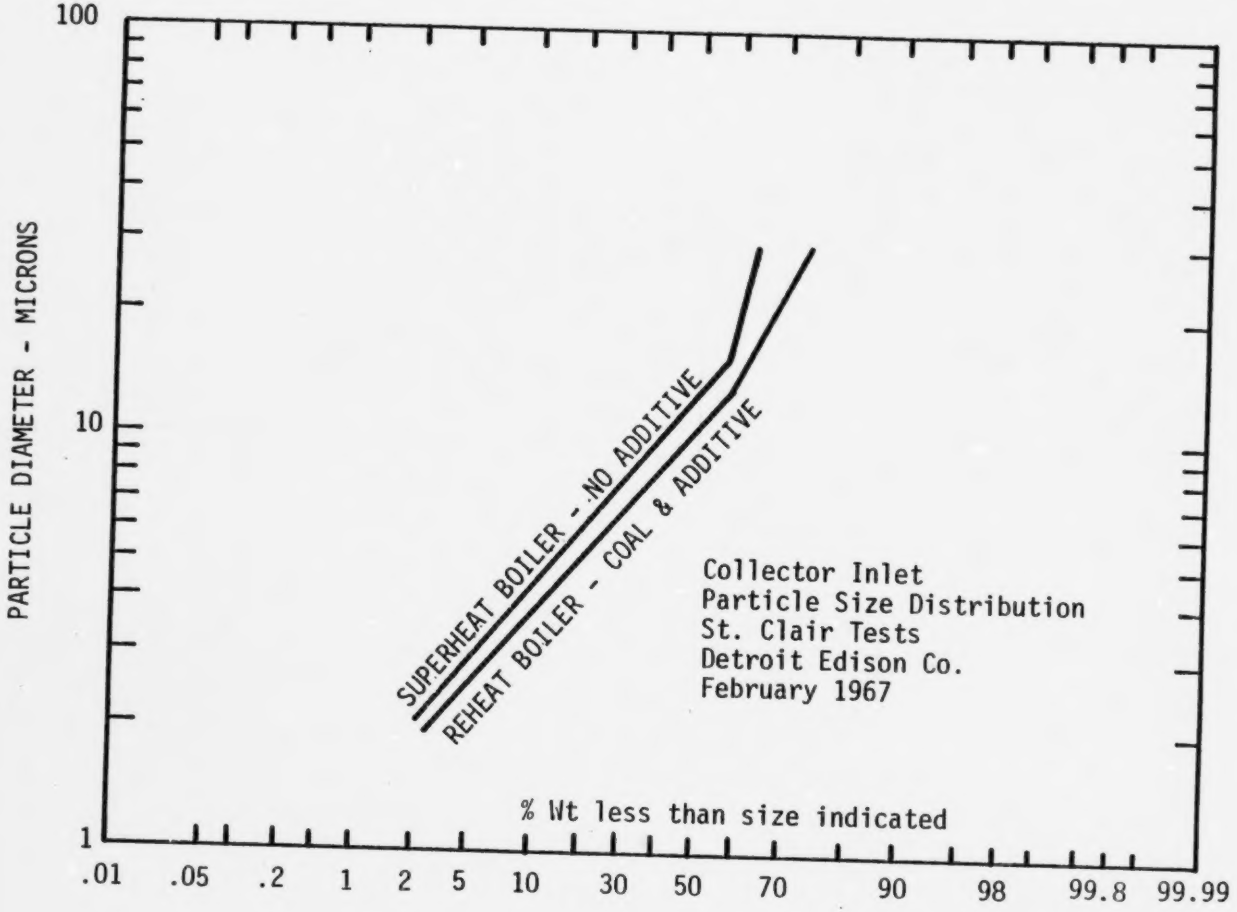

Figure 11-1. Size Distribution with and without added Sorbents; Detroit Edison Tests

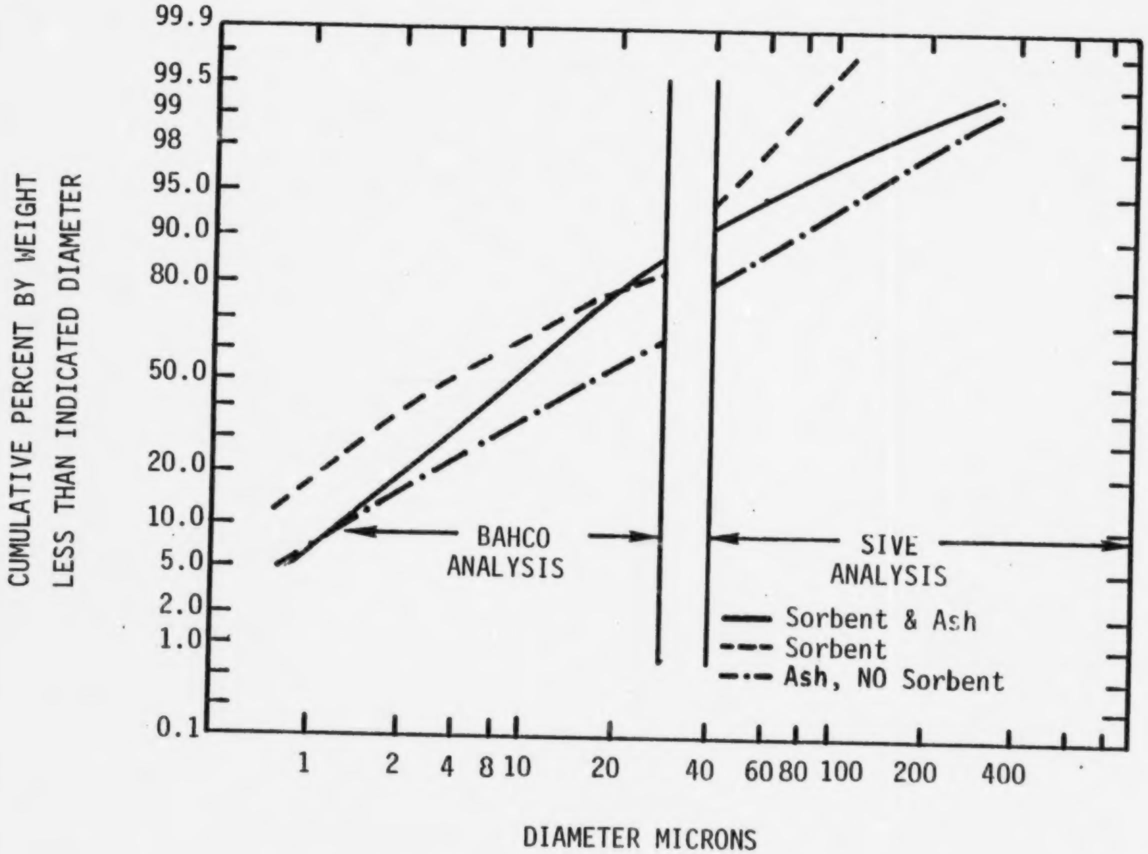

Figure 11-2. TVA Shawnee
Effect of limestone injection on
particle size - inlet of collector.

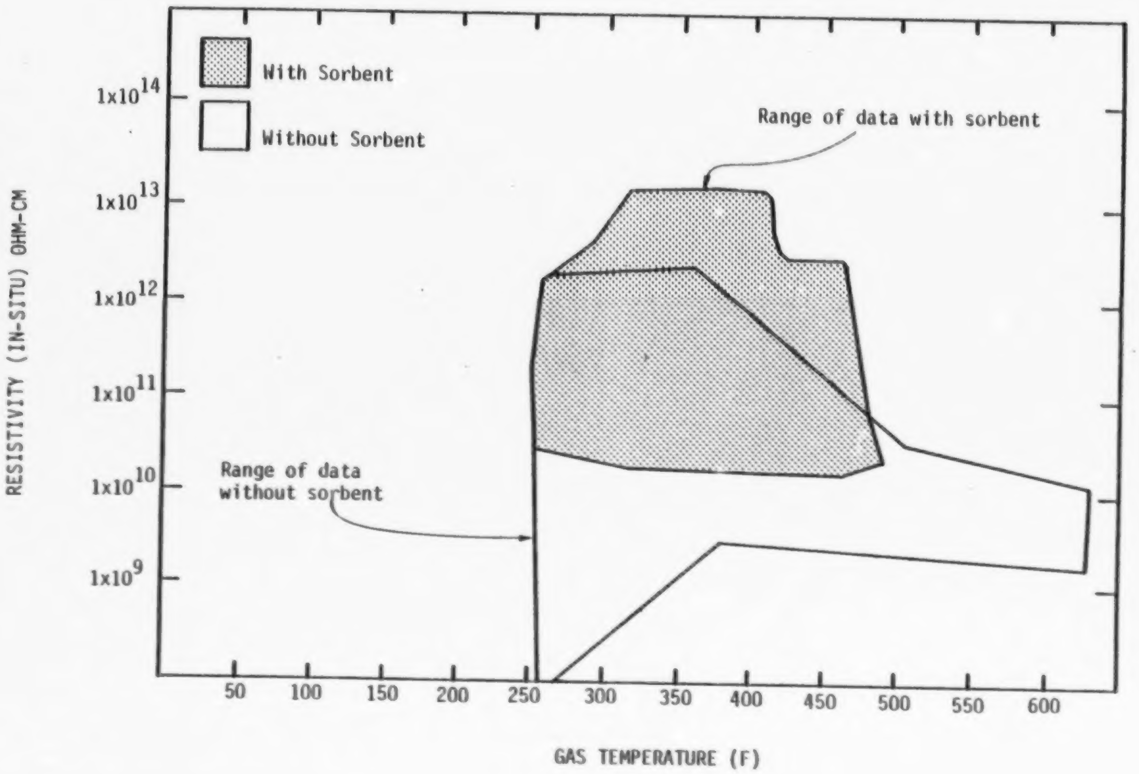

Figure 11-3. Effect of sorbent on fly ash resistivity TVA Shawnee, B & W - Pilot and Detroit Edison - St. Clair.

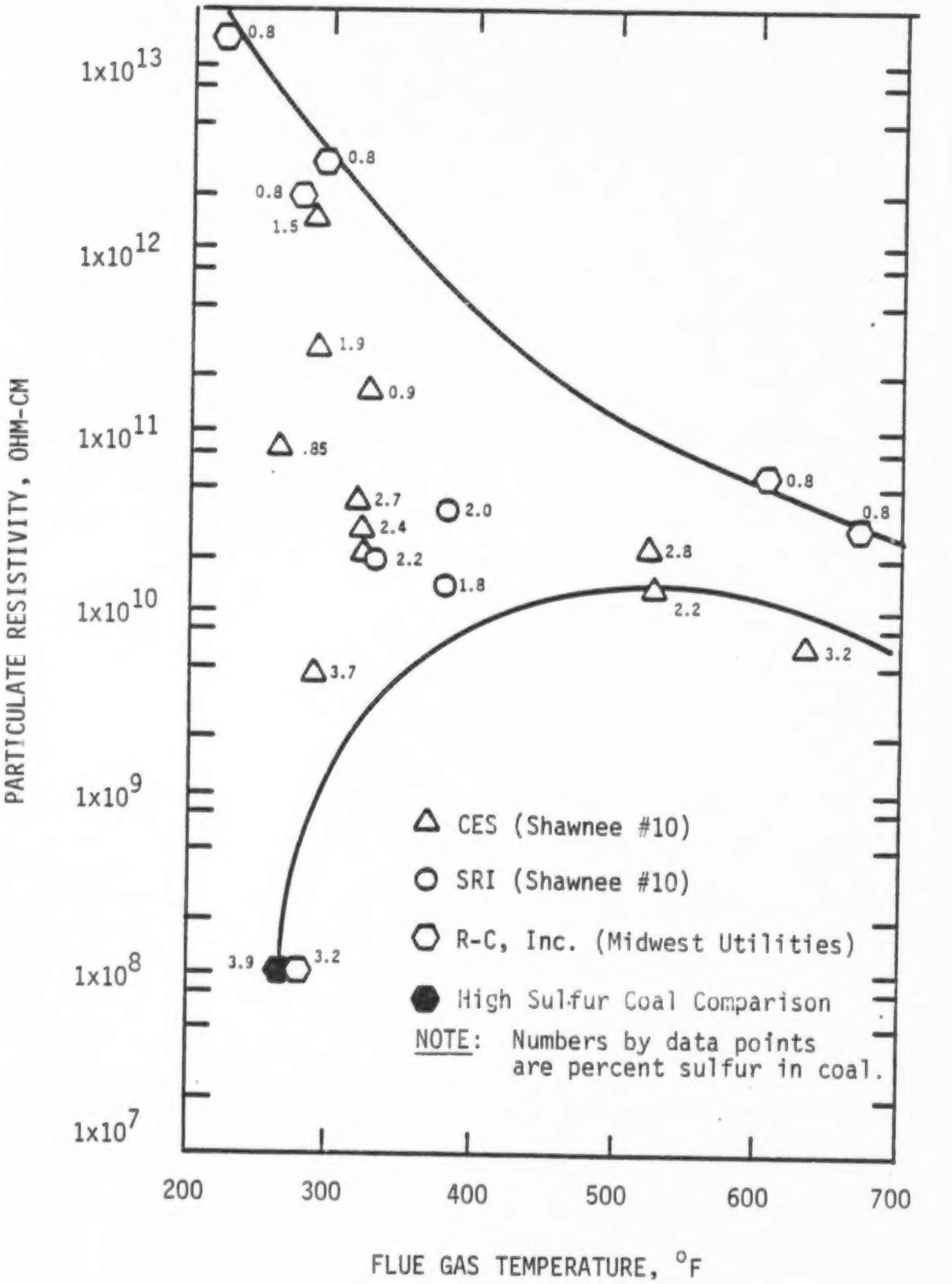

Figure 11-4. In-situ resistivity vs. temperature relationship for various coal sulfurs (no limestone injection).

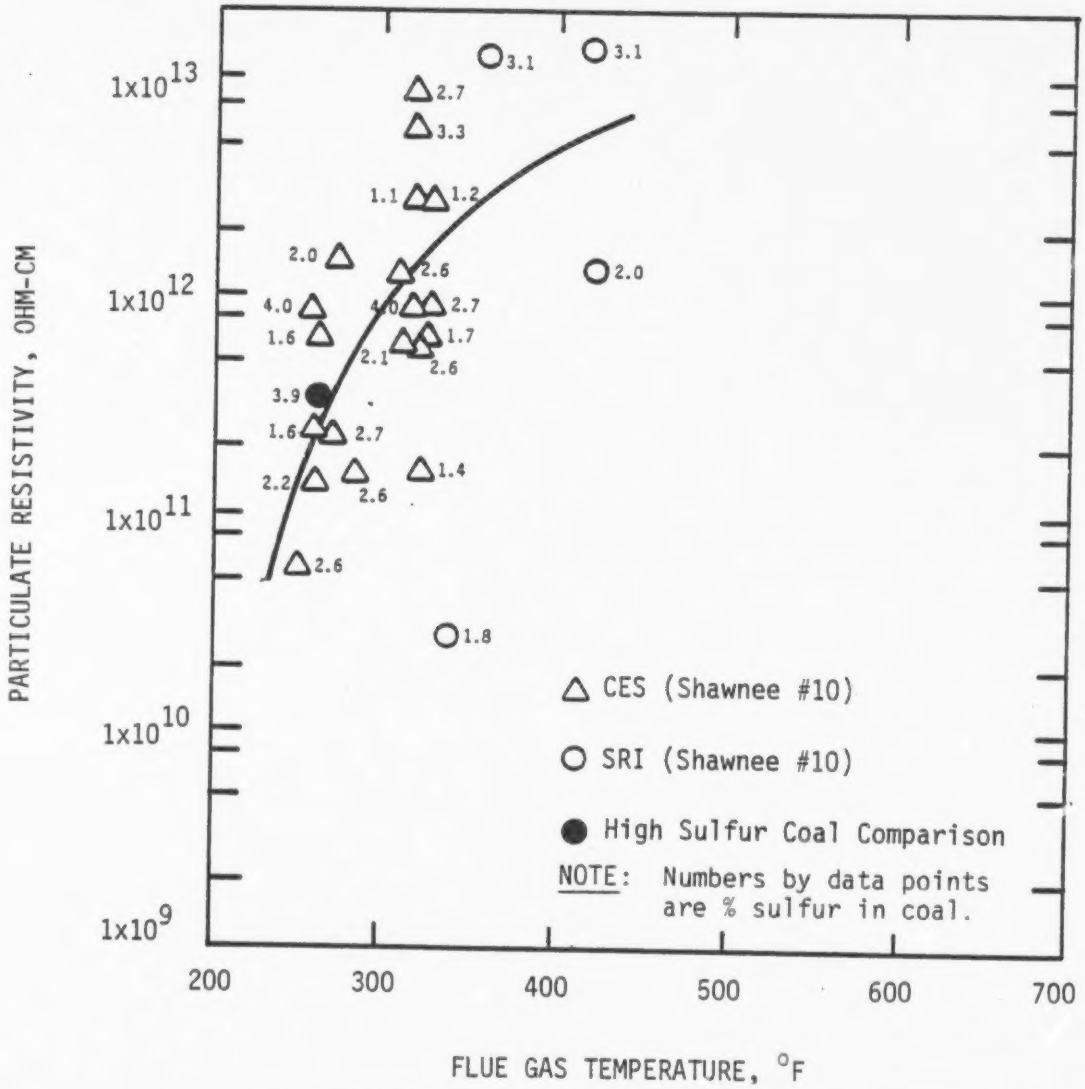

Figure 11-5. In-situ resistivity vs. temperature relationship for various coal sulfurs (with limestone injection).

addition increased resistivity. Sorbent addition had the most dramatic effect on the resistivity of high sulfur coals, increasing it as much as 10^3 ohm. cm (see solid symbols, Figures 11-4 and 11-5).

Electrostatic precipitator performance has been reported to be very adversely affected by sorbent injection. Particulate removal efficiencies at Shawnee have been reported to decrease from 99 percent to as low as 72 percent. The performance ESP system at RWE has not been reported to be adversely affected by sorbent injection. The opacity of the plume from the Hoot Lake Station was observed to change from non-visible to approximately 20 percent. The less severe impact of sorbent injection on the ESP's at the lignite-fired plants was probably due to the stringent, and generally over-size, design basis usually used on lignite-fired systems. Estimates of required increases in ESP size for higher sulfur bituminous coal-fired facilities using sorbent injection range from 3.25 (Shawnee) to 2.5 times the original size in order to accommodate the increased solids loading and resistivity.

11.1.4 Effect on Downsteam Equipment and Effluent Streams

Sorbent injection was also reported to adversely affect ash handling equipment at TVA, due to over-loading and to alterted flow, mixing and handling characteristics of the collected particulate. The effect on plant waste-water quality at TVA was also monitored. An increase in total dissolved solids, hardness and sulfate and magnesium concentration of the discharge water was observed during limestone injection tests. Significant deterioration in waste-water quality, including increases in soluble heavy metals and toxic elements was anticipated for sytems using limestone injection. Problems with increased solid and liquid waste disposal due to limestone injection were also anticipated (Gartrell).

In summary, the potential problematic side effects of using sorbent injection to control SO_2 emissions are myriad. Reported effects include changes in: Slagging and fouling rates and characteristics, fly ash particle size and resistivity, solids loading, ESP efficiency, ash handling equipment reliability, and effluent water quality have all been reported. In addition, speculation that the sorbent will affect the flame itself, especially emissivity and thermal radiative characteristics, is probably in order. The magnitude and importance of these effects and how they affect boiler operation and availability has yet to be determined. Sorbent injection side effects will be further assessed as planned pilot, bench, and demonstration studies of LIMB progress.

11.2 Boiler Simulator Furnace Tests of Sorbent Effect on Ash Characteristics

A brief set of experiments was performed in the BSF to assess the effect of SO_2 removal by dry limestone sorbent injection on effluent stream (gas and solid) characteristics. The effects of LIMB on characteristics of two basic streams - effluents from firing a high-sulfur (3.5% S), eastern, bituminous coal (Illinois #6) and a low-sulfur (0.9% S), western coal (Utah) were investigated at the same general firing conditions using the same limestone sorbent.

11.2.1 Sulfur Capture

The effectiveness of sorbent injection for SO_2 emission control was assessed using both fuels. The test conditions were chosen to give 30 percent sorbent utilization with the Illinois coal. This required the use of cooling coils in the radiant furnace to alter the thermal history of the sorbent and flue gases. Figure 11-6 shows SO_2 capture through the BSF as a function of residence time for Ca/S of 2.0 with the Illinois coal. The furnace wall and gas temperatures are also shown. Two characteristics are striking. First, the SO_2 capture is essentially complete at the first sample point - the exit of the radiant zone. The second important characteristic is the increase in sulfur capture with run time, sorbent utilization was approximately 25 percent at port 3 after twenty minutes of injection and increased to a high of 35 percent after several hours of run time. The sulfur captures shown are based on the differences in SO_2 at the beginning of the run with and without sorbent injection.

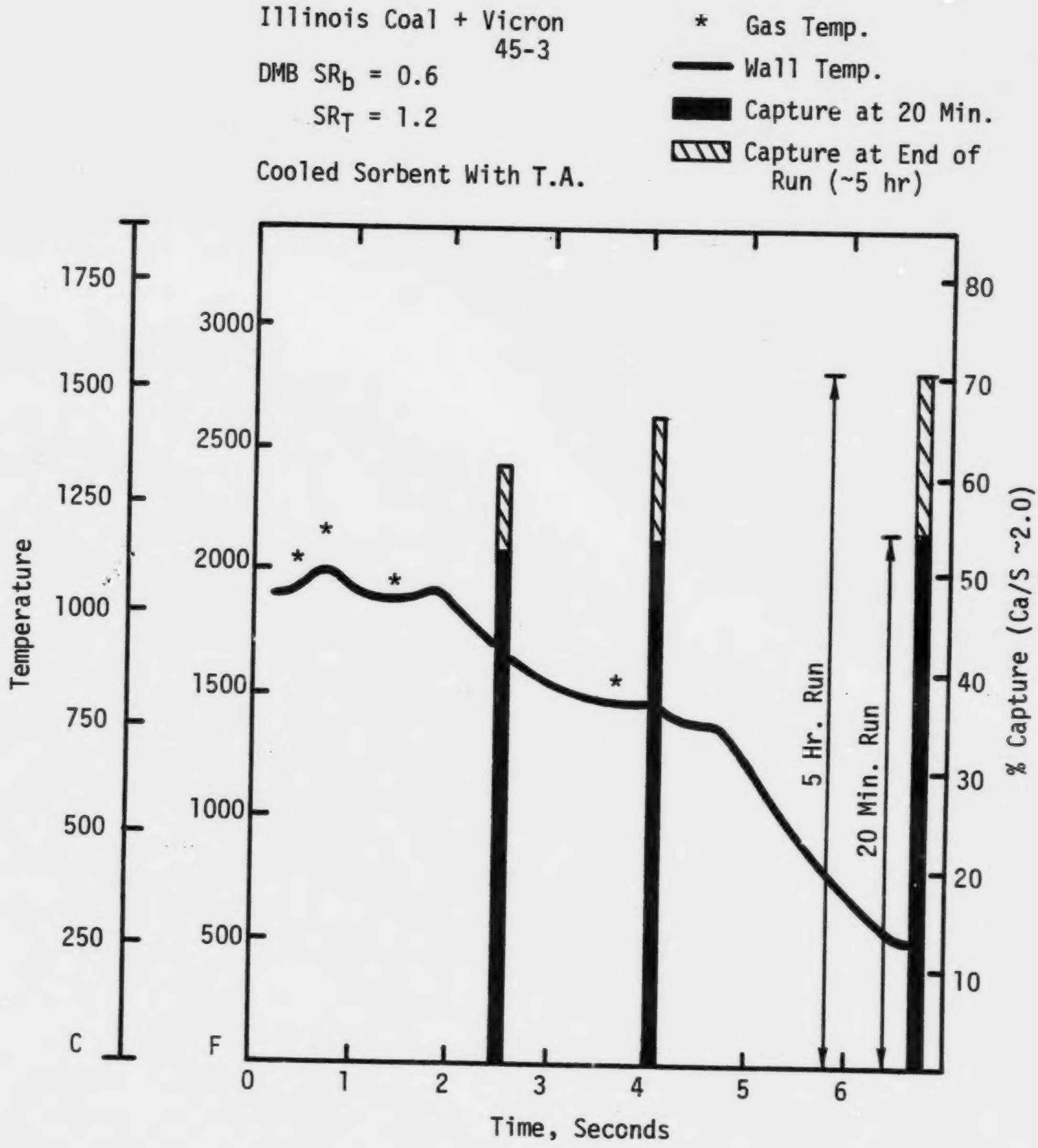

Figure 11-6. Furnace temperatures and sulfur capture - Illinois coal fired with Vicron 45-3.

Similar sulfur capture and temperature data for the Utah coal-fired test are shown in Figure 11-7. It is clear that for this fuel also, the sulfur capture is essentially complete at the exit of the radiant furnace and that sulfur capture increased during the test run.

11.2.2 Thermal Effects

The injection of limestone for SO_2 capture from pulverized coal-fired furnaces impacts the solids loading in the furnace and the thermal characteristics of the furnace. The effect of sorbent injection on furnace temperature profiles and on fouling of a simulated convective tube was assessed during the ash characterization tests. Typically, five hours of sorbent injection resulted in an increased furnace exit temperature and increased fouling rates. The flue temperature increased 50-100°F during the sorbent injection tests with the Illinois coal and 25-50°F with the sorbent/ Utah coal.

Fouling rates were assessed using a simulated convective tube. Heat transfer to the air-cooled tube and tube skin temperature were measured as a function of time for both coals with and without sorbent injection. Figures 11-8 and 11-9 show heat extraction and probe temperature for Illinois coal with and without Vicron 45-3. Similar data for the Utah coal are shown in Figures 11-10 and 11-11.

Fly Ash Resistivity

The effect of sorbent addition (and SO_2 capture) on fly ash resistivity of the two coals was determined. Fly ash resistivity was measured in-situ with a point-to-plane resisitivity probe designed and built by Southern Research Insittue. Resistivity measurements were made for both fuels with and without sorbent addition. SO_3 concentrations and water vapor content of the flue gas were also determined. The results of the resistivity measurements, along with other effluent stream characteristics, are summarized in Table 11-1. Sorbent addition resulted in an increase in fly ash resistivity of approximately 30 times for the Illinois coal while sorbent addition resulted

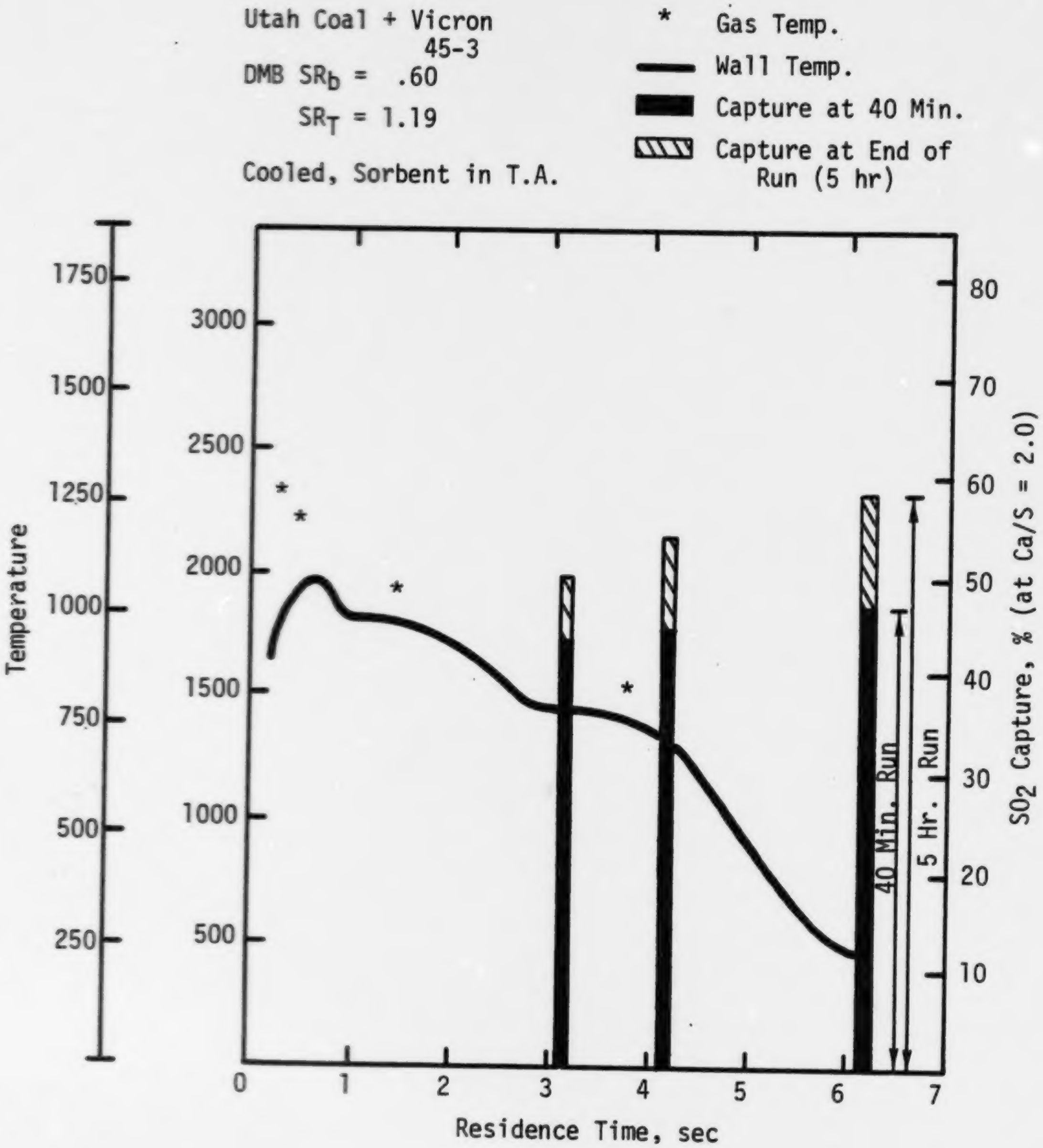

Figure 11-7. Furnace temperatures and sulfur capture - Utah coal fired with Vicron 45-3.

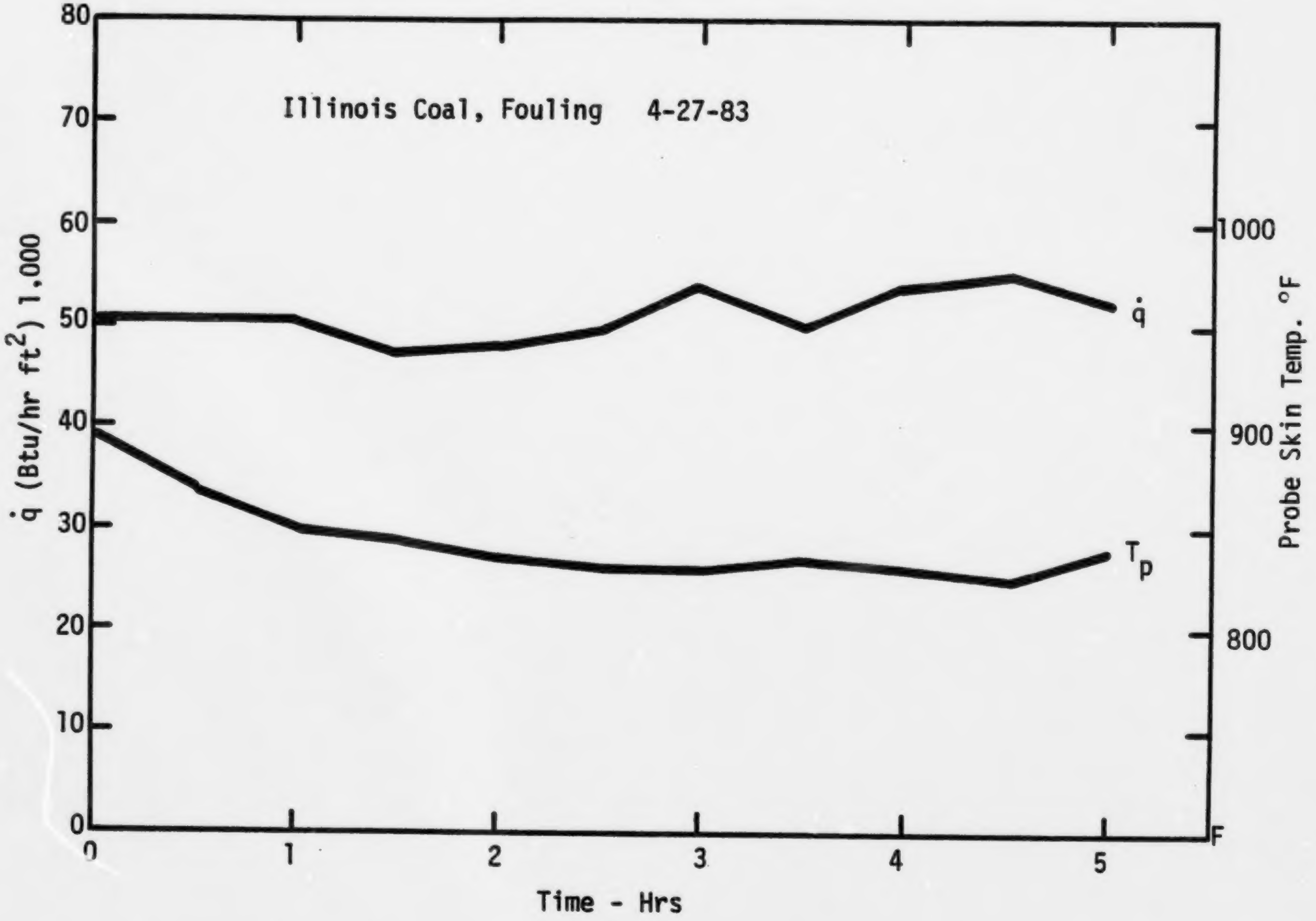

Figure 11-8. Fouling Characteristics - Heat Extraction ($\dot{q}$) and cooling Probe Temperature (T). Illinois Coal Fired.

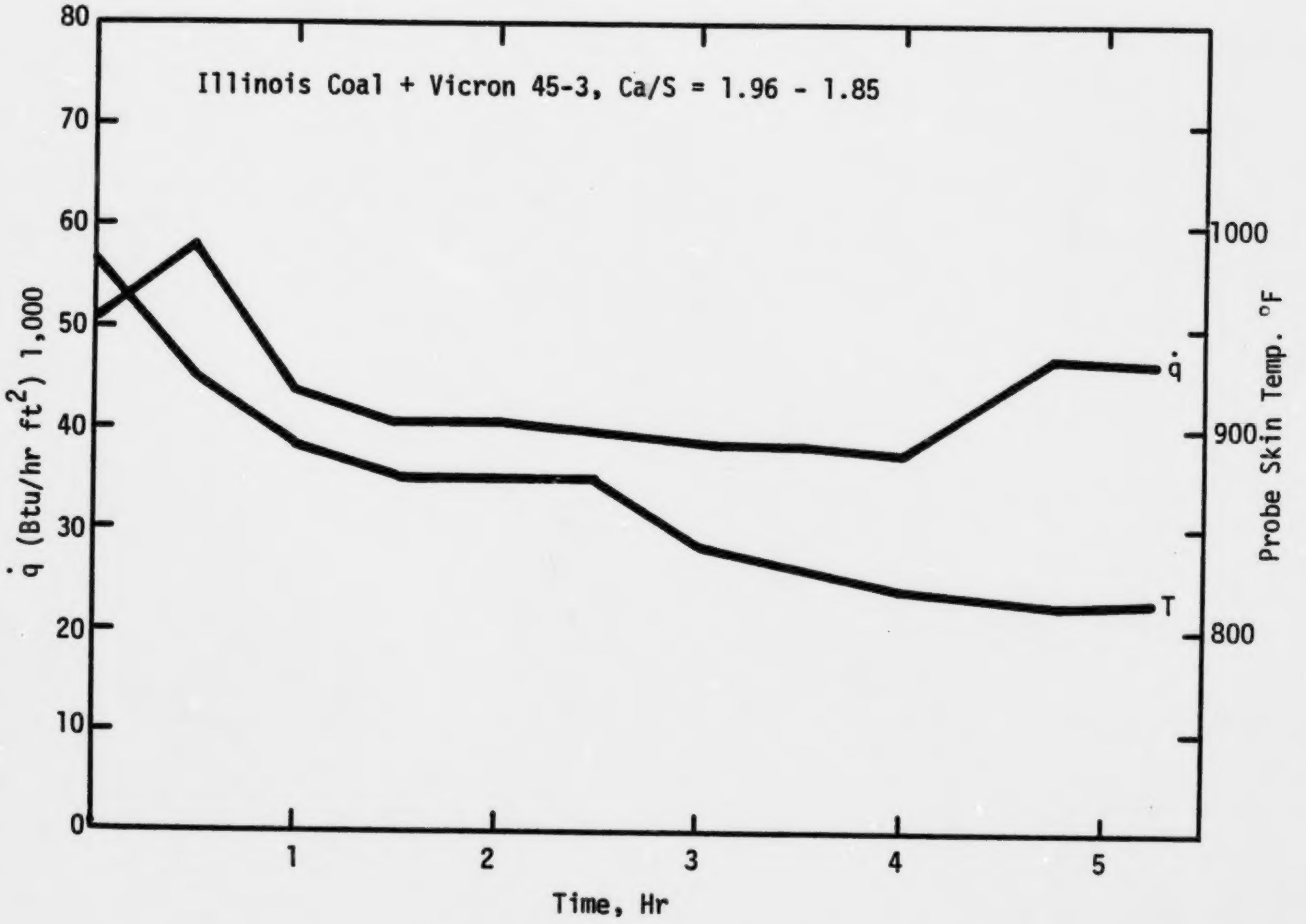

Figure 11-9. Fouling Characteristics - Heat Extraction ($\dot{q}$) and Cooling Probe Temperature (T). Illinois Coal with Vicron 45-3 (Ca/S = 2.0).

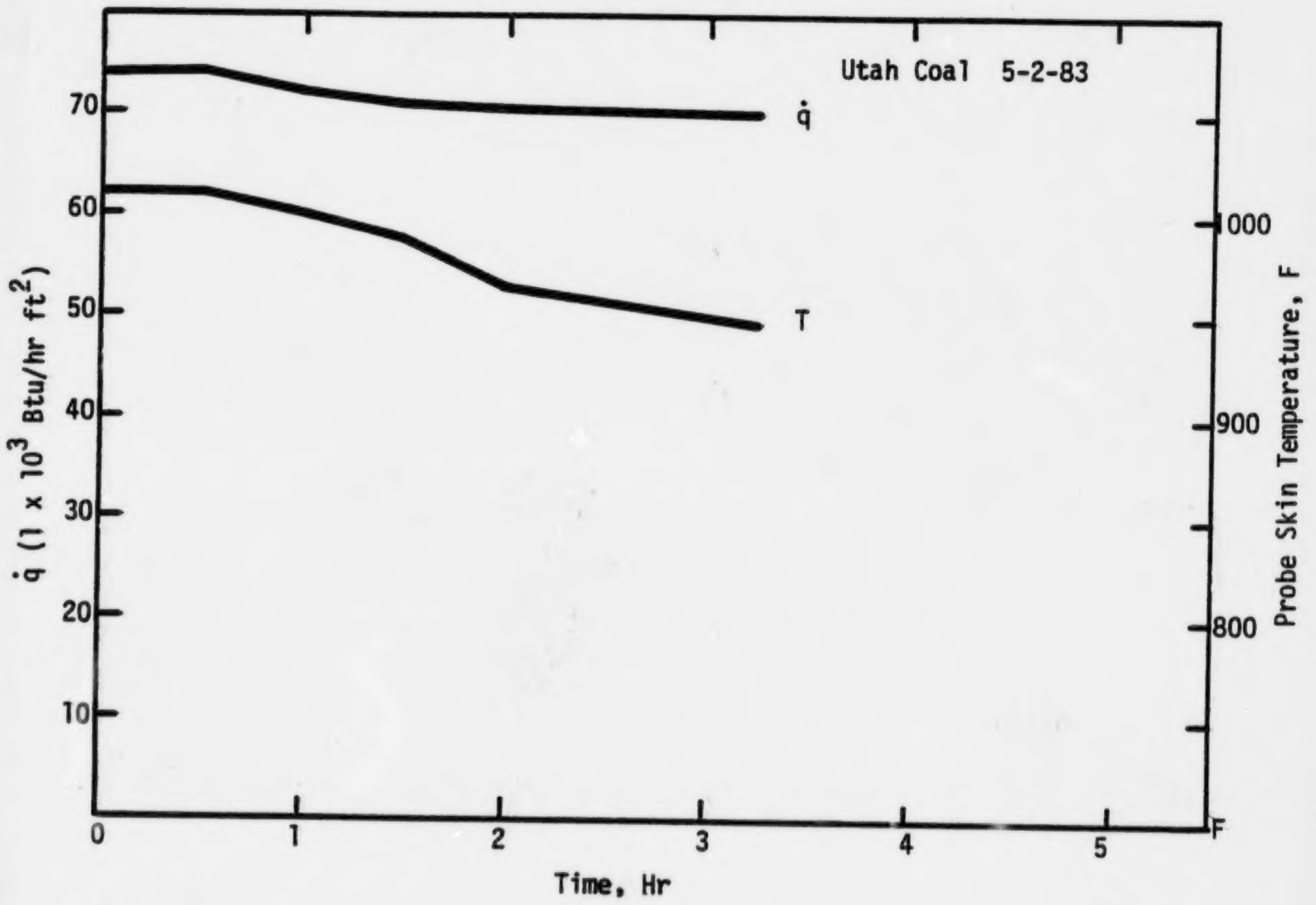

Figure 11-10. Fouling Characteristics - Heat Extraction ($\dot{q}$) and Cooling Probe Temperature (T). Utah Coal Fired.

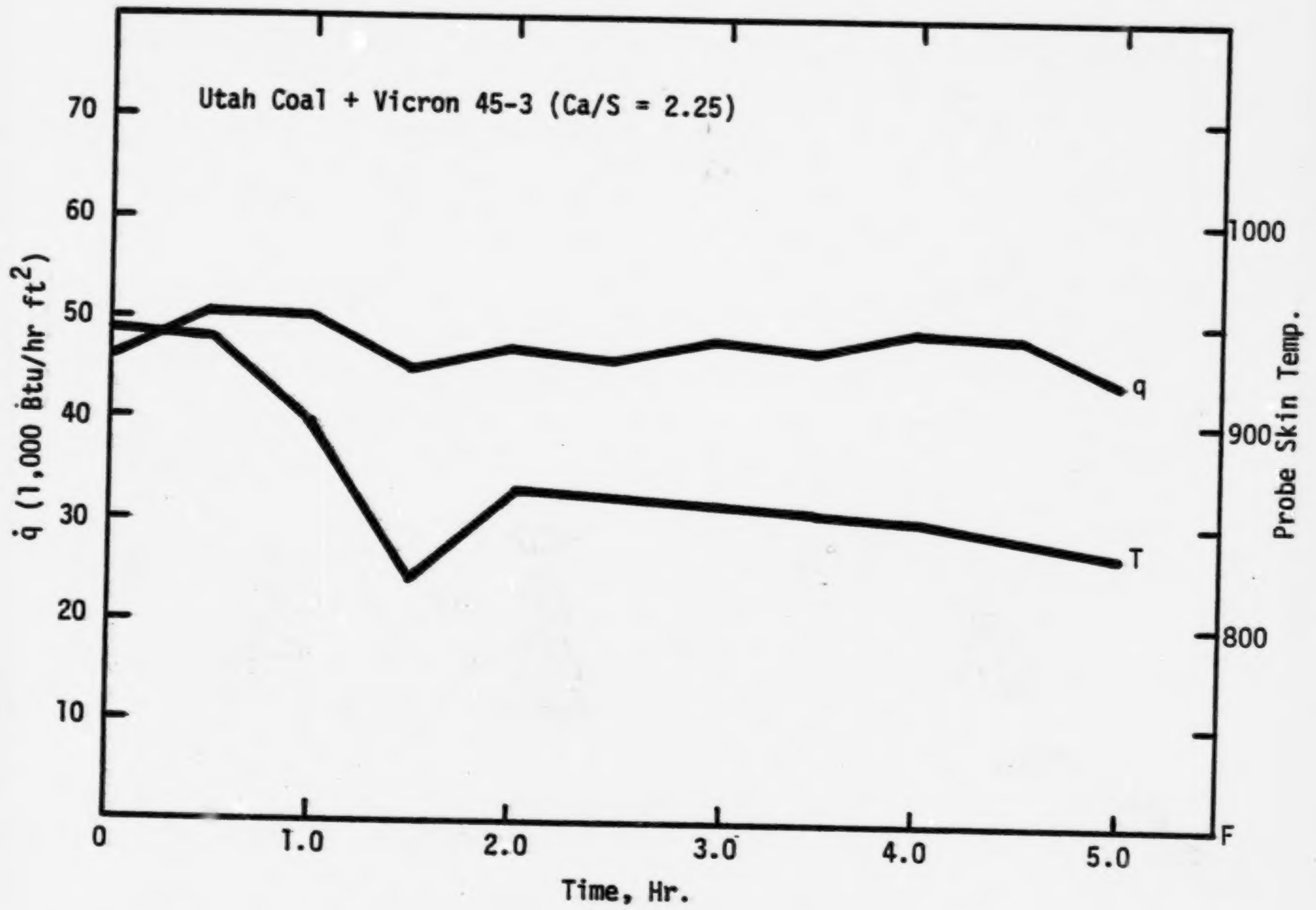

Figure 11-11. Fouling Characteristics - Heat Extraction ($\dot{q}$) and Cooling Probe Temperature (T). Utah Coal + Vicron 45-3 (Ca/S = 2.25).

TABLE 11-1. LIMB EFFLUENT STREAM CHARACTERISTICS

		FLUE GAS COMPOSITION		SOLIDS COMPOSITION		FLUE TEMP. F		SOLIDS LOAD gm/DNCM		SOLIDS SIZE gm/DNCM		RESISTIVITY OHM cm (Spark)		SO_2 UPTAKE (% ut.)	
SORBENT ADDITION		W.O.	WITH	W.O.	WITH	W.O.	WITH	W.O.	WITH	W.O.	WITH	W.O.	WITH	W.O.	WITH
INDIANA COAL						370	420	3.1	9.05			2.8×10^{13}	8.6×10^{14}	14.6	3.4.4
GAS	SO_2	3075	1019												
	SO_3	20	5.3												
	O_2 (%)	3.4	3.3												
	CO_2 (%)	18.5	18.9												
	NO_x	438	410												
	H_2O (%)	5.2	7.8												
SOLID	C			1.9	.5										
	CaO			10.9	30.2										
	S			3.8	11.0										
	Ash			95.5	92.7										
	CO_3			1.3	.78										
SIZE	< 2µm									0.44	1.50				
	< 1µm									0.12	0.66				
UTAH COAL						390	415	1.3	1.75			6.3×10^{13}	6.6×10^{13}	19.7	23.0
GAS	SO_2	540	300												
	SO_3	1.2	1.5												
	O_2 (%)	3.7	4.2												
	CO_2 (%)	18.4	18.5												
	NO_x	167	148												
	H_2O (%)	6.3	6.2												
SOLID	C			5.7	2.2										
	CaO			16.8	21.6										
	S			4.7	5.4										
	Ash			92.2	96.3										
	CO_3			1.47	.85										
SIZE	< 2µm									0.2	0.48				
	< 1µm									0.15	0.25				

in no measurable increase in resistivity for the Utah coal. The SO_3 content of the flue gas decreased by a factor of 4 with sorbent injection for the Illinois coal, while there was essentially no change due to sorbent injection with the Utah coal.

11.2.4 Solids Loading and Size Distribution

The effect of sorbent addition on flue gas solids loading and particle size distribution for both fuels was measured. Table 11-2 summarizes measured and theoretical solids loading for both fuels with and without sorbent addition. The addition of limestone sorbent resulted in an average increase in flue gas solids loading of three (3) times for the Illinois coal and thirty-five (35) percent increase in particulate load for the Utah coal-fired case. In neither case was percent solids drop-out in the furnace increased by the sorbent addition.

Particle size distributions were measured in-situ with Cascade impactors. Figures 11-12 and 11-13 show particle size distributions measured for the two fuels with and without sorbent addition. Particle size for the Illinois coal ash (50 percent aerodynamic cut size versus cululative mass) is shown in Figure 11-12. Five impactor runs are shown, three of the Illinois coal ash and two of the Illinois coal ash/sorbent mixture. It is clear that the sorbent addition results in an increase in the fines (particles $< 1 \mu m$) in the flue. Again, it appears that sorbent addition increases the fines loading, although the changes are not as clearly shown as in the Illinois coal-fired case.

11.3 Conclusion - Effect of LIMB on Boiler Operation

All of the results to date, in both pilot demonstration studies and in smaller scale work such as the BSF experiments indicate that injecting sorbent into the boiler will affect the boiler operating characteristics. Increases in fouling rates and convective section plugging have been documented. Limestone injection may affect both staging characteristics (decreasing or increasing ash fusion temperatures depending on the original fuel

TABLE 11-2. EFFECT OF SORBENT ADDITION ON TOTAL SOLIDS LOAD AND CARRYOVER

DATE	FUEL	LOAD gm/DNCM	THEORETICAL SOLIDS LOAD gm/DNCM	% DROP OUT
4-27 A2	Illinois	2.07	14.4	85.6
4-27 C4	Illinois	3.78	14.4	73.4
4-28 B5	Illinois + Vicron 45-3	10.06	33.8	70.0
4-28 C6	Illinois + Vicron 45-3	7.50	33.8	77.8
5-4 C9	Utah	1.29	9.31	86.1
5-4 B10	Utah + Vicron 45-3	1.48	14.63	89.9
5-4 A11	Utah + Vicron 45-3	2.06	14.63	85.9

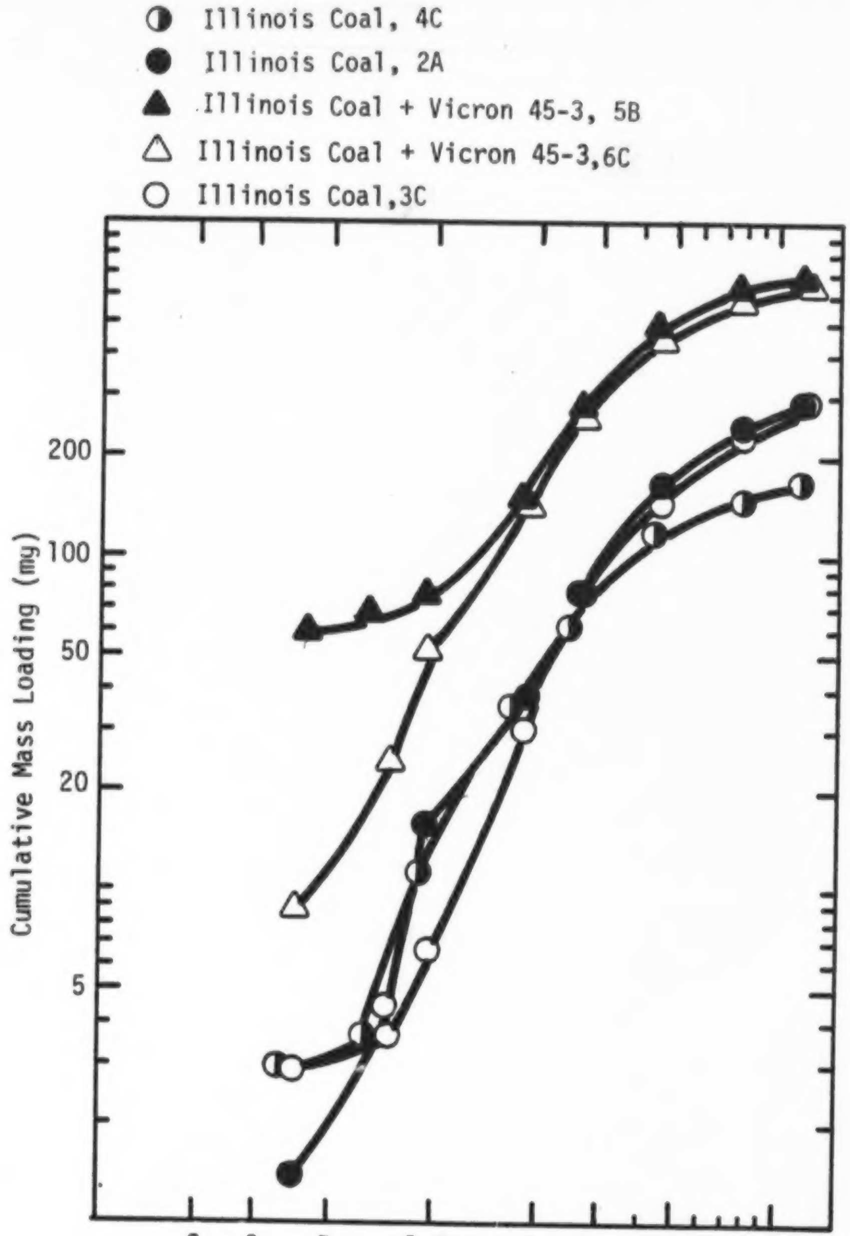

Figure 11-12. Particle Size Distribution, Flue, Illinois Coal With and Without Sorbent.

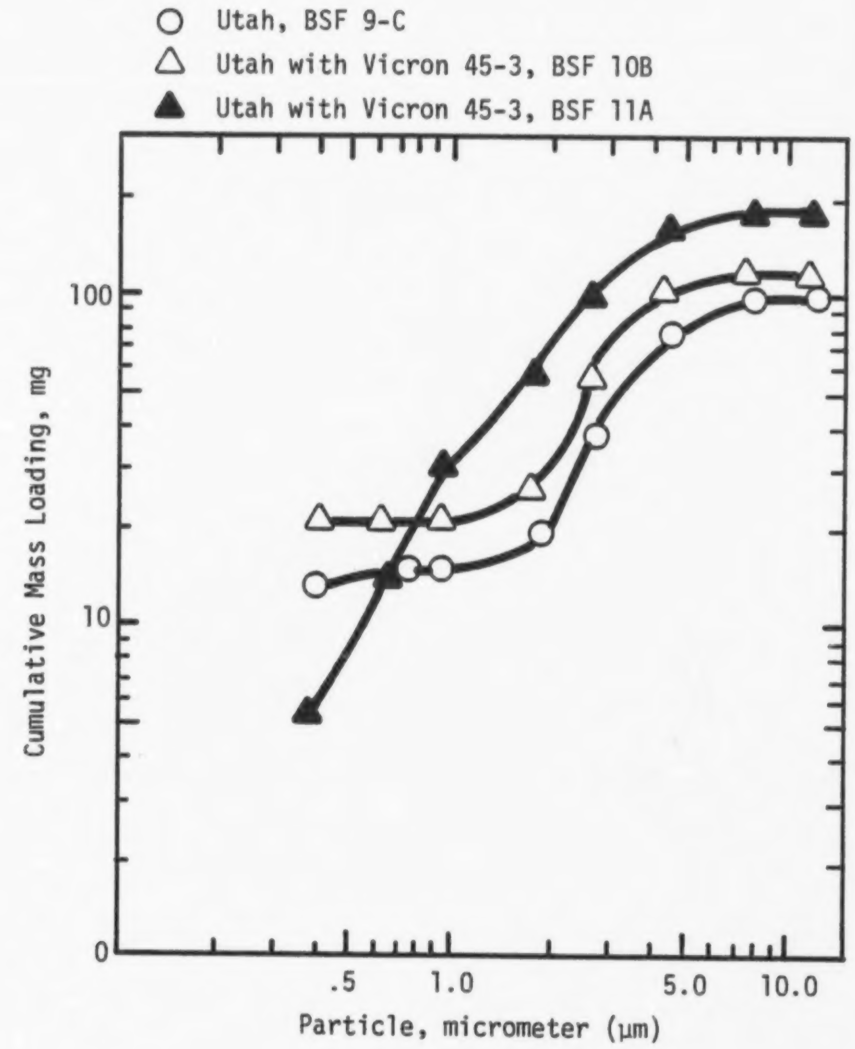

Figure 11-13. Particle Size Distribution, Flue, Utah Coal and Utah Coal with Sorbent.

characteristics) and the hardness of fouling deposits. Limestone injection may affect flame characteristics - changing emissivities, flame and/or wall temperatures - but such effects have not been studied.

Particulate removal systems will be affected by changes in solids loading and size distribution and in fly ash resistivity and flue-gas SO_3 content. All of these effects have been observed and general trends can be predicted - such as increased resistivity and fouling - but the data base needed to predict the particular effects of LIMB on the operation characteristics of a given boiler is simply not yet available. More experience with limestone injection in various systems is required in order to begin assessing actual effects on operating systems.

12.0 CONCLUSIONS AND RECOMMENDATIONS

The acronym LIMB is from Limestone Injected Multi-stage Burners. The LIMB process is for simultaneous control of NO_x (using distributed mixing or multi-stage burners) and SO_2 (using sorbent, i.e., limestone, injection) from pulverized coal-fired boilers. The overall goals of this research was clarification of the processes which control sulfur capture by dry sorbents injected directly into a pulverized coal-fired system, and the development of methods for generalizing data from one test furnace to another and from test facilities to field application.

The experimental portion, carried out in the Boiler Simulator Furnace (BSF), included investigation of:

- the effect of fuel type and fuel mineral material on sulfur;
- the effect of sorbent type on sulfur capture;
- detailed temperature and species characteristics of flames which gave significantly different sulfur captures;
- the effect of operational characteristics such as fuel injector, burner zone stoichiometry, peak flame temperature, and load on sulfur capture;
- the effect of sorbent injection location;
- and the effect of LIMB on various furnace operational characteristics such as slagging, fouling, solids loading and size distribution, and fly ash resistivity.

The analytical portion included the development of a computer code to model sulfur capture by sorbents and the application of an existing boiler performance/heat transfer code to model facilities at EER and provide a prediction of thermal characteristics. A scheme for applying the two computer models to experimental systems and predicting sulfur capture was developed and applied to the pilot-scale facilities at EER.

12.1 Conclusions - Experimental Results

Detailed measurements of temperatures, gas species and solids in the region near the BSF burner were performed to better define two flames (coal and gas) which gave disparate sorbent utilizations. These detailed measurements showed slight differences in flame shape and peak flame temperatures (the coal flame was somewhat shorter and hotter near the burner than the gas flame) and confirmed the difference in sorbent utilization in the two flames. There was some loss of calcium (sorbent) in the furnace when coal was fired and considerable dropout of solids through the furnace with either fuel. The measured differences in temperature and flame shape did not seem sufficient to account for the observed difference in sulfur capture. It appeared that some fuel effect not directly responsible for the lower sulfur capture in the coal flame.

Investigation of the effect of various thermal conditions on sulfur capture from gas flames indicated that overall sulfur capture in the BSF was only slightly affected by very significant increases in flame temperature. Changes in burner characteristics, including fuel injector and staging level also had minor effects on sulfur capture. The change in sulfur capture produced by altering the thermal characteristics of the natural gas flame were much less dramatic than the difference in capture between gas and coal flames. Capture for gas flames with peak temperatures both higher and lower than the coal flame gave better captures than the coal-fired system. These results combined with the detailed measurements indicate that the effect of fuel type on sulfur capture is not a simple, direct result of thermal differences in the flames.

The hypothesis that some component of the coal, most likely the ash, was responsible for the difference in captures between coal and gas firing was investigated. The addition of coal fly ash to Vicron 45-3 (limestone) caused a dramatic reduction in sulfur capture by the sorbent in a natural-gas/H_2S flame. Fly ash from a pf-fired furnace is not necessarily the same as the original mineral matter in the coal so two clay minerals were mixed with two sorbents to investigate the role of coal mineral matter. The addition of kaolin had a strong effect on vicron utilization and a similar effect on dolomite. Bentonite, a different clay material, also decreased sulfur capture, but not as dramatically as the kaolin. There was a reasonably good inverse correlation between the alumina (Al_2O_3) content of a sorbent/mineral mixture and the sulfur capture by that mixture using either Vicroni 45-3 or dolomite.

The concentration of SO_2 in the natural gas-fired tests had a slight effect on sulfur capture, increasing capture at Ca/S = 2 from 26 percent at 500 ppm to 40 percent at 3500 ppm SO_2. The concentration of mineral matter (correlated as gm Al_2O_3 per dry normal cubic meter of flue gas) in the system had a very strong impact on capture at all of the SO_2 concentration levels and Ca/S ratios tested. At a calcium-to-sulfur mole ratio of 2 and 3500 ppm SO_2, the capture went from 40 percent with no mineral material to 8 percent with 7 gm/DNCM Al_2O_3 in the flue gas.

Electron micrographs of sorbent mineral samples taken from the BSF show particles composed of a mixture of AlSi and Ca. The particles are spherical and have been molten at some point in the furnace. It appears that the sorbent/mineral interaction accounts for the observed effect of coal ash on sulfur capture. The mechanism of mineral deactivation is not clear and should be the subject of further investigation.

A fairly extensive data base of sulfur capture in the BSF for various fuel sorbent pairs was established. Six fuels and five sorbents were tested (not all possible combinations of fuel-sorbent pairs were included).

The effect of sorbent type on capture with a given fuel was dependent on the firing conditions - including sorbent injection location and thermal conditions. The hydrated limes seemed to be most sensitive to thermal conditions and the Vicron least sensitive. The German hydroxide gave better capture than the Colton hydroxide - it was not clear why the two had different captures. Dolomite gave the highest capture with all of the fuels tested.

The effect of fuel type on capture with a given sorbent was also system (injection method, firing characteristics and thermal conditions) dependent. Capture with natural gas was higher for all of the sorbents than with coal - due, in part, to deactivation of the sorbent by coal mineral matter. Sulfur capture for the fuels tested with Vicron 45-3 and dolomite showed a fairly consistant inverse correlation with the calculated Al_2O_3 content of the ash sorbent mixture (at a $Ca/S = 2.0$).

In general, sorbent size affected capture only for large particles, at mean sizes less than 10 μm particle size had little effect on sulfur capture. The effect of particle size was greater when firing Indiana coal than when firing natural gas. A comparisoin of the predicted effect of particle size and the observed effect using various sizes of vicron was in fairly good agreement.

Injecting the sorbent downstream from the main flame resulted in improved utilization in coal flames. Experiments with natural gas flames showed that the sorbents had somewhat higher surface areas in the reaction zone when injected downstream. Gas-fired experiments using mineral matter additives showed that mineral material deactivation of the sorbent could be reduced by injecting the sorbent downstream of the main flame. Electron micrographs of solid samples from experiments where kaolin was injected with the fuel (natural gas) and the sorbent was injected downstream showed discrete irregular sorbent particles and spherical mineral material particles. Electron micrographs of samples taken from coal-fired, downstream sorbent injection tests showed spherical ash particles and discrete irregular sorbent particles.

Injecting sorbent to control SO_2 emissions from pulverized coal-fired boilers will result in changes in the boiler operating characteristics. Changes measured in the BSF due to sorbent injection included:

- increased solids loading from 35 percent to as much as three times depending on the fuel sulfur content;
- changes in particle size distribution resulting in an increase in fines;
- increased fouling on the simulated convective passes; and
- increases in fly ash resistivity of as much as 30 times for the high-sulfur coal tested.

The experiments performed have provided some clarification of the effect of various system parameters on sulfur capture by direct injection of sorbents. Fuel mineral matter has been shown to deactivate the sorbent if the two are injected together in a high-temperature (> 2300°F). Downstream sorbent injection (at temperatures around 2200°F) gave higher captures than injection with the fuel for coal-fired tests, because of decreased mineral matter interference and some increase in sorbent surface area. Further experimental work investigating the mechanism of mineral deactivation, the possibility of generating high surface area (highly reactive) sorbents and the effect of sorbent injection on boiler operating characteristics (especially heat transfer concerns such as flame emissivity).

12.2 Conclusions - Analytical Methods Development

One goal of this program was to develop tools to enable engineering analysis of various systems where sorbent injection for SO_2 control might be applied. The tools developed included a computer program which modeled the sulfur capture processes and the application at an existing boiler performance heat transfer code to specify thermal characteristics of a given system. The two computer programs were used to analyze three pilot-scale facilities at EER.

The general approach to sulfur capture modeling was to divide the process into the two zones; sorbent activation, which includes the processes which ultimately determine sorbent reactivity and sorbent sulfation capacity; these processes include: particle interfering chemical reactions. The second zone, sulfate formation includes: diffusion within the particle pores, chemisorption, reaction with the solid, diffusion through the reactant layer, blockage of the pores due to sulfate formation, and the thermal stability limits of the sulfate.

The activation portion of the model is basically empirical and was derived from data produced by another EPA Contract (68-02-3633) described in detail by Cole, et al., (1983).

The sulfur capture portion of the model was based on an approach developed by Bhatia and Perlmutter (1981) which treats the calcined (CaO) particles as spheres enveloping a random distribution of cylindrical pores which provide the overall particle surface areas. The sensitivity of the model to various parameters including pore-size characteristics, surface area, temperature, calcium-to-sulfur ratio, the selected intrinsic rate constant (derived from kinetic data and subject to some variation in interpretation) sulfate product layer diffusivity and Sherwood number (which influences the SO_2 concentration gradient at the particle surface) was tested. The parameters which had a significant effect on capture were the porosity/pore size/surface area of the sorbent (these are interreleated), and to a lesser extent, time, temperature, SO_2 concentration and Ca/S ratio.

The sulfation portion of the model is probably adequate for the model application needs except that the predicted effect of SO_2 concentration does not match the available data very well. The sorbent activation portion of the model is the best currently available, but is over-simplified and should be refined as data on the effects of calcination conditions and input sorbent characteristics becomes available.

In addition to modeling the sulfur capture process, engineering analysis work performed included the thermal modeling of three experimental facilities at EER, and the coupling of the two models (thermal and sulfation) to predict SO_2 capture. An existing boiler performance code, developed by Wolfgang Richter at EER was used for the thermal modeling. The code allows predictions of local and overall heat transfer and fuel burnout in boiler combustion chambers and industrial furnaces. The results are dependent on furnace geometry and operating conditions, fuel characteristics, and characteristics of wall deposits. The flow pattern within the furnace and the distribution of heat release due to combustion of volatile or gaseous fuel species is prescribed. Predictions of local furnace variables include:

- gas temperatures;
- incident and net radiative and total heat fluxes to heat sink surfaces;
- temperatures of refractory walls and wall deposits;
- burnout of solid fuel particles of up to ten size classes;
- equilibrium concentrations of major gaseous species corresponding to the progress of fuel burnout;
- complete time/temperature histories of real or imaginary tracer particles or material within the furnace;
- time dependent representation of all considered dependent variables, if requested.

There are two and three-dimensional codes available at EER; the three-dimensional code was used to model the LWS and the two-dimensional code was used to model the axi-symmetric SWS and MT furnaces.

The scheme developed for combined thermal sulfation modeling condisted of the following steps:

- The furnace heat transfer model was used to produce a temperature/flow map of the furnace.
- A large number of particles were tracked through the furnace, passing from zone to zone at random, weighted by the gas flow.
- The distribution of peak particle temperatures was used to calculate a mean particle surface area according to the sorbent activation correlation.
- The mean temperature and the mean residence time were used to calculate sulfation according to the sorbent sulfation model.

The combined thermal/sulfation modeling approach was used on the SWS, MT, and LWS furnaces. The importance of assumptions inherent to the approach was investigated, and the results from the three furnaces were compared with each other and with results obtained by applying the sulfation model to measured temperature profiles on the BSF.

Effects of scale were investigated by comparing sulfur capture predictions for the four furnaces under baseline conditions for sorbent injection with the fuel. The predicted sulfur capture of 44 percent for the LWS was highest due to its long residence time and high surface area which more than offset its low mean temperature. Sulfur capture of 39 percent was predicted for the MT, still fairly high, due to its high mean temperature, but relatively flat temperature profile resulting in a fairly high surface area. The SWS had a predicted sulfur capture of only 23 percent. Its average temperature was cool, but its peak temperatures were not, so its mean surface area was not high. The 13 percent capture predicted for the BSF was the lowest. The BSF had highest peak temperature resulting in the lowest surface area and the shortest residence in the sulfation temperature region. (All capture values discussed here are for Ca/S = 2.0.)

The model predictions of capture in the three pilot facilities are fairly good at predicting overall ranking of capture in the furnaces - LWS better than MT better than SWS. Captures measured in the LWS ranged from 40 to 53 percent depending on the burner and sorbent injection location. (The model predicts slightly higher capture for sorbent injection with the tertiary air in the LWS which was also apparent in some of the LWS tests.) Captures measured in the MT ranged from 10 to 29 percent again depending on burner and sorbent injection location. The highest capture measured in the SWS was 30 percent, higher than the predicted 23 percent. The model also does not predict a difference in capture due to sorbent injection location in the SWS, while experimental results showed a difference as great as from 10 percent to 30 percent capture.

A general analytical scheme, and some of the tools for applying this scheme have been developed to allow generalization and rationalization of LIMB data taken in various facilities. The prediction of some general capture trends is possible, but several gaps in the data and in modeling techniques remain. The available analytical methods do not give sufficient refinement of the processes occurring in the near-burner region which, from the experimental results, can have a profound impact on sorbent reactivity and sulfur capture. The prediction of sorbent reactivity from measurable properties and projected thermal history is still very inadequate. Insufficient data on the effects of parent stone characteristics, such as grain size, composition and particle size, as well as the effect of various flame - calcinatin regimes (heating rate, peak temperature, quench rate, etc.) on sorbent reactivity currently exist. These areas should receive further experimental and analytical attention.

13.0 REFERENCES

Attig, R. C., P. Sedor "Additive Injection for Sulfur Dioxide Control. A Pilot Plant Study". The Babcock and Wilcox company, NTIS PB226 761, March, 1970.

Bhatia, S. K. and D. D. Perlmutter. The Effect of Pore Structure on Fluid-Solid Reactions: Application to the SO_2-Lime Reaction. AICHE. J. 1981, 27 (2), 226-234.

Blythe, G. M., "Dry Limestone Injection Test at a Low-Rank Coal-Fired Power Plant", November, 1982, DOE/FC/10200-T5.

Borgwardt, R. H., G. R. Gillis, N. F. Roache, "IERL-RTP Research on Sulfur Capture in LIMB". Presented at Joint Symposium on Stationary Combustion NO_x Control - EPA, EPRI, Dallas, TX, November, 1983.

Case, P. L., L. Ho, M. P. Heap, R. Payne, D. W. Pershing, "Development of Criteria for Extension of Applicability of Low Emission, High Efficiency Coal Burners" - Final Report of Bench-Scale Studies of Limestone Injection for SO_2 Control, EPA Contract No. 68-02-2667, August, 1983.

Cole, J. A., et al. Fundamental Studies of Sorbent Calcination and Sulfation for SO_2 Control from Coal-Fired Boilers, Irvine, CA: EER Corporation, Final Report, EPA Contract 68-02-3633, October, 1983.

Faber, A. And S. Michelfelder, The Calculation of Flame Length and Chemical Heat Release Distribution, The International Flame Research Foundation, 1978, Document No. G02/a/27.

Field, M. A., D. W. Gill, B. B. Morgan, and P. G. W. Hawksley, Combustion of Pulverized Coal, Chapter 2, Flow Patterns and Mixing, The British Coal Utilization Research Association, 1967.

Flament, G., "The Simultaneous Reduction of NO_x and SO_x in Coal Flames by Direct Injection of Sorbents in a Staged Mixing Burner:, International Flame Research Foundation (IFRF) Doc. No. G19/a/10, September, 1981.

Gartrell, F. E., "Full-Scale Desulfurization of Stack Gas by Dry Limestone", Vols. 1, 2, 3, EPA-650-2- 73-019 a, b, c, 1973.

Hein, K. and W. Glazer, "Dry Additive Process for SO_2 Removal During the Combustion of Brown Coals", Proc. Sixth Members Conference IFRF, 1981.

Johnson, J. W., G. I. Clinard, L. G. Felix, J. D. McCain, "A Computer-Based Cascade Impactor Data REduction System", EPA-600/7-78-042, March, 1978.

Kerr, N. M. and D. Fraser, 1965, J. Inst. Fuel 38, 519-526.

Payne, R., P. L. Case, M. P. Heap, J. Lee, C. N. McKinnon, P. Nelson, D. W. Pershing, Fourth Annual Report - Development of Criteria for Extension of Applicability of Low-Emission, High-Efficiency Coal Burners, EPA Contract 68-02-2667, October, 1982.

Smith, W. B., K. M. Cushing, J. D. McCain, "Procedures Manual for Electrostatic Precipitator Evaluation", EPA-600/7-77-059, June, 1977.